APTD-1290

AUTOMOTIVE GAS TURBINE OPTIMUM CONFIGURATION STUDY

U.S. ENVIRONMENTAL PROTECTION AGENCY
Office of Air and Water Programs
Office of Mobile Source Air Pollution Control
Advanced Automotive Power Systems Development Division
Ann Arbor, Michigan 48105

APTD-1290

AUTOMOTIVE GAS TURBINE OPTIMUM CONFIGURATION STUDY

Prepared by

E. S. Wright, L. E. Greenwald, R. R. Titus
United Aircraft Research Laboratories
East Hartford, Connecticut 06108

Contract No. 68-04-0013

Project Officers:

T. M. Sebestyen (EPA), A. W. Nice (NASA)

Prepared for

U.S. ENVIRONMENTAL PROTECTION AGENCY
Office of Air and Water Programs
Office of Mobile Source Air Pollution Control
Advanced Automotive Power Systems Development Division
Ann Arbor, Michigan 48105

May 1972

[FINAL REPORT TITLE PAGE REVERSE SIDE FORMAT]

The APTD (Air Pollution Technical Data) series of reports is issued by the Office of Air Quality Planning and Standards, Office of Air and Water Programs, Environmental Protection Agency, to report technical data of interest to a limited number of readers. Copies of APTD reports are available free of charge to Federal employees, current contractors and grantees, and non-profit organizations - as supplies permit - from the Air Pollution Technical Information Center, Environmental Protection Agency, Research Triangle Park, North Carolina 27711 or may be obtained, for a nominal cost, from the National Technical Information Service, 5285 Port Royal Road, Springfield, Virginia 22151.

This report was furnished to the U.S. Environmental Protection Agency by United Aircraft Research Laboratories in fulfillment of Contract No. 68-04-0013 and has been reviewed and approved for publication by the Environmental Protection Agency. Approval does not signify that the contents necessarily reflect the views and policies of the agency. The material presented in this report may be based on an extrapolation of the "State-of-the-art". Each assumption must be carefully analyzed by the reader to assure that it is acceptable for his purpose. Results and conclusions should be viewed correspondingly. Mention of trade names or commercial products does not constitute endorsement or recommendation for use.

Publication No. APTD - 1290

FOREWORD

This report describes a comprehensive analysis of gas turbine engines designed for automotive propulsion. The study was performed by the United Aircraft Research Laboratories under contract to the Environmental Protection Agency, Office of Air Programs, Department of Advanced Automotive Power Systems Development (Contract No. 68-04-0013).

The Contractor's study team involved the participation of the United Aircraft Research Laboratories (UARL), Pratt and Whitney Aircraft Division (P&WA), United Aircraft of Canada Limited (UACL), and Hamilton Standard Division (HSD), all of United Aircraft Corporation. Additionally, several outside organizations representing potential vendors of selected critical components assisted in the study on a voluntary no-cost basis. Program management, economic analysis, and mission analysis were provided by UARL. Engine cycle analysis was provided by P&WA, base-line technology and preliminary design by UACL, and fuel control design by HSD.

Within UARL, the program was managed by Edward S. Wright. Vehicle performance and mission analysis were performed by Dr. Larry E. Greenwald, transmission analysis and vehicle integration by Richard R. Titus, and manufacturing cost studies by W. Richard Davison.

The program monitor for EPA was Mr. Thomas Sebestyen, and technical direction was provided by Mr. Arno W. Nice, of the NASA-Lewis Research Center.

Report L-971249-7

Automotive Gas Turbine
Optimum Configuration Study

TABLE OF CONTENTS

TABLE OF CONTENTS (cont'd)

TABLE OF CONTENTS (cont'd)

Report L-971249-7

Automotive Gas Turbine Optimum Configuration Study

SUMMARY

A wide variety of candidate gas turbine cycles was evaluated for application to automobile propulsion. Simple cycles, regenerated and recuperated cycles, cycles including intercooling and reheat, single-shaft and free-turbine engines, and a combined gas turbine and Rankine cycle were evaluated over a range of pressure ratios and turbine inlet temperatures for an initial total of 60 separate candidate cycles. Following a preliminary evaluation on the basis of total lifetime costs of all designs, three leading candidates were chosen for more detailed analysis -- a simple cycle, a regenerated cycle, and a recuperated cycle, all of which were single-shaft designs.

The selected engines were subjected to a more detailed preliminary design analysis which included a comprehensive study of fuel control, transmission, and installation considerations. The installed engines were analyzed on the basis of vehicle performance over a number of driving cycles for two candidate transmission types. In these analyses, the acceleration performance, fuel economy, and emissions characteristics were calculated. A direct manufacturing cost estimate was made as part of an overall economic analysis in which total lifetime engine-related automobile ownership costs were estimated. Also, estimates were made of the probability of achieving 1976 federal emissions standards, probable automobile first cost, and probable vehicle fuel economy. These estimates were compared with estimated values for both present and future emissions-treated Otto-cycle engines.

A broad outline of a development plan was generated for one of the selected engines, the single-shaft, simple-cycle configuration, and some of the problems associated with achieving a demonstration of this engine by 1975 are discussed.

RESULTS AND CONCLUSIONS

1. In an engine selection process which considered 60 potential gas turbine cycles, three engines were selected for detailed analysis. These were:

(1) A single-shaft simple-cycle gas turbine (designated SSS-10)
(2) A single-shaft regenerated gas turbine (designated RGSS-6)
(3) A single-shaft recuperated gas turbine (designated RCSS-8)

2. The SSS-10 has the best potential of meeting the 1976 Federal NO_x emission standards but careful combustor development is required to establish the fact. Heat exchanger engines inherently pose a more difficult problem from the NO_x emission standpoint and the combustor development program would be correspondingly greater. Federal standards for carbon monoxide (CO) and unburned hydrocarbons (UHC) are expected to be met by all three of the selected engines.

3. The single-shaft engines recommended require an advance in transmission capability to provide adequate driving characteristics. Several potentially eligible concepts are under study. It is important to ensure that engine and transmission developments proceed concurrently.

4. The gas turbine engines analyzed can be produced at a cost which would result in an automobile selling price on the same order as today's cars, and considerably lower than for a 1976 automobile powered with an emissions-treated Otto-cycle engine (OC-76). The SSS-10-powered automobile is expected to have the lowest cost.

5. Total engine-related lifetime cost predictions for 105,000 miles of operation are approximately the same for all three selected gas turbine engines. The lower capital and maintenance costs associated with the simple-cycle engine compensate for its higher fuel cost when compared with heat-exchanger engines.

6. The heat-exchanger engines exhibit superior fuel economy when compared with either the simple-cycle gas turbine engine or emissions-treated Otto-cycle engines. While the simple-cycle engine is predicted to fall short of the EPA goal of 10 miles per gallon over the Federal Driving Cycle, it may compare favorably with the emission treated OC-76. It is reasonable to postulate that future refinements of the first generation turbine-transmission combination will effect substantial improvements in fuel economy.

7. All three selected engines are compatible, in terms of size and weight, with the installation requirements of standard-sized automobiles. The simple-cycle engine has the greatest flexibility, due to its relatively small size and weight.

8. The design of the selected engines is based on advanced, but demonstrated, technology. The resulting high specific output (power-to-airflow ratio) leads to small size of critical components and consequently requires a minimum of high-cost materials. The high engine shaft speed associated with these high-work components is consistent with demonstrated bearing technology.

9. Of the three gas turbine cycles selected for detailed study, the SSS-10 offers the highest probability of meeting the Office of Air Programs goals for emissions and performance, and capable of being developed by 1975. The base-line engine is a simple-cycle, single-shaft engine rated at 130 hp, under standard conditions, utilizing a high-efficiency single-stage centrifugal compressor capable of a pressure ratio of 10:1, and a single-stage radial inflow turbine. Its performance is based on state-of-the-art technology and, while improvement in emissions is required relative to estimated levels based on current state of the art, it is highly probable that these can be achieved by 1975 if adequate programs are implemented.

10. A meaningful demonstration of the SSS-10 could be accomplished by 1975. The necessary concurrent transmission program requires further definition.

11. The "normal" period for introducing a novel concept into large-scale automotive production is on the order of 10 years. With sufficient impetus and support this time could probably be materially shortened. Again, the definition of such a program requires additional study.

RECOMMENDATIONS

1. It is strongly recommended that a high-priority program be initiated for the development and demonstration of the simple-cycle, single-shaft engine (SSS-10) defined herein. This recommendation is based on the prime result of this study that the SSS-10 is clearly the best solution for a low-emissions automobile powerplant, this engine offering the highest probability of meeting all systems requirements, including low cost, low pollution, and satisfactory fuel economy.

2. Concurrently with the engine program, a parallel study, with a subsequent development program, is recommended to define and demonstrate the optimum transmission(s) for the single-shaft engines defined herein.

3. It is recommended that a parallel engine development program be initiated for the development and demonstration of the RCSS-8 recuperated gas turbine, defined herein, to gain the advantage of superior fuel economy for those applications (such as trucks and buses) in which this characteristic is of prime importance, and also to allow for the possibility that an extraordinary future increase in fuel price may add significance to fuel economy. This program can have a somewhat lower priority than that for the recommended automobile engine because of the fewer numbers of applicable vehicles and consequent lesser pollution problems, as well as greater technological risk.

INTRODUCTION

Gas turbines for automotive applications have been considered for many years but, up until recently, they have been rejected as either too costly to produce or too expensive to operate. However, with increased emphasis on air pollution, their favorable emissions characteristics have stimulated more intensive investigation.

One such study was reported in Ref. 1* which was intended to determine if the application of new technology could result in a cost-competitive solution as compared with the cleaned-up Otto-cycle engine. In that study, a simple-cycle gas turbine was found capable of low emissions, superior performance (i.e., lower weight and volume for a given power output), adequate fuel economy, and competitive initial and lifetime operating costs. The significant technological innovation which contributed to this result was a highly efficient centrifugal compressor which, in a single stage, could produce pressure ratios high enough to achieve a cycle efficiency sufficient to avoid the necessity of regeneration, a feature which had been largely responsible for the high cost associated with the traditional approach to gas turbine design.

The simple-cycle design approach resulted in a small engine, relatively insensitive to design tolerances, which offered the possibility of low material and labor costs. While adequate substantiation was offered in Ref. 1 to lend confidence in the results, the limited scope of that study did not permit extensive optimization of the simple-cycle engine or a comprehensive comparison with all of the many gas turbine cycle options available. Consequently, a more detailed optimization of gas turbine alternatives, represented by the present study, was needed.

Accordingly, the objectives of this study were (1) to define the optimum gas turbine engine(s) capable of meeting the 1976 federal emissions standards and of being developed by the year 1975, and (2) to outline the research and development programs necessary to develop and demonstrate a selected optimum engine(s) by 1975 and mass-produce vehicles powered by such a low-emission engine at the earliest possbile date after 1975.

The study was organized into three sequential phases as summarized in Fig. 1. Within each phase, specific tasks are noted, but these were not necessarily time sequenced as shown, there being a strong requirement for iteration to account for interdependencies among the tasks. Phase I required the establishment of state-of-the-art technology to permit the estimation of realistic performance for all of the 60 gas turbine cycles initially considered. Out of a preliminary evalutation of these cycles emerged three candidates for detailed analysis.

*References are located beginning on page 241.

STUDY SCOPE

PHASE I – CANDIDATE SELECTION

- ESTABLISHMENT OF BASE-LINE TECHNOLOGY
- PARAMETRIC INVESTIGATION OF MANY GAS TURBINE CYCLES
- PRELIMINARY EVALUATION OF PROPULSION SYSTEMS
- SELECTION OF CANDIDATE SYSTEMS FOR DETAILED STUDY

PHASE II – CANDIDATE OPTIMIZATION

- PERFORMANCE ANALYSIS OF SELECTED ENGINES
- MISSION ANALYSIS
  - VEHICLE PERFORMANCE, EMISSIONS, AND FUEL ECONOMY
  - ENGINE INSTALLATION INVESTIGATION
- DEFINITION OF OPTIMUM CONFIGURATIONS
- PRELIMINARY DESIGN OF OPTIMUM CONFIGURATIONS
- ECONOMIC ANALYSIS
  - MANUFACTURING COST ESTIMATION
  - LIFETIME COST PREDICTION
- FINAL ENGINE SELECTION

PHASE III – PROGRAM PLANS

- OUTLINE RECOMMENDED DEVELOPMENT PROGRAM
- DISCUSS IMPLICATIONS FOR ENGINE PRODUCTION

Phase II involved the optimization of the three engines selected from Phase I for the detailed requirements of low-polluting automobiles as established by the Office of Air Programs. This phase involved very close coordination among the noted tasks since the optimization process was essentially iterative in nature. The optimization program included design, performance, and economic analyses of the selected configurations. Finally, Phase III involved the preparation of an outline of a development program for the most attractive of the gas turbine engines considered.

This report consists of a description and results of the tasks performed under each phase, and is organized in very much the same order as the above tasks are described.

ESTABLISHMENT OF BASE-LINE TECHNOLOGY

General

Early in the study of automotive gas turbines at United Aircraft Research Laboratories, it became evident that, to be competitive, a gas turbine engine must be based on advanced-technology components. Advanced technology in this regard is defined as the best demonstrated level of sophisticated aerodynamic, thermodynamic, and mechanical design capable of large-volume, low-cost production. The failure of a successful automobile engine to emerge in some 20 years of previous effort by various highly competent individuals and organizations can be attributed primarily to the level of technology represented by the components used in these efforts. Low component efficiencies and low stage work components coupled with low achievable peak pressure ratios have led to only one path of development for automobile engines, i.e., the examination of large heat exchanger areas in an effort to compensate for deficiencies in the flow path efficiency in seeking reasonable fuel consumption characteristics. Ref. 1 documents the high costs associated with this approach.

Since the objective of this study was to define the best engine for future OAP development programs, the engines studied herein were based on the best applicable advanced technology. A previous study had identified the advantages of this approach for both a simple-cycle and regenerated engine (SSS-12 and RSS-7 of Ref. 1), but it was far from clear whether or not an advanced regenerated, a recuperated, or a simple-cycle engine might be the optimum choice of advanced-technology engines. The method of approach for this study used comparable levels of component technology, supportable by test results obtained within UAC wherever possible.

Another significant constraint which affected the results of the study was that regarding the 1975 demonstration requirement. In order to minimize the technical risk, several compromises in the performance previously reported in Ref. 1 were made. Specifically, compressor test data were used directly from test results with little or no improvements assumed for 1975 performance. In addition, specific speeds of the engines were reduced, thereby resulting in reduced rotational speeds and specifications for stresses and bearings which more closely adhere to the current state of the art. The pressure ratio was also reduced for the simple-cycle engine, and a reduction of up to 100 degrees in maximum uncooled turbine inlet temperature (to 1900) was assumed. These compromises were made at the expense of increased size of the engine and resulted in a technologically less advanced engine than that postulated in Ref. 1. Consequently, there is no doubt that the engines described in this report represent state-of-the-art

FIG. 2

TYPICAL HIGH-PRESSURE-RATIO COMPRESSOR PERFORMANCE PREDICTIONS

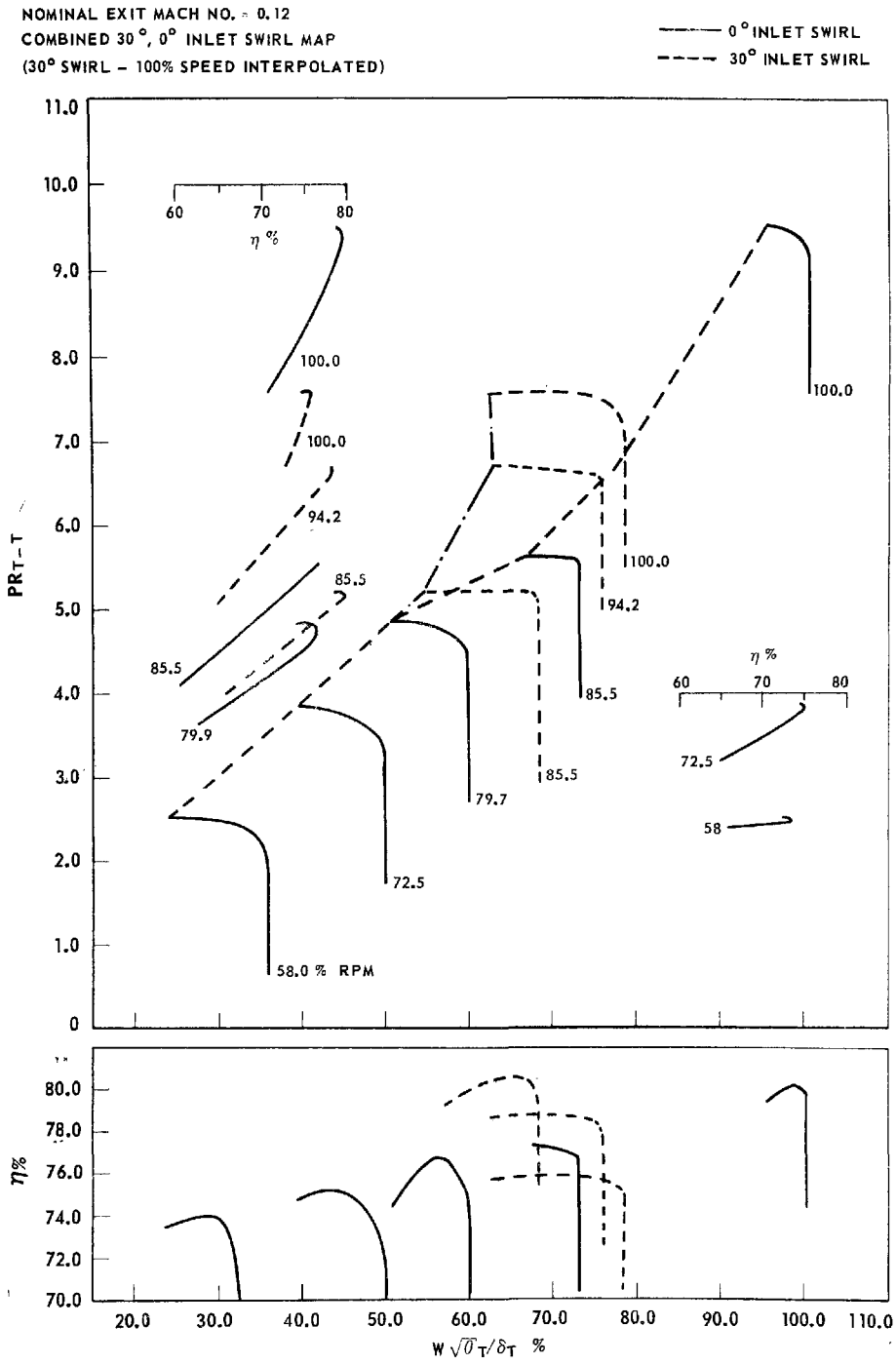

technology with no breakthroughs required to achieve the performance estimated, provided that a reasonable and thorough development program is followed.

A discussion of the base-line technology used for evaluation follows. Some design features examined for the base-line engines (such as internally cooled turbine blades) were eliminated in the Phase I review and, hence, did not enter into the detailed Phase II evaluation.

Compressors

The most critical component of a gas turbine engine (since it is generally the most difficult component for which to obtain advanced performance) is the compressor. United Aircraft Corporation has achieved a significant breakthrough in the area of small centrifugal compressor performance largely as a result of research conducted at UACL. Both rig demonstration and actual engine application of advanced centrifugal compressors have confirmed that these compressors, which feature UACL's patented pipe diffuser, are the most advanced in the world from the standpoint of efficiency, pressure ratio, flow capability, handling ease, and predictability.

An example of the performance believed to be achievable from these compressors is shown in Fig. 2. This compressor map is an estimate previously reported in Ref. 1, and is representative of those used for performance calculations in this study.

Single-Stage Design Point Performance

Figure 3 shows the relationship between stage efficiency (η_{T-S}) and stage total-to-static pressure ratio (PR_{T-S}) which was used for this study, at design poi The curve shows the predicted level available for engine demonstration in 1975 following a suitable research program. Because the time period for this research is short, UACL considered it advisable to assume only modest improvements over currently available technology. It is for this reason that this curve has an irregular form between 8 and 9.50 PR. It has been constructed from experimental data from series of tests on two different types of impellers, identified as the "F" and the "K" impellers. The "F" impeller incorporates prewhirl and the inducer is designed to be subsonic below about 5.5:1 pressure ratio, which also has the effect of reducing impeller loading. However, for a given pressure ratio, this approach results in higher diffuser entry Mach number, and as pressure ratio increases, this Mach number increases to the point where losses become significant. Above 6.0:1 the inducer also becomes supersonic, resulting in a

PREDICTED DESIGN POINT COMPRESSOR STAGE EFFICIENCY AND PRESSURE RATIO

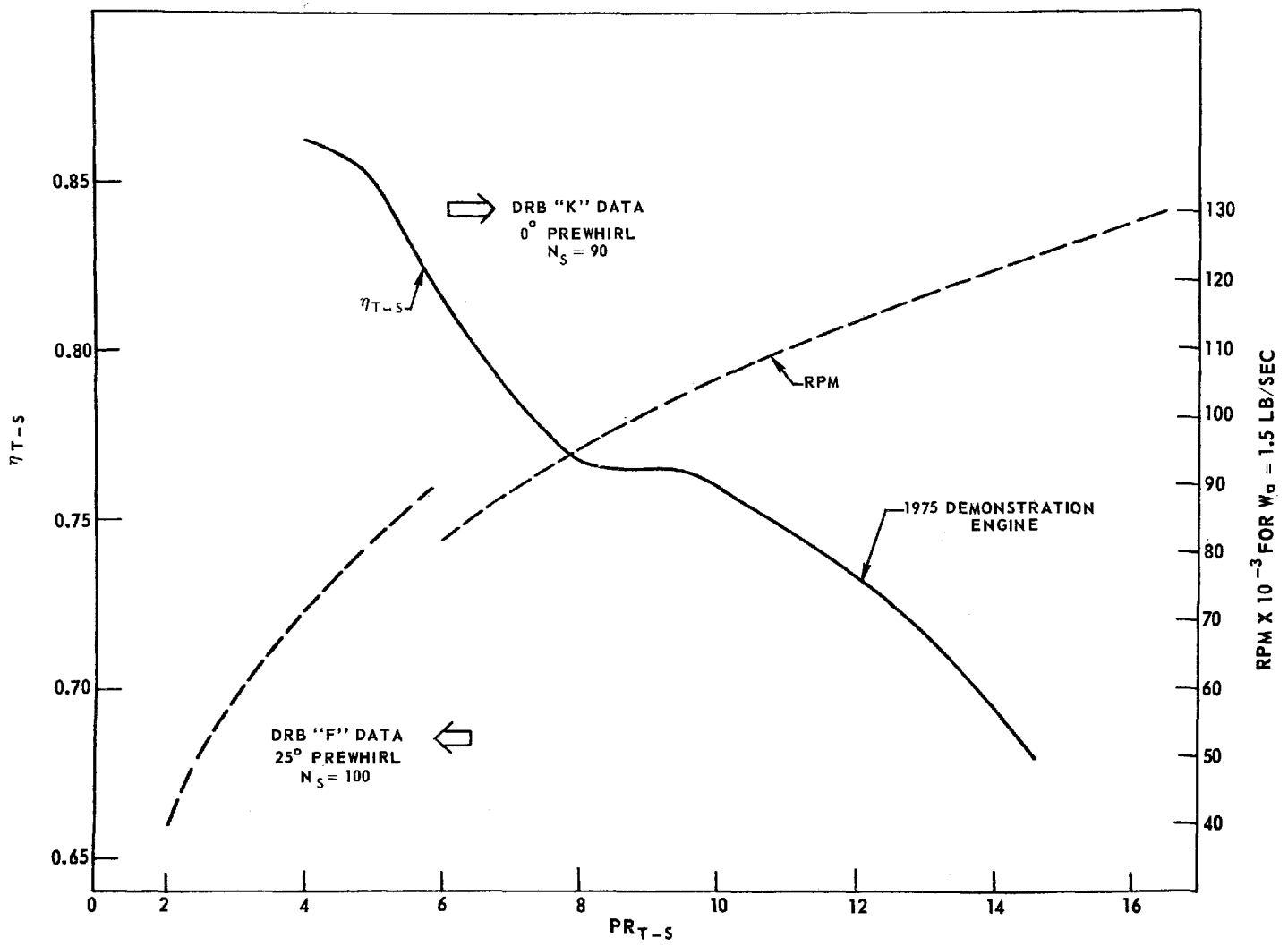

FIG. 3

fairly steep gradient in efficiency with pressure ratio. These effects are discussed in greater detail in Ref. 5 which includes test data on this class of impeller up to 14.0:1 pressure ratio. Substantial improvements are possible at high pressure ratio as the result of the development of supersonic inducers which give efficient impellers and reduced diffuser inlet Mach numbers. The potential performance of this class of impeller is represented by the right-hand branch of the curve, above 8.0:1 PR.

As a result of this approach, i.e., essentially assuming that demonstrated performance levels could be improved by roughly the same amount at all pressure ratios, the predicted efficiency levels reflect the variation experienced with current compressors. To remove the apparent "dip" in this curve between 8 and 9.5 PR would mean assuming that the efficiency at 8.0:1 PR could be increased by a further 4 points. It was considered unwise to assume that this could be done for a 1975 demonstrator engine.

Two-Stage Design Point Performance

The staging of two such compressors provides an excellent level of technology with which to investigate multispool engines. The point of maximum efficiency for each overall pressure ratio was found (Fig. 4) and the corresponding values of first-stage pressure ratio are shown in Fig. 5. As can be seen from Fig. 5, the optimum first-stage pressure ratio for a two-spool machine is approximately the square root of the overall pressure ratio.

In a single-shaft compressor, equal specific speeds would give a high first-stage pressure ratio, while equal pressure ratios would give a large difference in specific speed. Therefore, the shape of the efficiency vs. pressure ratio characteristic will establish two regimes. At low pressure ratios this curve is flat and the effect of specific speed will dominate (i.e., pressure ratio across the first stage, PR_I, will be high).

When the first-stage pressure ratio exceeds 4:1, the optimum will start to shift toward equal stage pressure ratios, and when both stage pressure ratios exceed 5:1 the effect of pressure ratio dominates and $PR_I \approx \sqrt{PR_{overall}}$. In Fig. 5 the two-spool curve is a simple transform of the single-stage characteristic while the single-shaft curve shows the effect of the further constraint on the stage specific speeds.

FIG. 4

OPTIMUM TWO-STAGE CENTRIFUGAL COMPRESSORS - OVERALL EFFICIENCY VS. OVERALL PRESSURE RATIO

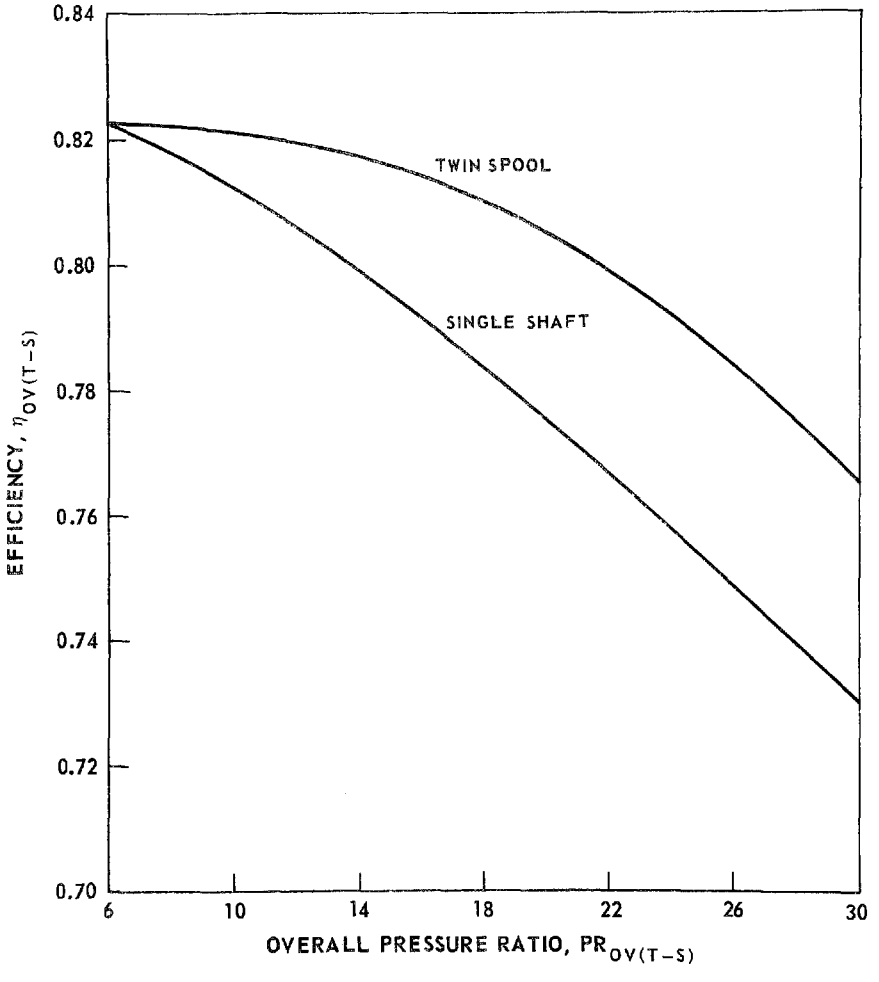

FIRST STAGE PRESSURE RATIO VS OVERALL PRESSURE RATIO

OPTIMUM CENTRIFUGAL COMPRESSORS

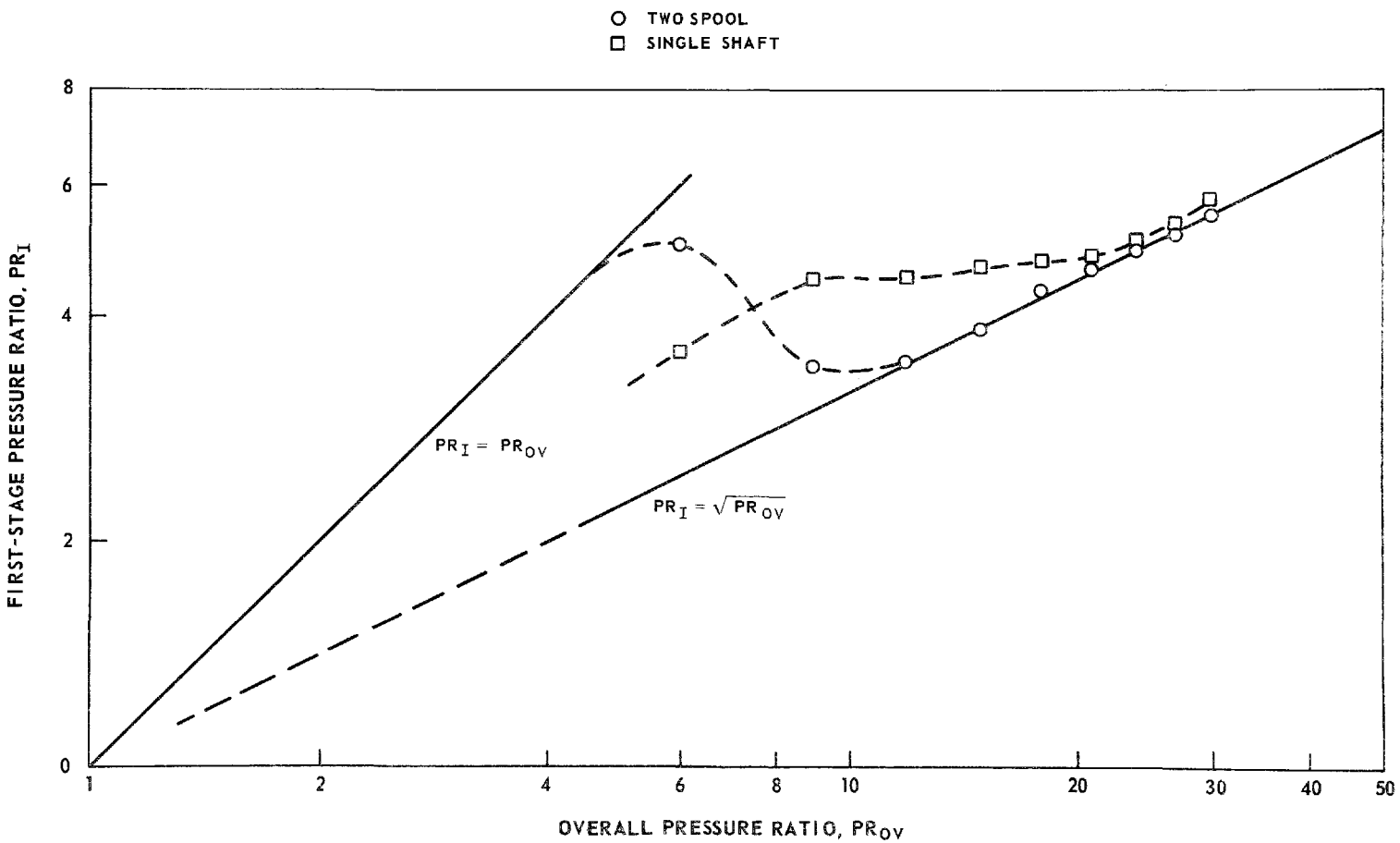

FIG. 5

FIG.6

AXIAL TURBINE FULL-POWER EFFICIENCY

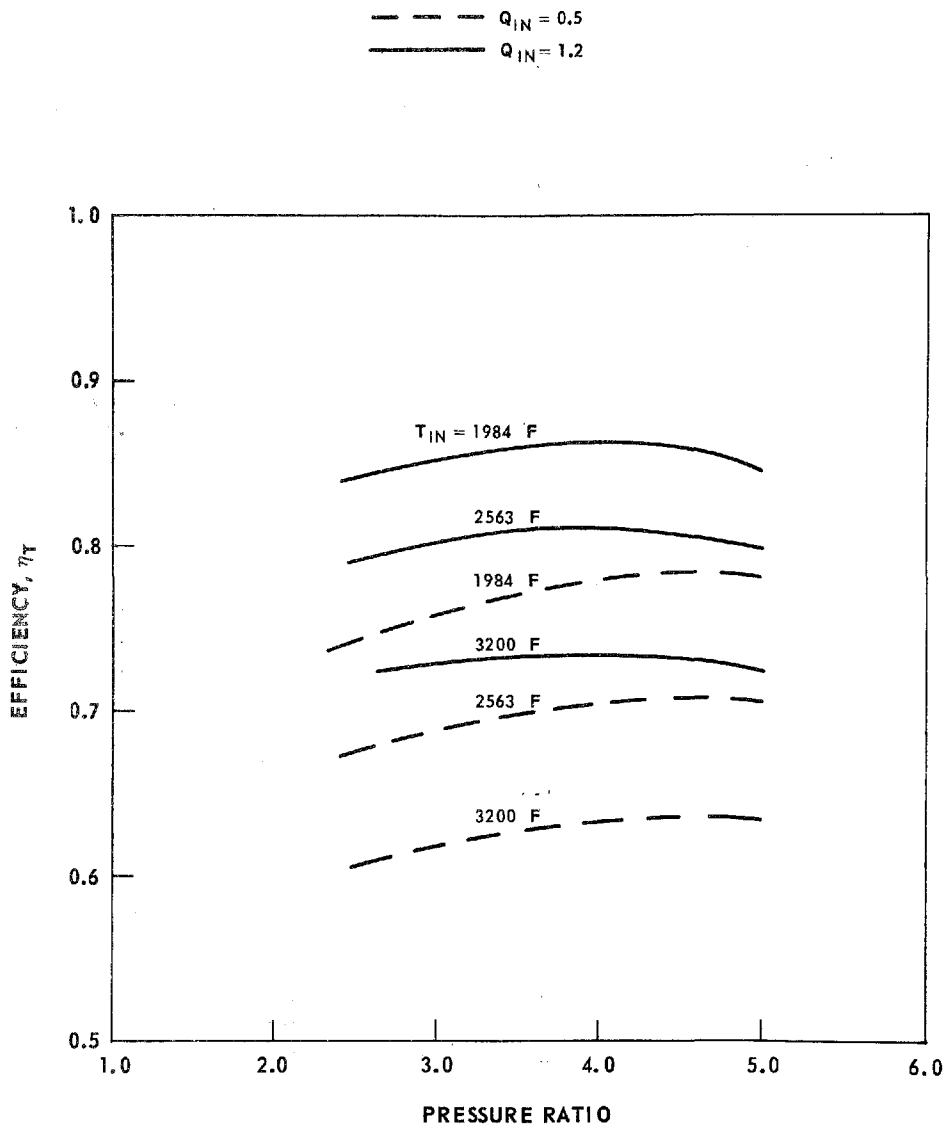

Turbines

The aerodynamic design of turbines at UACL is largely based on a fundamental analysis of fluid flow within the turbine flow passages. This approach was used for the design of the turbines for the original PT6 engines, and this sophisticated technique has been progressively refined since then with a series of uprated PT6 versions, the JT15D turbofan engine, research turbines, and advanced engine design studies. This emphasis on analytical design requires a continuing effort to refine design and analysis techniques. UACL has, since 1963, been engaged in a series of aerodynamic turbine research programs on both axial and radial turbines. Current axial turbine research at UACL is funded jointly by the DRB* and UACL, and is concentrated on high-work stages. A stage of 3.6 total-to-total pressure ratio is being tested along with a number of variations to establish design criteria for high-work regimes. The effects of cooling compromises such as low aspect ratio and thick trailing edges are being tested. Extended stage loadings were chosen for the present research program due to the potential for performance improvement in the high-work regime of small, cooled axial turbines.

Aerodynamic research on radial turbines has been carried out at UACL since 1963. A design point efficiency of 88.7% at 5.9:1 pressure ratio, and a peak efficiency of 90% at 7.15:1 pressure ratio were achieved on the first build of a test turbine early in this program. Results of turbine test work have been partially reported in Refs. 6 through 9.

The base-line technology data were selected to adequately cover the required turbine inlet temperature (TIT) range. Three levels were selected such that the first TIT would require no airfoil cooling; the second would require conventional amounts of convection cooling; and the last would require some advanced form of cooling. Two different sets of the flow parameter, $W\sqrt{T/P}$, were selected: two for axial turbines and another two for radial turbines. The philosophy followed in this investigation was to design the turbines aerodynamically for a part-load design point and then correct the information to maximum power conditions.

Axial Turbines

Preliminary designs and efficiency estimates were made for several single-stage axial turbines with different pressure ratios, turbine inlet temperatures, and inlet nondimensional flows. The results are shown in Figs. 6, 7, 8 and 9. From the inlet conditions and assumptions, turbine annuli were constructed and the airfoil numbers and chords were estimated. Stage efficiency estimates followed, including cooling air effects. For the lowest-TIT case, no airfoil

*Canadian Defence Research Board.

AXIAL TURBINE GAS TEMPERATURE RELATIVE TO BLADE MEAN SPAN

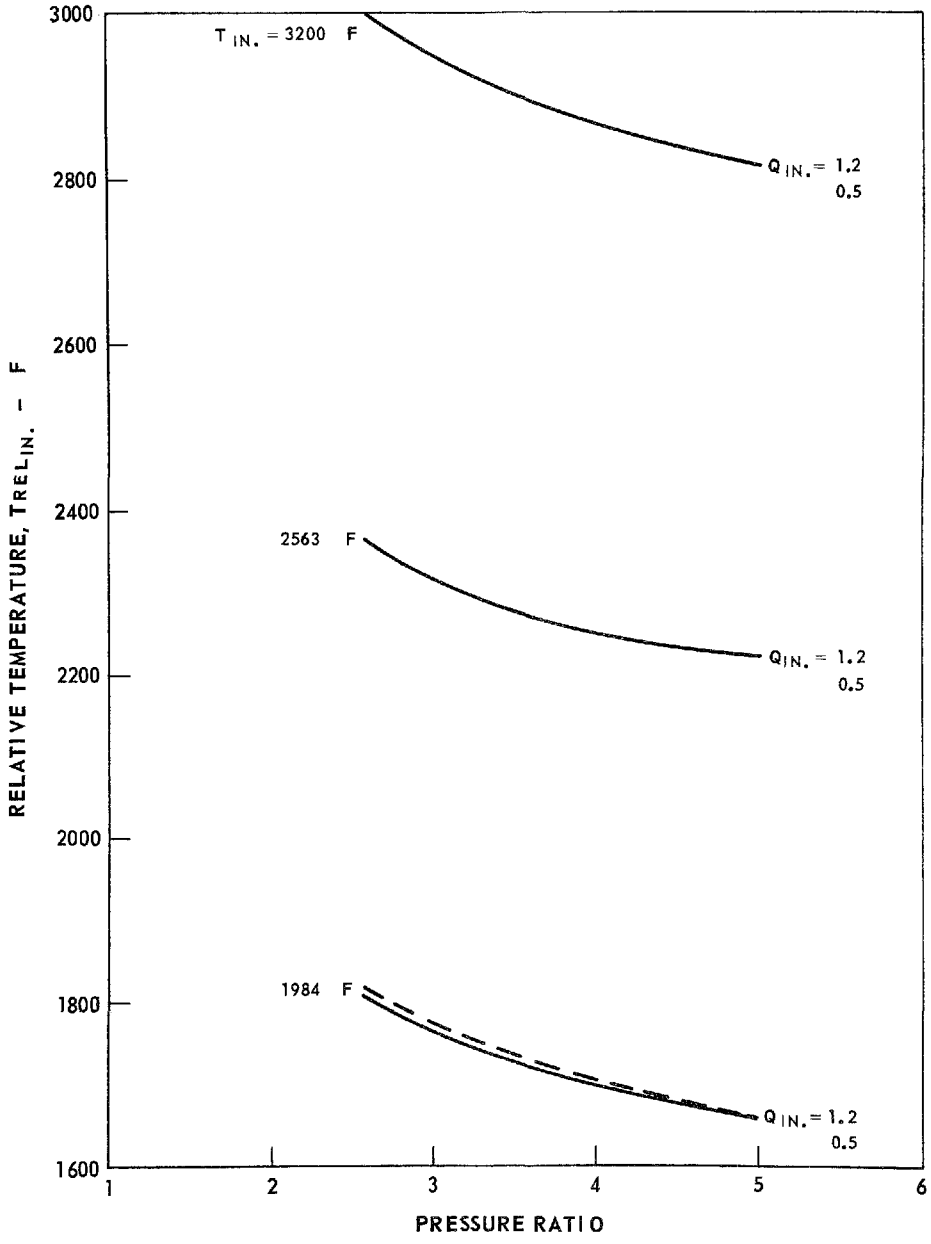

AXIAL TURBINE BLADE STRESS PARAMETER

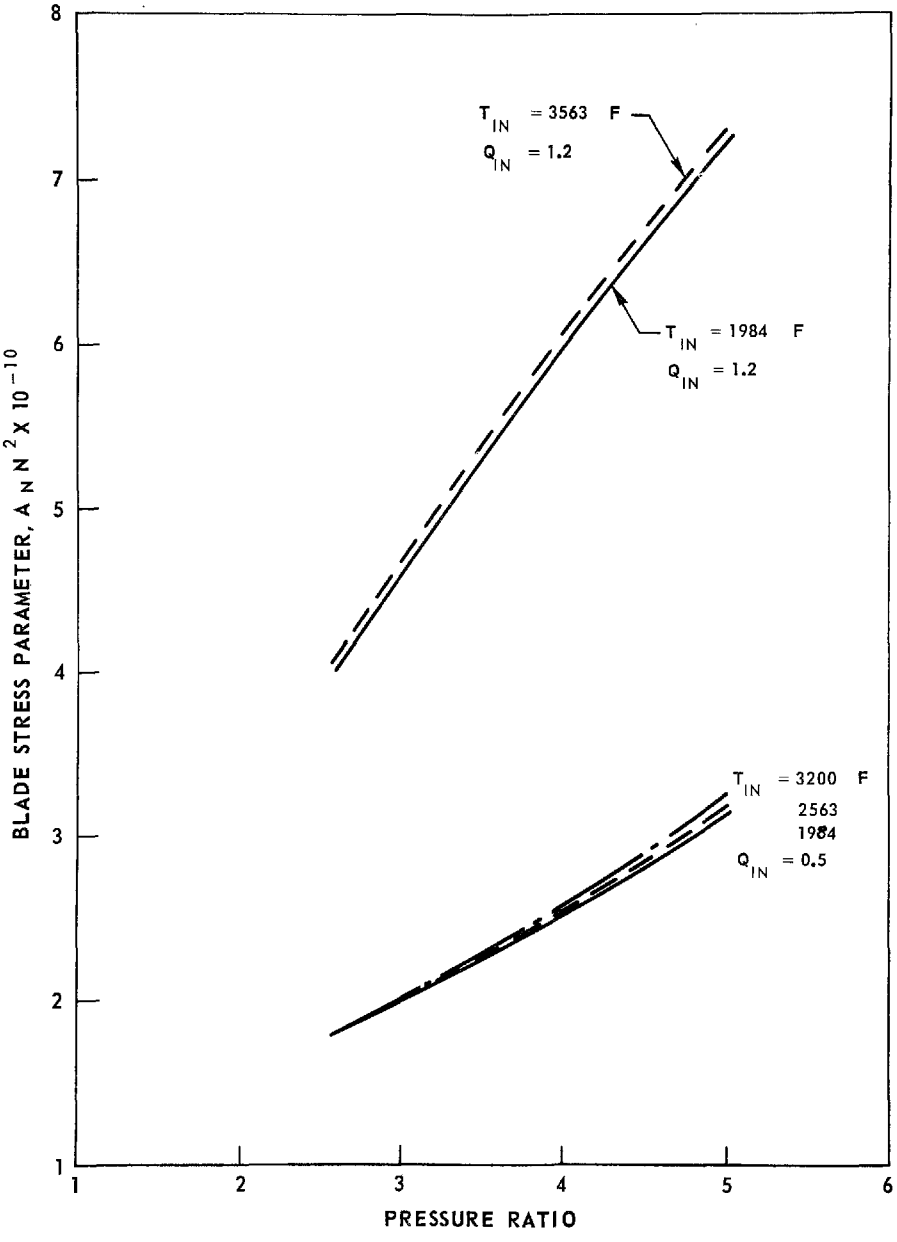

FIG. 9

RADIAL TURBINE EFFICIENCY AT FULL POWER

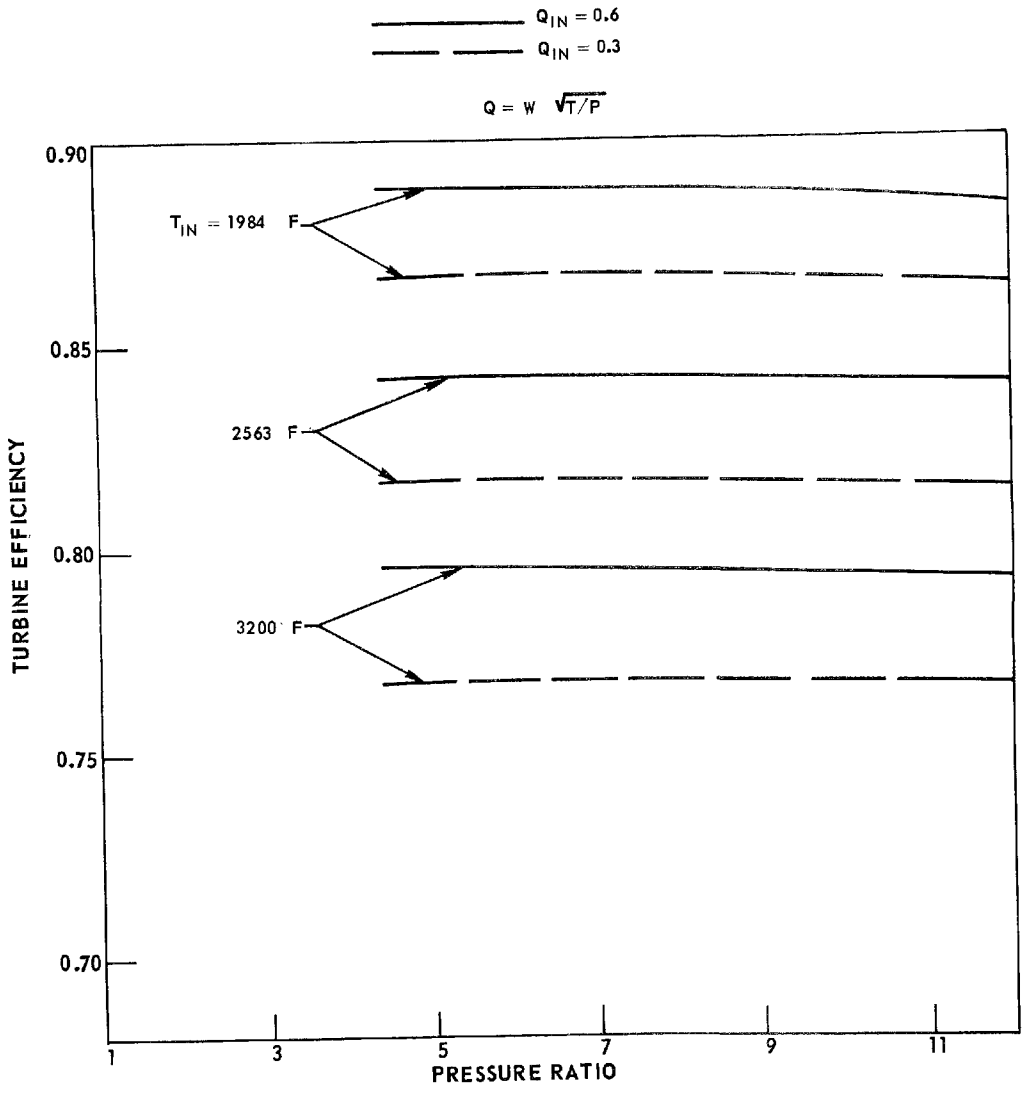

cooling was required. For the intermediate TIT, airfoil cooling was assumed with 1.5% of vane cooling air and 2% blade cooling air. For the highest-TIT cases, efficiency decrements typical of transpiration cooling were used.

The procedure for two-stage axial turbine designs was similar to the one described above. For the intermediate TIT, cooling of only the first stage was assumed, with cooling flows similar to those given above. For the case of the highest turbine inlet temperature, transpiration cooling of airfoils of both stages was assumed and the accuracy of information for the two-stage axial designs was of the same order as for the single-stage cases. The results are not shown in this report, since none of the designs which were selected for cycle analysis included the use of two-stage axial turbines.

Radial Turbines

For the small sizes under consideration in this study, radial turbine efficiency (Fig. 9) tends to be higher than that of an axial turbine designed to the same conditions. Because of the high cycle pressure ratios under consideration, the radial turbine was also an obvious choice since it is capable of higher expansion ratios. For this reason, major effort was applied to the radial turbine preliminary designs and efficiency estimations. The pressure ratio range investigated was from 4 to 12. In the process of this investigation, the efficiency estimation technique had to be revised to cover the cases with very low inlet nondimensional flows, very high pressure ratios, and very high inlet temperatures. The results are shown in Figs. 10 through 12.

Radial turbine off-design performance was predicted using Fig. 12. In order to use this figure, the following steps are used:

a. Calculate U/C_o' for the required off-design point, noting that $\Delta h'$ is the isentropic enthalpy drop

b. The upper curve is entered to find η/η_{DESIGN}

c. The lower curve is entered for the correction to η/η_{DESIGN} for the selected pressure ratio

d. Calculate η from the design point η_{DES}

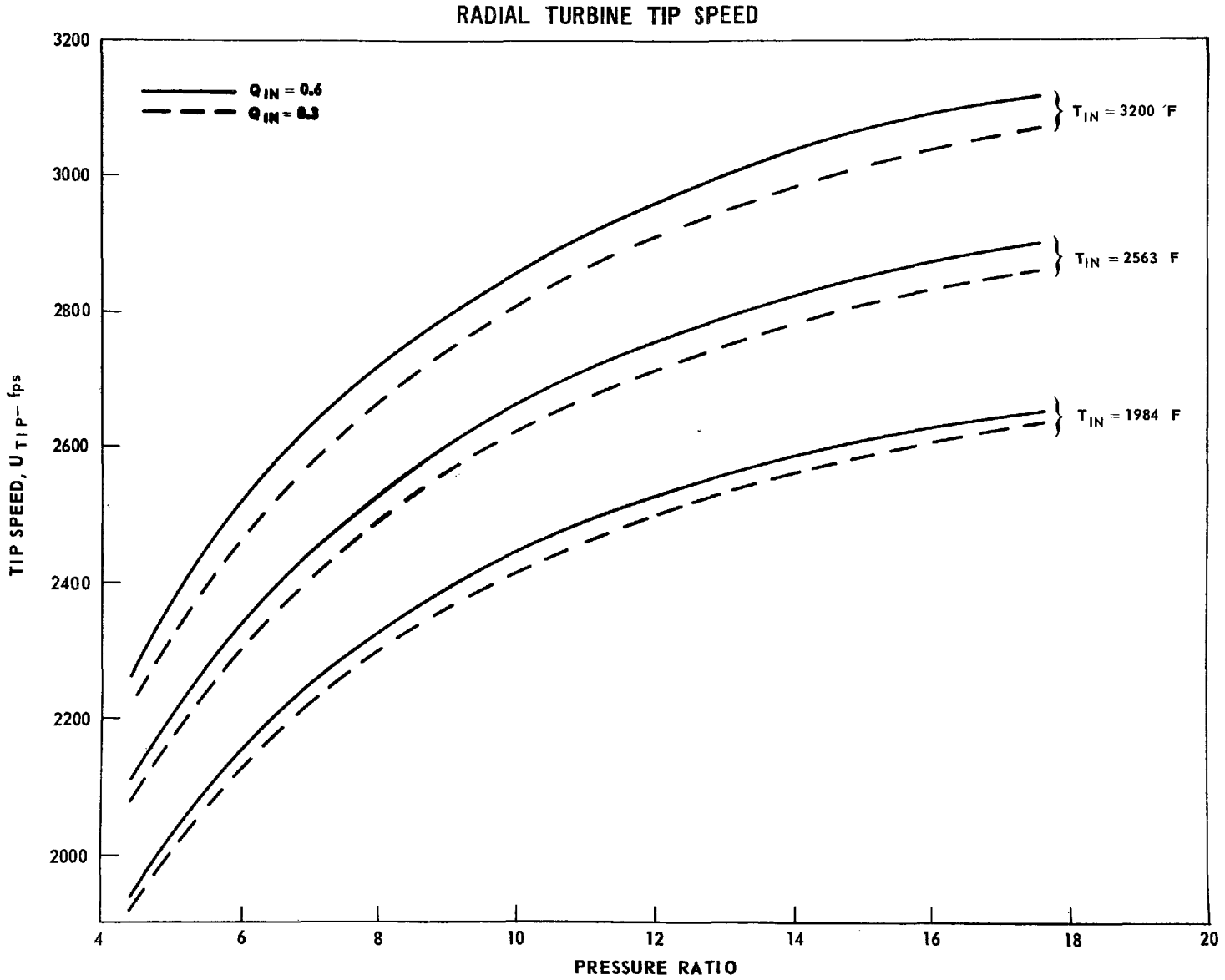

L-971249-7

FIG. 10

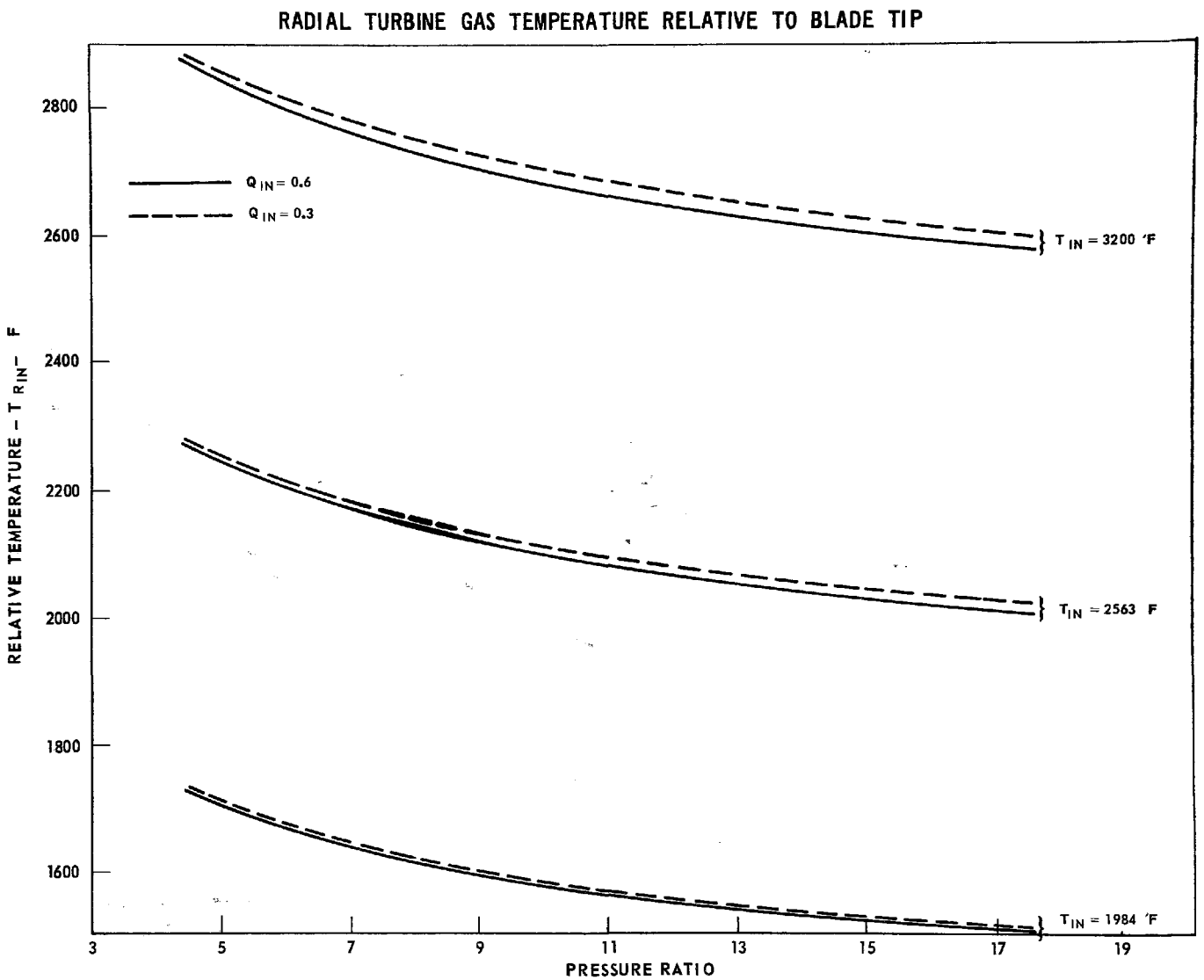
RADIAL TURBINE GAS TEMPERATURE RELATIVE TO BLADE TIP
RELATIVE TEMPERATURE – $T_{R_{IN}}$ – F
2800
2600
2400
2200
2000
1800
1600
Q_{IN} = 0.6
Q_{IN} = 0.3
T_{IN} = 3200 °F
T_{IN} = 2563 F
T_{IN} = 1984 °F
3
5
7
9
11
13
15
17
19
PRESSURE RATIO

FIG. 11

FIG. 12

RADIAL TURBINE OFF-DESIGN PERFORMANCE CORRECTIONS

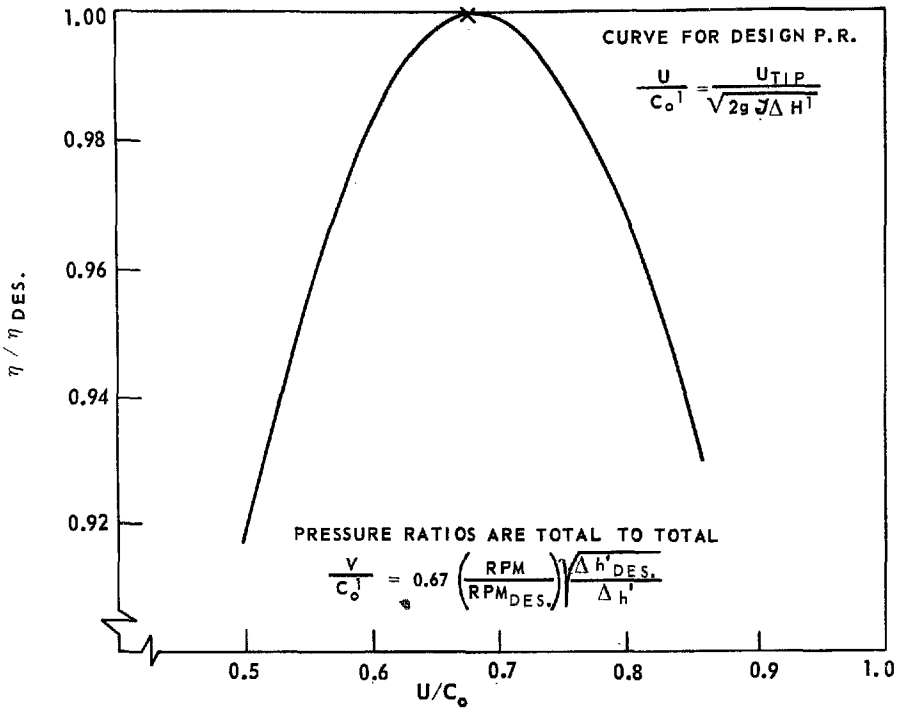

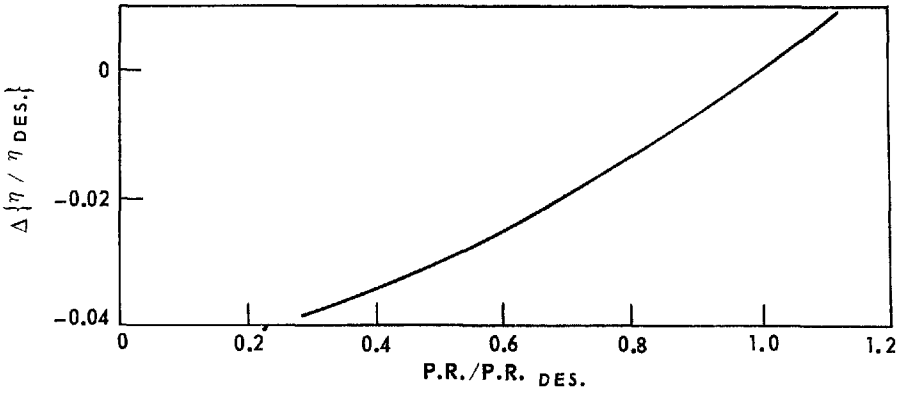

Stress Data

Axial Turbine Stress Limits

Stress limits for integrally cast axial turbines were developed to serve as a preliminary guide in the selection of feasible rotors. Figures 13 and 14 show the maximum allowable relative gas temperature at the blade mean section and the maximum rotational speed limits for various $A_A N^2$ blade stress parameter values, where A_A is the mean gas annulus area in square inches, and N is rotational speed in revolutions per minute. The material shown in Fig. 13 is IN-100, while Fig. 14 shows similar data for INCO-713 material.

If the rotors are solid with no bore, the rotational speed limits are indicated by burst requirements or rim low-cycle fatigue requirements. The data presented have been based on the following assumptions:

1. Design limits are for the maximum power conditions.
2. Rotors have a constant blade mean peripheral speed of 1350 ft/sec.
3. The blades are unshrouded.
4. The blade creep life is 150 hr.
5. The ratio of disc bore radius to rim radius is approximately 0.3.
6. The rotor burst speed margin is 1.2.
7. The disc fatigue life is 25,000 to 30,000 start-stop cycles.
8. The thermal stresses were assumed constant.

Radial Turbine Stress Limits

The maximum allowable relative gas temperature at the blade tip for the radial turbines is given in terms of the tip peripheral speed for various rotational speeds, as shown in Fig. 15.

The data presented in Fig. 15 are valid for the following design conditions:

1. Design limits are for the maximum power condition.
2. Material is forged Udimet 700 (PWA-689), which is believed to be the best for this application. Certain engine cycles may allow the use of cheaper materials.

AXIAL TURBINE STRESS LIMITS

MATERIAL IN-100

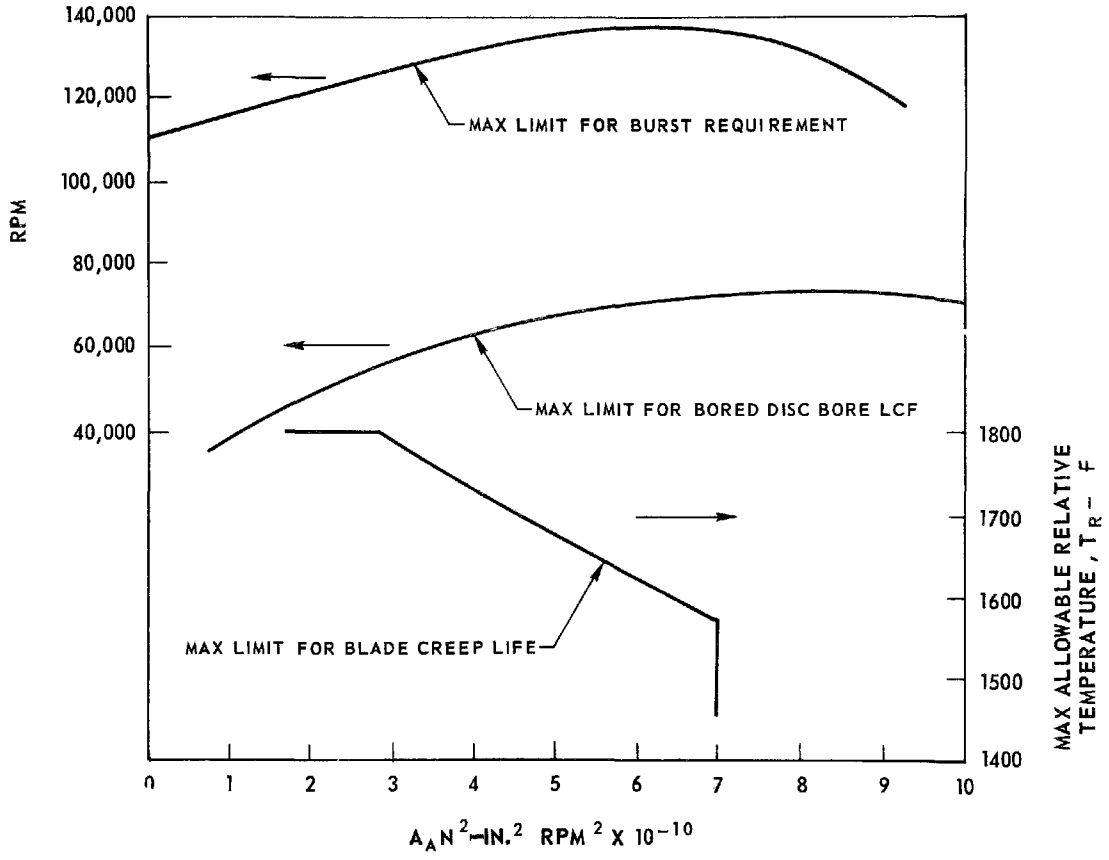

AXIAL TURBINE STRESS LIMITS

MATERIAL INCO-713

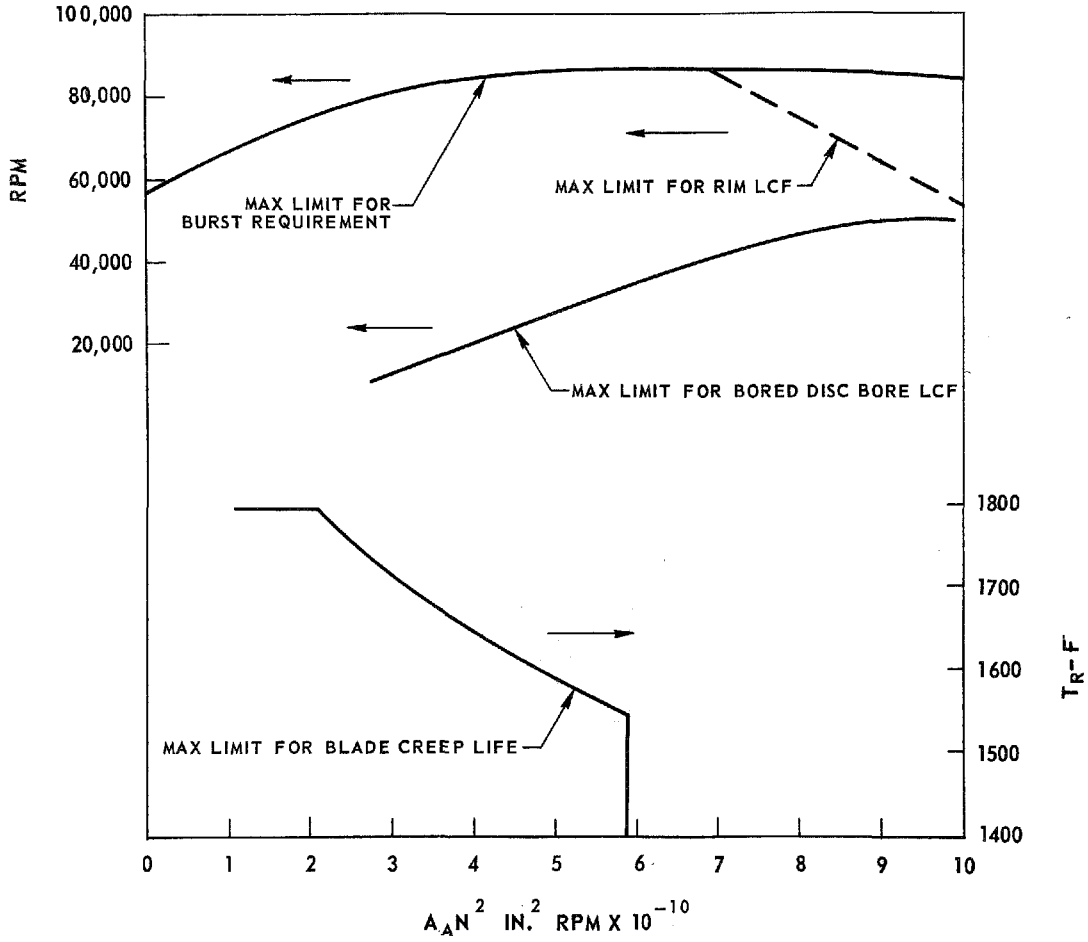

STRESS–RELATED TEMPERATURE LIMITS FOR RADIAL TURBINES

UDIMET 700

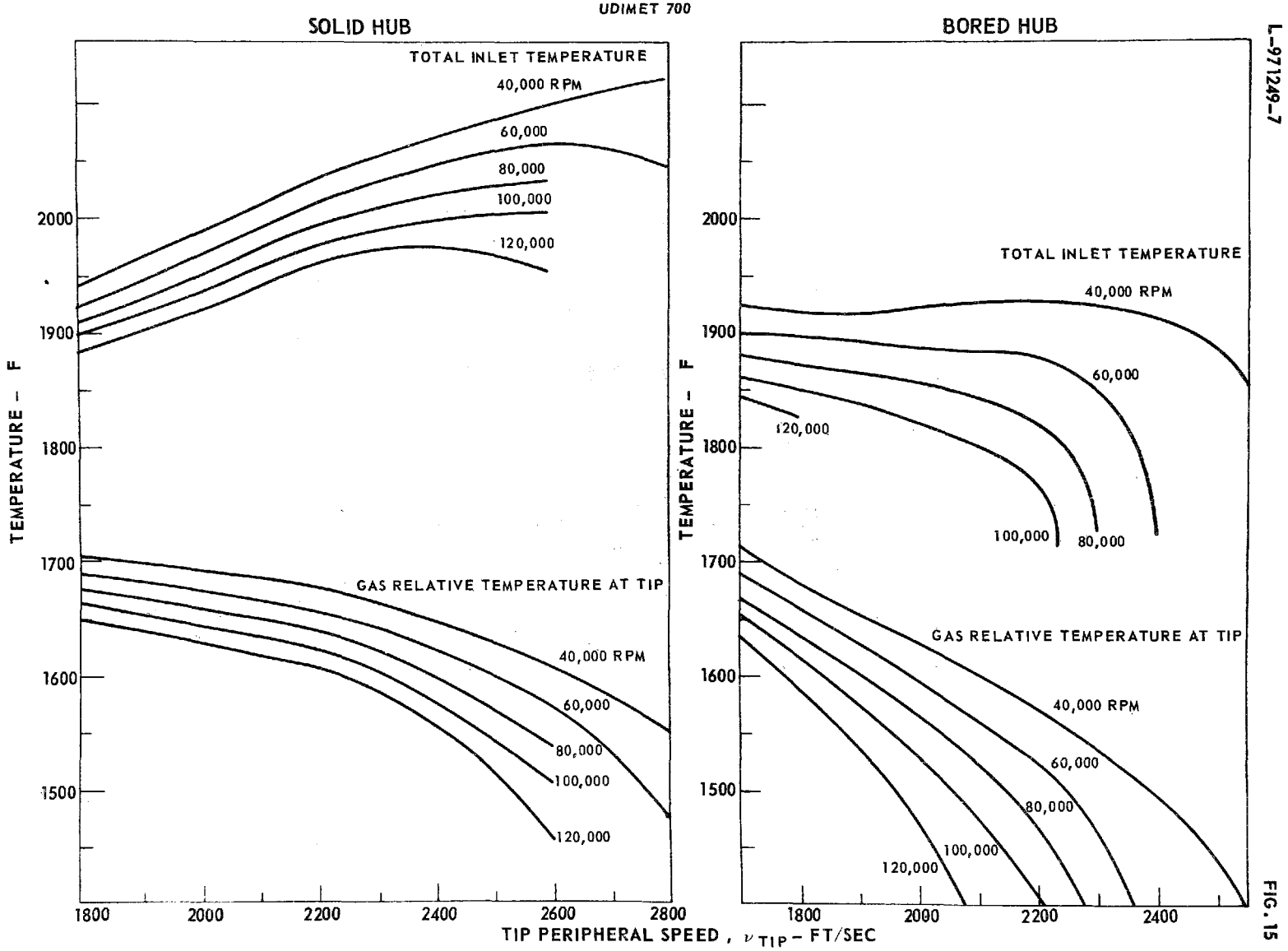

L-97149-7

FIG. 15

3. The blade creep life is 150 hr at design limit.

4. The hub ratio is selected to give maximum temperature capability, but was limited to a maximum value of 0.55.

5. The bore ratio for the bored hub is 0.2.

6. The maximum allowable theoretical strip analysis stress was kept at 125 ksi for the bore, 75 ksi for the rim, and 90 ksi for the blade root; presently these limits are believed to permit a fatigue life of 25,000 start, max. power, stop cycles.

7. The effect of blade tolerance is considered in the blade definition (tolerance $\pm$ 0.005 in. wavelength = 20% of tip radius). Nominal blade weight only is considered for disc stress calculation.

Turbine Blade Cooling

Because cooling air mass flow is a function of stress as well as temperature level, it has been correlated with the primary stress criteria. Other limitations due to high stress or high temperature must be established since there are major areas of concern regarding the combinations of high temperatures and high speeds, erosion of blade tip coating at high temperatures, requirements for relatively large cooling holes and small turbine rotors, and small-size effects on material properties and component strength. The limitations due to the low-cost requirement are difficult to establish. However, it was felt that this problem would be faced following the selection of engine cycles should the engines with cooling requirements appear to be particularly attractive. However, in no case was an internally cooled turbine selected for detailed analysis.

The cooling air mass flow was obtained from a cooling effectiveness correlation shown in Fig. 16 for which the material application and stress parameter have to be known. Materials which were considered for the automotive engine include: NX-188 and WI-52 for turbine vanes, forged Udimet 700 and cast IN-100 for radial turbine rotors, and cast IN-100 and INCO-713 for axial turbine rotors. The allowable temperature (T_{ALL}) to be used in the cooling effectiveness calculation is given here for typical designs. In the case of rotors, T_{ALL} has been correlated with the following stress parameters:

axial: AN^2, where: A is gas path annulus area, N is rotational speed; units are $\frac{\text{in.}^2 \ \text{RPM}^2}{10^{10}}$

FIG. 16

COOLING AIR FLOW VS COOLING EFFECTIVENESS

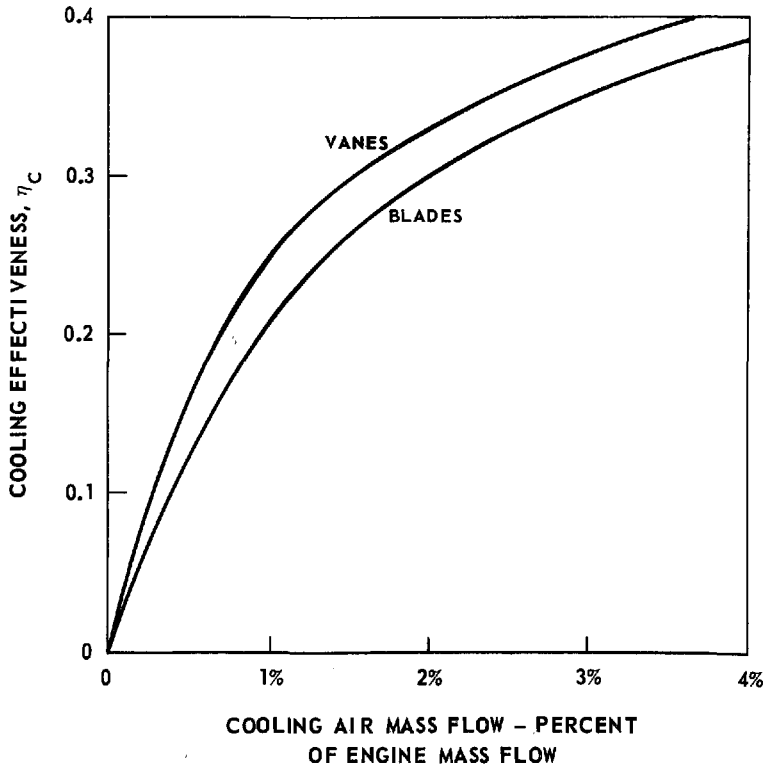

radial: U_T, Blade tip peripheral speed, (ft/sec)

Material	Application	Allowable Temperature T_{ALL}, deg F
NX-188	Turbine vane	1780
WI-52	Turbine vane	1750
UDIMET 700	Radial turbine rotor	$1710 - 57\ (U_T/1000)^2$
IN-100	Radial turbine rotor	$1770 - 57\ (U_T/1000)^2$
IN-100	Axial turbine rotor	$1810 - 45\ AN^2$
INCO-713	Axial turbine rotor	$1730 - 45\ AN^2$

The cooling effectiveness used in the cooling air mass flow determination was defined as follows:

for vanes $$\eta_c = \frac{TIT - T_{ALL}}{TIT - T_{CA}}$$

for radial turbines $$\eta_c = 1.25\ \frac{T_{RTIP} - 32\ \frac{(U_T)^2}{(1000)} - T_{ALL}}{T_{RTIP} - 32\ \frac{(U_T)^2}{(1000)} - T_{CA}}$$

for axial turbines $$\eta_c = 1.25\ \frac{T_{RMEAN} - T_{ALL}}{T_{RMEAN} - T_{CA}}$$

where: TIT = turbine temperature, F

T_{ALL} = allowable temperature, F (obtained from Table I)

T_{CA} = cooling air temperature, F (which is assumed equal to compressor delivery total temperature plus 100 degrees)

TABLE I

ENGINE CYCLE LOSSES

	SSS-10*	RGSS-6*	RCSS-8*
1. Intake pressure loss	1.3%	→	→
2. Primary burner pressure loss	3%	→	→
3. Duct pressure loss between turbine exhaust and heat exchanger	0	4%	→
4. Duct loss from turbine or heat exchanger to nozzle	3.3%	→	→
5. Nozzle loss	4.7%	→	→
6. Nozzle dump loss	1.2%	→	→
7. Reduction gearbox loss (ΔSHP)	4.23	→	→
8. Exchanger cold side Δp/p	0	0.0125	0.0057
9. Exchanger hot side Δp/p	0	0.0213	0.0231
10. Carryover flow loss	0	1.5%	0
11. Exchanger leakage flow loss	0	4.5%	0
12. Turbine leakage flow	1.0%	1.0%	1.0%
13. Bearing seal leakage flow loss	0.5%	0.5%	0.5%

*For definition of engine designationa, see p. 73

T_{RTIP} = total relative temperature at blade tip, F

T_{RMEAN} = total relative temperature at blade mean section, F

Cooling mass flows are obtained from correlation with the cooling effectiveness as plotted in Fig. 16 for static vanes and rotor blades. This correlation is applicable to simple convection cooling of small-size blades and vanes.

Engine Loss Data

The major losses which were factored into the engine performance program were estimated based on experience and detailed analysis of installation requirements. Table I shows the cycle losses which were included for the optimization portion of this study.

Heat Exchangers

Recuperator

Two candidate recuperator types were evaluated for the automotive engine application -- plate-fin and tubular -- and the tubular type was chosen. The main factors influencing the choice of an axisymmetric, tubular type were as follows:

1. Engine Layout. The axisymmetric heat exchanger possible with the tubular type allows for more compact, low-loss ducting, particularly in the turbine exit diffuser. This duct will be much more tolerant of the large swirl variations which it will have to accept. The plate-fin exchanger does not lend itself readily to this configuration, and would require the exhaust stream to be split into discrete flows feeding rectangular heat exchangers. These split ducts would have larger losses and bulk than the design chosen, thereby tending to minimize the advantage in compactness normally associated with plate-fin heat exchanger matrices.

2. Heat Exchanger Durability. Cyclic thermal stresses affect all heat exchangers. Experience at Hamilton Standard Division (HSD) with the plate-fin type has shown tendencies for progressive increases in leakage as the closure joints crack open under this cycling. This problem is aggravated by the additional restraints at the corners of a rectangular-section heat exchanger. The best

AXISYMMETRICAL TUBULAR RECUPERATOR

SINGLE PASS – HOT

DOUBLE PASS – COLD

2140 TUBES, 0.012 IN. O.D.

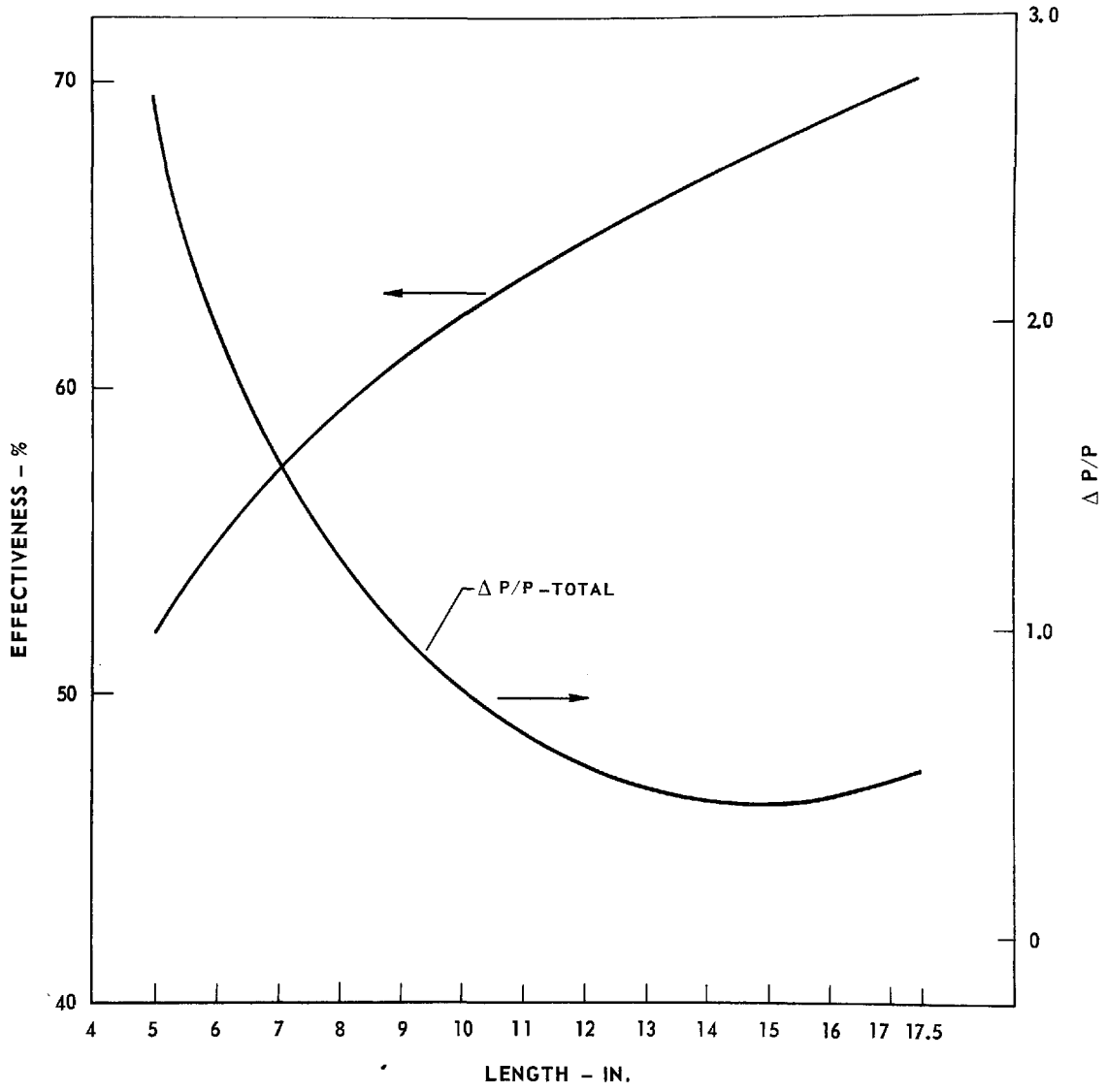

solution to this problem at present is to use material with good cyclic fatigue properties. The tubular type appears to suffer much less from these difficulties. The braze joints will not tend to open up under the pressure loads; thus, even if cracked this should not exhibit much leakage. Furthermore, the annular headers can be arranged to float radially inside the engine casing, thus eliminating a large source of thermal stress. This feature opens up the prospect of a cheaper material for the tubular exchanger.

3. Manufacturing Cost. The potential manufacturing cost of a plate-fin exchanger is apparently relatively low. However, experience with actual production at HSD shows that it is extremely difficult to avoid leakage at the closure joints on newly brazed parts. This difficulty must be resolved at low cost for the plate-fin design to be acceptable. The major difficulty for the tubular heat exchanger is the cost of the tubes themselves. The solution to this problem may be some form of helically wound strip welded or brazed into tubes and drawn, if necessary, to the finished size. The other fabrication problems do not appear to be too difficult. No clear distinction can be drawn between the fabrication cost of these two types, but the possibility of less expensive materials for the tubular type may provide some cost savings.

The disadvantage of the axisymmetric tubular recuperator is its somewhat larger matrix size when compared to a compact plate-fin type. This disadvantage is somewhat offset when the volume of the entire recuperator, including headers and ducting, is considered; nevertheless the practical effectiveness of the tubular recuperator is probably limited, for the automobile application, to values of less than 70%. The variation of effectiveness with recuperator length is presented in Fig. 17. It is noted that, for the recuperator considered, it is necessary to double the length (from 8.5 in. to 17.5 in.) to increase effectiveness from 60 to 70%. In the optimization portion of the study, it was initially attempted to design the recuperator for an effectiveness of 70%; however, it soon became apparent that packaging and installation problems, and the increased manufacturing cost, could not justify the relatively small gain in fuel economy (approximately 1 mile per gallon) for the higher value of effectiveness.

Regenerator

The heat exchanger of the rotary type considered (regenerative) was considered to be of the CERCOR® ceramic configuration. Data entered into the program are shown in Fig. 18 and Table II. These data were supplied by the manufacturer, Corning Glass.

Although metallic-matrix rotary regenerator cores have been used for truck-type engines, their material cost precludes serious consideration in

FIG. 18

f AND j FACTORS FOR CERCOR MATRIX HEAT EXCHANGER

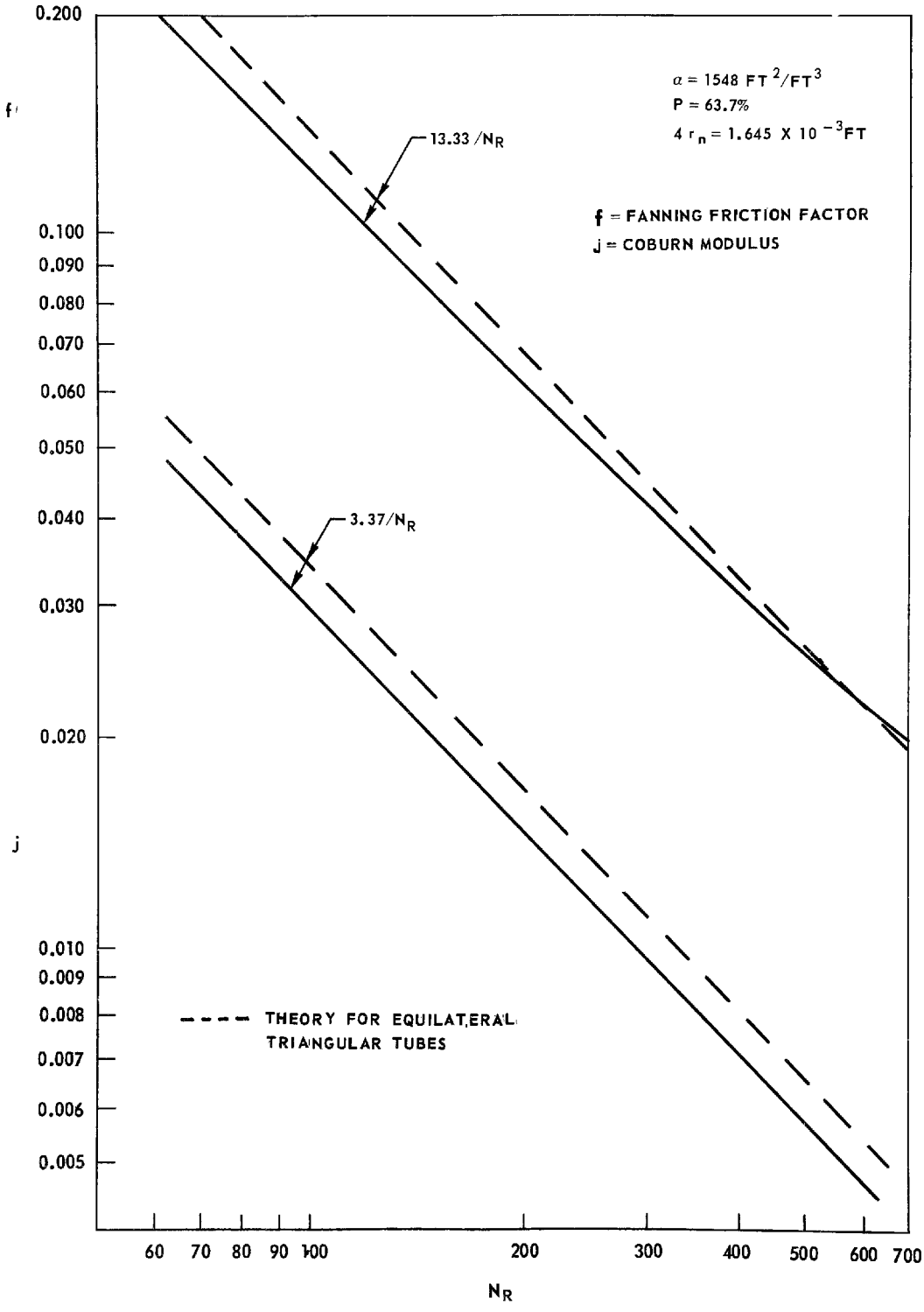

TABLE II

HEAT EXCHANGER CORE GEOMETRY FOR DATA REDUCTION

(Single-Blow Transient Technique)

Core Designation	507 (Corning 22-02*)	Date: 6/4/68
Core Mass	0.8964* (406.6 grams)	
Core Dimensions	width 3.312 in. height 3.296 in. length 2.830 in.	
Core Volume	30.892+ $in.^3$	
Solidity	0.3633	
Porosity, p	0.6367	
Area Density, α	1548 ft^2/ft^3	
Heat Transfer Area, A	27.67 ft^2	
Frontal Area, A_{fr}	10.92 $in.^2$	
Flow Area, $pA_{fr} = A_c$	6.95 $in.^2$	
Hydraulic Diameter, $4r_h$	0.001645 ft	
L/r_h	575.2	
Specific Heat, c	0.200* Btu/(lb-F)	
Density, solid, ρ	138*+ lbm/ft^3	
Thermal Conductivity, k	0.42 Btu/(hr ft-F)	
Conduction Area, A_k	3.97 $in.^2$	
Number of Cells per $in.^2$, N	1041.6+	
Cell Height/Cell Width, d/c	0.853+	

* Manufacturer's specifications

\+ Inputs for p, α, and r_h evaluations

automobiles. Another ceramic material for this application is provided by Owens-Illinois, but its properties are very similar to those of the Corning Glass material for engine cycle analysis purposes.

Transmissions

The transmission is the power-train component which provides the torque flexibility required for proper operation of an automobile. The selection of this unit is primarily influenced by the engine torque/speed characteristics. An internal combustion (IC) automobile engine can provide high torque over most of the engine speed range and therefore requires gear-ratio changes (torque multiplication) only for starting from a standstill. The free-turbine gas turbine engine also has relatively high low-speed torque. Consequently, a standard three-speed automatic transmission can be used, with or without a torque converter, or a manual shift could be employed.

The single-shaft gas turbine has torque characteristics which make the selection of a transmission an acute problem. The full-load torque decreases rapidly as speed is reduced until, at 50% rated speed, the engine produces no appreciable torque at all. Therefore, the transmission must provide considerable torque multiplication over the entire speed range to make the single-shaft gas turbine suitable for an automobile.

Previous studies had identified the extreme importance of the transmission in determining the engine characteristics and the output of optimization studies. Therefore, considerable emphasis was placed on the selection of proper base-line technology transmissions. The transmission analysis for this study is directed mainly toward identifying and determining the operating characteristics of those units which may be suitable for a single-shaft engine.

Geared Systems

Geared systems provide torque multiplication via a set of gears which are alternatively meshed or demeshed to provide discretely stepped gear ratios.

Slipping-Clutch System

The simplest mechanical device is a multigeared stepped transmission, such as an 8-speed unit suggested by Borg-Warner and examined for single-shaft automotive gas turbines in Ref. 1. This unit incorporates a controlled, mechanical, slipping clutch which is fully engaged and disengaged within a relatively narrow engine

speed range. The clutch permits transmission of a constant engine torque (determined by clutch input speed) at any clutch output speed up to and including input speed. The shifts would occur automatically, governed by throttle setting and road speed, in a fashion similar to that employed in current automotive transmissions. The rate of deceleration of the slipping clutch during upshifts is assumed to be controlled at a rate sufficient to assure passenger comfort. Figure 19 illustrates a steady-state horsepower/speed profile for the 8-speed gearbox with a 150-hp simple-cycle gas turbine. Similar data are shown for an equal-output spark-ignition (SI) engine with a three-speed torque converter automotive transmission. Considering the shift points from a steady-state standpoint, for both systems, there is a large torque (horsepower) mismatch which needs to be smoothed. From steady-state considerations, the average power for the 8-speed transmission up to 60 mph is about 106 hp, but transient analyses indicate the availability of a substantially higher average power, as shown in Fig. 20. Here, the effects of engine inertial energy are seen to increase the average power to about 120 hp for the conditions analyzed.

As presently conceived by Borg-Warner, the shifting control will be a function of engine speed and vehicle speed, and not dependent on road load as in current transmission practice. Thus, the shifts take place at the same speeds, regardless of throttle setting.

The slipping clutch must have sufficient life to avoid costly and frequent repairs, and it is the Borg-Warner belief that this durability is current state of the art. However, the torsional vibration associated with a pure mechanical system may not be damped to any significant degree. The cost of an 8-speed transmission consisting of a standard four-speed automatic gearbox preceded by a two-speed planetary splitter and a controlled slipping clutch may not be higher than present automatic transmissions with torque converters. In addition, efficiencies should be high for this completely mechanical system. The weight of such a unit is still somewhat uncertain since detailed designs have not been executed, but is estimated to be less than 200 lb for a 150-hp engine.

Fluid-Coupling System

An alternative to the slipping clutch for this transmission may be a fluid coupling. The first major advantage would be extremely long lifetimes with little maintenance. Secondly, a fluid coupling is an excellent "shock absorber" and greatly reduces torsional vibration transfer to the passengers.

If the fluid coupling were located between the turbine and the transmission, a variable-fill system could be incorporated for starting from a stop. At idle,

FIG. 19

POWER VS SPEED

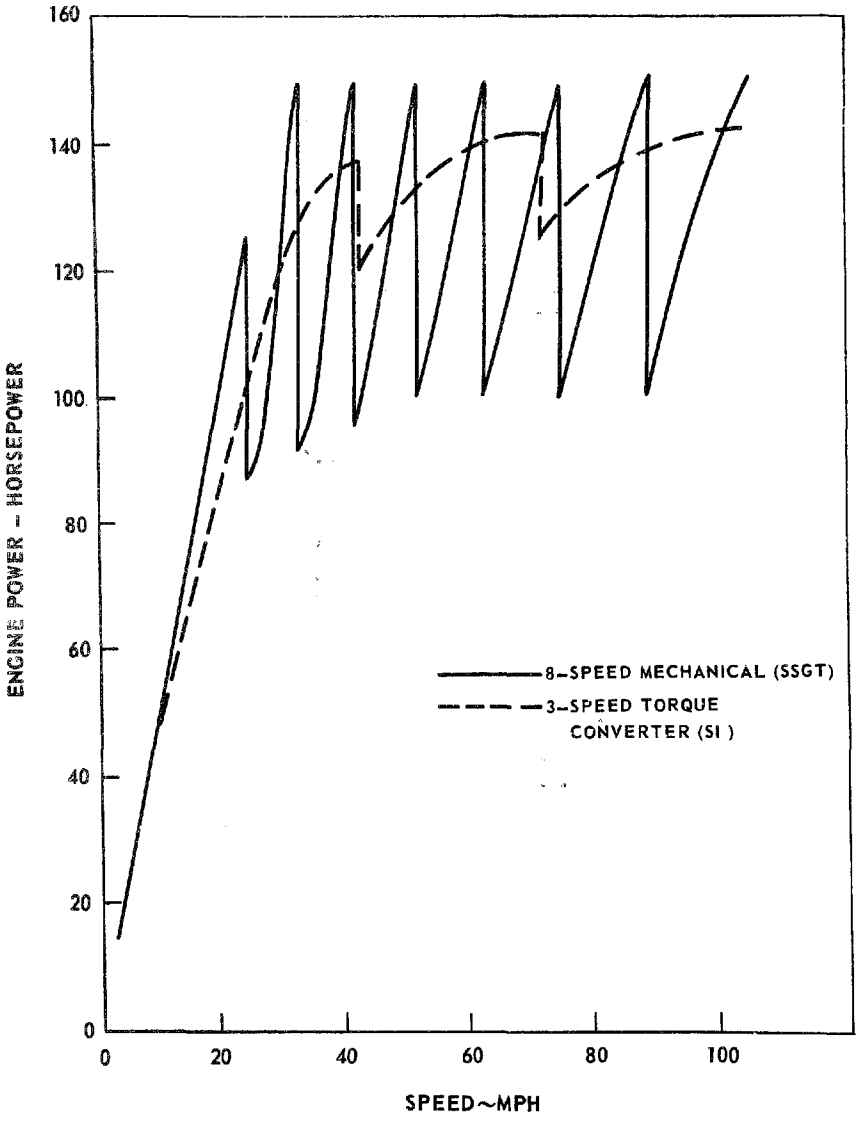

PERFORMANCE OF SINGLE-SHAFT GAS TURBINE WITH BORG-WARNER 8-SPEED TRANSMISSION

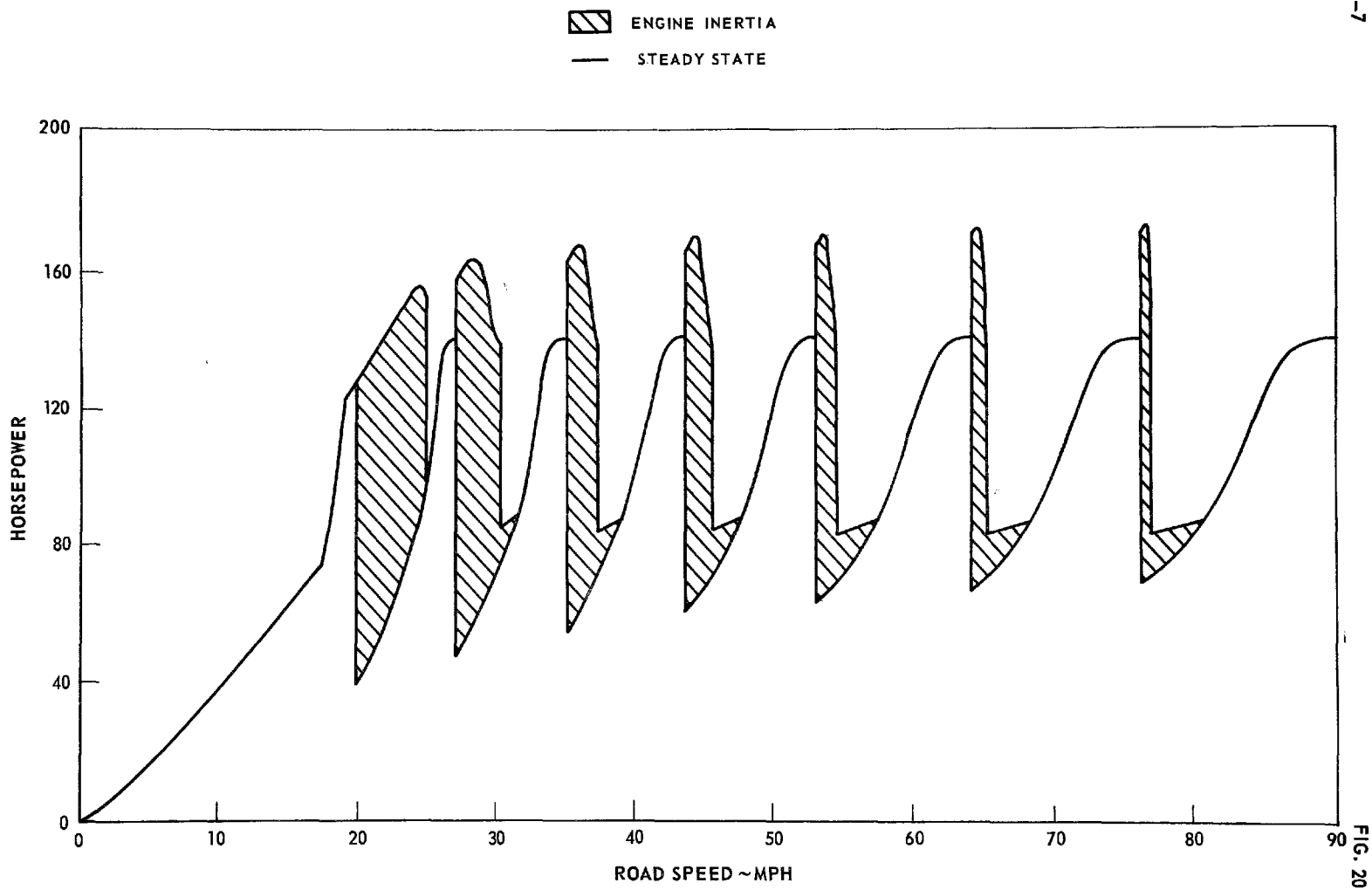

L-971249-7

FIG. 20

ELECTRIC-DRIVE SCHEMATIC

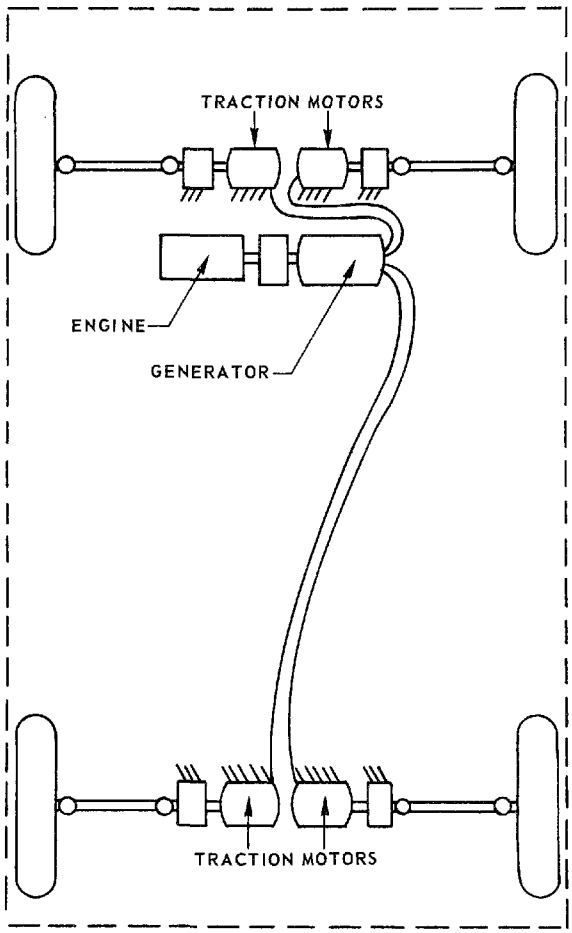

the coupling would be sufficiently empty to avoid automobile "creep." As the accelerator is depressed, the coupling would fill at a rate which would vary with throttle setting and road load. Thus, wheel spin could be avoided from a standing start at full throttle. At part throttle, the coupling would fill rapidly to provide maximum available torque to the transmission. At high slip ratio, the power loss through the coupling is converted to heat which tends to break down the coupling fluid. However, the variable-fill system would incorporate an external oil reservoir, which would also act as an oil cooler. Partially-filled fluid couplings have a tendency to "foam" under high slip conditions, thus greatly reducing efficiency. Therefore, the coupling should be as near full as possible.

If the coupling were located behind the transmission, it would experience the combined speed range of the engine and transmission, thus possibly eliminating the need to reduce the fluid level at idle since the torque transmitted varies as the square of the input speed.

Since the fluid coupling transmits torque at a maximum of 98% efficiency, its overall efficiency would approach that of a mechanical clutch. Also, the coupling would probably be cheaper than the clutch, but the added oil reservoir/cooler unit and pumping system would result in an overall higher cost.

Electric Drive

Rather than to rely on high gear ratios to achieve high torque multiplication at low speeds, other systems might be incorporated which have the desired characteristics. One such system is electric drive. Here, the gas turbine drives a generator (or alternator) which produces electrical power to drive traction motors which are connected to the vehicle's wheels (Fig. 21). The controlled-speed traction motors allow the engine to operate near peak efficiency at all times, since engine speed is not a function of road load. Electric-drive systems have been successfully used for off-road equipment where great flexibility is required, and where cost and weight considerations are secondary. In these applications, four basic types of electric motors have been used -- shunt and series-field d-c motors, a-c induction motors, and a-c synchronous motors. D-c motors generally have good speed control but are speed-limited due to the brushes and commutator. A-c motors can operate at higher speeds and are more rugged than d-c motors but are more difficult in speed control.

The costs of electric-drive systems used to date have normally been quite high, due primarily to low production rates. Also, the components have been heavy and bulky to a degree which has made an electric-drive system appear infeasible

FIG. 22

A-C INDUCTION MOTOR WEIGHT CORRELATION

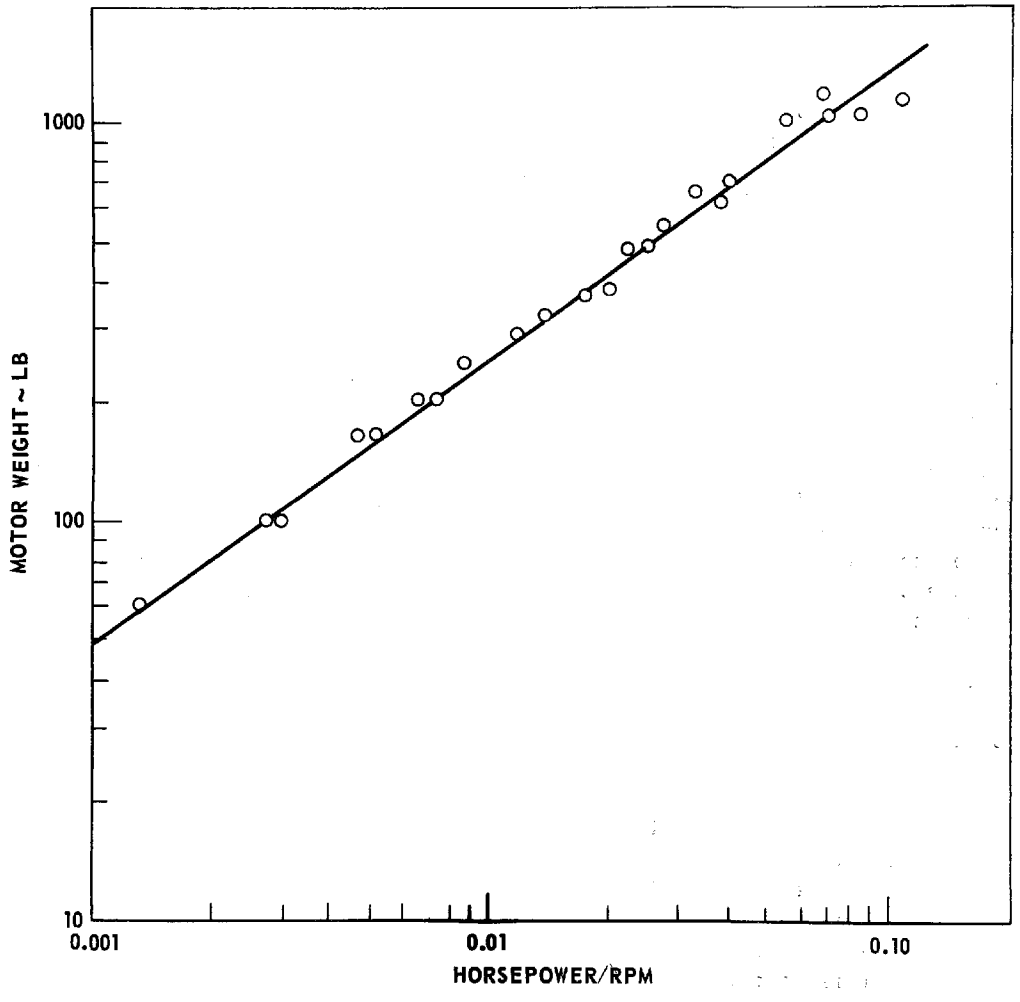

for an automobile. As an example, assume two electric traction motors are used, each rated at 50 hp and 3000 rpm. Figure 22 indicates that each would weigh about 300 lb and have a retail cost of about $450 at low-volume production rates. A conventionally-sized 100-hp generator, which is driven by the gas turbine, may weigh 600 to 700 lb and cost about $1000. While these prices could be greatly reduced if millions were produced annually specifically for the automotive market, a redirected technology to design lightweight units for automotive use would appear to be a necessary first step.

Recent developments in electric-drive systems indicate that significant advances could be made in system weight and performance. Delco-Remy Division of General Motors has tested a high-speed a-c drive system in a 2 1/2-ton truck (Ref. 10). The traction motors are brushless, self-synchronous units which have torque and speed control characteristics much like a d-c motor. They are electronically commutated as a function of rotor position, thus eliminating rotor windings, the rotor commutator, and brushes. The motor can be operated at high speeds (17,000 rpm) and also provide high continuous torque (essentially constant hp). These high-speed units should result in significant weight reductions. It is estimated that a 50-hp motor would weigh less than 100 lb and have a retail cost of about $200 at smaller production rates than is normal for automobiles. Likewise, the alternator can be similarly designed and would be estimated to weigh under 200 lb and cost $500.

Similar developments have been advanced by the Pratt & Whitney Division of United Aircraft for d-c systems (Ref. 11). Rather than eliminate the brushes and commutator, the design of these elements was improved to the point where rotational speeds of 15,000 rpm were successfully run on a 30-kw prototype unit. This unit weighed only 112 lb. It is estimated that a 50-hp mass-produced unit could be designed to weigh about the same.

The Solar Division of International Harvester has developed a small 10-kw turbo-alternator on a common shaft which operates at 100,000 rpm. Similar technology would allow a single-shaft gas turbine and alternator to be used for an electric-drive automobile.

It appears that significant advances could be made in electric-drive technology for automotive applications if a directed effort were to be made. Possibly the high-speed alternator (or generator) would weigh no more than today's transmissions, and the traction motors and control systems would weigh no more than the drive shaft, differential, and axle they would replace. The control systems have been estimated to cost about $20/kw on a high-production basis and may approach $2/kw for automobile production rates.

FIG. 23

EFFICIENCY OF GENERAL ELECTRIC HYDROMECHANICAL TRANSMISSION

$$\eta = 0.80\left[1-(1-P)^{12}\right]\left[\text{SIN}^{1/3}\left(\frac{N\pi}{2P^{0.366}}\right) + 0.10\ \text{SIN}\left(\frac{N\pi}{P^{0.366}}\right)\right]$$

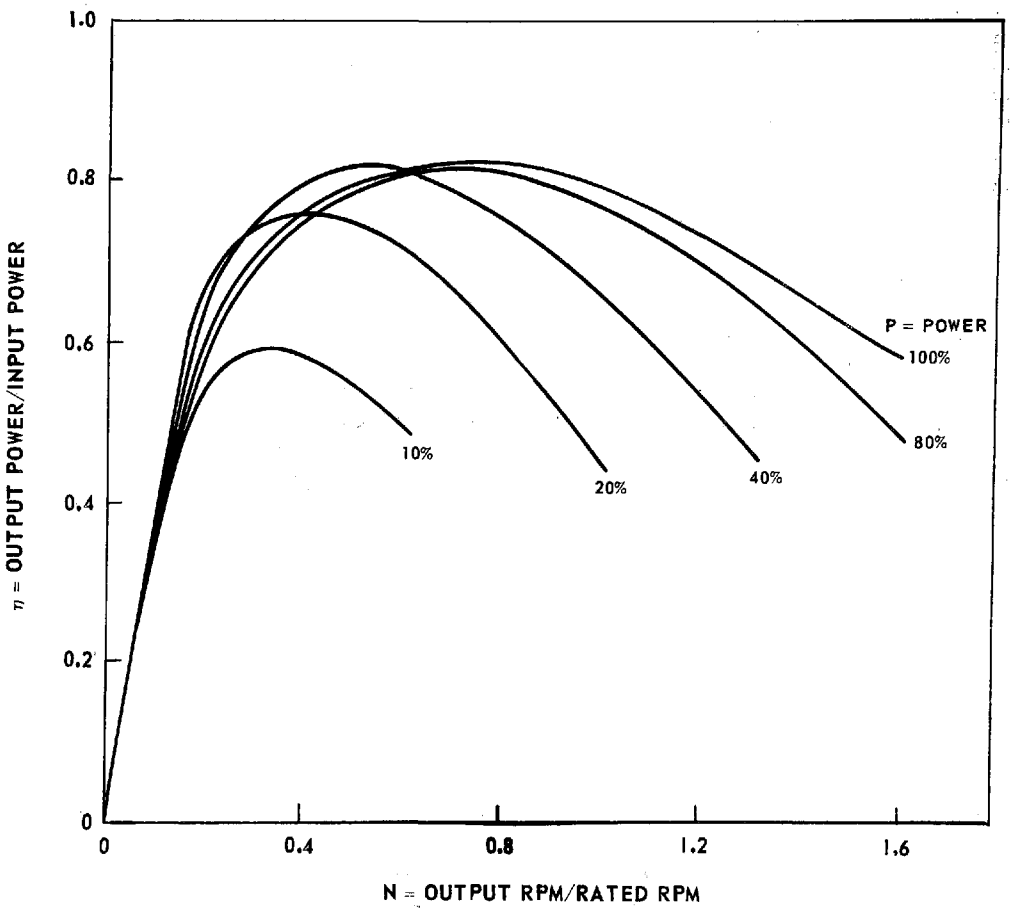

Hydrostatic Transmissions

Pure hydrostatic transmissions have been tested in automobiles for years, but the systems have suffered from hydraulic noise, low overall efficiency (~80%), and appear to be subject to speed limitations (approximately 5000 rpm maximum). They have also been heavy and somewhat bulky.

The pure hydrostatic system can be greatly improved by combining it with an epicyclic gear system to produce a transmission which has higher efficiency and greater versatility than the basic system. These hydromechanical transmissions (HMT) are sometimes called "split-torque" transmissions in which the input torque is divided between the hydraulic system and the mechanical gear train. One hydraulic unit is attached to the input of the transmission system; the other is geared (or attached) to the remaining planetary shaft which does not connect to the output. Depending on load conditions, either hydraulic unit may act as a pump or motor.

Another variation is the "split-speed" system in which one hydraulic unit is attached to the output and the other is attached to the floating member of the planetary gear system.

A third type employs two planetary gear systems where each hydraulic pump is attached to the floating member of one of the planetaries. From Ref. 12, it appears that the split-speed and double-planetary systems can provide efficiencies of 90% over a wide speed range. However, the split-torque configuration would probably be the cheapest because of simplicity.

All HMT's allow a smooth, infinitely variable change in gear ratio and allow the engine to operate near peak efficiency.

The literature suggests that the gear systems coupled with the hydraulic pumps and controls will be quite expensive, even on a mass-produced basis. The hydraulic noise problem must also be solved, along with weight reduction. However, conversations with General Electric personnel indicate that a hydromechanical transmission can be produced as cheaply as a modern torque-converter transmission and would probably weigh less. The potential noise problem remains to be resolved. However, GE has isolated the source of the major contributors to noise in its HMT and has redesigned its units, although absolute noise levels have yet to be measured. Figure 23 presents efficiency characteristics for a General Electric HMT with an 8.7-cu in. capacity. The equation shown on the figure very closely represents test data derived from this unit.

FIG. 24

TORQUE CONVERTER CHARACTERISTICS

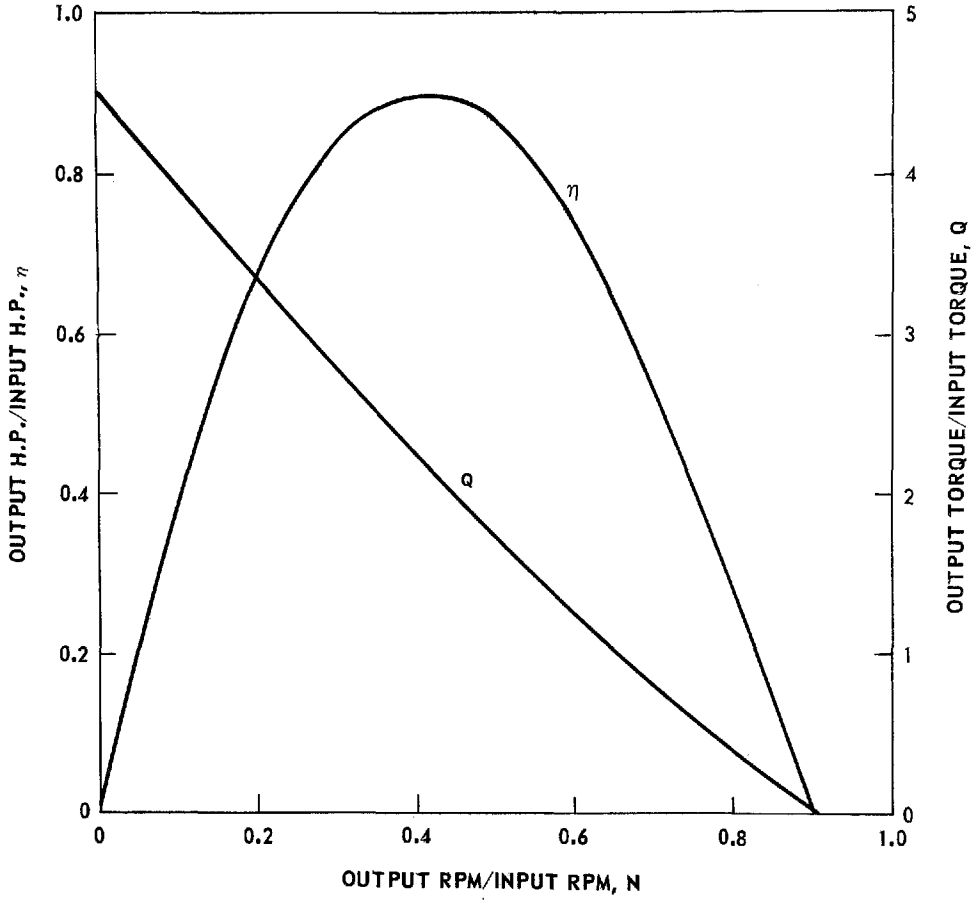

Sundstrand Corporation has also built hydromechanical transmissions for large trucks and is currently preparing to market its unit for the trucking industry. This transmission is a dual-mode configuration (DMT) which incorporates two internal clutches. These clutches allow the DMT to operate in a pure hydrostatic mode at low speeds and then shift to a hydromechanical mode through a planetary gear system. This system would allow higher part-load efficiencies than the HMT and better full-load performance at somewhat greater expense. This unit, as now marketed for the trucking industry, is too expensive for automobiles and weighs 675 lb.

Hydrokinetic Transmissions

A pure hydrokinetic coupling (fluid coupling) does not provide torque multiplication but merely transfers torque. However, a torque converter (TC) similar to those used with today's automatic transmissions can multiply torque as much as 5-to-6:1 at stall. Thus, the torque converter may be adaptable to the single-shaft gas turbine. If so, its low cost due to fully developed technology and manufacturing techniques, plus its high reliability and relatively good efficiency, would make it a good candidate. Several authors (see Ref. 13, for example) have suggested the torque converter for use with single-shaft engines and have shown preliminary data to support their positions. However, these authors considered only the torque-multiplication ratio and efficiency variations as a function of output speed (or slip ratio). For various slip ratios, the input torque was multiplied by the torque multiplication factor to obtain output torque. This approach in essence assumes that the torque converter is infinitely small; i.e., there is no retarding torque which tends to reduce input speed. Simultaneously, it assumes the torque converter is infinitely large and can absorb whatever torque is applied to it.

Actually, one must examine the torque absorption characteristics of the converter and match these with the engine output torque over the entire speed range. The converter must be sized and matched to a specific engine power level. Converters are often characterized by a set of curves of torque multiplication factor (Q) and efficiency (η) vs. output/input speed ratio (N), as shown in Fig. 24. Since efficiency (η) is defined as output/input horsepower, it can also be defined as the product of N and Q, i.e.,

$$\eta = \frac{hp_2}{hp_1} = \frac{(\text{torque})_2\ (\text{output speed})}{(\text{torque})_1\ (\text{input speed})} = QN$$

FIG. 25

TORQUE CONVERTER-ENGINE CHARACTERISTICS

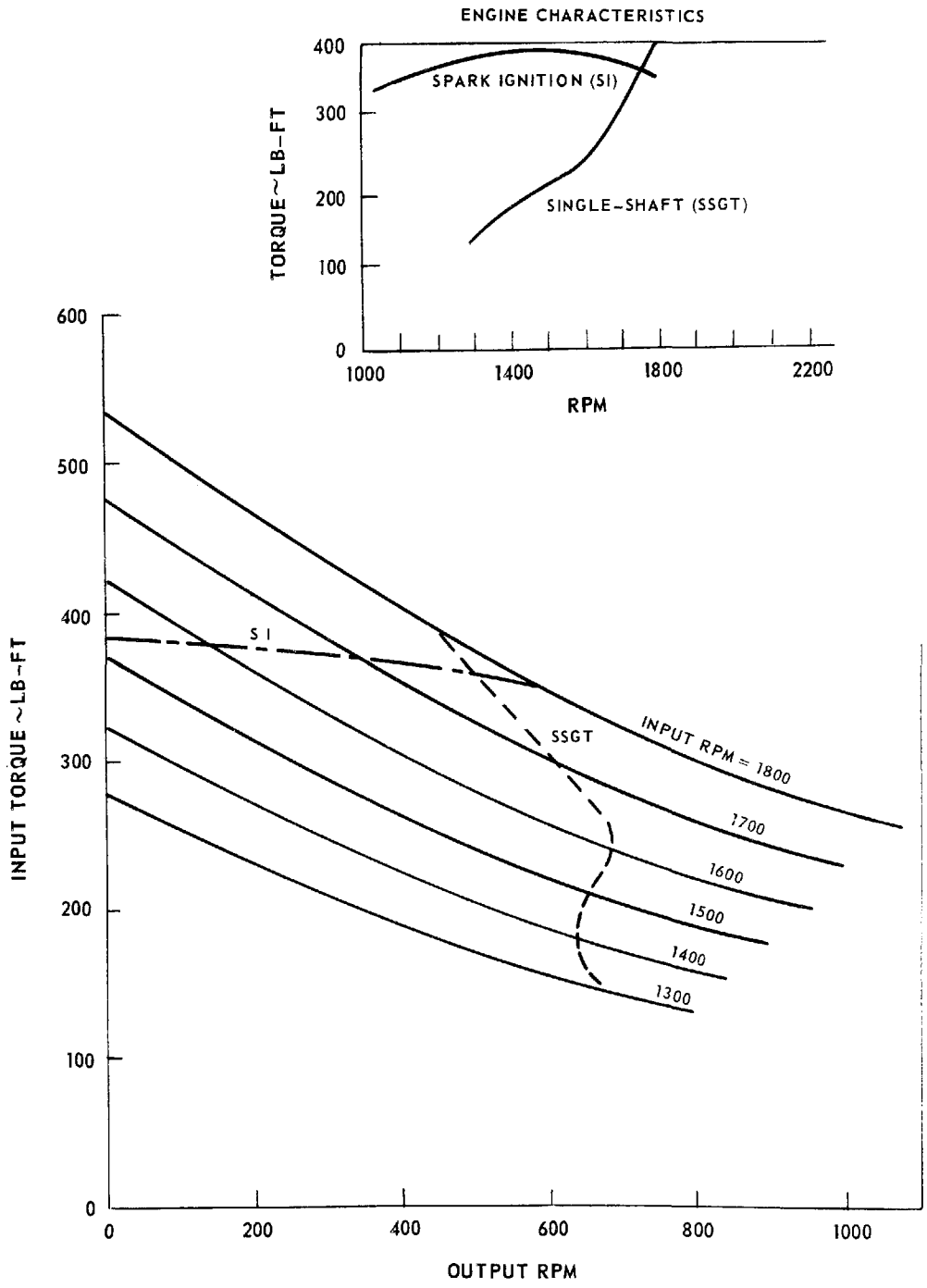

Thus, a curve of Q vs. N could define a converter. However, these characteristic curves are not sufficient for determining how it will perform when mated to a specific engine. Figure 25 presents a set of torque absorption curves for a spark-ignition (SI) engine. The intersections of the SI torque curve with the converter curves represent a locus of operating points. If this particular converter were mated to the single-shaft gas turbine (SSGT), one would again superimpose the engine torque curve as shown by the dashed line in Fig. 25. The resulting locus of operating points indicates that over most of the input speed range, the output speed will be about constant. Also, there is no stall condition, i.e., zero output speed. Therefore, this converter and the SSGT are incompatible.

Another means of determining compatibility between engine and converter is to examine a curve of torque vs. engine speed upon which is superimposed a typical parabolic converter stall curve which is matched to the maximum engine torque (Fig. 26). The torque of the SSGT is below the converter stall requirement over a large percentage of the operating range. In this region, the converter will tend to reduce engine speed until a torque match can be found. However, the more the rpm is reduced, the greater the mismatch and eventually the engine will stall. A smaller converter could be used, but a governor would be required to control maximum rpm and much less torque would be delivered.

Torque converters can be made with many different torque absorption characteristics and torque multiplication ratios. One type has torque characteristics which appear to be more compatible with the SSGT. The primary torque of this converter at a given input rpm decreases as the output rpm approaches stall over a range of about 0.40 to 0 (output rpm/input rpm). By combining a properly sized converter and the proper gear reduction ratio for the SSGT engine, a match between engine and converter can be achieved as shown in Fig. 27. The engine would not be operated to full rated rpm to circumvent the "curl" at the top of the curve. Therefore, 10 to 15 hp would be lost at the top end of the operating range.

Idle conditions must also be examined. With the converter and SSGT engine defined above, the engine would stall at idle speed when the power train is engaged. To prevent stall, one could automatically increase the throttle setting when the shift lever is moved from neutral. Another means of preventing stall at idle speed is to change the ratio of the reduction gear, thus changing the engine idle torque to a high enough level to avoid stall. This approach, exemplified by Fig. 28, leads to a split transmission in which a gear change can be made before and after the converter. Thus, good idle conditions and full-power performance would be attainable.

TORQUE CONVERTER STALL CHARACTERISTICS

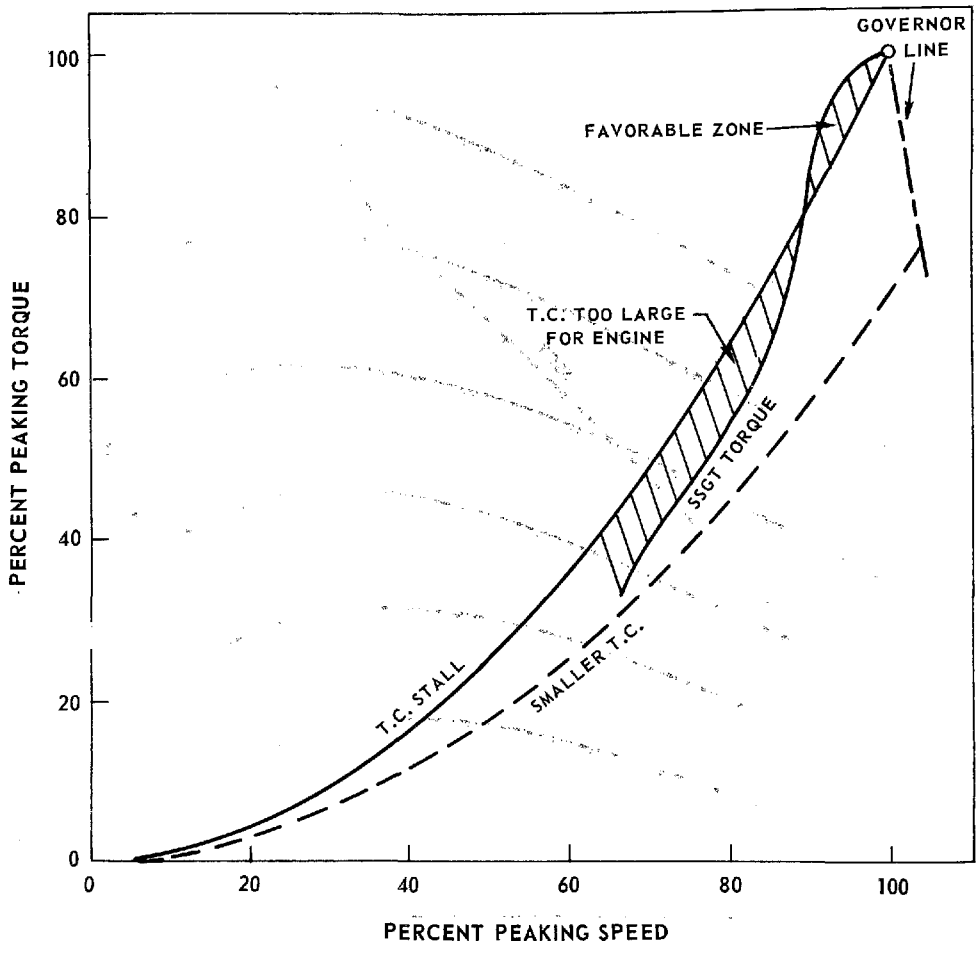

FIG. 27

TORQUE ABSORPTION CHARACTERISTICS FOR SINGLE-SHAFT GAS TURBINE APPLICATION

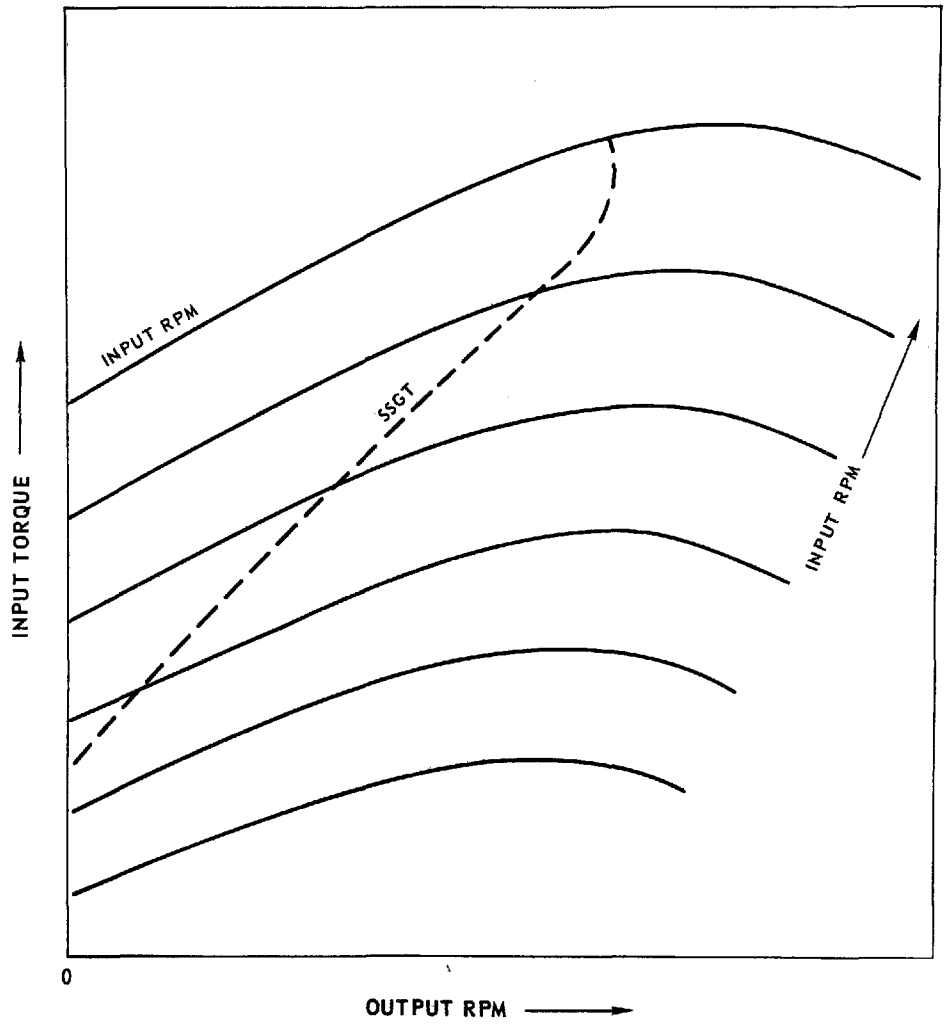

FIG. 28

TORQUE CONVERTER–ENGINE MATCHING

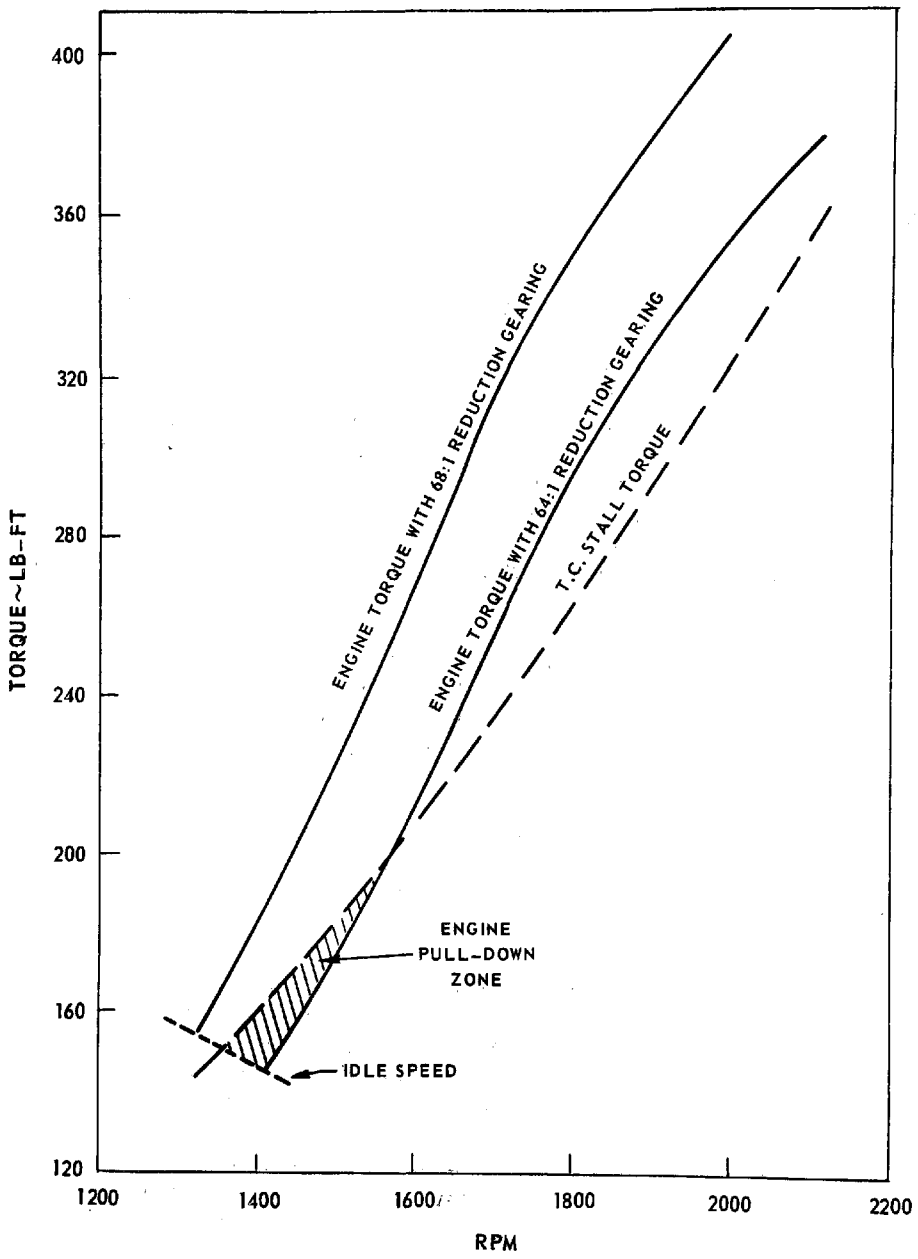

Another means of providing satisfactory idle conditions may be to use a variable-fill converter in which fluid is pumped in and out according to some schedule. By reducing the mass of the working fluid, the converter characteristics would be changed to allow idle without engine stall. However, partially filled TC's tend to "foam" and can rapidly lose efficiency. Thus, one would have to carefully study this problem and determine to what practical degree the converter could be emptied.

Traction Drives

Traction drives (TD) have been in use for many years and have been incorporated in systems ranging from small toys to large industrial machinery. The principle involves rolling friction, rather than gear teeth, to transfer power. For small torque levels, dry mating surfaces can be employed. However, as the torque to be transferred increases, the compressive force between the components must be increased to prevent slippage, thus producing large amounts of heat (lost power), which destroys the contact surfaces, and excessive repetitive Herzian stresses, which lead to fatigue (shelling) failures. The use of lubricants allows the transfer of high torque without excessive heat build-up. Recent development in lubricants by Monsanto are reported to have resulted in efficiencies of about 97%, and can greatly reduce surface stresses by effectively enlarging the total contact area (Ref. 14).

Transmissions using traction-drive principles have been built on a small scale and have proven very successful from the standpoints of both efficiency and endurance. One basic design problem is that of achieving stable zero output speed on a device which does not also include a clutch and a separate reversing device.

It appears that traction-drive transmissions would require precision contact surfaces to ensure smoothness and roundness. This precision is generally expensive, as compared with a torque converter, for instance, which is made from stampings and automatically assembled.

A multitude of traction transmission designs have been suggested. The New Departure Division of General Motors has developed a nonratio-changing gear reduction unit which automatically increases the compressive forces between the rolling elements as the torque load increases. No data are available as to costs but efficiencies have been quoted as being over 95%.

The General Motors Hydramatic Division Toroidal transmission was tested extensively in several automobiles, and is reported to have high efficiencies, long life, and competitive manufacturing cost. It offers little advantage when coupled

TABLE III

TRANSMISSION RATINGS

(Each Transmission Weighted by Category - Max. = 7)

	Type of Transmission				
Category	Hydrokinetic	Hydromechanical	Traction Drive	Mechanical	Electric
Efficiency	5	4	6	7	6
Weight	5	6	4	4	5*
Smoothness	6	7	7	3	7
Durability	5	5	3**	4	7
Temp. Sensitivity	5	4	5	7	7
Eng. Braking	5	6	7	7	6
Noise	6	4	6	5	6
R&D Costs	5	7	4	6	2
Manuf. Costs	7	6	4	5	4
Availability	5	7	4	6	2

* Considering elimination of drive shaft, differential, and gear box
** Highly questionable, dependent on R&D effort

with a standard V-8, but might be adapted for a single-shaft gas turbine. Additional devices are being tested by TRACOR and AirResearch. Confirmation of reported efficiency figures for test devices in practical automotive units would lead to significant improvements for automotive transmissions, regardless of powerplant type used.

Transmission Ratings

A general comparison of the basic transmissions is shown in Table III. For each category, the transmissions are rated from 1 to 7, where the higher numbers reflect in favor of the system. The ratings shown were derived from both quantitative and qualitative sources, including literature surveys, manufacturer contacts, and computations. It should be emphasized that these ratings are very interdependent and could change during development and/or manufacture. Research and development status is a dominant factor, not only because of the contract requirement to demonstrate the optimum engine by 1975, but since progress can greatly affect the ratings of efficiency, weight, smoothness, durability, etc. It is currently judged that these ratings should be representative for reasonable research and development costs.

Each category will also carry its own ratings as to overall importance in a program to develop an automotive transmission. When considering the ultimate goal of customer acceptance of the system, one must surely place high emphasis on research, development,and manufacturing costs, each of which directly affect the cost to the customer. Probably as important is the vehicle performance delivered by the transmission system. A measure of performance would include smoothness, engine braking capability, temperature sensitivity, and to a lesser degree, efficiency. Although the engineer, designer, and salesman stress operating efficiency, rarely does a driver show concern for gas mileage variations in a given vehicle, as long as the vehicle is running smoothly and starts reliably. The driver is seldom aware that worn spark plugs and pitted distributor points can cost him a 10%-to-30% increase in fuel consumption. The same is true of low fluid levels and/or clogged filters in a torque converter. Variations in driving habits can cause significant variation in gas mileage as evidenced by average driving versus the Mobil mileage runs. Therefore, it is felt that theoretical operating efficiency is not as important as consistency, smoothness, reliability, and initial cost.

Similarly, the transmission weight is important if significant weight savings are attainable which could measurably affect vehicle performance, vehicle cost, and gas mileage. However, from a fuel economy standpoint, a 3000-lb automobile with a single-shaft engine will show only a 1 mpg increase in fuel economy over a 5000-lb automobile.

Transmission noise must be related to engine noise rather than absolute values, since driver awareness to noise is relative. As an example, an HMT, which is thought to have high pumping noise, is barely audible when installed in a heavy truck or track-laying vehicle, but might be the dominant source of noise in an automobile.

The "availability" category reflects the timetable set by the Federal Government for meeting the 1976 emissions requirements. If it is assumed that these requirements will be strictly enforced, then the transmission development must start almost immediately to allow lead time for "bench" testing and prototype vehicles. Again, availability is a function of applied development effort, where a four-year crash program with unlimited funds could probably develop any transmission considered here by 1976. However, in the initial phase, it is obviously prudent to use an available unit (such as the HMT, rated "7") rather than one requiring much R&D effort (such as the electric system, rated "2").

An importance (or weighting) factor, ranging from 1 to 5, was also assigned to each of the ten categories as follows:

Category	Weighting Factor
Efficiency	2
Weight	1
Smoothness	4
R&D Costs	5
Manufacturing Costs	5
Durability	4
Braking	3
Temperature Sensitivity	2
Availability	4
Noise	4

These weighting factors were multiplied by the rating factors assigned in Table III to obtain the modified relative ratings which are shown in Table IIIa along with the total rating for each transmission.

This analysis favors the HMT mainly because of availability, smoothness of operation, and because units have been built under other programs which substantially reduces the required development costs and technological risk for a 1975 demonstration.

Differential

For the transmission systems studied (except electric), a mechanical differential system is employed to split the total torque between the driving wheels and to also provide a means of compensating for speed variations between the wheels, such as when turning a corner.

The system employed in this study is an epicyclic gear system (planetary) (Fig. 29), where the ring gear is driven by a silent-running chain connected to an output pinion from the transmission. This system is similar to that currently used in General Motors' front-wheel drive cars, such as the Oldsmobile Toronado. One axle is connected to the sun gear and the opposite axle is connected to the carrier which contains the planet gears. To provide proper rotational direction, the planet gears also have a corresponding set of idlers. This epicyclic system eliminates bevel gearing and the associated thrust loads on the bearings.

In a standard planetary system, the rotation speed relationship among the planet, carrier, and ring gear is

$$\omega_r r_r + \omega_s r_s = \omega_c (r_r + r_s)$$

where $\omega_{r,s,c}$ = speed of ring, sun, and carrier, rpm

$r_{r,s}$ = radius of ring and sun gears, in.

The chain drive serves three major functions. First, a large distance between centers can be traversed with low reduction ratios (≈3:1) for a small weight penalty. By incorporating an idler in the chain system, the differential reduction ratio can be easily changed by changing the transmission output pinion diameter. The idler is then used to compensate for chain tension.

TABLE IIIa

TRANSMISSION RATINGS*

(Each Category Weighted by Importance - Max. = 5)

		Type of Transmission				
Category	Rating	Hydrokinetic	Hydromechanical	Traction Drive	Mechanical	Electric
Efficiency	2	10	8	12	14	12
Weight	1	5	6	4	4	5
Smoothness	4	24	28	28	12	21
Durability	4	20	20	12	16	28
Temp. Sensitivity	2	10	8	10	14	14
Eng. Braking	3	15	18	21	21	18
Noise	4	24	16	24	20	24
R&D Costs	5	25	35	20	30	10
Manuf. Costs	5	35	30	20	25	20
Availability	4	20	28	16	24	8
TOTALS **		188	197	167	180	160
		(79%)	(82.8%)	(70.2%)	(75.6%)	(67.2%)

*Each transmission rating = (category rating) x (importance rating)
maximum = 7 x 5 = 35

**100% = 238

FIG. 29

PLANETARY DIFFERENTIAL

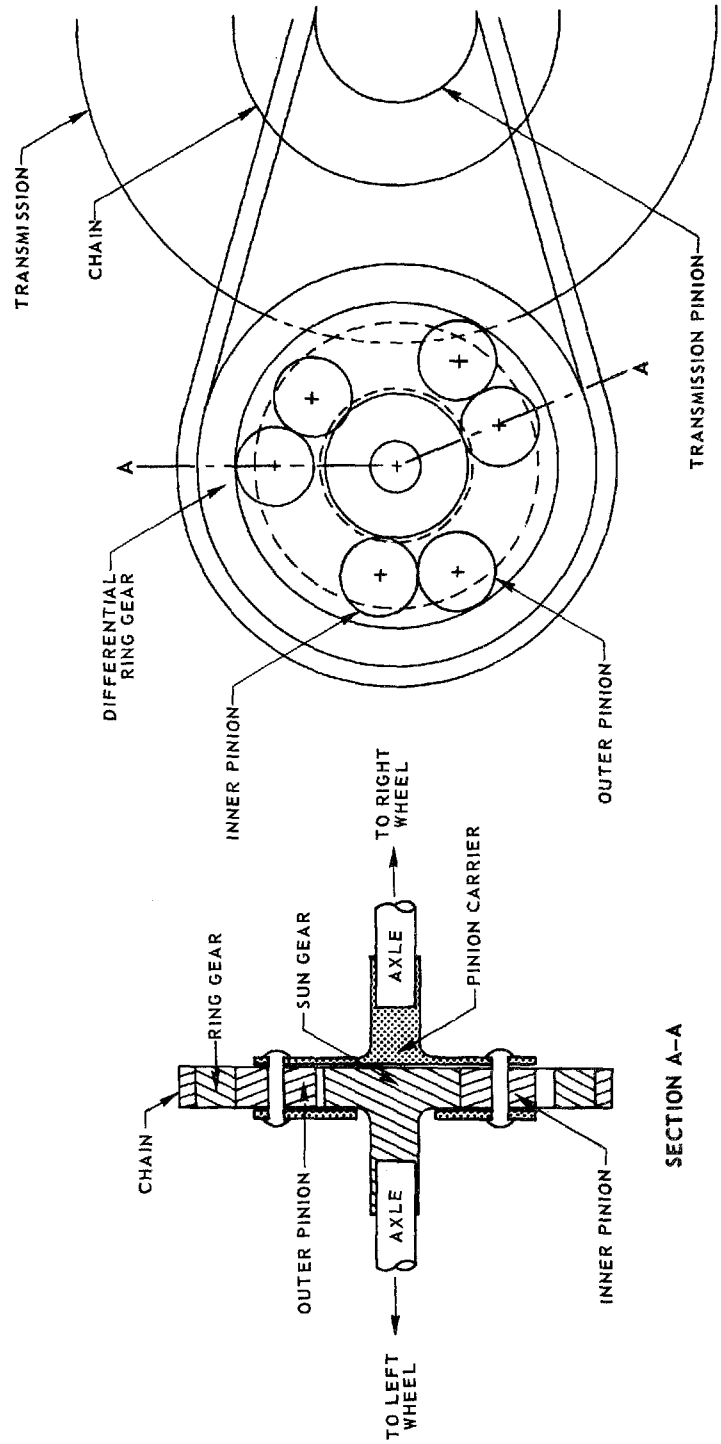

CYCLE ANALYSIS AND PRELIMINARY CANDIDATE SELECTION

Task 2 of Phase 1 (see Fig. 1) involved a parametric design-point cycle study of a large number of potential candidate engines for the gas turbine application. Task 3 comprised the selection of the three most attractive candidates for further optimization studies in Phase 2.

Engine Cycles Evaluated

A total of 60 engine cycles was evaluated during the parametric design-point cycle study. These were as follows:

1. Regenerative with large-size regenerator/recuperator ($\varepsilon = 0.90$)
2. Regenerative with medium-size regenerator/recuperator ($\varepsilon = 0.70$)
3. Regenerative with small-size regenerator/recuperator ($\varepsilon = 0.50$)
4. Simple cycle with single shaft
5. Intercooled with dual shaft
6. Reheated version of free-turbine engine
7. Simple-cycle gas turbine combined with Rankine cycle (COGAS)
8. Simple cycle with variable inlet turbine nozzle area and free turbine
9. Simple cycle with free turbine
10. Simple cycle, single shaft with water injection for power augmentation
11. Simple cycle with power-transfer free turbine

Cycle combinations 1 through 7 above were each evaluated for two levels of turbine inlet temperature and four levels of cycle pressure ratio, thereby making a total of 56 cycles among these types. The turbine inlet temperature level selected represented an uncooled version at 1900 F and a cooled version at 2300 F. The levels of cycle pressure ratio selected were dependent on the cycle and ranged from 4:1 to as high as 30:1. The final four combinations 8 through 11, were evaluated for a single most attractive pressure ratio and turbine inlet temperature, as determined from the preceding 56 evaluations, for a total of four cycles.

TABLE IV

SAMPLE ENGINE PERFORMANCE COMPUTER PRINTOUT

SINGLE SPOOL REGENERATIVE ENGINE (SSR), COUNTERFLOW

DESIGN POINT INFORMATION

ALTITUDE	0. FT	AMBIENT TEMP.	59.0 F
AIRFLOW	1.230 LBS/SEC	DELTA AMBIENT TEMP	-.0 F
T.I.T.	1900. F	BURNER INLET TEMP.	1025.4 F
PRES. RATIO	8.00	BURNER INLET PRES.	115.2 PSIA
DESIGN RPM	95000. RPM	FUEL FLOW	62.4 LBS/HR
EXH. AREA	8.73 SQ.IN.	DESIGN HORSEPOWER	130.0 HP
TRANS. AREA	391.0 SQ. FT.	EFFECTIVENESS	.75

OFF-DESIGN DATA

O/O HP	O/O N1	HP (HP)	N1 (RPM)	WF (LB/HR)	BURNER IN. TEMP	T.I.T. (F)	TURB.EXH TEMP.	EXH. TEMP.	AIRFLOW (LB/SEC)	COMP. PR	ENG. EXH FLOW	F/A	HEX EFF	ENGINE TORQUE	O/O TORQUE
1.000	1.000	129.9	95000.	62.36	1025.4	1900.3	1162.1	770.1	1.2304	8.000	1.2478	.0141	.751	7.18	1.000
.900	1.000	116.9	95000.	59.48	982.5	1823.9	1106.3	754.7	1.2317	7.896	1.2483	.0134	.749	6.46	.900
.800	1.000	103.9	95000.	56.57	939.8	1747.4	1050.9	739.1	1.2322	7.786	1.2479	.0128	.746	5.75	.800
.700	1.000	90.9	95000.	53.62	897.9	1670.7	995.7	723.0	1.2318	7.672	1.2467	.0121	.744	5.03	.700
.600	1.000	78.0	95000.	50.70	855.5	1593.4	940.1	707.2	1.2316	7.551	1.2457	.0114	.741	4.31	.600
.500	1.000	65.0	95000.	47.82	815.7	1518.3	887.2	691.6	1.2310	7.433	1.2443	.0108	.739	3.59	.500
.400	1.000	52.0	95000.	44.95	778.8	1445.5	836.8	676.2	1.2300	7.320	1.2425	.0102	.736	2.87	.400
.300	1.000	39.0	95000.	42.29	740.8	1372.8	787.1	662.9	1.2310	7.206	1.2428	.0095	.734	2.15	.300
.200	1.000	26.0	95000.	39.57	703.6	1299.6	737.1	648.7	1.2311	7.091	1.2421	.0089	.731	1.44	.200
.100	1.000	13.0	95000.	36.86	668.2	1227.6	688.7	634.7	1.2311	6.974	1.2413	.0083	.728	.72	.100
.050	1.000	6.5	95000.	35.53	651.4	1192.6	665.7	628.1	1.2311	6.918	1.2409	.0080	.727	.36	.050
.020	1.000	2.6	95000.	34.71	640.5	1170.6	650.9	623.9	1.2311	6.882	1.2407	.0078	.726	.14	.020
.800	.950	103.9	90250.	51.43	921.4	1702.0	1037.7	692.5	1.1648	7.240	1.1791	.0123	.756	6.05	.842
.700	.950	90.9	90250.	48.73	871.6	1615.8	974.2	676.5	1.1702	7.154	1.1838	.0116	.752	5.29	.737
.600	.950	78.0	90250.	45.96	823.9	1530.8	912.1	659.8	1.1741	7.052	1.1869	.0109	.748	4.54	.631
.500	.950	65.0	90250.	43.17	778.3	1447.9	852.2	643.5	1.1758	6.939	1.1878	.0102	.745	3.78	.526
.400	.950	52.0	90250.	40.39	734.9	1367.1	794.8	627.7	1.1763	6.820	1.1875	.0095	.742	3.02	.421
.300	.950	39.0	90250.	37.63	693.8	1288.4	740.1	612.5	1.1756	6.701	1.1860	.0089	.739	2.27	.316
.200	.950	26.0	90250.	34.92	653.2	1209.2	685.6	597.3	1.1765	6.581	1.1862	.0082	.736	1.51	.210
.100	.950	13.0	90250.	32.22	614.4	1131.7	633.3	582.6	1.1763	6.460	1.1853	.0076	.733	.76	.105
.050	.950	6.5	90250.	30.88	595.8	1093.5	607.9	575.4	1.1762	6.399	1.1848	.0073	.731	.38	.053
.020	.950	2.6	90250.	30.07	584.2	1070.0	592.1	571.0	1.1762	6.361	1.1845	.0071	.731	.15	.021
.400	.800	52.0	76000.	22.72	1030.7	1637.2	1147.0	529.4	.6612	4.122	.6675	.0095	.847	3.59	.500
.300	.800	39.0	76000.	20.16	833.3	1364.3	924.5	487.6	.6938	4.069	.6994	.0081	.832	2.69	.375
.200	.800	26.0	76000.	17.60	682.0	1142.9	748.9	453.2	.7178	3.985	.7224	.0068	.819	1.80	.250
.100	.800	13.0	76000.	15.02	573.3	968.9	619.6	426.5	.7289	3.874	.7331	.0057	.810	.90	.125
.050	.800	6.5	76000.	13.65	522.6	884.8	557.7	413.1	.7316	3.802	.7354	.0052	.807	.45	.062
.020	.800	2.6	76000.	12.82	491.4	833.4	519.7	405.2	.7335	3.755	.7370	.0049	.804	.18	.025
.200	.650	26.0	61750.	11.24	1187.2	1644.2	1291.1	416.3	.4285	2.786	.4317	.0073	.897	2.21	.308
.150	.650	19.5	61750.	10.11	919.6	1318.1	1005.4	383.1	.4629	2.785	.4657	.0061	.882	1.66	.231
.100	.650	13.0	61750.	8.91	719.3	1063.4	787.0	354.5	.4920	2.766	.4945	.0050	.868	1.11	.154
.050	.650	6.5	61750.	7.56	553.1	842.1	601.0	325.4	.5161	2.720	.5182	.0041	.854	.55	.077
.020	.650	2.6	61750.	6.79	473.8	730.5	510.4	309.8	.5263	2.681	.5282	.0036	.847	.22	.031
.100	.500	13.0	47500.	4.89	1891.4	2241.0	1986.8	328.1	.2316	1.914	.2330	.0059	.947	1.44	.200
.075	.500	9.7	47500.	4.46	1384.5	1681.4	1464.4	301.2	.2557	1.913	.2569	.0048	.937	1.08	.150
.050	.500	6.5	47500.	3.76	976.3	1223.5	1041.5	270.0	.2837	1.903	.2847	.0037	.923	.72	.100
.020	.500	2.6	47500.	3.18	638.6	833.1	685.9	241.5	.3196	1.896	.3205	.0028	.905	.29	.040

I-971249-7

For each combination, the end output item consisted of performance data at full- and part-load operating points, including specific fuel consumption and output shaft rpm vs. horsepower. The tabular design point output included airflow, turbine inlet temperature, pressure ratio, burner inlet temperature, burner inlet pressure, fuel flow, exhaust area, heat exchanger surface area, and heat exchanger effectiveness. A sample output is shown in Table IV.

The rationale for the selection of the cycles is described in the following paragraphs.

Turbine Inlet Temperature

Central to the problem of automotive gas turbines is the question of maximum allowable turbine inlet temperature which involves a discussion as to whether turbine blade cooling technology should be advanced to the stage where highly cooled turbines are a practical proposition or whether only uncooled turbines should be considered. Of the two turbine inlet temperatures selected for study (1900 and 2300 F), the 1900-deg level represents current state of the art for the gas turbines under consideration, where this maximum value is attained only at the full power point at any operating speed and does not represent a continuous operating line. The higher turbine inlet temperature, which is typical of the current state of the art for internally cooled blades of aircraft gas turbines, was not necessarily believed to be cost effective for an automobile engine, but was selected to quantify its relative advantages or disadvantages.

Cycle Pressure Ratios

All engines employing heat exchangers were evaluated at cycle pressure ratios of 4, 6, 8, and 10, whereas simple-cycle engines were evaluated at pressure ratios of 6, 10, 15, and 30. Single-stage compressors were assumed for all pressure ratios up to and including 10:1, and two-stage compressors were considered for all other pressure ratios. Single-stage radial turbines were considered for the first stage of expansion in all engines with pressure ratios up to 10:1. Free-turbine engines consisted of a radial turbine driving the gas generator shaft, and an axial-stage power turbine.

Description of Cycles Evaluated

The first three cycles above (regenerative) were chosen to evaluate the heat exchanger engine. It was determined that, for the purpose of the preliminary evaluation, there would be no need to differentiate between recuperated and regenerated engines; therefore, only one set of data, representative of both,

was run. The large-size regenerator had an effectiveness of 90%; the medium size regenerator had an effectiveness of 70%; while the small regenerator had an effectiveness of 50%. The fourth engine type (simple-cycle single-shaft) was selected as being similar to an engine in a previous study (Ref. 1) which provided acceptable fuel consumption characteristics at a minimum manufacturing cost. The fifth engine cycle (intercooled with dual shaft) was selected to see if there were advantages in efficiency to be gained by intercooling the flow between stages of a two-stage compressor. The sixth cycle, which was a reheat version of the free-turbine engine, was selected since it is assumed that full-power requirements will size the basic engine, whereas fuel consumption and emission requirements at partial load will determine its other characteristics. The reheated engine, with its characteristic high specific power, would thus have a smaller basic engine size and a smaller compressor and, consequently, would be working at a higher percentage of full (no reheat) power during the typical mission, with a corresponding improvement in specific fuel consumption at the average mission power. The associated high specific fuel consumption at the design point due to adding heat at a point in the cycle where the pressure is low is likely to be of little consequence in normal automobile applications, where operation at full power is of very limited duration.

The seventh cycle, a simple-cycle engine combined with a Rankine-cycle engine operating from exhaust heat, was included in the evaluation for the following reasons. It is the system with the greatest assurance of meeting 1976 emissions standards and offers additional advantages, when compared with the simple-cycle engine, with regard to exhaust cooling, silencing, torque-speed characteristics, and heat for the car interior. When compared with the regenerated engines, it would offer greater power per pound of airflow and greatly improved emissions for a comparable level of fuel economy. At the same time, when compared with a straight Rankine cycle, the system would be smaller, less costly, lighter, and permit startup without undue complexity.

The last four cycles were evaluated at a 10:1 pressure ratio at 1900 degrees turbine inlet temperature. They included a free-turbine engine with and without variable inlet turbine nozzles, and a power transfer device to transfer power in scheduled amounts from the free turbine to the single-shaft engine as has been demonstrated in the General Motors GT309 engine. One of the engines evaluated considered using water injection for power augmentation. This engine shares, with the reheat engine, a similar advantage of producing a higher specific output and therefore a smaller basic engine size than the simple-cycle engine, thereby resulting in expected improvements in cost and fuel economy. The problem of obtaining pure water for injection was not considered in the preliminary evaluation since it is a problem which would have to be faced only if the cycle showed sufficient advantage for further design study.

Selection Criteria

The selection criteria which were applied to all 60 engine cycles and used to select the three engines for further study in Phase II of the program are described below. The final rankings were expressed in dollars, representing the total engine-related lifetime costs (TLC) for seven years and 105,000 miles of automobile life. These costs represent approximately one-fourth of the total lifetime cost of the vehicle, as reported in Ref. 15, appropriately adjusted for the cost of money. Therefore, an engine-related cost ranking which was below 140% of present experience represents compliance with the contract requirement that overall cost of operation not exceed 110% of the cost of operation of an equivalent 1970 automobile, if it is assumed that the other 75% of the expenses do not vary with engine type. The lifetime cost calculations were derived as follows. First, it was assumed that the total lifetime engine-related costs were: all fuel consumed by the engine, and engine-related costs of depreciation, maintenance, cost of money, and taxes. The fuel costs were derived, as detailed below, from calculations from the mission analysis program using the fuel consumption figures which were the output of the engine cycle analysis program of Task 2. The remaining items are as derived from the following table which resulted in a total cost of 235% of the basic engine cost, using an average of the high and low tabular values:

Item Related to Price of Engine	Lifetime Costs as a Percentage of Engine Cost	
Depreciation	100%	100%
Maintenance	70%*	100%
Sales Tax	0%	7%
Property Taxes	0%	15%**
Excise Tax	0%	7%
Interest Lost/Finance	18%***	36%****
Totals	188%	285%
Average	235%	

* as per Ref. 1

** 5% of annual value of engine

*** interest lost at 6%

**** finance charge of 12% for 3 years, plus 6% interest lost on equity; refinanced once

TABLE V

DERIVATION OF ENGINE COMPLEXITY FACTORS (CF_E)

Direct Manufacturing Costs (DMC)
SSS-12 Engine with Direct Labor at
$5.50/hour (9.15¢/min)

Group	Parts	DMC	CF
Casings	Diffuser Case	10.12	
	Air Inlet Housing	16.33	
	Accessory Drive Cover	5.01	
	Pressure Vessel	15.35	
		46.81	0.29
Compressor Rotor	Inducer, Impeller	9.38	0.06
Hot Sheet, etc.	Turbine Shroud	8.55	
	Scroll	9.37	
	Fuel Nozzle	3.50	
	Burner Liner	8.55	
	Turbine Shroud	6.00	
	Compressor Shroud	2.74	
		38.71	0.20
Turbine	Star Exducer	11.39	
	Nozzle	20.14	
		31.53	0.20
Gears, Bearings, Seals	All Gearing	5.95	
	Compressor Shaft	1.15	
	Output Shaft	1.29	
	Bearings-	12.00	
	Seals	3.50	
		23.89	0.15
Assembly, Test, Miscellaneous	All Others	16.18	0.10
		CF_E Total	1.00

The basic engine cost was derived by, first, estimating the manufacturing cost of the engine. This value was obtained by multiplying the cost of the simple-cycle engine, derived carefully in Ref. 1, by a complexity factor estimated as a function of the needed components of each engine relative to the configuration of the simple-cycle engine, as detailed below. A retail price of each engine was then derived by multiplying its manufacturing cost times 2.7 to obtain an average retail price of that portion of the vehicle believed due to the engine. This price was finally multiplied by 235%, the estimated lifetime cost factor, as derived above.

The total lifetime cost was then derived by summing the costs of the engine, the cost of its control, and the cost of fuel.

The fuel cost derivations were made by assuming that mileage driven was one-half urban and one-half rural as per national averages reported in Ref. 16. It was assumed that the urban mileage was represented by the Federal Driving Cycle and that rural mileage was approximately equal to the UARL country cycle of Ref. 1 which is approximately equivalent, for fuel economy, to driving at 70 mph. An adjustment was made to reduce the mileage reported in Ref. 15 to that more representative of national averages as reported in Ref. 16. Turbine fuel was assumed to weigh 7 lb/gal and was costed at 33¢/gal. Gasoline, for Otto-cycle engines, was assumed to weigh 6.2 lb/gal and was costed at 35¢/gal.

The engine complexity cost factors were derived in the following manner: From Ref. 1 the direct manufacturing costs of the simple-cycle single-shaft engine (SSS-12) were normalized to the value 1.0. This derivation is shown in Table V. The derivation of complexity factors for all engines was then derived from this base of data by adjusting for airflow, heat exchanger surface area, and design changes required. In general, differences in airflow were accounted for by adjusting costs by the square root of the ratio of the airflow of the candidate engine to that of the original SSS-12 of Ref. 1. Heat exchanger areas were compared by contrasting effectiveness to that of the RSS-7 of Ref. 1 and then adjusting for the area of the heat exchangers by the cube root of the surface area of the heat exchangers. Free-turbine engines were costed on the basis of comparisons between the SSS-12 and SFT-12 of Ref. 1. Controls were compared on a complexity basis according to estimates furnished by Hamilton Standard. The tabulation of engine complexity factors for all 60 engines is shown in Table VI.

The engine costs as derived from the complexity factors, plus fuel and control costs, are presented in Table VII along with the values of total lifetime costs for all 60 engines plus the 1970 Otto-cycle engine (OC-70). The total lifetime costs are also shown in Fig. 30 as a function of pressure ratio.

TABLE VI

ENGINE COMPLEXITY FACTORS

Series Designation	W_a/A_{HEX}	Complexity Factors							CF_E
		Casings	Compressor	Hot Sheet	Turbines	Gears, Bearings and Seals	HEX	A&T	TOTAL
1. RSS-4 (50%)	1.6/106	0.38	0.04	0.26	0.23	0.18	0.76	0.10	1.95
RSS-6	1.4/92	0.34	0.06	0.24	0.22	0.18	0.68	0.1	1.82
RSS-8	1.45/96	0.35	0.07	0.24	0.22	0.18	0.70	0.1	1.86
RSS-10	1.51/102	0.36	0.07	0.25	0.23	0.18	0.73	0.1	1.92
RSS-4C	1.38/73	0.31	0.04	0.24	0.62	0.18	0.62	0.12	2.13
RSS-6C	1.17/62	0.27	0.05	0.22	0.57	0.18	0.54	0.12	1.95
RSS-8C	1.19/64	0.28	0.06	0.22	0.57	0.18	0.55	0.12	1.98
RSS-10C	1.21/65	0.28	0.06	0.22	0.58	0.18	0.56	0.12	2.0
2. RSS-4 (75%)	1.67/324	0.56	0.05	0.26	0.24	0.18	1.13	0.12	2.54
RSS-6	1.4/275	0.49	0.06	0.24	0.22	0.18	0.98	0.11	2.28
RSS-8	1.47/285	0.51	0.07	0.25	0.22	0.18	1.01	0.11	2.35
RSS-10	1.52/297	0.52	0.07	0.25	0.23	0.18	1.04	0.11	2.40
RSS-4C	1.44/204	0.45	0.05	0.24	0.63	0.18	0.90	0.14	2.59
RSS-6C	1.19/173	0.39	0.05	0.22	0.57	0.18	0.77	0.13	2.31
RSS-8C	1.21/175	0.39	0.06	0.22	0.58	0.18	0.78	0.13	2.34
RSS-10C	1.23/179	0.40	0.06	0.22	0.58	0.18	0.79	0.13	2.36
3. RSS-4 (90%)	1.85/1008	0.87	0.05	0.27	0.25	0.18	1.73	0.14	3.49
RSS-6	1.47/786	0.71	0.06	0.25	0.22	0.18	1.42	0.13	2.97
RSS-8	1.50/807	0.73	0.07	0.25	0.23	0.18	1.46	0.13	3.05
RSS-10	1.54/870	0.75	0.07	0.25	0.23	0.18	1.50	0.13	3.11
RSS-4C	1.6/557	0.66	0.04	0.26	0.66	0.18	1.32	0.15	3.27
RSS-6C	1.24/428	0.53	0.05	0.23	0.58	0.18	1.07	0.14	2.78
RSS-8C	1.24/435	0.54	0.06	0.23	0.58	0.18	1.07	0.14	2.80
RSS-10C	1.25/454	0.55	0.07	0.23	0.59	0.18	1.09	0.14	2.85
4. SSS-6	1.1	0.28	0.05	0.20	0.19	0.18	0.00	0.08	0.98
SSS-10	1.22	0.30	0.06	0.21	0.20	0.18	0.00	0.08	1.03
SSS-15	1.35	0.39	0.14	0.23	0.21	0.18	0.00	0.10	1.25
SSS-30	2.85	0.57	0.20	0.33	0.31	0.18	0.00	0.13	1.72
SSS-6C	0.93	0.26	0.05	0.19	0.51	0.18	0.00	0.10	1.29
SSS-10C	0.98	0.27	0.06	0.19	0.52	0.18	0.00	0.10	1.32
SSS-15C	1.03	0.34	0.12	0.20	0.53	0.18	0.00	0.11	1.48
SSS-30C	1.51	0.41	0.14	0.24	0.64	0.18	0.00	0.13	1.74
5. SFT-6I	2.23*	0.53	0.10	0.21	0.46	0.54	0.1	0.16	2.1
SFT-10I	2.0*	0.50	0.12	0.19	0.44	0.54	0.09	0.15	2.03
SFT-15I	1.0	0.5	0.12	0.19	0.44	0.54	0.09	0.15	2.03
SFT-30I	1.33	0.57	0.13	0.22	0.50	0.54	0.10	0.17	2.23
SFT-6IC	0.91	0.48	0.09	0.19	0.74	0.54	0.09	0.17	2.30
SFT-10IC	0.81	0.45	0.00	0.17	0.70	0.54	0.08	0.17	2.21
SFT-15IC	0.78	0.44	0.10	0.17	0.69	0.54	0.08	0.17	2.19
SFT-30IC	0.88	0.47	0.11	0.18	0.73	0.54	0.08	0.17	2.28
6. SFT-6R	1.06	0.56	0.05	0.40	0.65	0.36	0.00	0.16	2.18
SFT-10R	1.01	0.55	0.06	0.39	0.63	0.36	0.00	0.16	2.15
SFT-15R	0.99	0.60	0.12	0.39	0.63	0.36	0.00	0.17	2.27
SFT-6RC	0.96	0.53	0.05	0.38	0.95	0.36	0.00	0.18	2.45
SFT-10RC	0.91	0.52	0.06	0.37	0.93	0.36	0.00	0.18	2.42
SFT-15RC	0.87	0.57	0.11	0.36	0.91	0.36	0.00	0.18	2.49
SFT-30RC	1.39	0.72	0.14	0.46	1.15	0.36	0.00	0.22	3.05
7. WSS-6	0.71	0.23	0.04	0.16	0.16	0.18	0.6	0.08	1.45
WSS-10	0.82	0.25	0.05	0.18	0.17	0.18	0.6	0.08	1.51
WSS-15	0.92	0.32	0.11	0.19	0.18	0.18	0.6	0.09	1.67
WSS-20	1.15	0.36	0.12	0.21	0.20	0.18	0.6	0.10	1.77
WSS-6C	0.52	0.20	0.03	0.14	0.38	0.18	0.6	0.09	1.62
WSS-10C	0.57	0.21	0.04	0.15	0.40	0.18	0.6	0.09	1.77
WSS-15C	0.61	0.26	0.09	0.15	0.41	0.18	0.6	0.10	1.79
WSS-20C	0.68	0.28	0.10	0.16	0.43	0.18	0.6	0.11	1.86
8. SFT-10VG	1.22	0.48	0.06	0.21	1.07	0.36	0.00	0.17	2.35
9. SFT-10	1.21	0.48	0.06	0.21	0.48	0.36	0.00	0.13	1.72
10. SSS-10W	1.22	0.48	0.06	0.34	0.20	0.18	0.00	0.11	1.37
11. SFT-10PT	1.22	0.48	0.06	0.21	0.48	0.69	0.00	0.15	2.07

* 2 x actual

TABLE VII

TOTAL LIFETIME COSTS

	Engine	Urban MPG	Rural MPG	CF_F	Fuel Cost ($)	CF_E	Engine Cost ($)	CF_C	Control Cost ($)	Total Lifetime Cost ($)	% of OC-70
0.	OC-70	9.5	12.2	1.04	2652	0.90	945	0.50	235	3832	100
1.	RSS-4 (50%)	12.5	13.6	0.87	2218	1.94	2048	1.50	705	4971	130
	RSS-6	15.3	16.9	0.70	1785	1.82	1911			4401	115
	RSS-8	17.2	17.5	0.65	1658	1.86	1953			4316	113
	RSS-10	17.6	17.2	0.65	1658	1.92	2016			4379	114
	RSS-4C	9.1	12.0	1.07	2728	2.13	2237			5669	148
	RSS-6C	13.3	15.1	0.80	2040	1.95	2048			4793	125
	RSS-8C	14.0	16.1	0.73	1862	1.98	2079			4646	121
	RSS-10C	15.9	16.7	0.70	1785	2.00	2100			4590	120
2.	RSS-4 (75%)	15.6	17.9	0.69	1760	2.54	2667	1.50	705	5132	134
	RSS-6	20.1	20.2	0.56	1428	2.28	2394			4527	118
	RSS-8	18.9	18.5	0.61	1556	2.35	2468			4729	123
	RSS-10	18.6	18.5	0.61	1556	2.40	2520			47.81	125
	RSS-4C	13.2	16.1	0.77	1964	2.59	2720			5389	141
	RSS-6C	18.1	18.4	0.62	1581	2.31	2426			4712	123
	RSS-8C	18.1	18.4	0.62	1581	2.34	2457			4743	124
	RSS-10C	18.1	18.3	0.62	1581	2.36	2478			4764	124
3.	RSS-4 (90%)	17.5	20.5	0.60	1530	3.49	3664	1.50	705	5899	154
	RSS-6	20.0	22.8	0.53	1352	2.97	3118			5175	135
	RSS-8	20.0	21.5	0.55	1402	3.05	3202			5309	139
	RSS-10	22.0	20.6	0.53	1352	3.11	3266			5323	139
	RSS-4C	12.6	15.2	0.82	2091	3.27	3434			6230	163
	RSS-6C	17.7	20.4	0.60	1530	2.78	2919			5154	134
	RSS-8C	19.3	18.8	0.60	1530	2.80	2940			5175	135
	RSS-10C	22.5	18.8	0.55	1402	2.84	2992			5099	133
4.	SSS-6	7.3	12.2	1.17	2984	0.98	1029	1.00	470	4483	117
	SSS-10	9.2	13.5	1.00	2550	1.03	1082			4102	107
	SSS-15	10.3	14.3	0.92	2346	1.25	1312			4128	108
	SSS-30	6.7	12.1	1.21	3086	1.72	1806			5362	140
	SSS-6C	7.6	11.2	1.21	3086	1.29	1354			4910	128
	SSS-10C	8.1	12.7	1.09	2780	1.32	1386			4636	121
	SSS-15C	10.0	13.7	0.96	2448	1.48	1554			4472	117
	SSS-30C	9.8	14.0	0.95	2422	1.74	1827			4719	123
5.	SFT-6I	5.8	10.1	1.43	3646	2.10	2205	1.08	508	6359	166
	SFT-10I	11.7	13.8	0.89	2270	2.03	2132			4910	128
	SFT-15I	13.4	15.4	0.79	2014	2.03	2132			4654	121
	SFT-30I	7.8	12.9	1.10	2805	2.23	2342			5655	148
	SFT-6IC	5.8	10.2	1.42	3621	2.30	2415			6544	171
	SFT-10IC	9.2	13.0	1.02	2601	2.21	2320			5429	142
	SFT-15IC	10.6	15.1	0.88	2244	2.19	2300			5052	132
	SFT-30IC	9.6	14.6	0.94	2397	2.28	2394			5299	138
6.	SFT-6R	5.7	11.1	1.35	3442	2.18	2289	2.05	964	6695	175
	SFT-10R	7.1	12.7	1.15	2932	2.15	2258			6154	161
	SFT-15R	8.0	13.2	1.07	2728	2.27	2384			6076	159
	SFT-6RC	7.1	10.9	1.26	3213	2.45	2572			6749	176
	SFT-10RC	8.1	12.4	1.11	2830	2.42	2541			6335	165
	SFT-15RC	10.2	14.5	0.92	2346	2.49	2614			5924	155
	SFT-30RC	5.2	8.5	1.65	4208	3.05	3202			8374	219
7.	WSS-6	16.4	19.2	0.64	1632	1.45	1522	1.50	705	3859	101
	WSS-10	16.4	19.2	0.64	1632	1.51	1586			3923	102
	WSS-15	16.4	19.2	0.64	1632	1.67	1754			4091	107
	WSS-20	10.6	16.1	0.85	2168	1.77	1859			4732	123
	WSS-6C	17.4	20.4	0.60	1530	1.62	1701			3936	103
	WSS-10C	17.2	21.3	0.59	1504	1.77	1859			4068	106
	WSS-15C	17.8	21.9	0.57	1454	1.79	1880			4039	105
	WSS-20C	15.3	21.0	0.63	1606	1.86	1953			4264	111
8.	SSS-10 V.G.	9.2	13.5	1.00	2550	2.35	2468	1.45	682	5700	149
9.	SFT-10	9.2	13.5	1.00	2550	1.72	1806	1.28	602	4958	129
10.	SSS-10W	9.2	13.5	1.00	2550	1.37	1428	1.15	540	4528	118
11.	SFT-10PT	9.2	13.5	1.00	2550	2.07	2174	1.85	870	5594	146

ENGINE-RELATED TOTAL LIFETIME COSTS

(UNCOOLED TURBINE, 1900-F MAX. INLET TEMP.)

ENGINE DESIGNATIONS

SERIES

1	REGENERATED, ϵ = 50%, SINGLE SHAFT
2	REGENERATED, ϵ = 75%, SINGLE SHAFT
3	REGENERATED, ϵ = 90%, SINGLE SHAFT
4	SIMPLE CYCLE, SINGLE SHAFT
5	SIMPLE CYCLE, INTERCOOLED, FREE TURBINE
6	SIMPLE CYCLE, REHEAT, FREE TURBINE
7	COGAS,
8	SIMPLE CYCLE, VARIABLE TURBINE
9	SIMPLE CYCLE, FREE TURBINE
10	SIMPLE CYCLE, WATER INJECTED
11	SIMPLE CYCLE, POWER TRANSFER

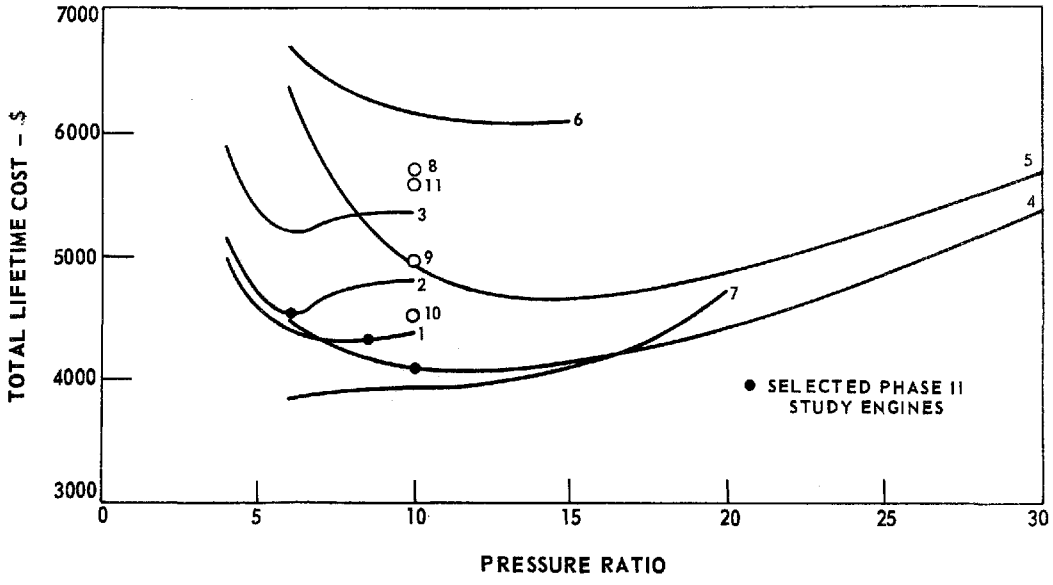

Preliminary engine selections for Phase II study are noted on Fig. 30. However, slight modifications, principally with respect to the low-effectiveness regenerated engine (Series 1) were made at the request of the Office of Air Programs, and the selected configurations are as follows:

RGSS-6 - Regenerated, Single-Shaft engine, 6:1 pressure ratio, 75% regenerator effectiveness

RCSS-8 - Recuperated, Single-Shaft engine, 8:1 pressure ratio, 60% regenerator effectiveness

SSS-10 - Simple-Cycle, Single-Shaft, 10:1 pressure ratio

Additional Iterations

While some of the engines shown in Fig. 30 appear to show better potential than the ones chosen (notably Series 7, the COGAS cycle), the final selection was made on the basis of additional iterations in the selection process as requested by the Office of Air Programs. Those iterations included an elimination of the COGAS system on the basis of technical and economic uncertainties. They also included further consideration of free-turbine engines, taking into account transmission effectiveness and costs required. The final selection also considered the use of the OAP-furnished driving cycle which is described in more detail in a subsequent section. In the case of the fuel cost comparisons, the effect of the OAP-supplied driving cycle (which consists of equal times over the FDC, the suburban driving cycle, and the rural driving cycle) is to increase overall fuel consumption and to favor more strongly the part-load operation of the engine. It was found that the fuel costs for the Series 4 SSS-10 engine increased by 12%, and those of the Series 1 RSS-8 and the Series 2 RSS-6 increased by 6%. The total lifetime cost comparisons are then as follows.

Series	Engine	Original TLC	Revised TLC	Selected Engine
4	SSS-10	$4102	$4402	SSS-10
1	RSS-8	4316	4413	RCSS-8
2	RSS-6	4527	4619	RGSS-6

Since it was obvious that changes of this magnitude would not affect the choice of engines to be studied in Phase II, no further revisions to the original calculations were made. The OAP-supplied driving cycle was, however, used for the economic analysis and the optimizations which were performed in Phase II.

Comparison of Free-Turbine and Single-Shaft Engines

Comparisons relative to the transmission complexity required for free-turbine and single-shaft engines were developed subsequent to the above work. These comparisons confirmthe elimination of the free-turbine version as described below.

The direct manufacturing cost (DMC) estimates for presently used automatic transmissions for 4000-lb automobiles are as follows:

1. Three-speed with torque converter - $62

2. Four-speed with torque converter - $75

3. Torque converter alone - $15

Therefore, a four-speed automatic for a free-turbine engine would have a DMC of approximately $60 if the torque converter were eliminated. This transmission would provide fuel economy approximately comparable with the single-shaft engine coupled to an infinitely variable transmission which allows the engine to follow its optimum fuel flow schedule, since the four-speed transmission coupled with the free turbine would not allow the free-turbine engine to follow its optimum fuel control schedule, and the resulting fuel consumption degradation of from 8 to 10% negates the inherently greater efficiency of the geared transmission. The three-speed transmissions without torque converter coupled to the free-turbine engine would result in an additional fuel economy degradation of approximately 4 to 5% for the free-turbine engine.

Either of the above resulting free-turbine propulsion systems is still unsatisfactory for automobile use since engine braking (negative torque) is not provided. The lowest-cost approach to this problem would probably be to add a hydraulic retarder to the transmission. This fluid coupling, plus piping, radiator, and control would have a DMC of at least $10. If this braking method is unacceptable from a safety standpoint, i.e., if negative torque must be supplied by the engine itself, the best alternative is to use variable geometry in the power turbine nozzles at an estimated DMC of $32.50 plus an additional engine control DMC of $8. In addition, the variable geometry results in an estimated fuel consumption penalty of 3 to 4%. Since these higher costs are clearly unacceptable, the most likely transmission for the free-turbine engine appears to be a four-speed automatic without the torque converter but with a hydraulic retarder with a consequent estimated DMC of $70. On a basis consistent with the previous calculations, this DMC would amount to a complexity factor for the transmission of $CF_T = 70/165 = 0.42$.

In the case of the single-shaft engine, the transmission assumed is the hydromechanical transmission (HMT) designed by General Electric. It is possible that its DMC will not exceed that of the present transmission and, based on an in-house manufacturing survey, it appears that the $90 DMC assumed is conservative. The CF_T = 90/165 = 0.55 for that assumption, and the fuel economy for this propulsion system, as mentioned above, is comparable with the free turbine with the four-speed transmission selected above.

Using the general methods previously derived, an overall complexity factor may be assigned to both single-shaft and free-turbine versions of the engine by adding the engine complexity factor from Table VI to that of the transmission required as described above. This procedure is followed below for the Series 2 RSS-8 engine and a free-turbine version of this engine, designated the RFT-8.

	W_a/A_{HEX}	Casings	Compr.	Hot Sheet	Turbine	GB&S	HEX	A&T	CF	CF_t Trans	CF_{PS}
RSS-8	1.47/285	0.51	0.07	0.25	0.22	0.18	1.01	0.11	2.35	0.55	2.90
RFT-8	same	0.66	same	same	0.50	0.36	same	0.13	2.98	0.42	3.40

From the above it can be seen that the cost of the transmission assumed for the single-shaft engine would have to almost double for its complexity factor to equal that of the free-turbine engine. The resulting DMC of $172 for the transmission appears to be completely unrealistic.

As a result of this analysis, it is concluded that the free-turbine version cannot be competitive with the single-shaft version even when the most favorable economic assumptions are made for the free-turbine and the least favorable are made for the single-shaft engine. Therefore, the selection of a free-turbine engine for Phase 2 optimization was not justifiable on either a technological or economic basis.

DESIGN

Engines

The three engines designed for the Phase 2 optimization comparisons are quite similar in all respects except for the inclusion of the heat exchanger. All engines are based on a single-shaft design with single-stage centrifugal impellers and single-stage radial turbines. All are designed to be robust, low-cost in construction consistent with high performance, and simple in concept and execution. All three designs make the minimum use of variable geometry. In each case, the only variable geometry is that for the compressor inlet guide vanes. These inlet guide vanes might possibly be eliminated during the development program as a result of further compressor development improvements, or they might be included in high-performance versions of a basic engine only. Their addition, including control complexity, raises the cost of the engine less than 10% and they provide a powerful means of optimizing engine operation during at least the development phase without the cost, performance, and mechanical reliability penalties of variable-geometry hot parts, such as power turbine nozzles. It is possible that some variable geometry might be associated in the combustor design, particularly for the regenerated and recuperated engines. For current lack of definition, this possibility was not included in the present design studies. Specific comments on engines follow.

Simple-Cycle Engine (SSS-10)

The simple-cycle engine is a single-shaft machine with all radial turbomachinery as are all Phase 2 study engines. It achieves a pressure ratio of 10:1 and a design mass flow of 1.15 lb/sec with a rotor speed of 106,000 rpm. Design and off-design point operational characteristics are shown in Table VIII, together with comparable detailed information for the other two study engines. The layout drawing of the SSS-10 engine is shown in Fig. 31 in cross section. The end view of the engine installed transversely with the GE HMT is shown in Fig. 32. An identical drawing numbered and keyed to a parts list is shown later, in Fig. 109.

The air intake is configured radially to achieve minimum installed length, and includes 18 variable inlet guide vanes. The inlet guide vanes are produced from plastic or aluminum strip stock and their actuation is automatically controlled by the fuel control unit. Structural support across the intake is provided by a series of axial struts. This configuration provides maximum flexibility for intake ducting.

The compressor is a centrifugal impeller of forged titanium alloy with 18 full vanes and 18 partial vanes, or splitters. Titanium is specified because of

TABLE VIII

ENGINE OPERATIONAL CHARACTERISTICS

Standard Day
Includes All Installation Losses

Engine	Power (hp)	N (Krpm)	W_f (lb/hr)	Burner Inlet Temp. (F)	TIT (F)	Airflow (lb/sec)	Fuel/Air Ratio	Equiv. Ratio ε	Compr. P.R.
RGSS-6	2.6	41.0	4.51	761	987	0.42	0.0033	0.92	1.70
	19.5	57.4	15.79	723	1130	0.79	0.0060	0.84	2.76
	130.0	82.0	69.00	1038	1900	1.49	0.0139	0.75	6.00
RCSS-8	2.6	47.5	4.88	620	877	0.38	0.0036	0.82	1.97
	19.5	66.5	17.10	636	1098	0.71	0.0068	0.72	3.50
	130.0	95.0	73.59	950	1900	1.36	0.0152	0.60	8.00
SSS-10	2.6	10.0	9.87	214	959	0.27	0.0105	--	1.99
	19.5	74.2	22.46	348	1266	0.47	0.0134	--	3.45
	130.0	106.0	82.16	692	1900	1.21	0.0191	--	10.00

FIG. 31

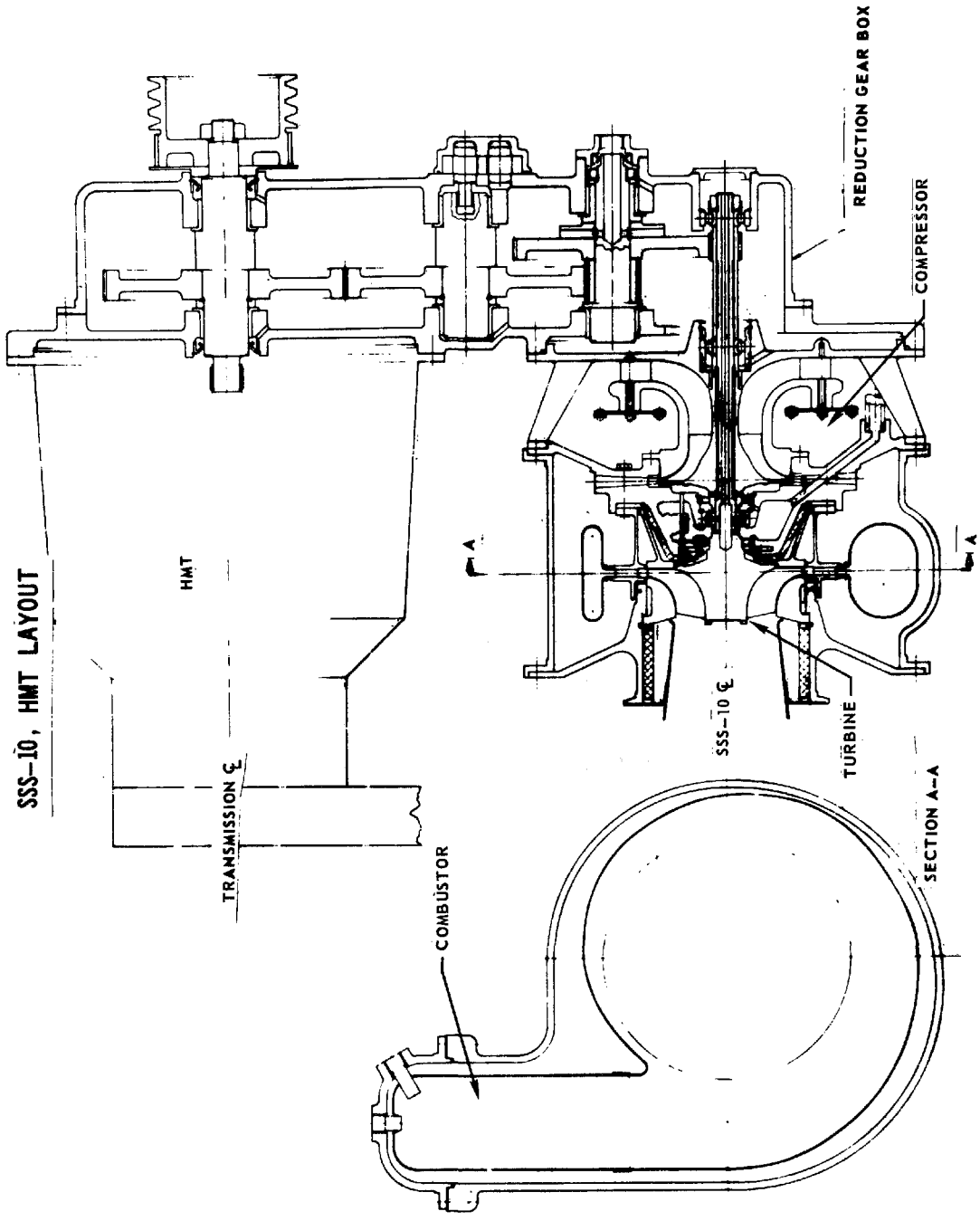
SSS-10, HMT LAYOUT
HMT
TRANSMISSION ℄
COMBUSTOR
SSS-10 ℄
TURBINE
REDUCTION GEAR BOX
COMPRESSOR
A
A
SECTION A-A

L-971249-7

FIG. 32

SSS-10, HMT POWER SYSTEM

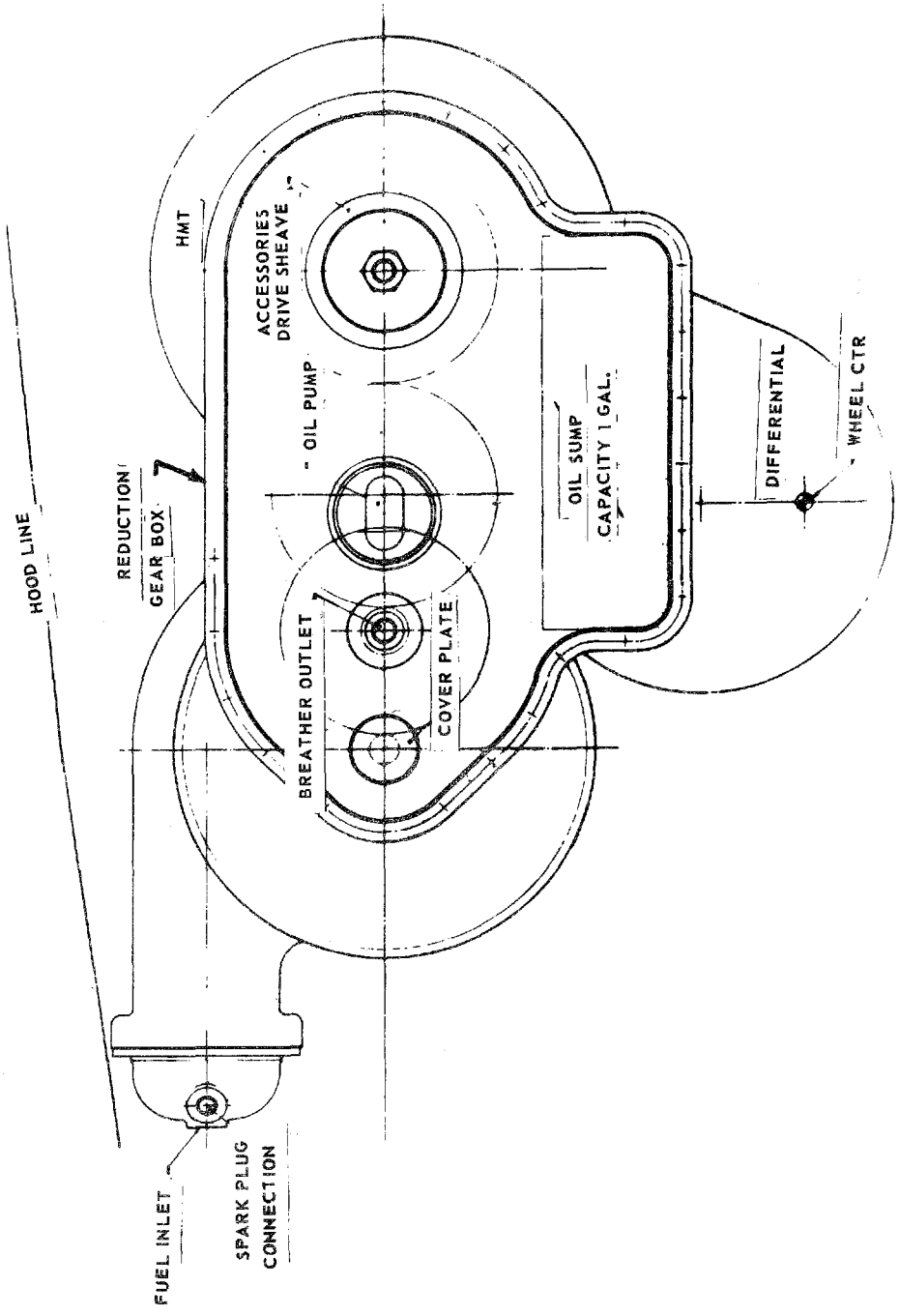

its superior fatigue strength in comparison with current steels. The particular grade of titanium (6 Al-2 Zn-9 Zr-6 Mo) was selected over the more common 6 Al-4V (used in the RGSS-6 and the RCSS-8) because of the higher temperatures encountered in the 10:1-pressure-ratio engine. The compressor, mounted on the turbine shaft, is driven by a friction joint provided by the axial lockup of components on the turbine shaft.

The diffuser passages are integrally machined in the ductile cast iron diffuser case with leading edges machined in a cast-in stainless steel ring to improve strength. The diffuser passages consist of straight and conical sections which intersect tangentially, providing a curved leading edge to the flow of gases leaving the impeller tip.

The combustor is a single-can design selected for reliability and low potential exhaust emissions. The gases are ducted from the combustor to the radial turbine nozzle by a toroidal scroll. The length of the combustor provides for a lengthened secondary combustion zone to thoroughly combust carbon monoxide and unburned hydrocarbons. Both the combustor and the turbine entry duct may be manufactured from either Hastelloy-X or INCO-625, depending on production economics.

The radial turbine nozzle is a one-piece investment casting with 15 airfoils. There are several alloy options for this component, including MAR-M-509 with MDC-9 coating, INCO-738 with PWA-73 coating, or WI-52 with MDC-9 coating. The final alloy selection would be based upon production economics and performance. The front and rear turbine shrouds may be constructed from the same material as the turbine nozzle or consideration may be given to using reaction-bonded silicon nitride ceramic as a potentially lower-cost material.

The turbine rotor would be manufactured from forged Udimet-700 and inertial welded to the AMS-4340 shaft. Among the high-production volume forging techniques which might be developed for this application, consideration should be given to superplasticity forging.

Exhaust gases are ducted away from the engine by an annular exhaust duct, part of which is shown in the cross section (Fig. 31). A straight diffusing length of approximately 9 inches is required. This duct may be manufactured from aluminized mild sheet steel.

The gearbox shown in Fig. 31 is configured to suit the particular installation as is discussed both in the previous section on base-line technology and in the following sections on installations. However, it is representative of the components required for a wide variety of installations. If a large offset were not required between the engine centerline and the output shaft, one gear and shaft could be eliminated from the gearbox. The gear train is shown as a double-reduction unit with an idler gear giving an output shaft speed of 3200 rpm.

RGSS–6, HMT LAYOUT

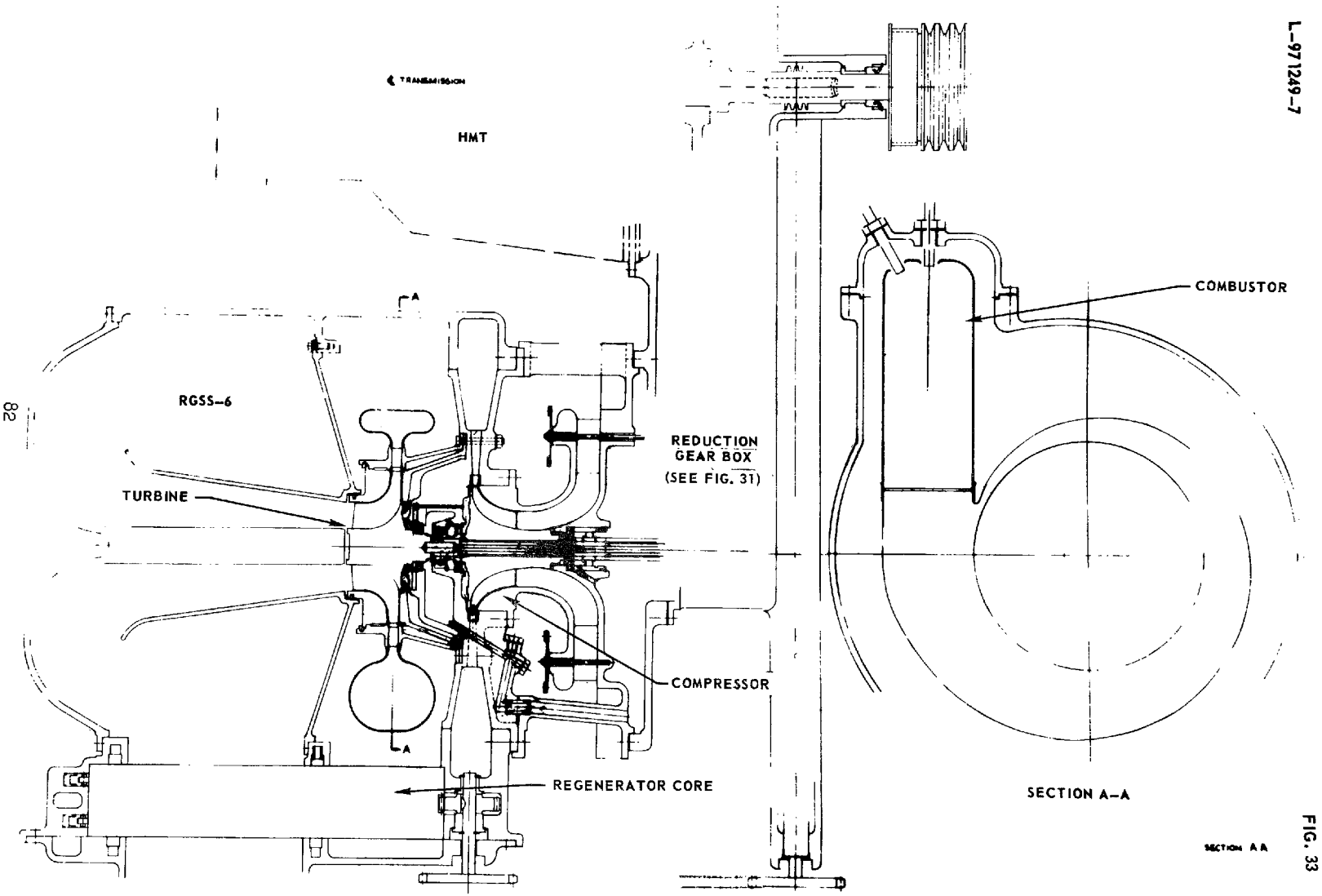

L-971249-7

FIG. 33

Another possibility is to replace the idler gear with a chain drive such as is now in use on such front-end-drive vehicles as the Oldsmobile Toronado. The initial reduction gear mesh requires carburized and ground gear teeth. Because of their lower pitch line velocities, the last two gear meshes may possibly make use of carburized, unground gear teeth.

All shafts are supported on plain bearings for low cost with the exception of the main engine shaft itself. Rolling-element bearings were retained for the input shaft since power losses in plain bearings at this speed become excessive. The specification of three main shaft bearings as shown in the layout, Fig. 31, could hopefully be reduced to two bearings.

Plain bearings were specified for low cost, except for the main shaft, where power losses would otherwise be excessive. Further engine optimization is expected to reduce the three main shaft bearings shown in Fig. 31 to two angular contact bearings, since designs for these have been satisfactorily demonstrated. For example, similar bearings designed for the Army's Mobile Equipment Research and Development Center 10 Kw Turbo-alternator have run without failure for more hours (4636 vs. 3500 design) at higher speeds (93,500 rpm vs. 74,000 rpm average).

Accessories are mounted on or are near the gearbox and are shown as belt-driven (Fig. 32). Sheaves for belt drives are provided on the 3200-rpm output shaft. In addition to driving such items as the generator and hydraulic pumps and perhaps air conditioning drives, a belt-driven starter is assumed feasible for the engine since starting torques are relatively low and cranking speeds relatively high. The gear casing contains an integral oil tank of the wet sump type. The oil pump is mounted on the casing and is directly driven by the idler shaft. A centrifugal breather impeller and hose connection is provided on the first intermediate shaft. The oil filter, oil cooler, and breather filter will be externally mounted and appropriate connections completed by hose. Exhaust from the breather filter will be connected back into the engine intake to further reduce emissions and solid oil separated from the air, and the breather filter will be drained back to the gearbox sump.

All major casings are shown as cast iron for low cost. Hot-end casings are of ductile cast iron, while the intake and gearbox casings are of gray cast iron. Aluminum could be substituted for some of the intake casings should further weight reductions be desired. The weight for the entire engine, less its accessories, is estimated to be 240 lb.

The performance of the SSS-10 engine is discussed in a subsequent section of this report.

Regenerative Engine (RGSS-6)

The regenerative-cycle engine is a single-shaft machine with all radial turbomachinery. Its layout is shown in Figs. 33 and 34. Its basic parameters are: a pressure ratio of 6:1, a mass flow of 1.49 lb/sec, a rotor speed of 82,000 rpm, and a design regenerator effectiveness of 75% using a regenerator comprising a single ceramic disc. Structural construction is quite similar to the SSS-10, except for the addition of the regenerator and its associated ducting passages. The material for the compressor is specified as titanium for long fatigue life and resistance to corrosion and is of alloy AMS 4928 (6 Al-4V). A conventional single-

FIG. 34

RGSS-6, HMT POWER SYSTEM

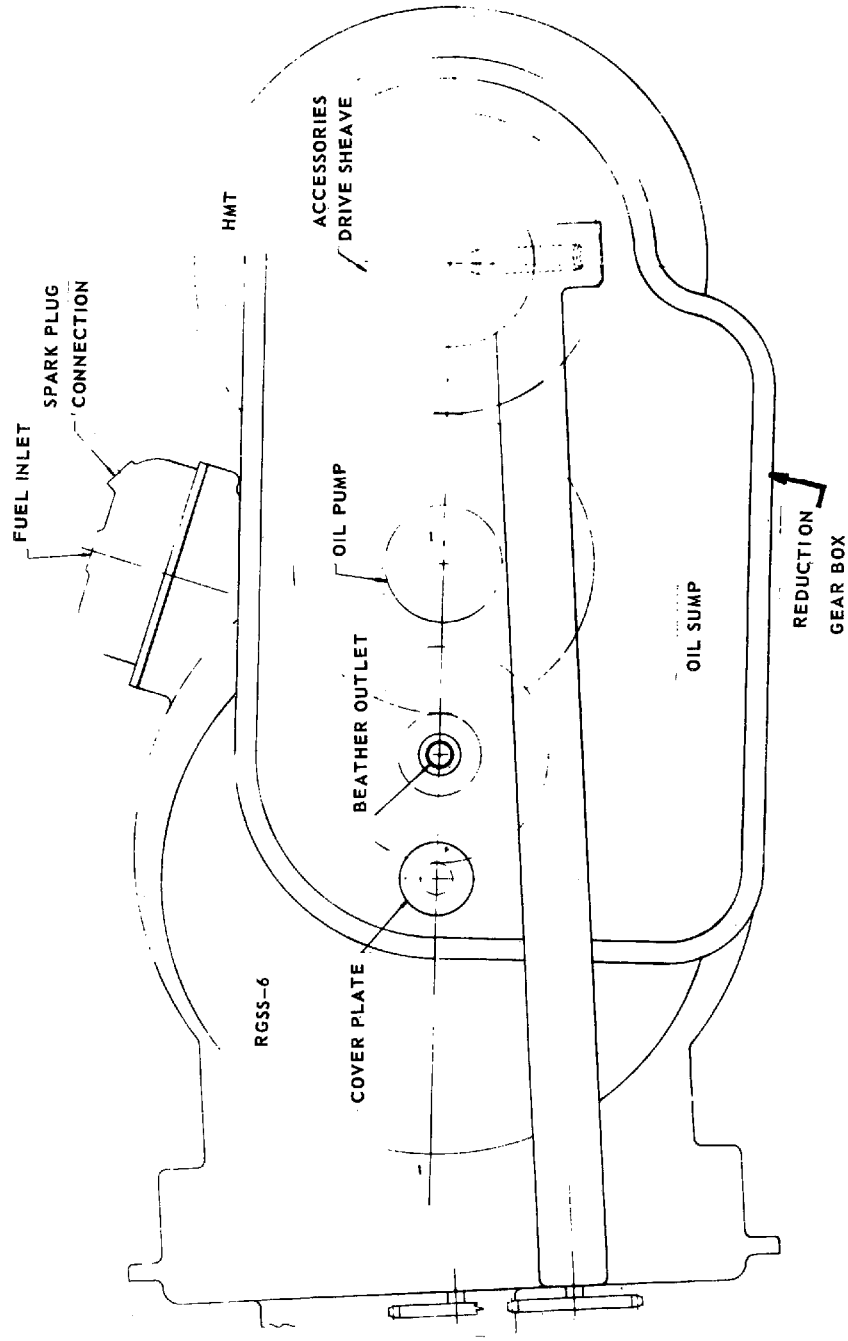

can combustor with one fuel nozzle and ignitor is shown for the regenerative engine. As will be pointed out later in the study, it is uncertain at the moment whether this type of a simple combustor can provide the required emissions reductions to meet OAP goals. It is most probable that a more complicated device involving variable geometry and perhaps multiple nozzles and multiple casings may be required to provide promise of meeting these requirements.

The exhaust gas from the turbine is diffused to reduce its Mach number and is passed through the regenerator matrix where it gives up heat to the ceramic core. It is then dumped into a plenum and makes its way to the single exit port.

The regenerator has a disc 13 inches in diameter and 2.8 inches thick and is composed of CERCOR material mounted in a steel drum. The regenerator disc rotates at approximately 20 rpm and is driven by a gearing system consisting of a worm gear set in the reduction gearbox, a cross shaft, and a chain drive to a spur gear pinion driving a ring gear on the outer drum of the regenerator core. Other candidate drive methods considered were an electric or hydraulic motor, but these were rejected as being higher-cost and less-reliable drives.

The gearbox is essentially the same as that shown for the simple-cycle engine except for (a) an increased distance between the engine centerline and the output shaft centerline to accommodate the larger engine diameter, (b) the addition of a worm gear set and cross shaft for the regenerator drive, and (c) a slight difference in reduction ratios required to achieve the 3200 rpm caused by the somewhat lower shaft speed. Design and off-design point information are shown for the RGSS-6 in Table VIII. The weight of the engine is estimated to be 520 lb.

Recuperated Engine (RCSS-8)

The recuperated engine is a single-shaft machine with all radial turbomachinery. The recuperator is a tube type which is annular in design. Its basic parameters encompass a pressure ratio of 8:1, a mass flow of 1.36 lb/sec, a rotor speed of 95,000 rpm, and a heat exchanger design effectiveness of 60%. The layout of the RCSS-8 engine and cross section is shown in Fig. 35 and an end layout is shown in Fig. 36.

The turbomachinery design of the RCSS-8 is very similar to that of the SSS-10 and RGSS-6 engines. The titanium alloy centrifugal impeller of AMS 4928 (6 Al-4V) has been selected for long fatigue life and resistance to corrosion.

Compressor air is delivered via 20 diffuser passages machined into the diffuser case to a cast passage which ducts the diffused air to the recuperator. The recuperator is a double-pass air, single-pass gas type constructed of 2280 U-tubes of 0.125 in. outer diameter and 0.010 in. thickness which are brazed to a header plate. The recuperator has a cylindrical shape with airflow axial through the tubes and gas flow radial. The material to be used in the recuperator is specified as a 300-series stainless steel.

FIG. 35

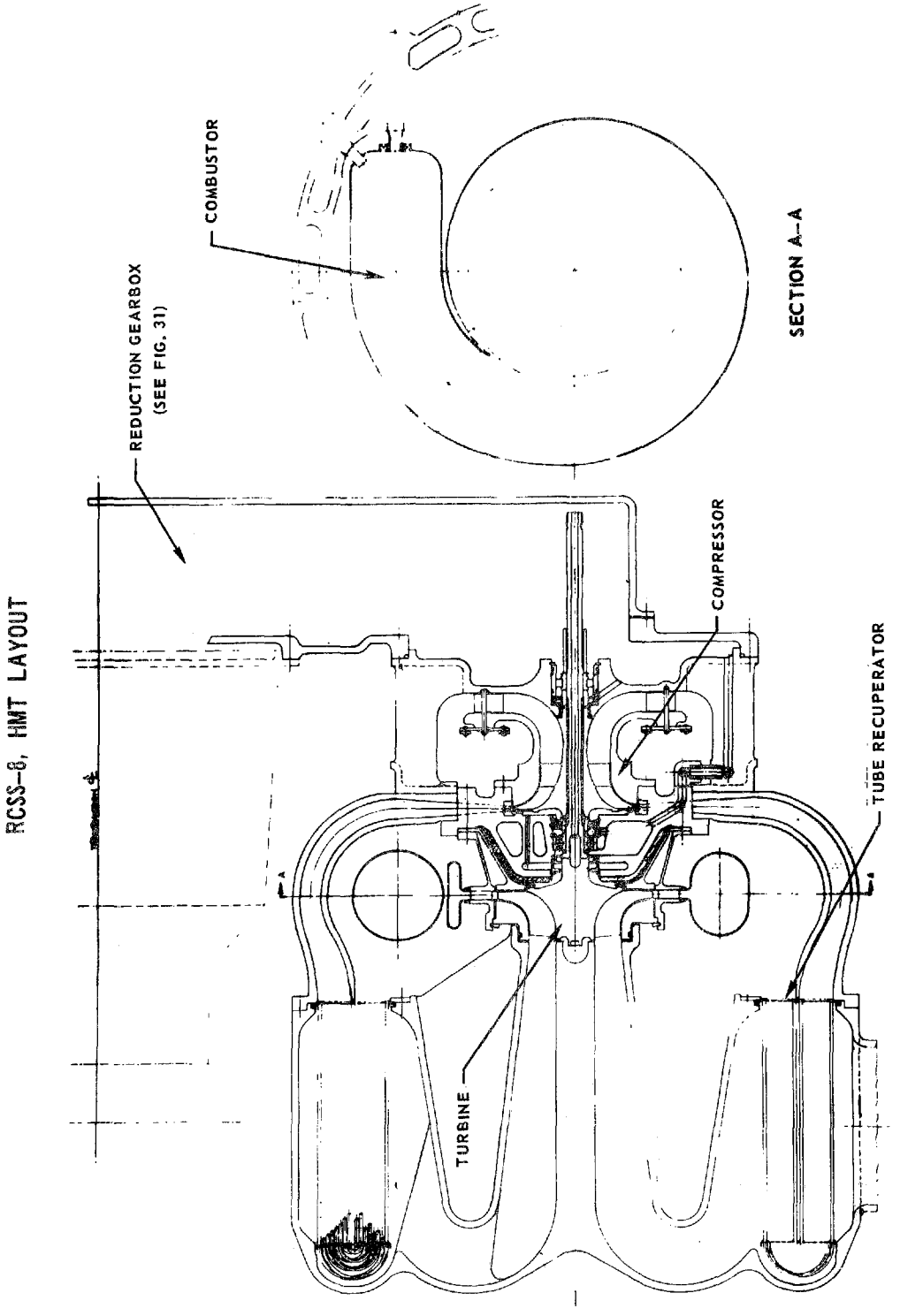
RCSS-8, HMT LAYOUT
REDUCTION GEARBOX
(SEE FIG. 31)
COMBUSTOR
SECTION A-A
COMPRESSOR
TUBE RECUPERATOR
TURBINE

FIG. 36

RCSS-8, HMT POWER SYSTEM

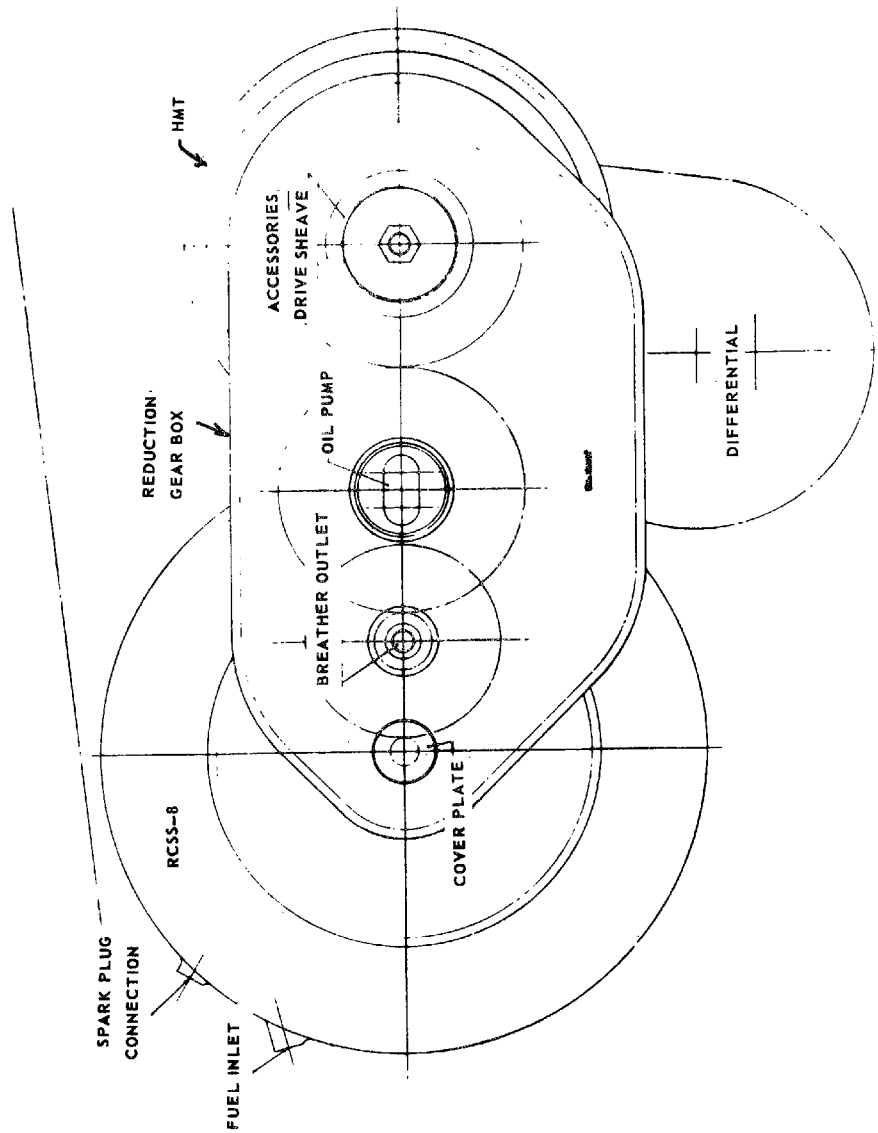

The combustor is a single-can design with a single fuel nozzle and ignitor for good combustion efficiency. In this engine, however, the combustor is buried beneath the diffuser-to-recuperator passage in order to minimize flow distortion at the entrance to the recuperator. Its size, therefore, directly influences the engine outside diameter. In order to minimize the engine diameter, the dilution portion of the combustor is curved on a radius about the engine axis. The primary zone remains cylindrical to avoid sacrificing combustion efficiency. The ignitor and fuel nozzle are fitted the flame tube through bosses cast into the diffuser passage and are accessible from outside the engine.

Exhaust ducting is constructed of ductile cast iron and may be configured either as a two-port or a single-port configuration as the installation dictates. The gearbox is essentially the same as that shown for the SSS-10 engine except that the distance between the engine centerline and the output shaft center has been increased to accommodate the larger engine diameter. As in the previous engines, all major casings are cast iron for low cost, with hot-end casings of ductile or heat-resistant cast iron, and intake and gearbox casings of gray cast iron. The weight for the entire engine, less its accessories, is estimated to be 480 lb.

Power Trains

The transfer of power from a power source to the traction (or reaction) members of a powered vehicle should ideally be performed with high efficiency (small power loss), quietness, and smoothness (small time rates of change of acceleration). The power must also be applied in the proper relationships of speed and torque to meet the wide range of conditions associated with an automobile's operation. Therefore, the power output of the engine must be controlled by engine throttle for varying loads, while the final reaction torque delivered to the wheels is controlled by a transmission system which is capable of changing the input torque to provide the required reaction force.

The power train for a gas turbine automobile essentially consists of a gearbox to reduce the engine speed to the rated speed of the transmission, a transmission which can provide varying gear ratios, a differential which provides a final overall gear ratio and a means of differentially splitting the power for a two-wheel drive, and, finally, an axle system to deliver the power to the wheels.

The design of these power-transfer components depends on the type of transmission employed, the installation configuration, the speed and torque to be carried, and the gear ratio(s) required.

Gear Reduction Box

Since the gas turbines considered in this study are rated at approximately 100,000 rpm, a large reduction in speed is required before the power can be input to the transmission. This reduction ratio is dependent on the type of transmission employed. The rated speed limits of various transmissions are assumed as follows:

Mechanical	- 6000 rpm
Hydromechanical	- 3200 rpm
Hydrokinetic	- 6000 rpm

In the case of electric transmissions, where the gas turbine drives a generator (alternator), the reduction ratio is much smaller since generators of advanced design have been operated at speeds up to 100,000 rpm.

The design of the gear system can take many forms, such as a planetary system, offset gearing, or double-reduction gearing. While one would tend toward the lightest-weight configuration, the actual installation characteristics and the mating of the engine to the transmission through the gearbox must be considered, as well as total cost.

For this study, a very compact propulsion system configuration can be achieved by mounting the engine and transmission transversely to the automobile centerline and side by side. The distance, d, between the engine output shaft and transmission input shaft varies between 17 in. and 20 in., depending on which of the three candidate engines is employed. The rated engine shaft speed among the three engines varies from 82,000 rpm to 106,000 rpm. For the specific engines, the overall reduction ratio for each engine-transmission combination is as follows:

	Transmission		
Engine	Mechanical	HMT	Hydrokinetic (TC)
SSS-10	17.7	33.1	17.7
RGSS-6	13.7	25.6	13.7
RCSS-8	15.8	29.7	15.8

Since the rotor of each engine has a high level of rotational energy (inertia), it is desirable to minimize the added inertia of the reduction gearbox to help maximize the transient response of the engine to throttle variations.

The kinetic energy, E, of each gear is

$$E = \frac{1}{2} I \omega^2 \qquad (1)$$

where "I" is the moment of inertia of the gear about its rotational axis and "ω" is its rotational velocity. Assuming each gear is a solid disc, the moment of inertia of each is

$$I = \tfrac{1}{2}\,\pi m r^4 t \tag{2}$$

where: m = mass density of gear, slugs/in.^{3}
r = pitch radius of gear, in.
t = gear thickness, in.

Combining Eqs. (1) and (2) yields:

$$E = \tfrac{1}{4}\,\pi m t \omega^2 r^4 \tag{3}$$

Simple offset gearing for large reduction ratios involves a large final gear which tends to be heavy and is volumetrically inefficient; therefore, double-reduction gearing is employed.

The radius of the pinion driven by the engine must be sufficiently small to avoid supersonic tip speed (creating a noise-producing shock wave and making it difficult to use spray lubrication) and yet large enough to carry the engine-produced torque. A one-inch radius pinion rotating at 106,000 rpm would have a tooth tip speed of 922 fps, which is nearly supersonic. Therefore, the maximum radius will be limited to about one inch.

The total rotational energy of the four gears in a double reduction system can be written as

$$E = \tfrac{1}{4}\,\pi m t (\omega_1^2 r_1^4 + \omega_2^2 r_2^4 + \omega_3^2 r_3^4 + \omega_4^2 r_4^4) \tag{4}$$

assuming the gears are made of the same material and are the same thickness. Then, an energy parameter, ε, can be defined as:

$$\varepsilon = \frac{4E}{\pi m t \omega_1^2} = r_1^4 + r_1^2 r_2^2 + \frac{r_1^2 r_3^4}{r_2^2} + \frac{r_4^4}{R_0^2} \tag{5}$$

where: R_0 = overall reduction ratio
$r_{1,2,3,4}$ = pitch radii of four gears, in.

For known values of r_1 and r_2, the radii of the remaining two gears are

$$r_3 = \frac{d-r_1-r_2}{1+\left(\frac{r_1}{r_2}\right)R_O}, \quad r_4 = \left(\frac{r_1 r_3}{r^2}\right)R_O \tag{6}$$

In Eq. (5), the gear face width (thickness), t, was assumed to be constant. However, the face width is a function of the power to be transferred and the rotational speed. This relationship is expressed as

$$D^2 t = \frac{31{,}500\ hp\ (R+1)^3}{k\ \omega\ R}, \tag{7}$$

where D = distance between gear center lines, in.
t = face width, in.
= input horsepower
R = reduction ratio
ω = pinion speed, rpm
= surface durability factor, lb/in.^{2}

Also:

$$D = r_1 + r_2 \tag{8}$$

where r_1 = pinion radius and r_2 = radius of mating gear. Equation (8) can also be written as

$$D = r_1(1 + R). \tag{9}$$

Substituting Eq. (9) into Eq. (7) yields

$$t = \frac{31{,}500\ hp}{k\omega_1 r_1^2}\left[\left(\frac{r_2}{r_1}\right)+ 1\right] \tag{10}$$

FIG. 37

INERTIAL ENERGY PARAMETER FOR DOUBLE-REDUCTION GEARING

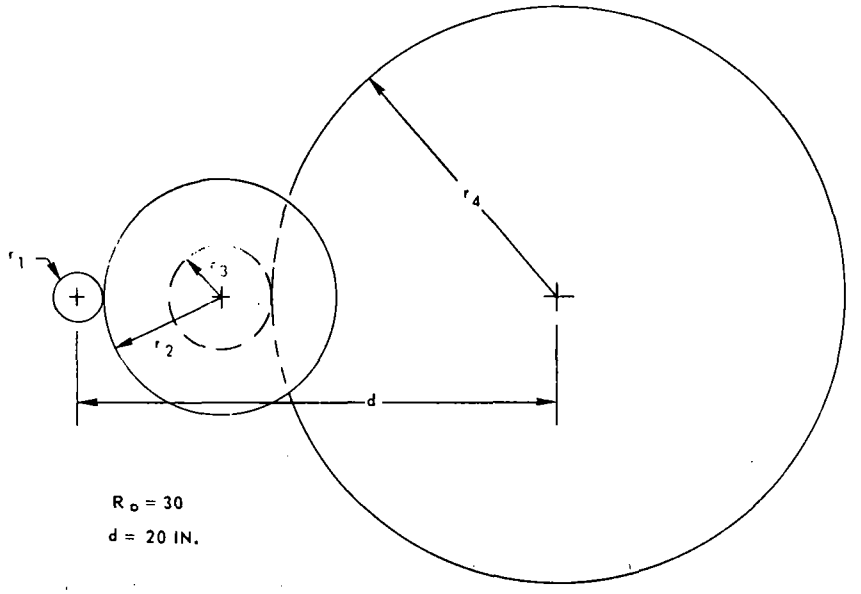

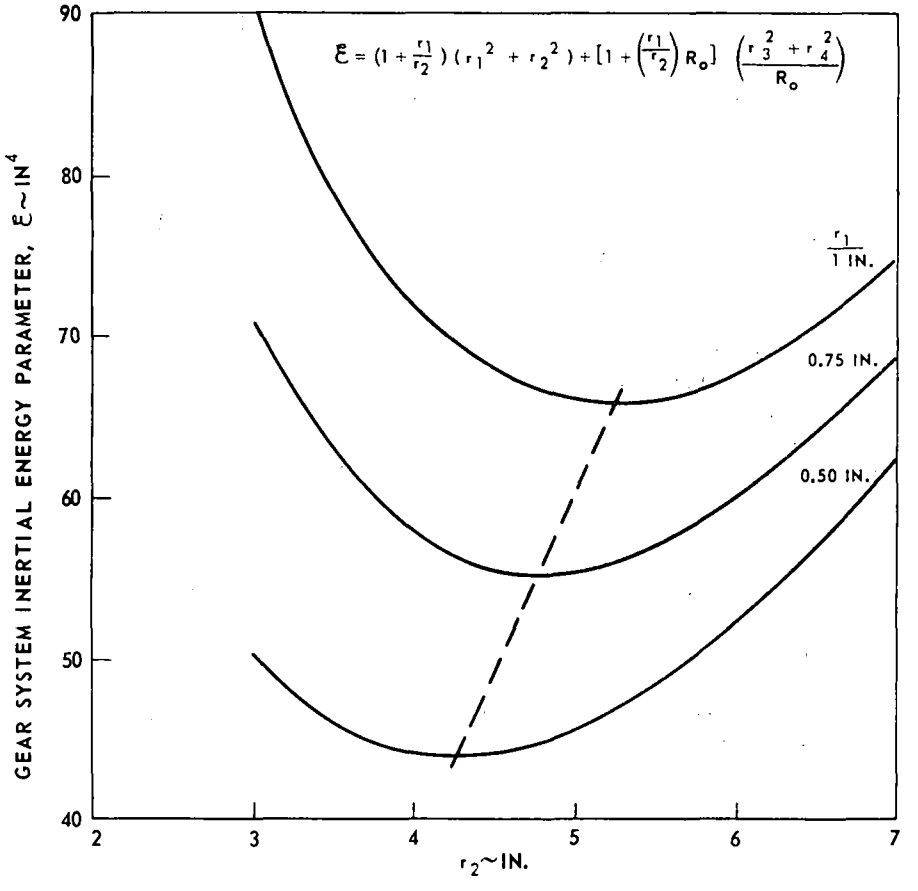

A face width parameter, τ, can be defined as

$$\tau_1 = \frac{\left[\left(\frac{r_2}{r_1}\right) + 1\right]}{r_1^2} \tag{11}$$

The second set of reduction gears can be analyzed in a similar manner, yielding

$$\tau_2 = \frac{r_2}{r_1 r_3^2}\left(\frac{\frac{r_2}{r_1} + R_o}{R_o}\right) \tag{12}$$

By applying Eq. (11) to the first two terms of Eq. (5), and Eq. (12) to the last two terms, Eq. (5), modified for gear thickness, becomes

$$\varepsilon = \left(1 + \frac{r_1}{r_2}\right)\left(r_1^2 + r_2^2\right) + \left[\frac{1 + \left(\frac{r_1}{r_2}\right) R_o}{R_o}\right]\left(r_3^2 + r_4^2\right) \tag{13}$$

Substituting Eq. (6) into Eq. (13) yields an expression for ε in terms of the characteristics of the pinion and mating gears.

$$\varepsilon = \left(1 + \frac{r_1}{r_2}\right)\left(r_1^2 + r_2^2\right) + \frac{(d - r_1 - r_2)^2}{1 + \left(\frac{r_1}{r_2}\right) R_o}\left[\frac{1}{R_o} + \left(\frac{r_1}{r_2}\right)^2 R_o\right] \tag{14}$$

Figure 37 presents the variation of the gear system inertial energy parameter, ε, with pinion gear and mating gear size. With a 0.5-in. radius pinion, the total inertial energy is about 30% less than that for the 1.0 in. radius pinion, for the minimum-ε cases. The 0.5-in. pinion requires a 4-in. mating gear. The corresponding third and fourth gears will have radii of 3.26 in. and 12.23 in., respectively.

Since the gearbox weight will be a small fraction of total vehicle weight, its weight effect on vehicle performance will be small. However, the gears' inertia directly affects the response of the engine to throttle changes and is therefore the dominant factor to be considered.

Figure 38 presents the radii of the third and fourth gears in the double reduction system. The radius of the final gear is rather large and contributes a significant amount to the total gear system inertial energy. The basic problem with using single-stage double reduction gearing is the relatively large span

FIG. 38

GEAR SIZE RELATIONSHIPS

d = 20 IN.

R_a = 30

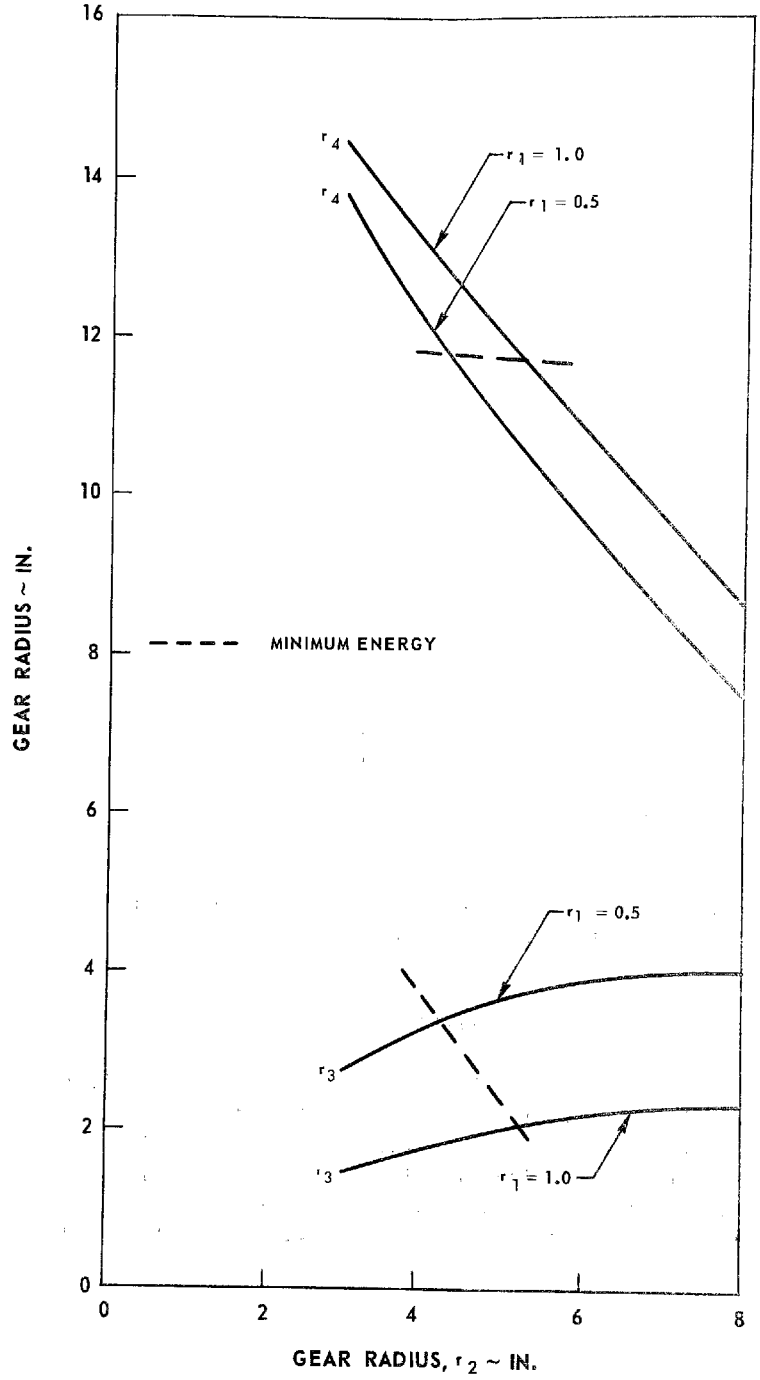

between the input and output shafts. If this distance were smaller, the final gear size could be reduced. The same effect can be achieved by adding a fifth gear the same size as the final gear, as an idler. A schematic is shown in Fig. 39

With the idler in the system, the energy parameter, ε, is defined as

$$\varepsilon = r_1^4 + r_1^2 r_2^2 + \left(\frac{r_1}{r_2}\right)^2 r_3^4 + \frac{2\, r_4^4}{R_o} \,. \tag{15}$$

The gear radii r_3 and r_4 are:

$$r_3 = \frac{d - r_1 - r_2}{1 + 3\left(\frac{r_1}{r_2}\right) R_o} \,, \quad r_4 = \left(\frac{r_1 r_3}{r_2}\right) R_o \tag{16}$$

The inertia energy parameter, corrected for varying gear thickness becomes

$$\varepsilon = \left(1 + \frac{r_1}{r_2}\right)\left(r_1^2 + r_2^2\right) + \left[\frac{d - r_1 - r_2}{1 + 3\left(\frac{r_1}{r_2}\right) R_o}\right]^2 \left[1 + 2\left(\frac{r_1}{r_2}\right)^2 R_o^2\right]\left[\frac{1 + \left(\frac{r_1}{r_2}\right) R_o}{R_o}\right] \tag{17}$$

The inertial energy for this gear train system is about 50% lower than for the standard double reduction system, as seen by comparing Figs. 37 and 39. Also, the gear sizes are significantly reduced, as evidenced in Fig. 40. Now the largest gear is only 5 in. radius. Consequently, the double reduction system with an idler was chosen for the reduction gearbox in this study.

Installation Concepts

The installation of any power/transmission system in an automobile should provide for easy maintenance, minimal susceptibility to impact damage, and should not encumber the driver or passengers. The selection of a single-shaft gas turbine offers great flexibility as to installation in a full-size six-passenger sedan, because of its small size and light weight. The HMT was chosen as a candidate transmission for purposes of examining the installation problem. The engine and transmission can be mounted transversely and neatly connected with a double

FIG. 39

INERTIAL ENERGY PARAMETER DOUBLE-REDUCTION GEARING WITH IDLER

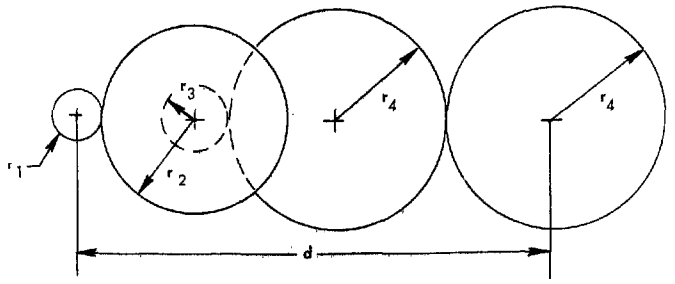

d = 20 IN.

R_o = 30

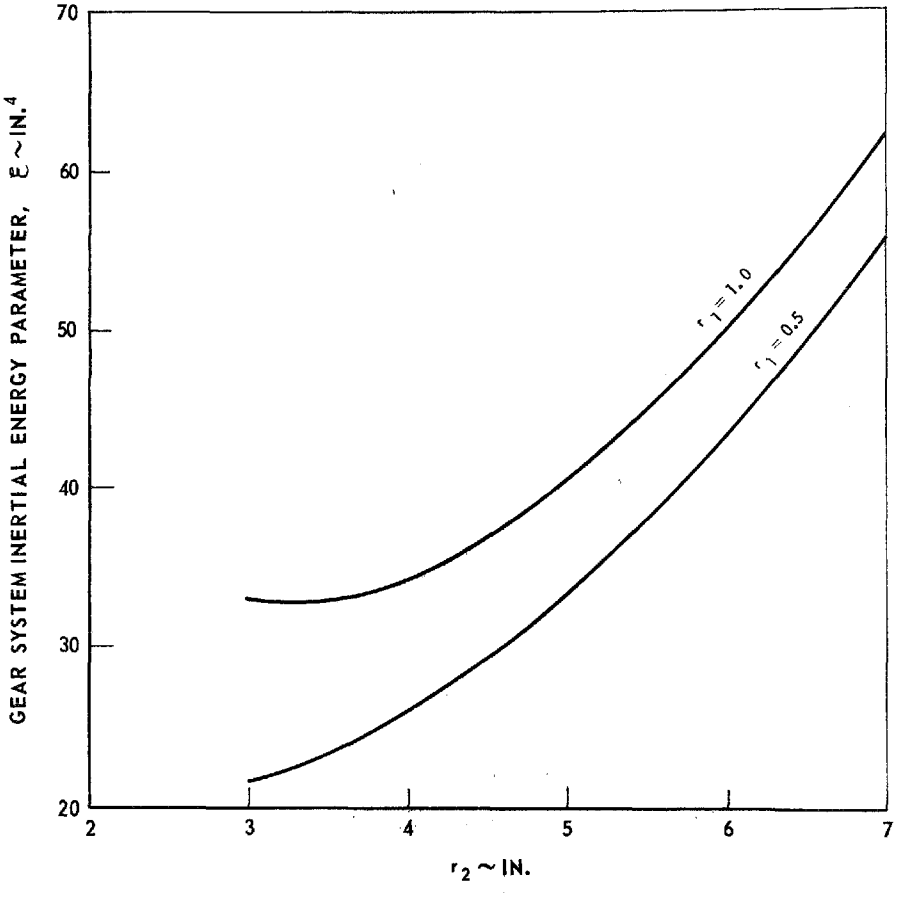

DOUBLE REDUCTION GEARING

GEAR SIZE RELATIONSHIPS

d = 20 IN.
R_o = 30

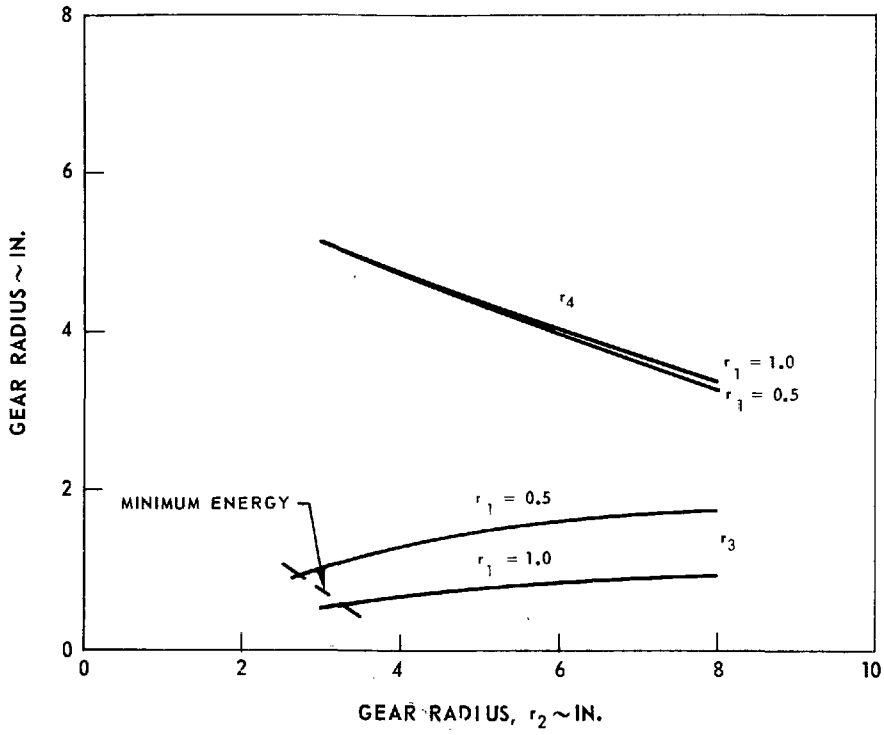

FIG. 41

INSTALLATION SKETCH, SINGLE-SHAFT GAS TURBINE WITH HMT, [illegible]

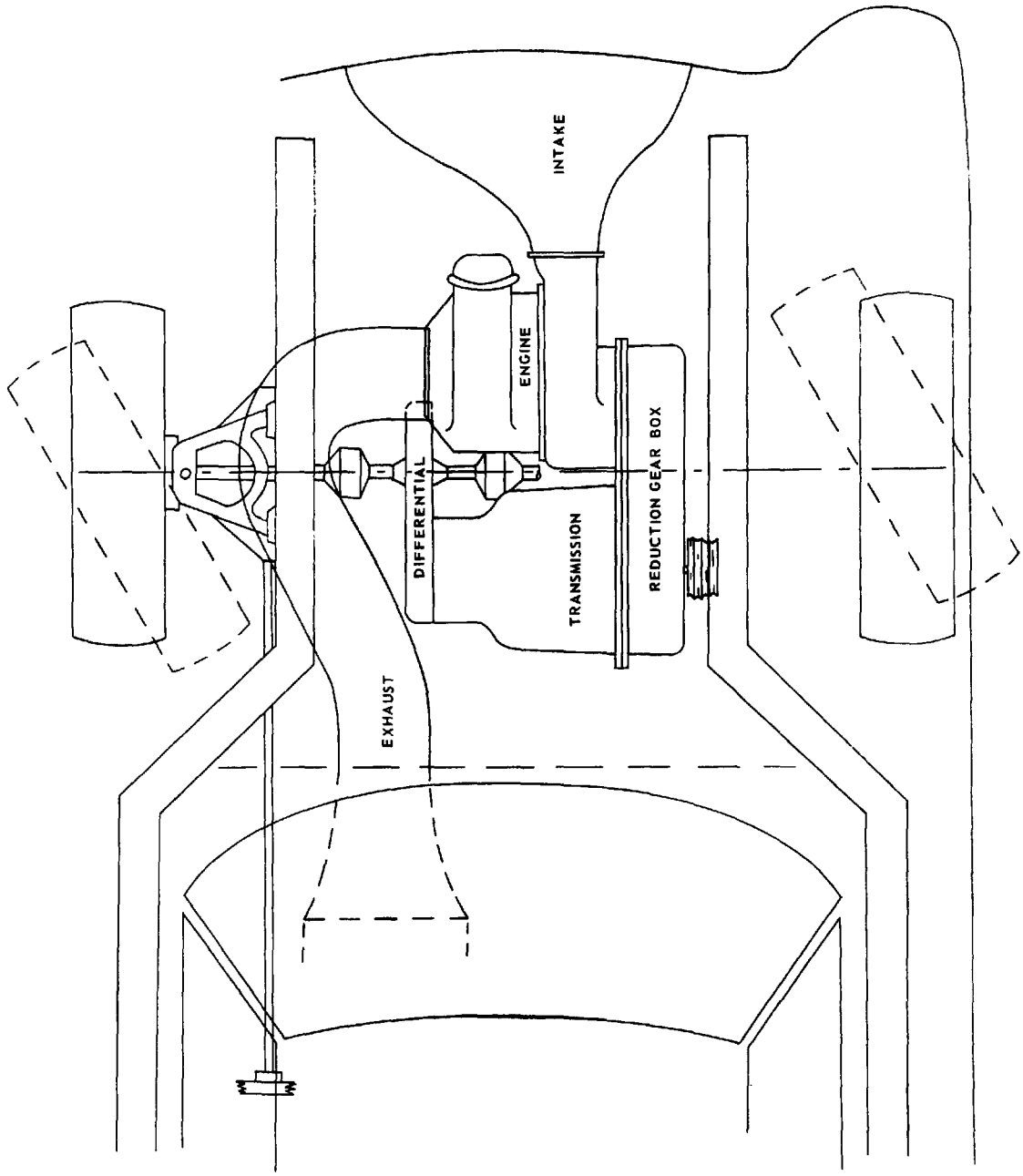

reduction gearbox incorporating an idler. The final drive would be through the epicyclic differential. This arrangement is so compact that a front-wheel drive (FWD) configuration could easily be developed. Such a system is shown in Figs. 41, 42, and 43 for a simple-cycle engine. Drive-line flexibility can be provided with Rzeppa joints. Figure 41 shows the entire unit neatly mounted between the frame members.

The air intake is shown only schematically; an actual system would incorporate a filter system and moisture trap. The exhaust system is conceived to be a straight-through system which is muffled by long-strand fiber glass, contained by inner walls perforated according to the noise profile over the length of the system. The 6-in. exhaust pipe will flatten beneath the vehicle to provide road clearance. The accessory drive is taken from the idler gear of the reduction gearbox in the form of a series of pulley belts. Because of the low engine torque, a belt-drive starter can be incorporated.

The installation shown would allow a large, flat floor space for the front-seat occupants, and more importantly provides a large amount of empty space between the engine and grill of the vehicle, which is vital in avoiding serious and expensive damage in light, to moderate, collisions. It is felt that the insurance companies will watch closely the development of the low-emission systems and would most certainly impose high rates on any system which is excessively vulnerable to light collisions. An example would be a collision in which a standard vehicle sustains a broken grill, a smashed radiator, and fan. A new radiator core costs about $60 and the fan about $25. This same collision would only bend the intake ducting for the single-shaft gas turbine-powered vehicle. Conversely, a Rankine-cycle system would probably sustain damage to the condensor, vapor generator, regenerator, condensor fans, and considerable plumbing. If such components were repairable at all, the total labor costs would be very high, and replacement costs would be similarly severe.

The same basic unit would also make an attractive rear-engine installation, as shown in Figs. 44 and 45. The air intake would be through openings near the rear of the car, using either protruding scoops or flush grilles, depending on the pressure distribution and airflow in that particular area, as well as styling features.

The exhaust would be serpentined to provide sufficient length for muffling and exhaust-gas cooling. Note that the rear-engine system also provides substantial crush-structure between the rear bumper and the engine.

The regenerated and recuperated single-shaft configurations are somewhat larger than the simple-cycle unit, but can still be installed quite nicely in the same basic configurations. Figures 46 and 47 illustrate the front-drive system using the recuperated engine. Note that the engine and transmission are reversed to allow hood clearance over the engine. The rear-drive installation for the recuperated engine is shown in Figs. 48 and 49.

L-971249-7

FIG. 42

INSTALLATION SKETCH, SSS-10 WITH HMT, FRONT-WHEEL DRIVE

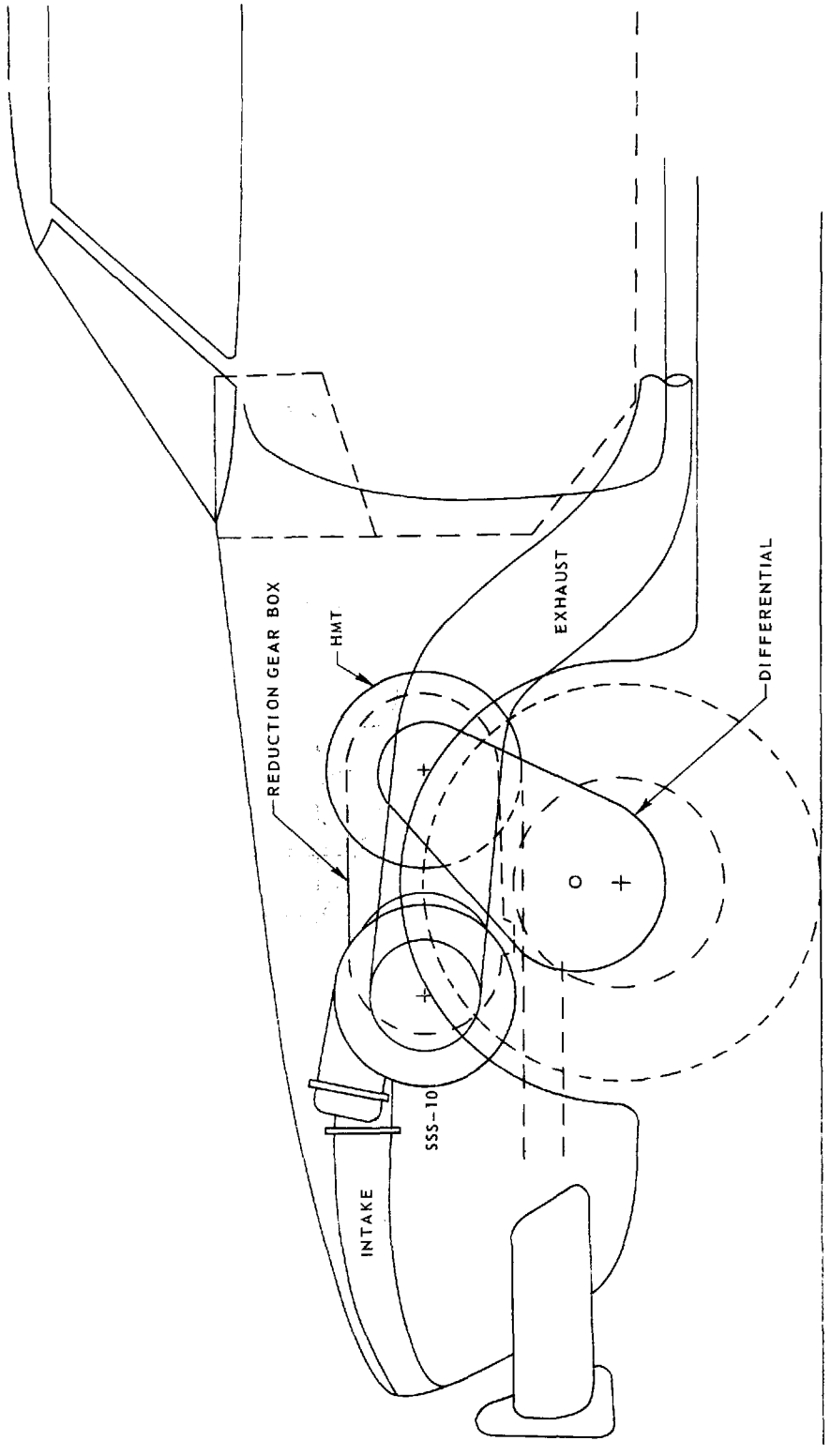

L-971249-7

FIG. 43

INSTALLATION SKETCH, SSS-10 WITH HMT, FRONT-WHEEL DRIVE

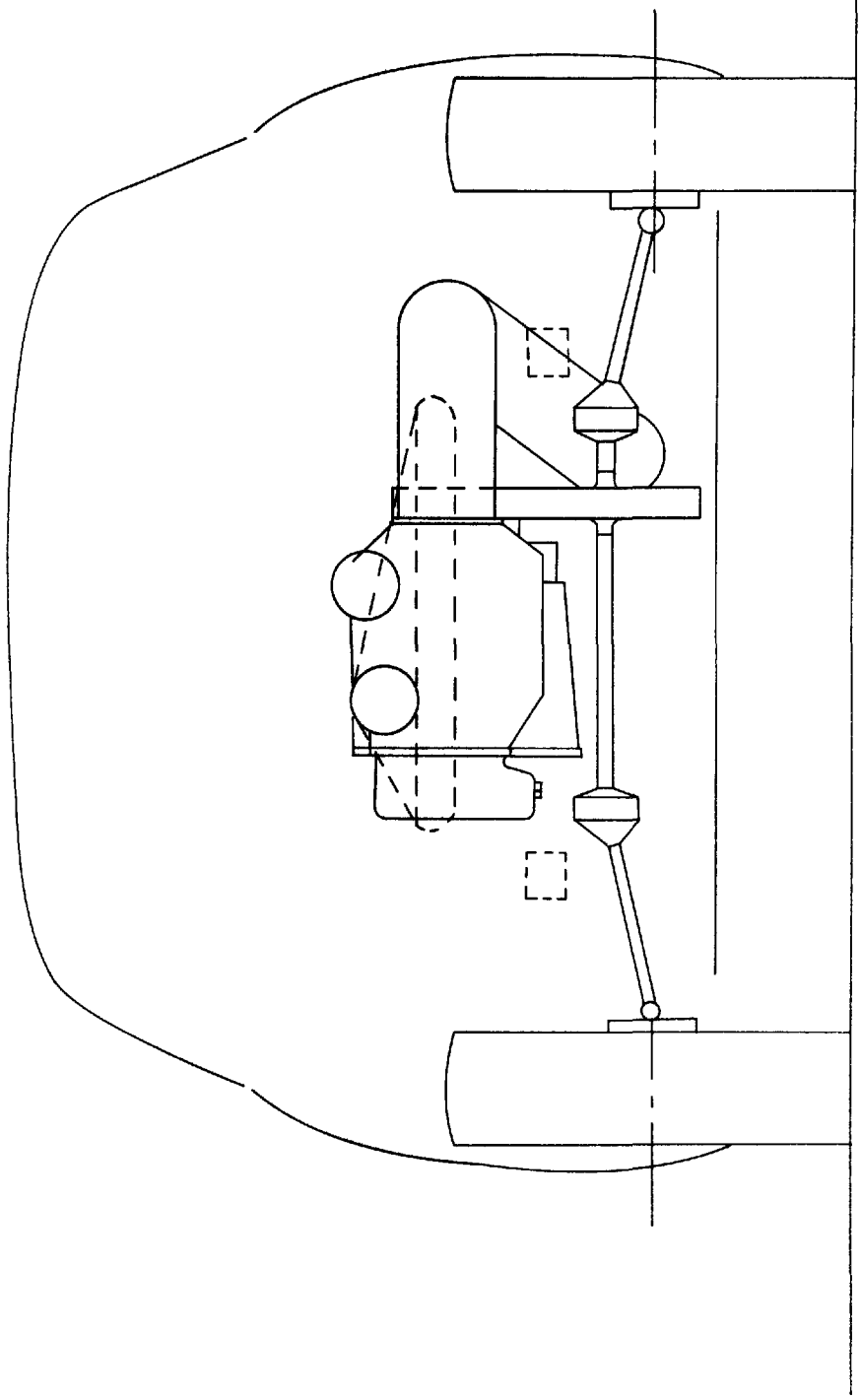

FIG. 44

INSTALLATION SKETCH, SINGLE-SHAFT GAS TURBINE, WITH FWT, REAR-WHEEL DRIVE

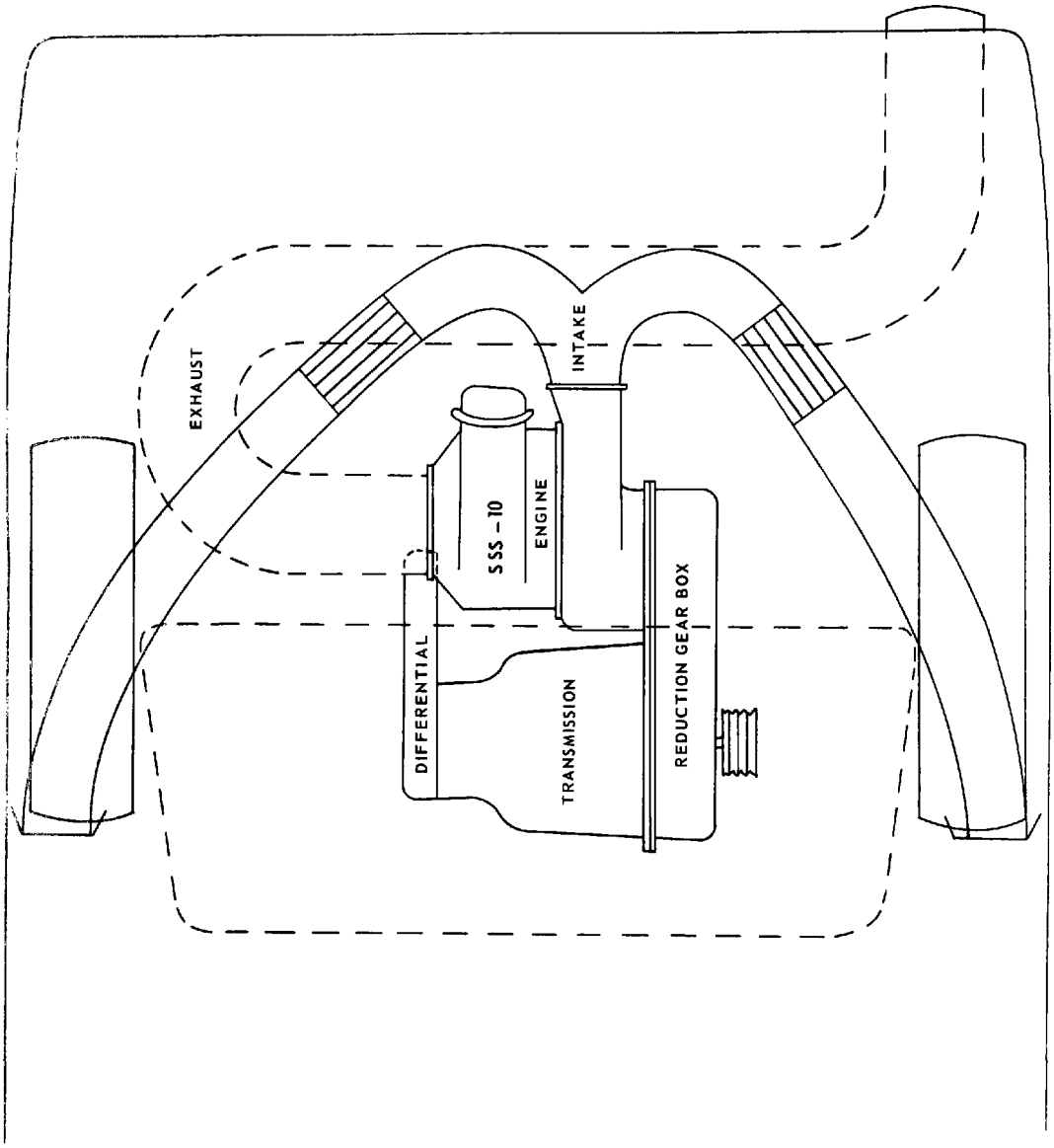

INSTALLATION SKETCH, SSS-10 WITH HMT, REAR-ENGINE DRIVE

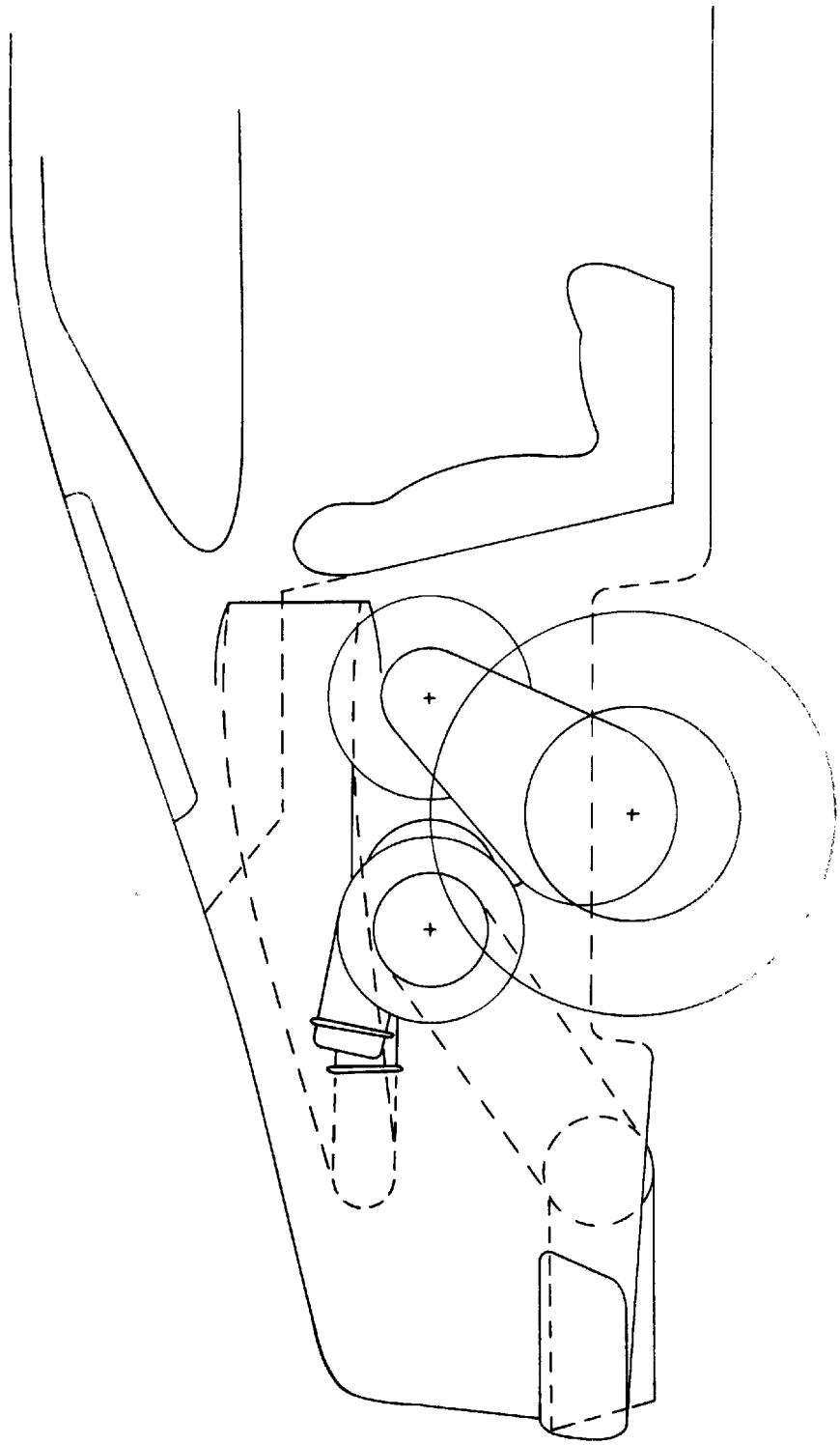

FIG. 46

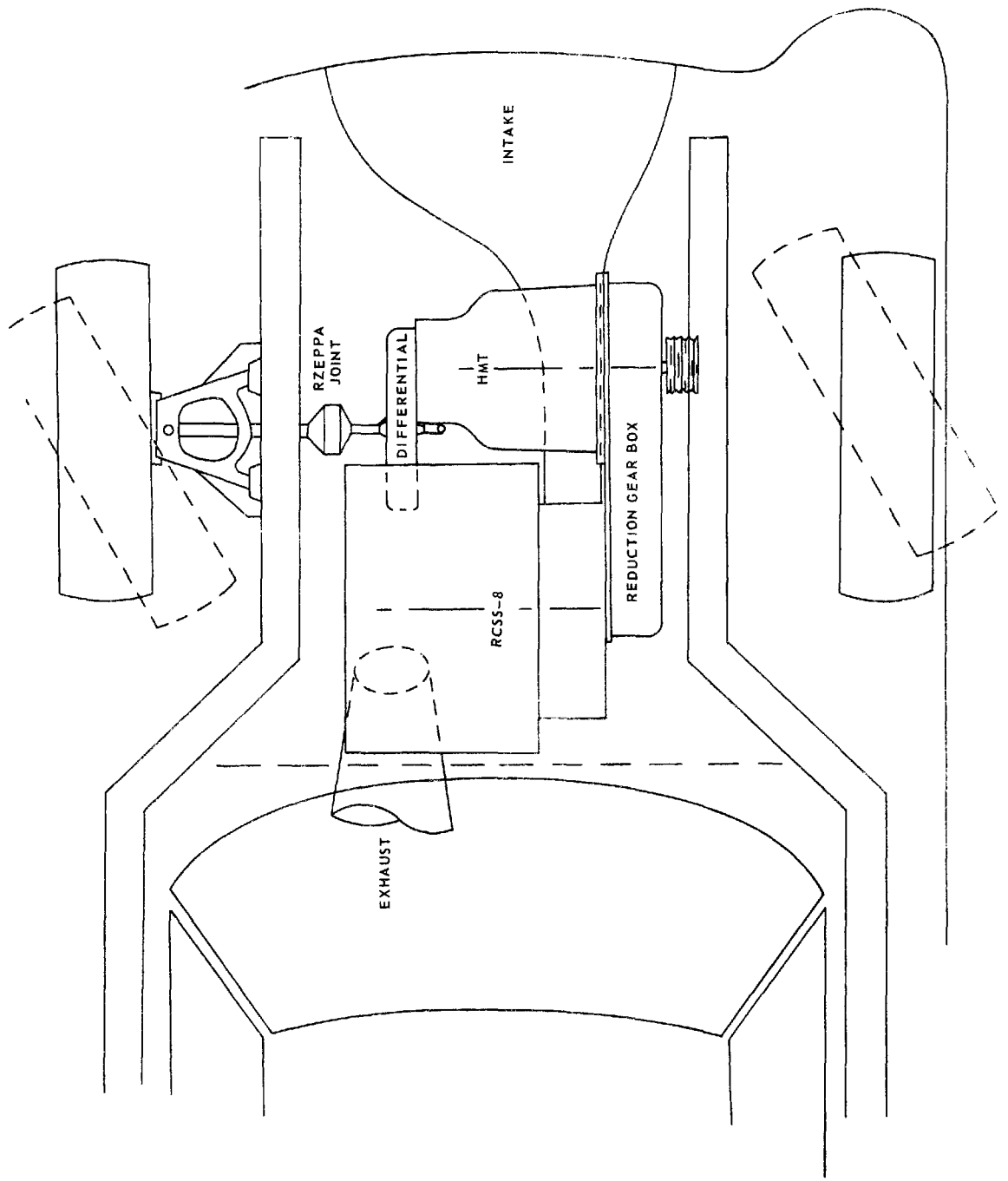

INSTALLATION SKETCH, RCSS-8 WITH HMT, FRONT-WHEEL DRIVE

L-971249-7

FIG. 47

INSTALLATION SKETCH, RCSS-8 WITH HMT, FRONT-WHEEL DRIVE

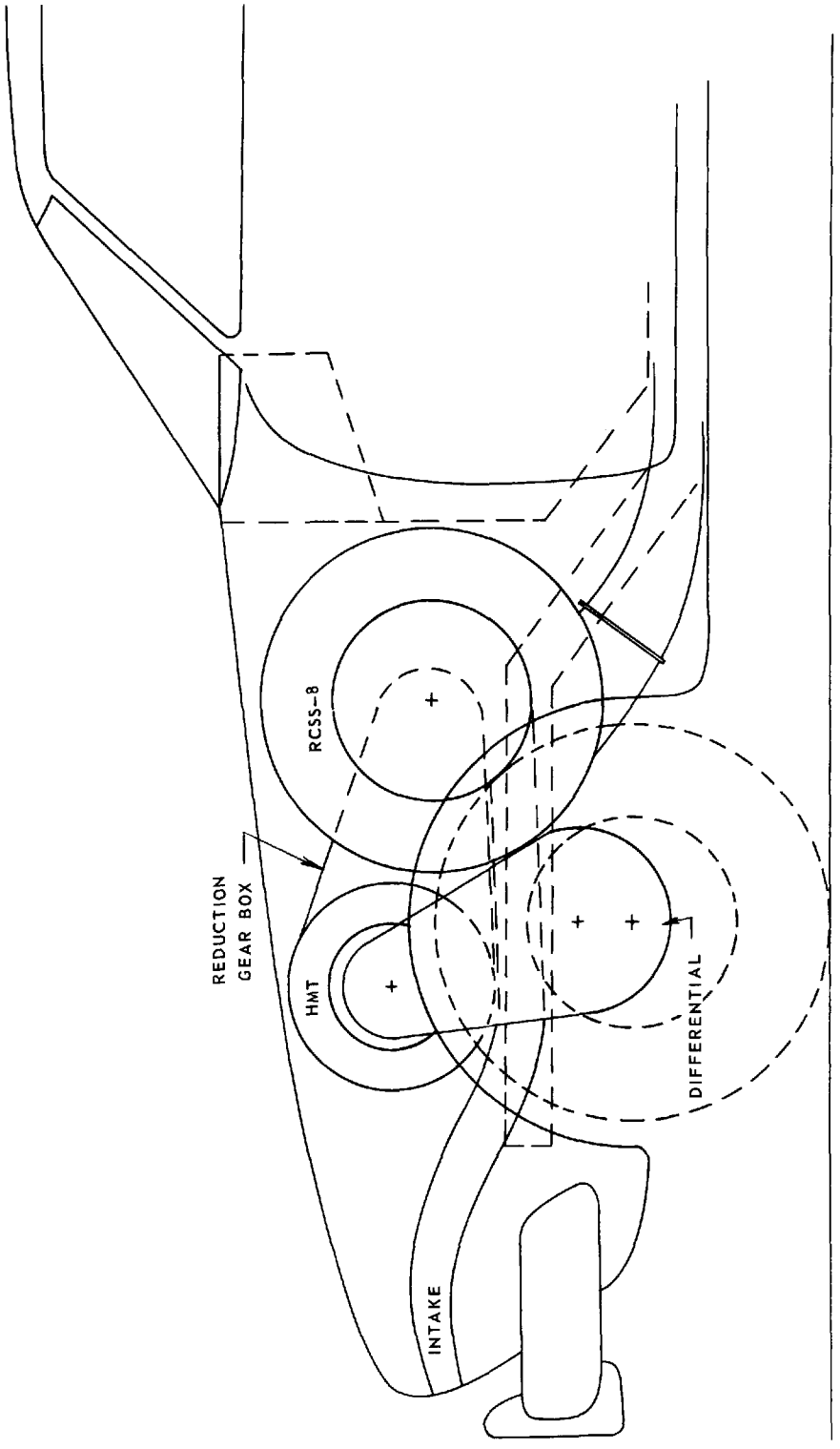

L-971249-7

FIG. 48

INSTALLATION SKETCH, RCSS-8 WITH HMT, REAR-ENGINE DRIVE

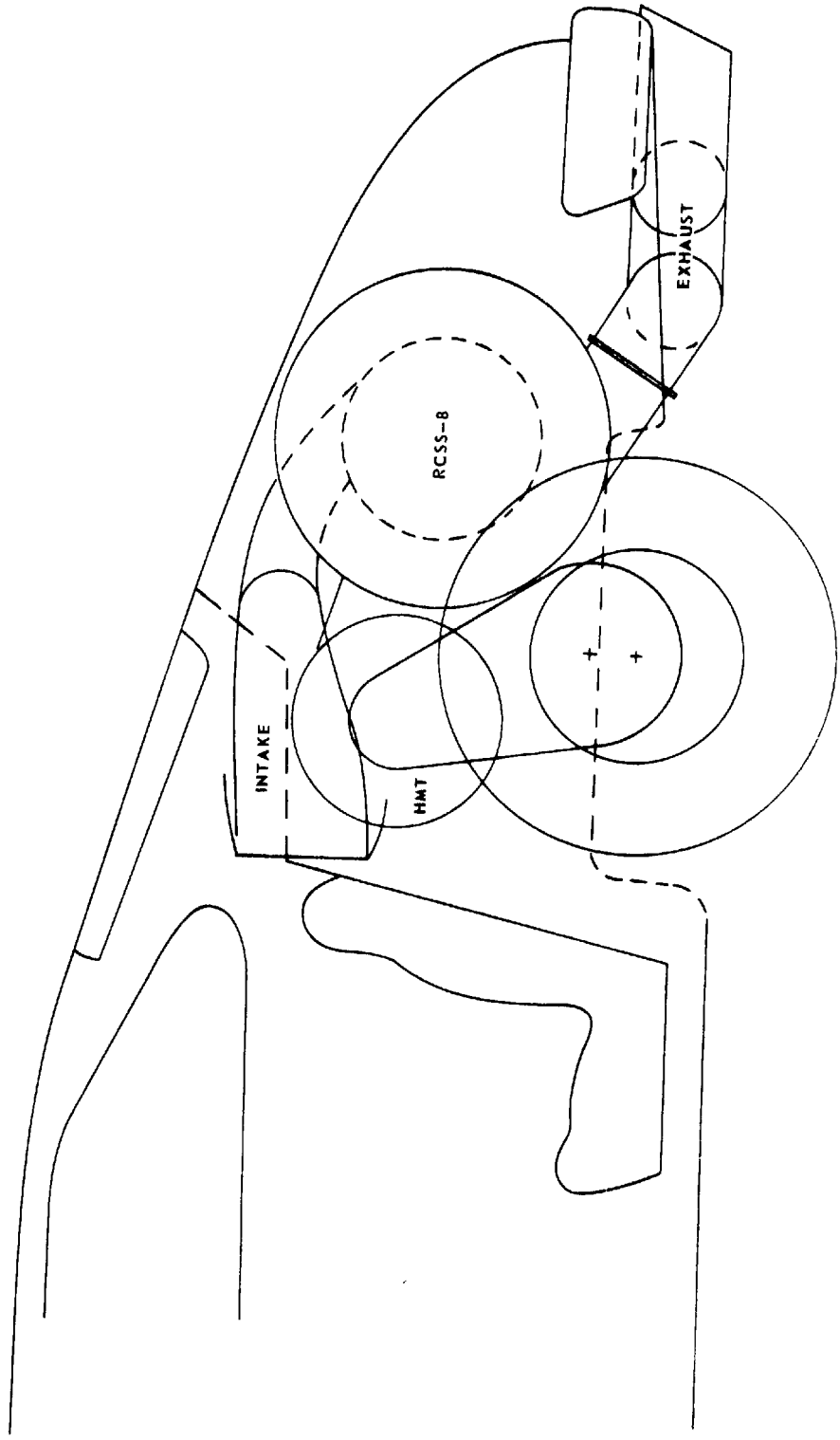

FIG. 49

INSTALLATION SKETCH, RCSS-8 WITH HMT, REAR-ENGINE DRIVE

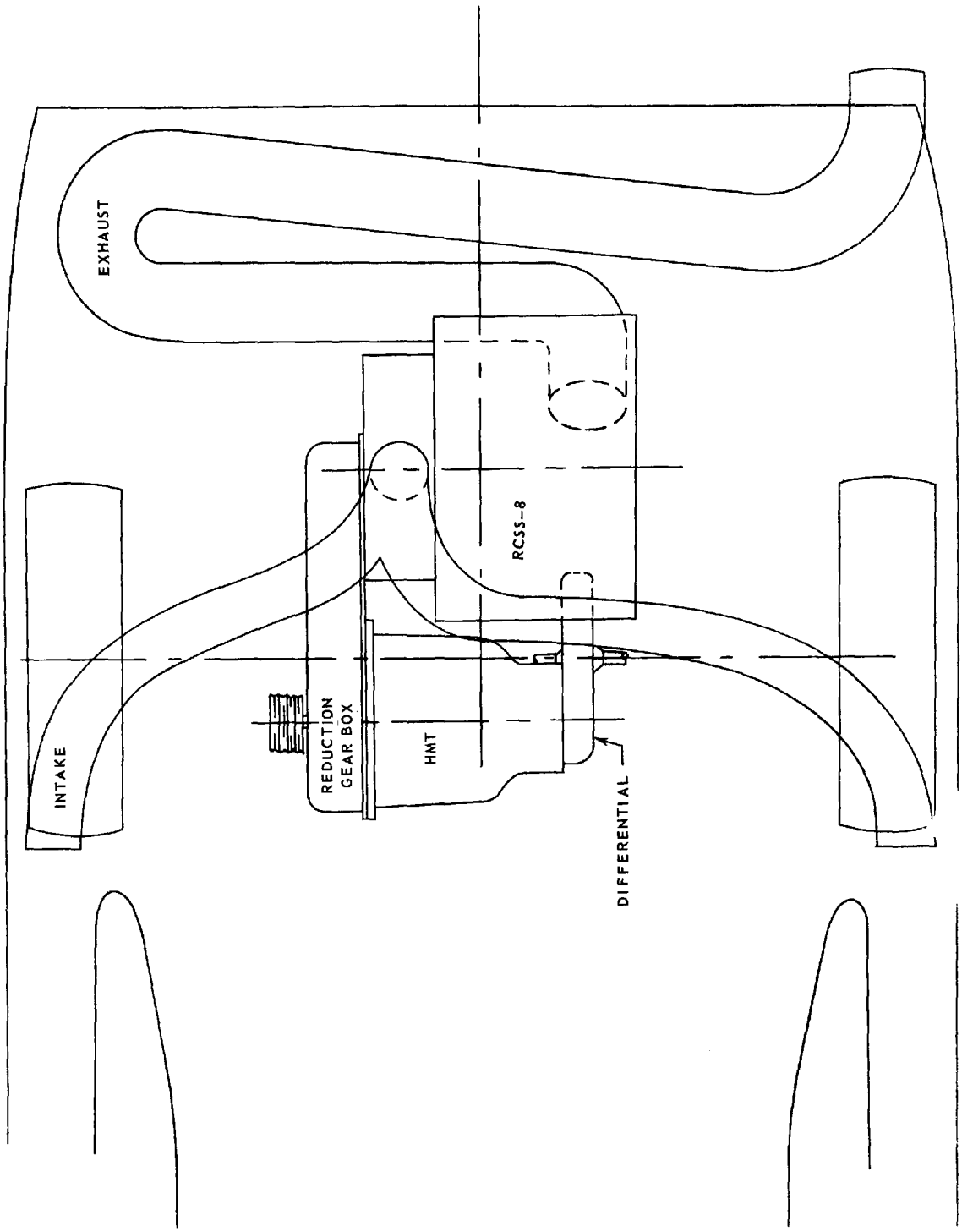

FIG. 50

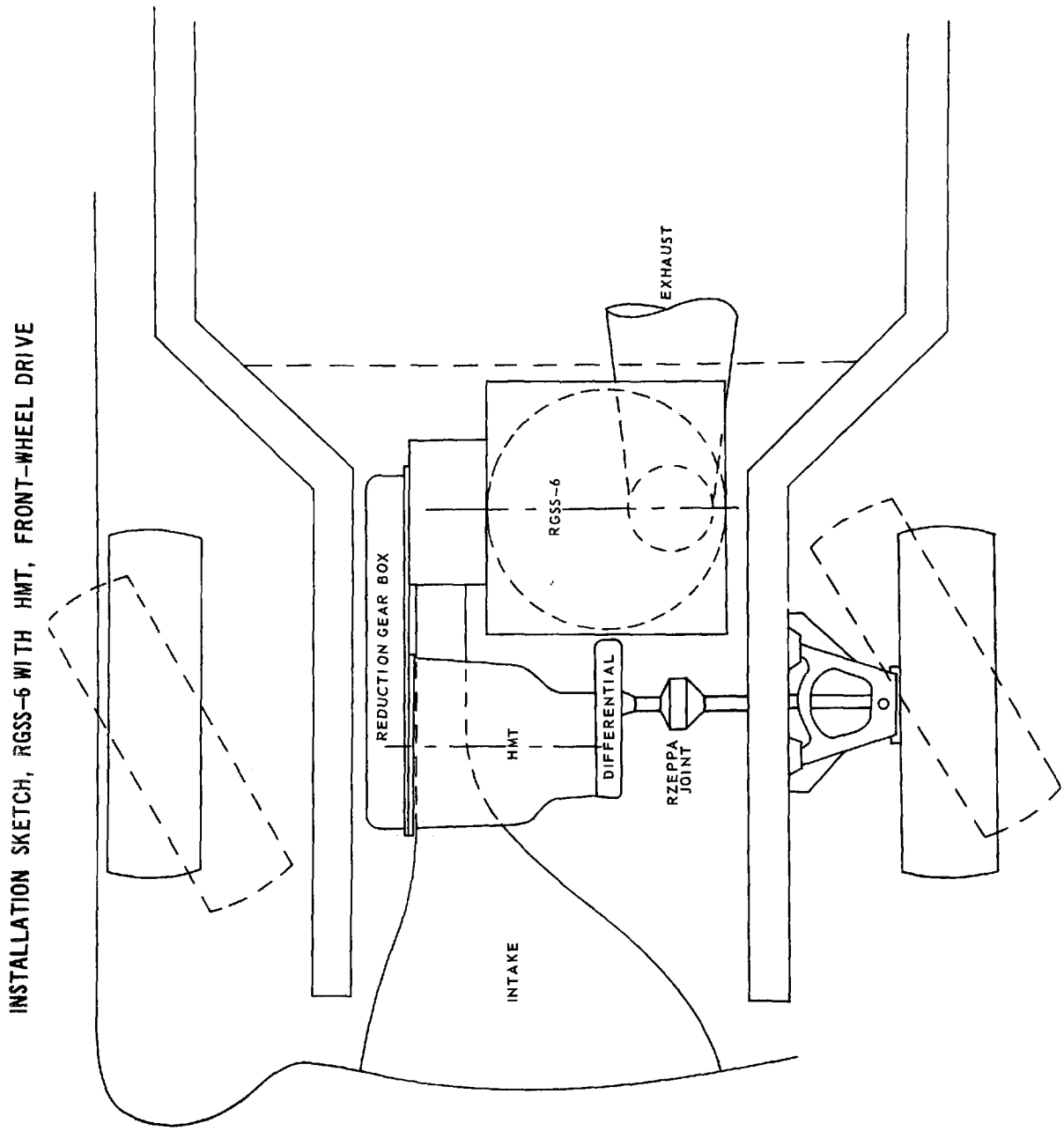
INSTALLATION SKETCH, RGSS-6 WITH HMT, FRONT-WHEEL DRIVE
EXHAUST
RGSS-6
REDUCTION GEAR BOX
HMT
DIFFERENTIAL
RZEPPA JOINT
INTAKE

FIG. 51

INSTALLATION SKETCH, RGSS-6 WITH HMT, FRONT-WHEEL DRIVE

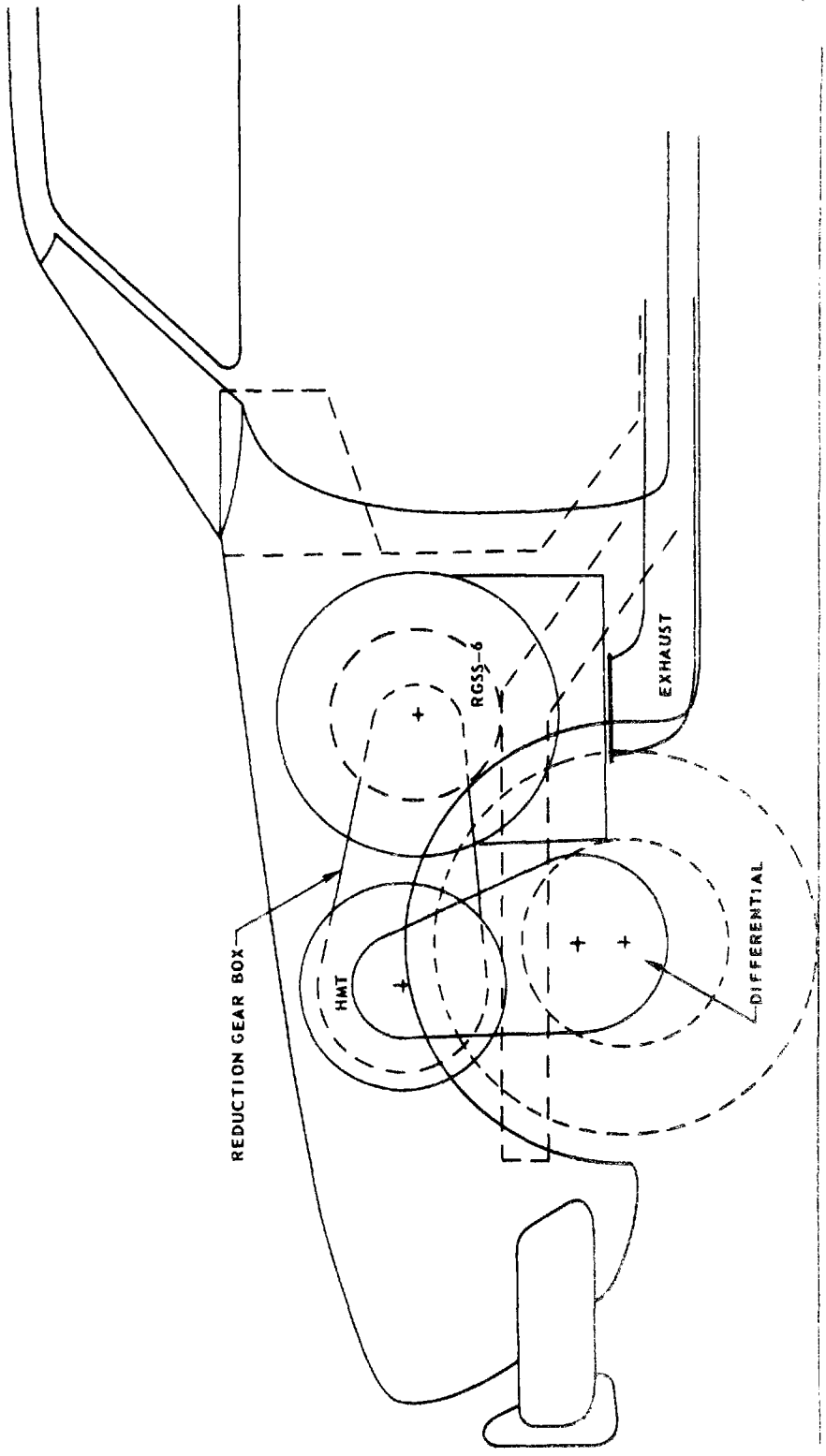

The large regenerated engine is shown in Figs. 50 and 51 for the front-wheel drive vehicle. The rear-engine system is very similar to the recuperated engine installation.

Fuel Control

Introduction

This section summarizes the study program conducted by the United Aircraft Hamilton Standard Division for a fuel control for an automotive gas turbine. The program was undertaken to conceptually design fuel control systems for three different engines; namely, single-shaft simple-cycle, single-shaft recuperative, and single-shaft regenerative engines. The fuel control system discussed in this report satisfies the requirements for all three engines when used in conjunction with the General Electric infinitely variable HMT transmission.

The selected mode of control for this application consists of a fuel flow/compressor discharge pressure (Wf/P3) schedule with exhaust gas temperature (EGT) limiting. A detailed discussion of the reasons for this mode selection is presented later. In addition, a schematic diagram and a control packaging concept have been generated and are discussed at length.

The control evolved during this study program is basically a hydromechanical unit with an integral fuel pump, a remote inlet guide vane (IGV) actuator and a remote EGT sensor. Specific design features of the control include the following:

1. Control of starting, acceleration, and deceleration fuel flow
2. Automatic start sequencing as a function of pump (and engine) speed
3. Exhaust gas temperature limiting
4. Automatic IGV actuation as a function of pump (and engine) speed
5. Foot pedal bias of fuel flow
6. Electrical shut-off
7. Automatic altitude compensation from sea level to 10,000 feet

Although the control which was conceptually designed for this application is hydromechanical, electronic implementation was also considered. Similar control logic was used for an electronic control, and a logic diagram and wiring schematic were prepared. Both methods of control implementation were then costed, and costs

to manufacture either the hydromechanical or electronic version compared favorably. However, it was decided that the electronic implementation presented a somewhat larger uncertainty than the hydromechanical version in both cost and performance. Therefore, a program decision was reached to implement the control hydromechanically. However, for future programs of this nature, it is recommended that an electronic control be given consideration. Electronic implementation may prove beneficial if the automotive engine requirements become somewhat more sophisticated.

Control Mode Determination

General

The mode of control presented is the result of discussions with UARL and UACL relating to implementation of a low-cost fuel control for the single-shaft regenerative and recuperative engines (RCSS-6 and RCSS-8) and the single-shaft simple-cycle engine (SSS-10). Fuel control requirements for these engines were considered in conjunction with the General Electric IVT-870 infinitely variable hydromechanical transmission, and although engine temperature, pressure, and fuel flows differ for the three engines, the operating characteristics allow a common mode of control for all three engines. Thus, only the detailed requirements of the SSS-10 have been considered in sizing control components, with the assumption that differences in the temperature, pressure, and flow requirements of the other two engines would have a negligible effect on cost, weight, and complexity.

Review of Engine and Control Requirements

A typical engine performance map, shown in Fig. 52, indicates engine fuel requirements for steady-state and acceleration operation of the engine. The maximum acceleration fuel flow is limited by turbine inlet temperature considerations.

The steady-state operating line is a result of the infinitely variable transmission controlling engine speed (as a function of foot pedal position) by varying transmission drive ratio to hold engine speed constant when the foot pedal is in a fixed position. Thus, the fuel control is not required to provide engine speed governing (as is required on aircraft engines) because of the combination of a fixed-shaft engine and an infinitely variable transmission. Therefore, fuel control requirements are reduced to providing acceleration and deceleration fuel limits and auxiliary functions such as IGV, starting, and shut-off functions.

Traditional aircraft engine control methods of controlling turbine inlet temperature during acceleration are by open-loop scheduling of fuel flow as a function of speed, inlet temperature, and compressor discharge pressure (P3) level. These techniques would result in excessive control cost and complexity for

FIG. 52

SSS-10 TORQUE CHARACTERISTICS

DESIGN SPEED = 106,000 RPM

DESIGN POWER = 130 HP

T.I.T. = 1900 F

AMBIENT TEMP = 59 F

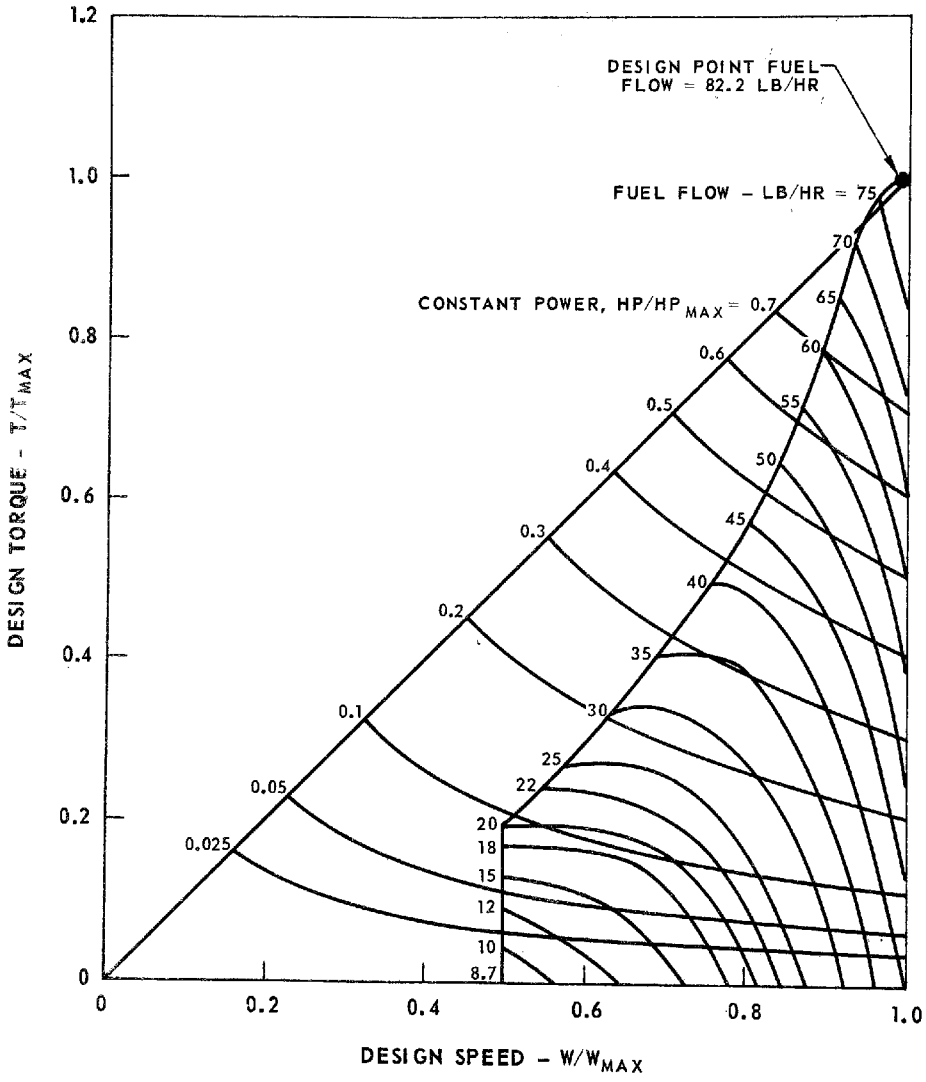

TURBINE EXHAUST GAS TEMPERATURE (EGT) VS TURBINE INLET TEMPERATURE (TIT)

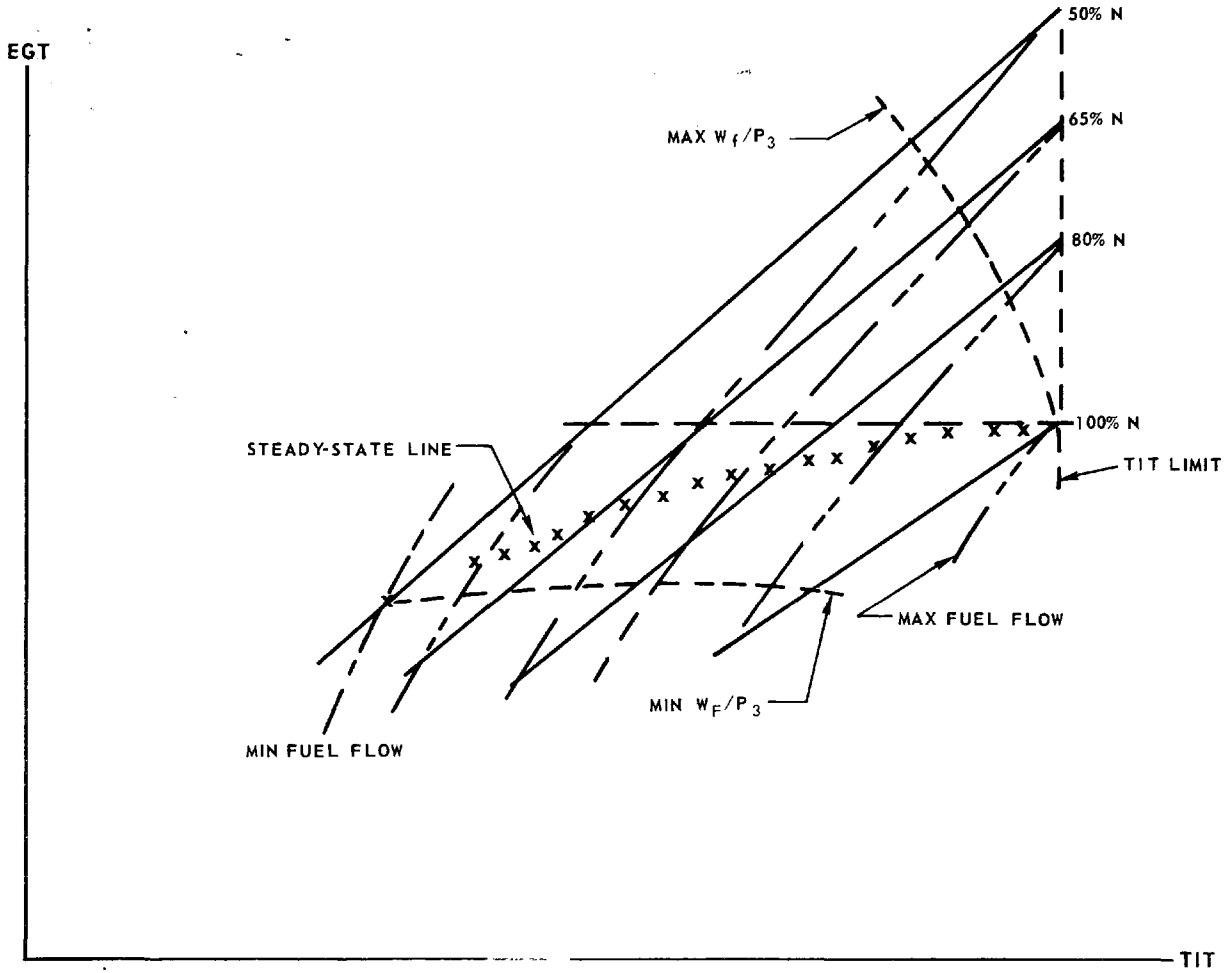

FIG. 53

FIG. 54

FUEL FLOW PARAMETER

SSS-10

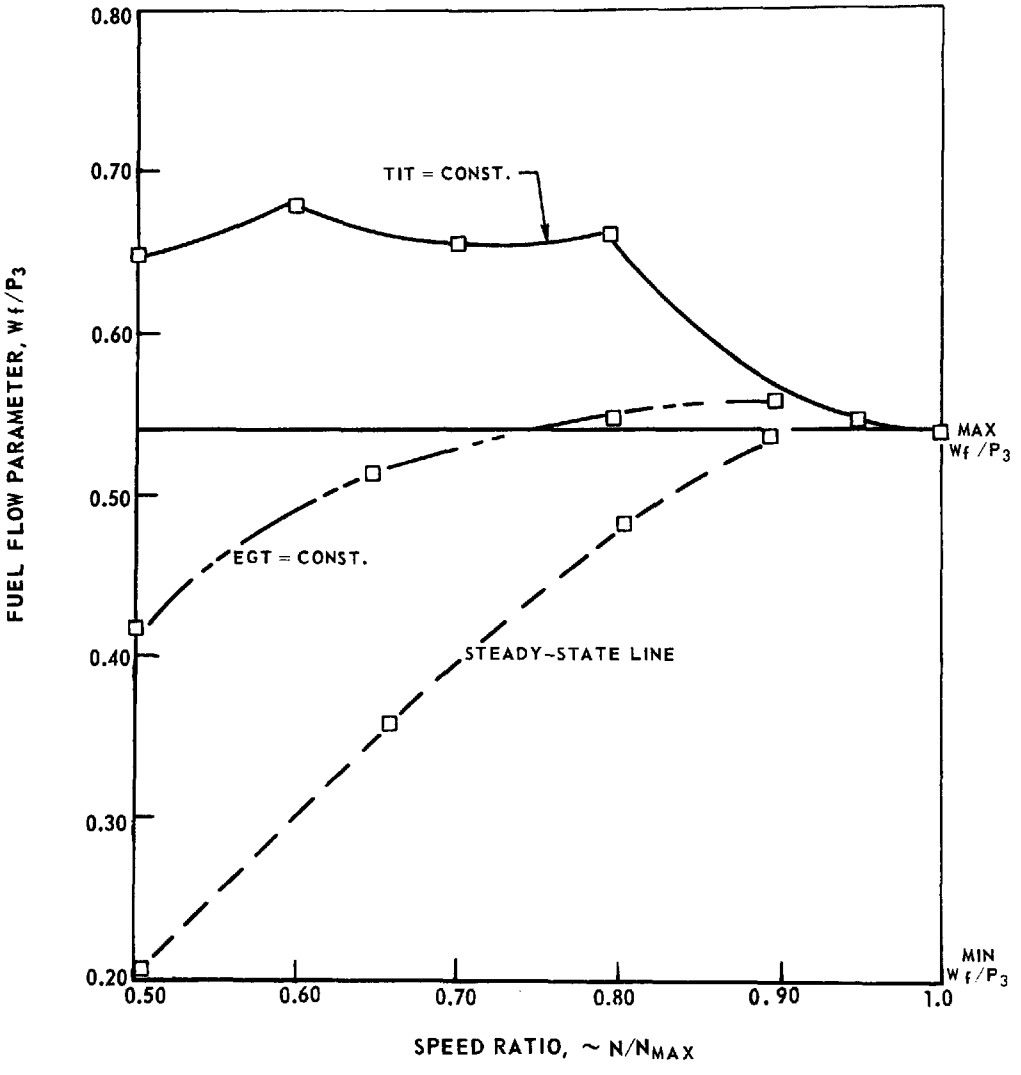

FUEL FLOW PARAMETER

RGSS-6

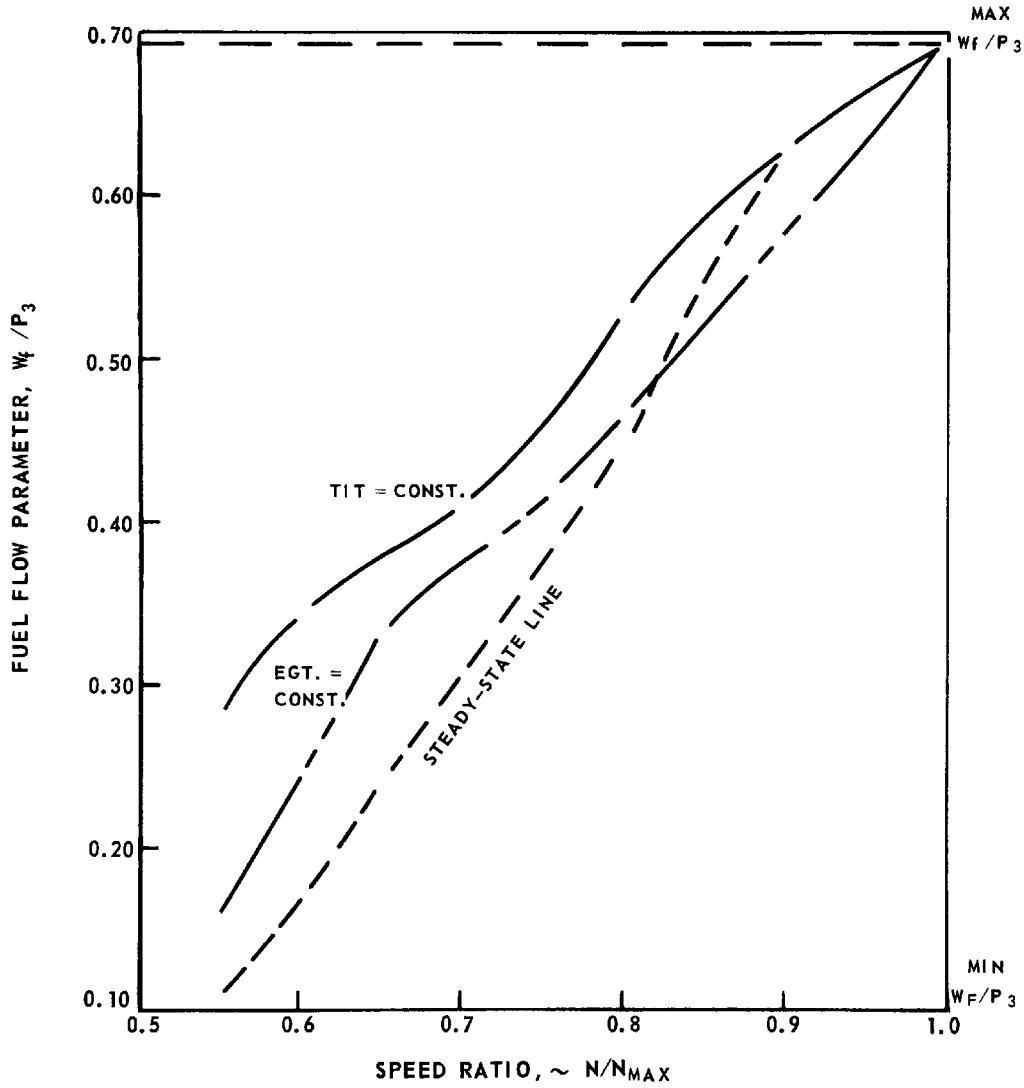

AUTOMOTIVE FUEL CONTROL LOGIC DIAGRAM

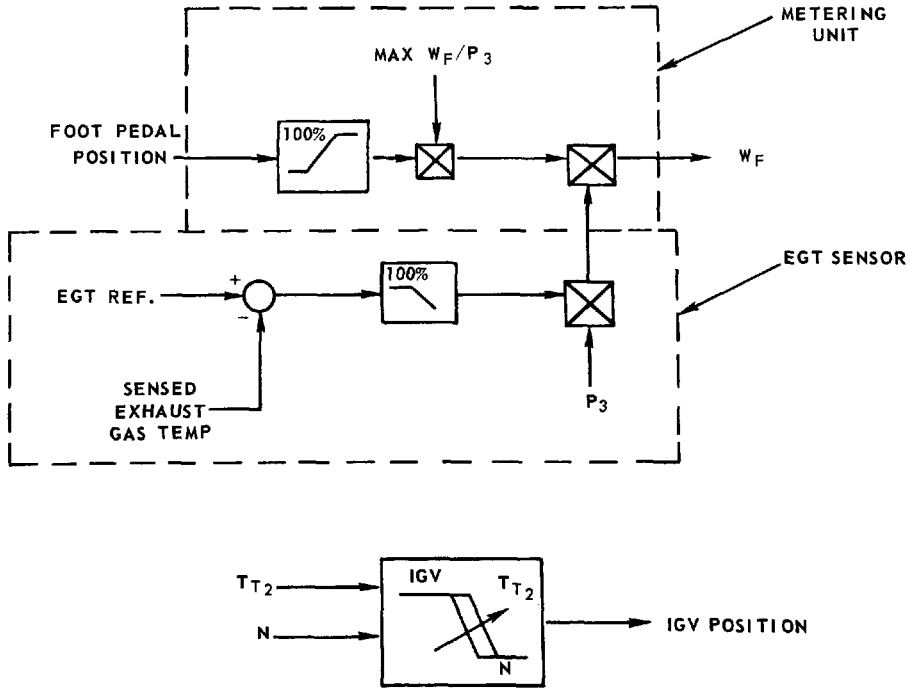

FIG. 56

an automotive fuel control, and would be further complicated by considerations for regenerative engines since ambient temperature, engine speed, and P3 do not uniquely define fuel flow for a given turbine inlet temperature for such engines.

Acceleration-limiting based on turbine exhaust gas temperature (EGT) presents a simplifying alternative and allows a common mode of control for the three engines under consideration. Figure 53 shows turbine exhaust gas temperature plotted vs turbine inlet temperature (TIT) as a function of engine speed and fuel flow. The curve indicates that holding EGT constant will result in a lower TIT at idle speed than at maximum speed. This feature is desirable to a certain extent since a constant inlet gas temperature would result in higher turbine temperatures at idle than at maximum speed. Acceleration at constant EGT would be relatively slower due to the lower TIT imposed by the EGT limit. Acceleration transients at constant EGT imply an EGT sensor with no time lags. Thus, proper selection of the sensor time constant can result in an acceptable overshoot in EGT which will allow higher transient turbine inlet temperature during acceleration throughout the operating range. Since the time constant of the temperature sensor varies with airflow, the EGT overshoot will be the greatest at low speeds, where the TIT margin is the greatest, and will be lowest at maximum speed.

Either fuel flow (Wf) or Wf/P3 could be used as the manipulated variable to provide temperature-limiting; however, Wf/P3 was chosen for several reasons which are illustrated in Fig. 54 which shows Wf/P3 vs engine speed for steady-state, constant EGT, and constant TIT. A maximum limit on Wf/P3 can be chosen so the TIT limit is not exceeded, even though a fixed EGT reference may be exceeded during transient operation. Also, the Wf/P3 mode provides for altitude bias, thereby permitting the EGT limiter to be implemented as a proportional control. Use of a Wf mode would require an EGT control that would allow fuel flow to integrate as a function of EGT error to hold the EGT limit regardless of altitude. Failure of the integrator would allow the engine to exceed the TIT limit; however, failure of the P3 sensor would be in a safe direction since it would result in underfueling the engine.

The use of Wf/P3 suggests the possibility of simplifying the control for the SSS-10 by eliminating the EGT sensor through an appropriate choice of the maximum Wf/P3 limit. It can be seen on Fig. 54 that a level of Wf/P3 can be picked (as a result of compromising acceleration potential), without exceeding the turbine inlet temperature limit. Elimination of the EGT sensor for the regenerative and recuperative engines is not feasible because, as shown in Fig. 55, a fixed Wf/P3 limit would cause excessive turbine inlet temperature. Thus, Wf/P3 was chosen as the manipulated parameter in the interest of reduced mechanical complexity and fail-safe considerations.

Proposed Mode of Control Logic

The logic for the proposed control mode is illustrated in Fig. 56. Wf/P3 level is scheduled between minimum and maximum limits as a function of foot pedal

AUTOMOTIVE FUEL CONTROL SCHEMATIC

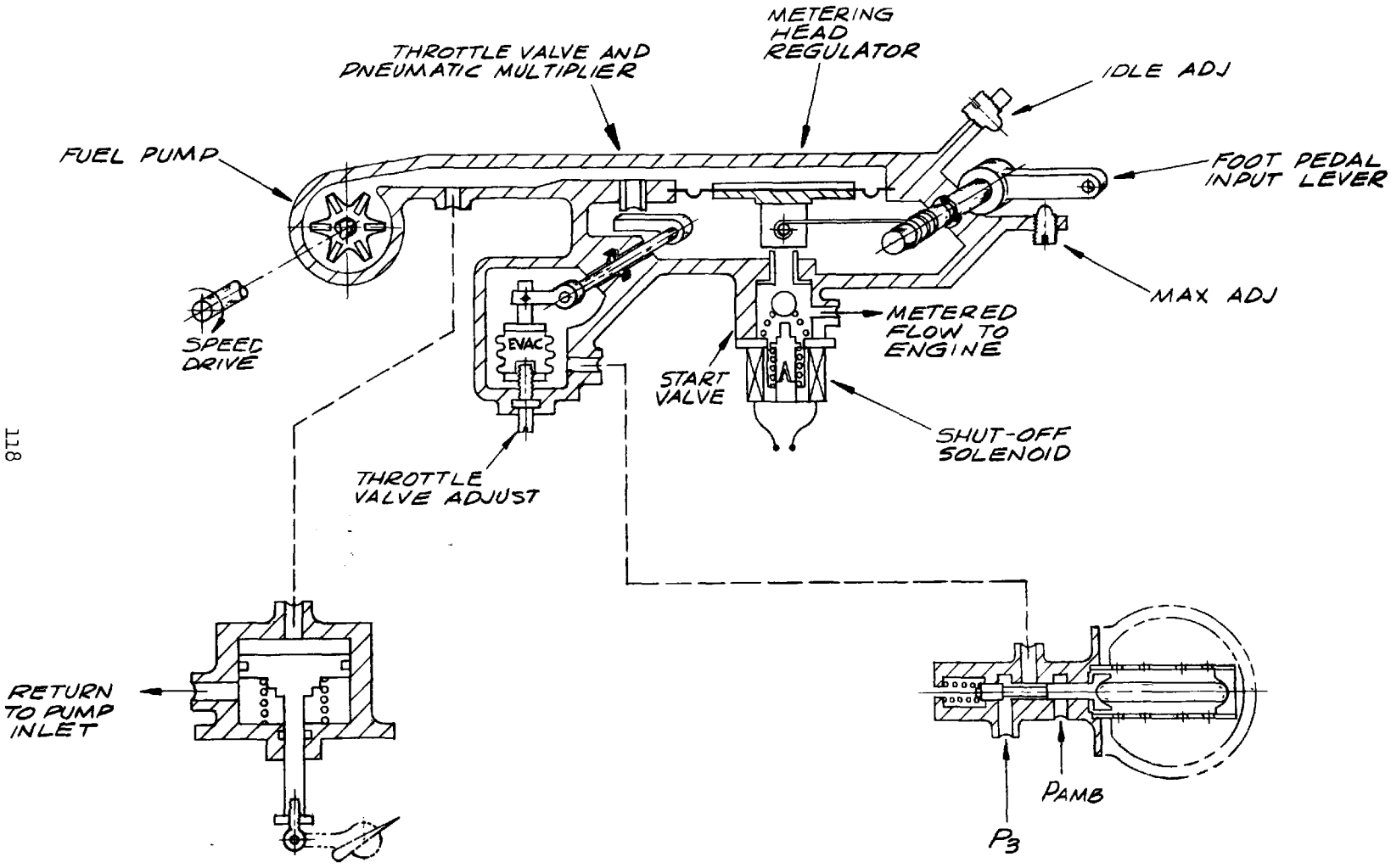

L-971249-7

FIG. 57

position. As long as the preselected exhaust gas temperature is not exceeded, the fuel flow to the engine will be proportional to foot pedal position and compressor discharge pressure level only, since Wf = (Wf/P3) x P3.

If the exhaust gas temperature limit is exceeded, the P3 level sensed by the control is reduced by the EGT sensor, thus making Wf = (Wf/P3) x K x P3, where K is a function of EGT error. Minimum Wf/P3 is scheduled at idle foot pedal position, resulting in (Wf) decel = (Wf/P3 min) x (P3), since the engine will be decelerating at a temperature below the EGT limit. The inlet guide vane control schedule is a linear combination of engine speed and inlet temperature and will be discussed in detail in the section treating the functional description of components. It is possible that the requirement for IGV's may be eliminated on production engines, particularly the RGSS-6 and RCSS-8 which have lower pressure ratios than the SSS-10.

The proposed mode of control, scheduling Wf/P3 as a function of foot pedal position with a proportional exhaust gas temperature bias, results in a control of minimum complexity suitable for the RGSS-6, RCSS-8, or SSS-10. It should be noted that a portion of this simplicity is due to the utilization of the infinitely variable hydromechanical transmission to provide engine speed control. Further potential simplification might result from elimination of the EGT sensor or IGV actuator as discussed above.

Functional Description

General

A hydromechanical implementation of the proposed mode of control is illustrated schematically in Fig. 57 . This system provides for acceleration and deceleration fuel flow scheduling as a function of foot pedal position, exhaust gas temperature, and compressor discharge pressure (P3) level. The system consists of a metering unit, a remote IGV actuator, and a remote exhaust gas temperature sensor. The metering unit contains an engine-driven centrifugal fuel pump, a throttle valve and pneumatic multiplier, a metering head regulator (biased by foot pedal position), a start valve, and a shut-off solenoid. A description of these components and their performance characteristics are presented below.

Fuel Pump

A forced-vortex centrifugal fuel pump has been chosen because its characteristics make it particularly suited to automotive gas turbine requirements. The forced-vortex pump shown schematically in Fig. 57 is an open-impeller type representing extreme simplicity in design. The pump design is based on the assumption that the liquid rotates in the housing like a solid body, along with the impeller, to form a perfect forced vortex, and that the quantity of liquid discharged is small relative to the rotating volume. This implies that rotational velocities are

predominant and that other components of the absolute liquid velocity are negligible. The noticeable distinctions from a conventional centrifugal pump are a straight radial open-bladed impeller, a circular housing concentric with the impeller (with ample clearances), and a wider cross section than is normally employed in conventional centrifugal pumps. A simple discharge nozzle is located tangentially to the periphery of the impeller bore. The open impeller offers the advantage of developing no end thrust since it is hydraulically balanced, which also results in essentially no pressure drop across the shaft seal.

Pump pressure and flow characteristics, as shown below, illustrate a flat pressure characteristic over a wide flow range at constant speed which is particularly advantageous to the IGV implementation. The sharp cutoff at high flows is typical of this type of pump and is influenced by discharge nozzle size, pump inlet pressure, and pump speed. Since the altitude range of the automotive control is from sea level to 10,000 feet, the discharge nozzle is easily sized to allow maximum flow at these extremes. Pump cutoff flow is essentially linear with speed, whereas the engine fuel requirements are reduced more sharply; therefore, sizing the nozzle for maximum speed and flow conditions results in ample flow margin at reduced speed.

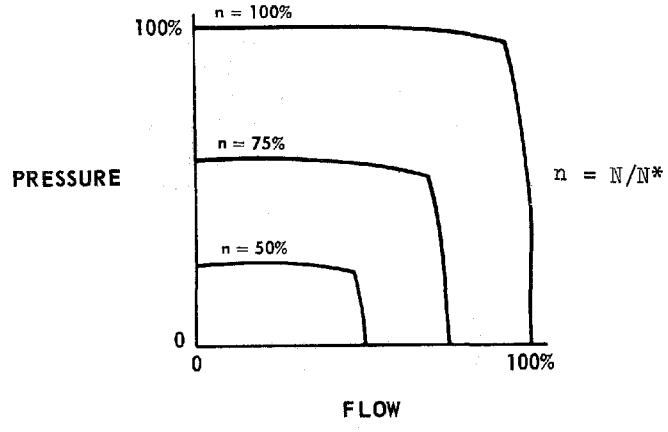

Pump discharge pressure level requirements are a function of compressor discharge pressure, burner fuel nozzle pressure drop, and fuel control metering valve and flow passage pressure drops. Pump sizing for the SSS-10 engine is based on 500 psi discharge pressure at maximum speed (N/N* = 100%). The allocation of pressure drops and level is tabulated as follows:

Compressor discharge pressure	148 psi at max speed
Burner fuel nozzle ΔP	200 psi at max flow
Throttle valve metering head ΔP	42 psi at max Wf/P3
Start valve ΔP (at 40% N*)	80 psi for start flow
Metering head regulator nozzle ΔP and line losses	30 psi at max flow
Required Pump Discharge Pressure	500 psi at 100% N*

In the interest of minimizing pump size and complexity, it is desirable to operate the pump by a direct drive from the engine. The current design for the SSS-10 (Fig. 31) indicates a three-stage reduction between engine output speed and transmission input speed with three speeds for consideration: 3200 rpm, 15,000 rpm or 105,000 rpm at maximum speed.

Considering the fuel pump horsepower requirements, pump efficiency might not be expected to be critical since the theoretical power requirements for a 100% efficient pump delivering 78 lb/hr at 500 psi is 0.06 horsepower. However, pump impeller diameter and speed determine disc friction loss (or "windage" loss), and this loss is independent of flow capacity of the pump. For a given discharge pressure requirement at a fixed speed, the impeller tip diameter is fixed since the output pressure is directly proportional to the square of the tip speed ($U \propto ND$). The friction force on the disc is dependent on the fluid density, the centrifugal energy (which is proportional to U^2), the area of the disc surface (which is proportional to D^2) and an empirical friction factor f'. Multiplying the product of these factors by U to obtain the power absorbed (P_{DF}) gives: $P_{DF} \propto f' \rho U^2D^2U = f' \rho U^3D^2$, and substituting $ND \propto U$, $P_{DF} \propto f' \rho N^3D^5$. This indicates that to minimize friction horsepower losses for a given pump delivery pressure, the impeller diameter should be minimized since $U \propto P^{3/2}$ and is fixed by the pressure requirements. A more detailed consideration of the pump disc losses for the forced-vortex pump leads to the following equation:

$$P_{DF} = 7.62 \times 10^{-6} \times S \times \nu^{.2} \times \left(\frac{N}{1000}\right)^{2.8} \times \left(d_2^{4.6} + 1.38\, d_1^{4.6}\right)$$

where: P_{DF} = disc friction, hp
S = fluid specific gravity
ν = fluid viscosity, centistokes
d_2 = impeller tip diameter, in.
d_1 = impeller inlet diameter, in.
N = shaft speed, rpm

A pump sized for 500 psi at 15,000 rpm results in an impeller tip diameter of 4 inches and the resultant disc friction is 7.0 horsepower. A pump sized for 500 psi

FIG. 58

INLET GUIDE VANE SCHEDULE

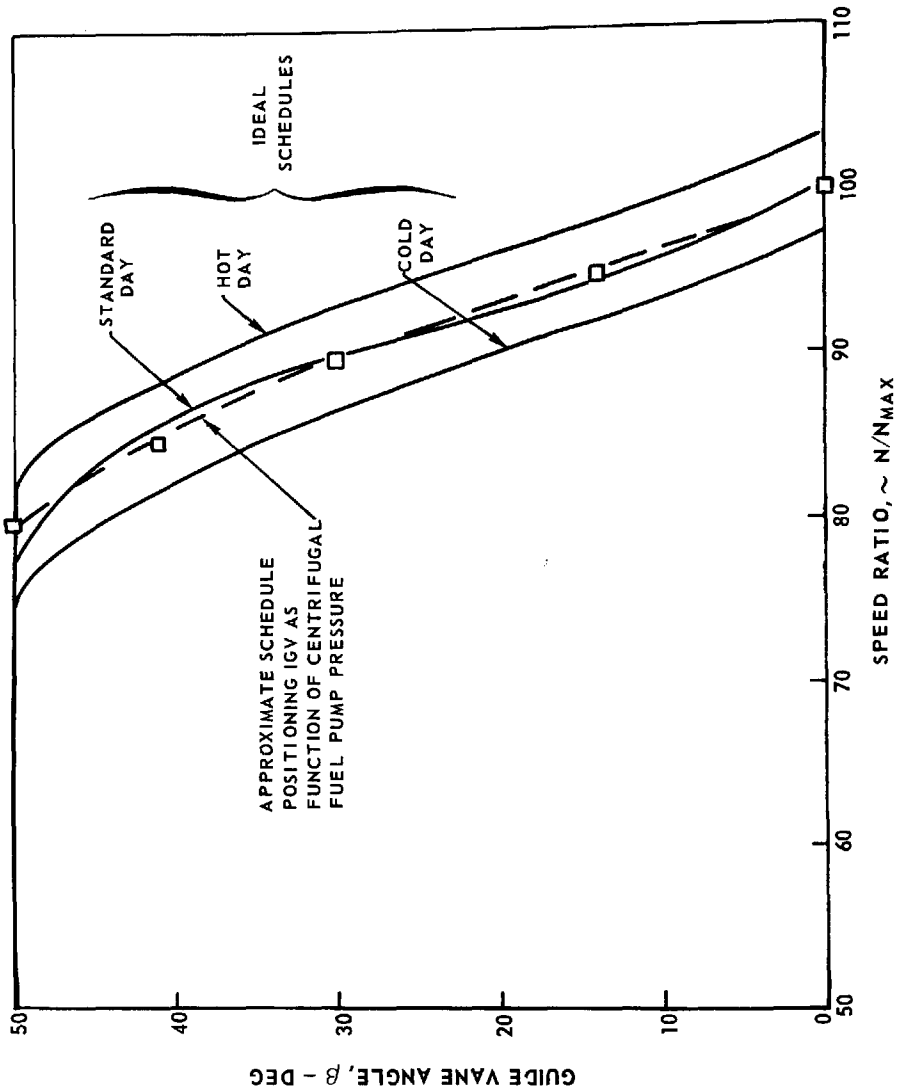

at 105,000 rpm results in an impeller tip diameter of 0.74 inches and the resultant disc friction is 0.12 horsepower, resulting in approximately 33% overall efficiency. Clearly, the operation of a pump sized for 500 psi at 15,000 rpm requiring 7 horsepower is not suitable for an engine required to develop 130 net horsepower. Thus, it is recommended that the fuel pump be designed to run at the maximum engine speed of 105,000 rpm.

Fuel pumps, seals, and bearing cartridges have been designed and developed by Hamilton Standard for turbopump applications in this speed range, although not at this low flow capacity. A carbon face seal backed up with a static "O"-ring and wave spring similar to "Cartriseal" 1-530 assembly should prove suitable for this application since the open impeller pump design results in low sealing force levels. It should also be noted that the engine is designed for 25 hours of operation at 105,000 rpm, and that the normal maximum operating speed is 80% of this or 84,000 rpm which leads to more favorable conditions for long seal life.

Inlet Guide Vane (IGV) System

A typical IGV schedule of blade angle (β) vs. speed for hot-day, standard-day, and cold-day conditions is shown in Fig. 58. The remote IGV actuator (shown schematically in Fig. 57) is spring loaded so that the actuator does not move until the fuel pump discharge pressure is sufficient to overcome the spring load. Since the pump discharge pressure is a function of speed squared, the resulting actuator motion closely approximates the desired schedule.

Several options exist regarding temperature bias of the IGV schedule. The first, in the interest of simplicity, is to eliminate the need for temperature bias by choosing a compromise schedule that could give adequate engine performance. Changes of schedule slope and position can be accomplished by choosing different spring rates and preloads. If such a compromise schedule proves unsatisfactory, two methods of providing temperature bias are suggested. The first method would bias the preload on the piston with a bimetallic disc so that, on hot days, the force, and hence the speed, required to initiate stator vane motion would be increased. The temperature bias of the point at which the actuator begins to move is at a constant $N/\sqrt{\theta}$ with this method, and can be illustrated by considering the following equilibrium force balance:

$$\text{Actuator pressure force} = K_1 N^2 = \text{Spring force} = K_2 \times \text{Temp}$$

$$\text{then } N^2/T \propto \text{constant}$$

$$\text{and } N/\sqrt{\theta} = \text{constant}$$

THROTTLE VALVE AND PRESSURE MULTIPLIER CHARACTERISTIC

SSS-10

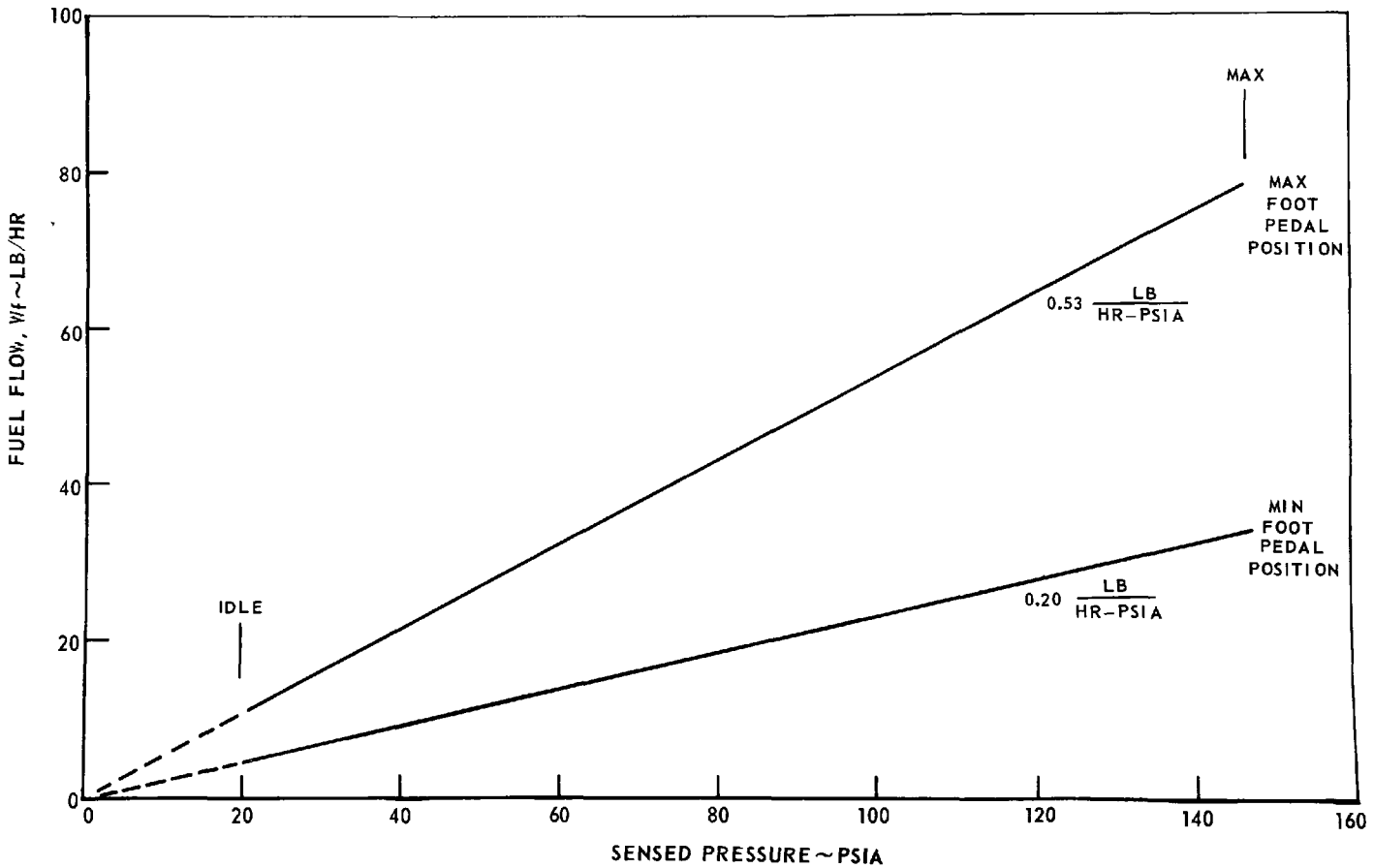

FIG. 59

Thus, this method can provide β vs. $N/\sqrt{\theta}$; however, the bimetallic disc would have to be sensitive to compressor inlet temperature. Placing the actuator in the compressor inlet air path is not feasible due to the actuator size required to provide 100 in.-lb torque through a 50-degree arc. A second method of biasing stator vane position with compressor inlet temperature would be to use bimetallic elements in the stator vane positioning linkage. This method will provide a more effective temperature bias since the IGV linkage is inherently in the compressor inlet airflow path.

The proposed IGV system which positions the stator vanes as a function of fuel pump pressure is recommended only in the interest of low cost and simplicity. If temperature bias should become a requirement, it is recommended that it be accomplished by incorporating bimetal elements in the stator vane positioning linkage in the compressor.

Throttle Valve and Pneumatic Multiplier

The throttle valve and pneumatic multiplier is a flapper valve positioned by an evacuated bellows. This system provides the compressor discharge pressure (P3) bias of fuel flow and the interface for the exhaust gas temperature sensor such that fuel flow is a linear function of sensed P3 pressure. This is illustrated by considering the following metering system equations:

$$W_F = K A\sqrt{\Delta P},$$

where Wf = fuel flow, pph
A = throttle valve metering area, $in.^2$
ΔP = throttle valve metering head, psi
K = constant

Setting $\sqrt{\Delta P} \propto (Wf/P3)$, and A ∝ sensed pressure, then

$$Wf \propto (Wf/P3) \times \text{Sensed Pressure},$$

where sensed pressure = KxP3 = f(P3, EGT), and Wf/P3 = f(foot pedal position). A typical fuel flow characteristic of this device is shown in Fig. 59 for pressure and foot pedal extremes. Absolute limits on fuel flow can be established by positioning the sensing bellows in conjunction with the foot pedal input limits.

Metering Head Regulator

The metering head regulator shown schematically in Fig. 57 regulates the metering head, or ΔP across the throttle valve by adjusting the flapper nozzle opening in response to force changes on the sensing diaphragm. The desired metering head is set by varying the torsion spring force applied to the diaphragm as a func-

MAXIMUM FUEL FLOW PARAMETER

SSS-10

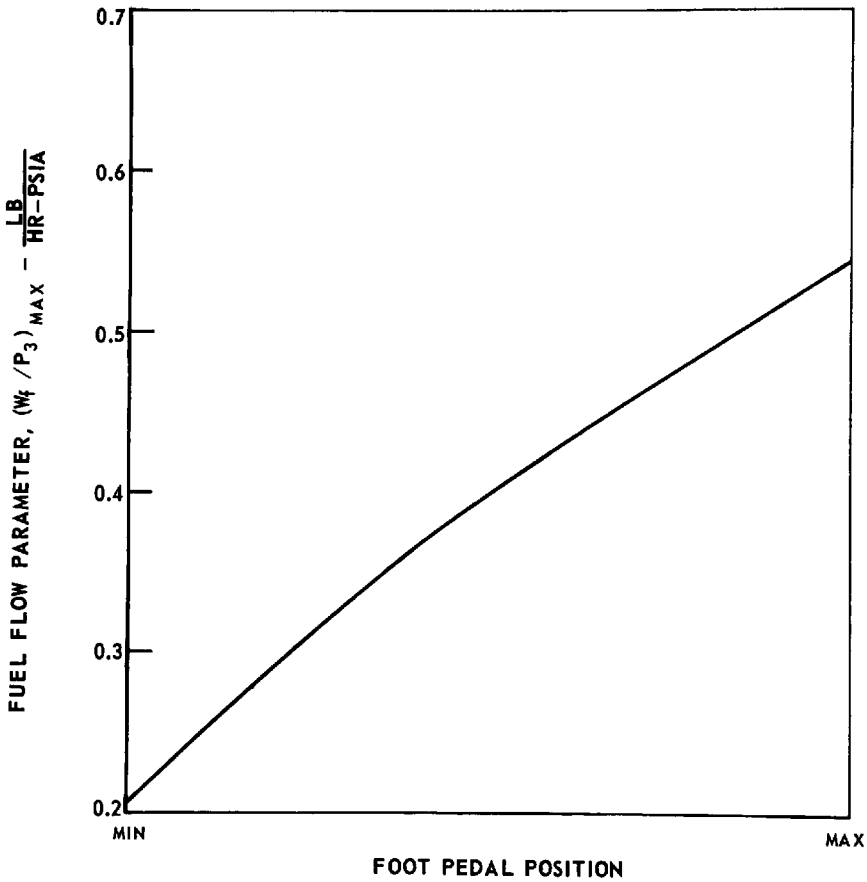

tion of foot pedal position. A simplified analysis of this force balance shows that $\Delta P = F/A$, where A is the diaphragm sensing area. The metering logic requires that Wf/P3 be proportional to the square root of the throttle valve metering head. Therefore, the Wf/P3 schedule vs. foot pedal position will be of the form Wf/P3 $\propto \sqrt{\text{foot pedal position}}$. The ratio of maximum to minimum metering head is equal to the square of the max.-to-min. ratio of Wf/P3. Thus, for the SSS-10 engine with a range of Wf/P3 from 0.2 to 0.53 pph/psia, a max.-to-min. metering head ratio of 7.0 is required. Preliminary metering system sizing indicates that a range of 6 to 42 psia results in reasonable component sizes.

Figure 60 illustrates the Wf/P3 vs foot pedal characteristic for the SSS-10 engine. Idle and max Wf/P3 limits can be varied by the adjustable stops on the foot pedal input lever.

Exhaust Gas Temperature (EGT) Sensor

The temperature sensing system selected to provide exhaust gas temperature biasing of acceleration fuel flow is shown schematically in Fig. 57. This system makes use of a bimaterial probe to sense turbine exhaust gas temperature by using the thermal differential expansion between the high-expansion element in the air stream and the low-expansion element shielded by the high-expansion element. The differential motion is used to position a spool valve which provides a pneumatic signal to the throttle valve and pneumatic multiplier. The spool valve is supplied with compressor discharge pressure (P3) and is essentially closed to ambient pressure ($Pamb_1$) and full open to P3 at temperatures below the EGT limit. As the EGT limit is approached, the spool valve bleeds a small amount of air from the P3 sensing line and reduces the signal to the throttle valve sensing bellows because of the series orifice pressure drop characteristic shown below.

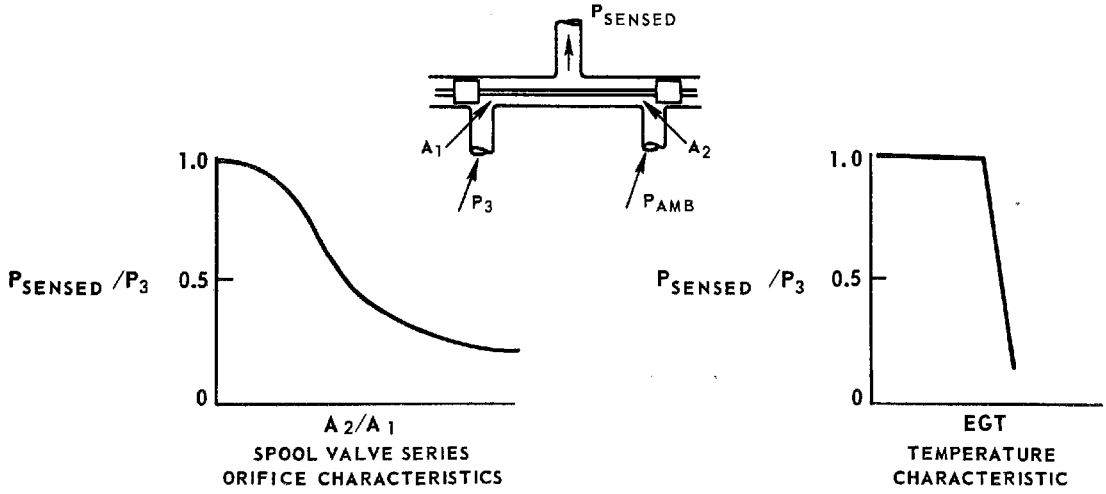

The rate of change of the reduction in pressure with EGT is a function of the temperature coefficients of the high- and low-expansion elements, the length of the probe, and the amount of spool valve underlap. A valve with 0.004 in. underlap would be capable of reducing fuel flow from effectively max. to min. Wf/P3 with an exhaust gas temperature change of 100 F when used with a probe 3.3 in. long, consisting of INconel-600 for the high-expansion element and lithium aluminum silicate (zero-X) for the low-expansion element. Zero-X material was chosen because of its low-expansion characteristic, high strength, and excellent thermal shock resistance.

Because the low-expansion element has a temperature coefficient that is negligible compared with that of INconel-600, the time response of the probe can be calculated by considering only the heat transfer between the Inconel sleeve and the exhaust gas. Thus, the time constant can be represented by the following equation:

$$\tau = \frac{Kt\ \gamma\ C}{h},$$

where K = constant
τ = wall thickness
γ = density of wall
C = specific heat of probe
h = film coefficient

A simplified expression for the film coefficient for a tube in air based on Reynolds number and Prandtl number variations is given by:

$$h = KG^{0.58}/D^{0.42}$$

where G = mass velocity, pps/ft^2
D = tube diameter.

Then the analytical representation of the sensor time constant becomes

$$\tau = KtCD^{0.42}/G^{0.58}$$

Variation of the sensor time constant with airflow density is shown in Fig. 61. The speed reference points indicated are based on the airflow-vs-speed data for the SSS-10 engine and assume the sensing probe is mounted in a 3.5-in. I.D. turbine exhaust passage, thus resulting in time constant variations from 3.5 seconds at idle to 1.5 seconds at max. speed.

Finalization of the EGT sensor dynamic and static operating characteristics will require further engine and control study to optimize engine acceleration performance.

Start Valve and Shut-Off Solenoid

The start valve, as shown schematically in Fig.57, is in the metered flow path. The ball valve is responsive to forces provided by the fuel pump and the solenoid.

During the starting sequence, the solenoid plunger would retract from the ball valve when the ignition or engine starter is energized. The spring on the ball valve will hold the valve closed until the engine speed, and hence the fuel pump pressure, is at a level that will assure that the engine will start. To shut off fuel flow to stop the engine, the solenoid is de-energized and the spring on the solenoid will close the ball valve.

Estimated starting fuel flow characteristics are illustrated in Fig. 62 for the SSS-10 and assume a nominal speed for starting fuel flow initiation of 40%. The spring load on the ball valve is set to open when the difference between compressor discharge pressure and pump discharge pressure is 65 psia. Thus, starting flow will be initiated at lower speeds at higher altitudes since the compressor discharge pressure level will be lower. The two-slope characteristic of the starting fuel schedule at a given altitude and foot pedal position is a result of the pressure rise characteristic of the fuel pump and the pressure drop characteristics of the metering unit. Although flow is initiated at nominally 40% speed, a further increase in speed is required to develop the pressure necessary to overcome the pressure drops needed to provide fuel flow at the levels associated with various foot pedal positions. In other words, the steep portion of the starting schedule is due to pump pressure limitations, and the shallow portion of the schedule is achieved when the pump produces sufficient pressure to allow the control to schedule fuel flow at the Wf/P3 level set by the foot pedal position.

CALCULATED EXHAUST GAS TEMPERATURE SENSOR TIME CONSTANT VS AIR FLOW

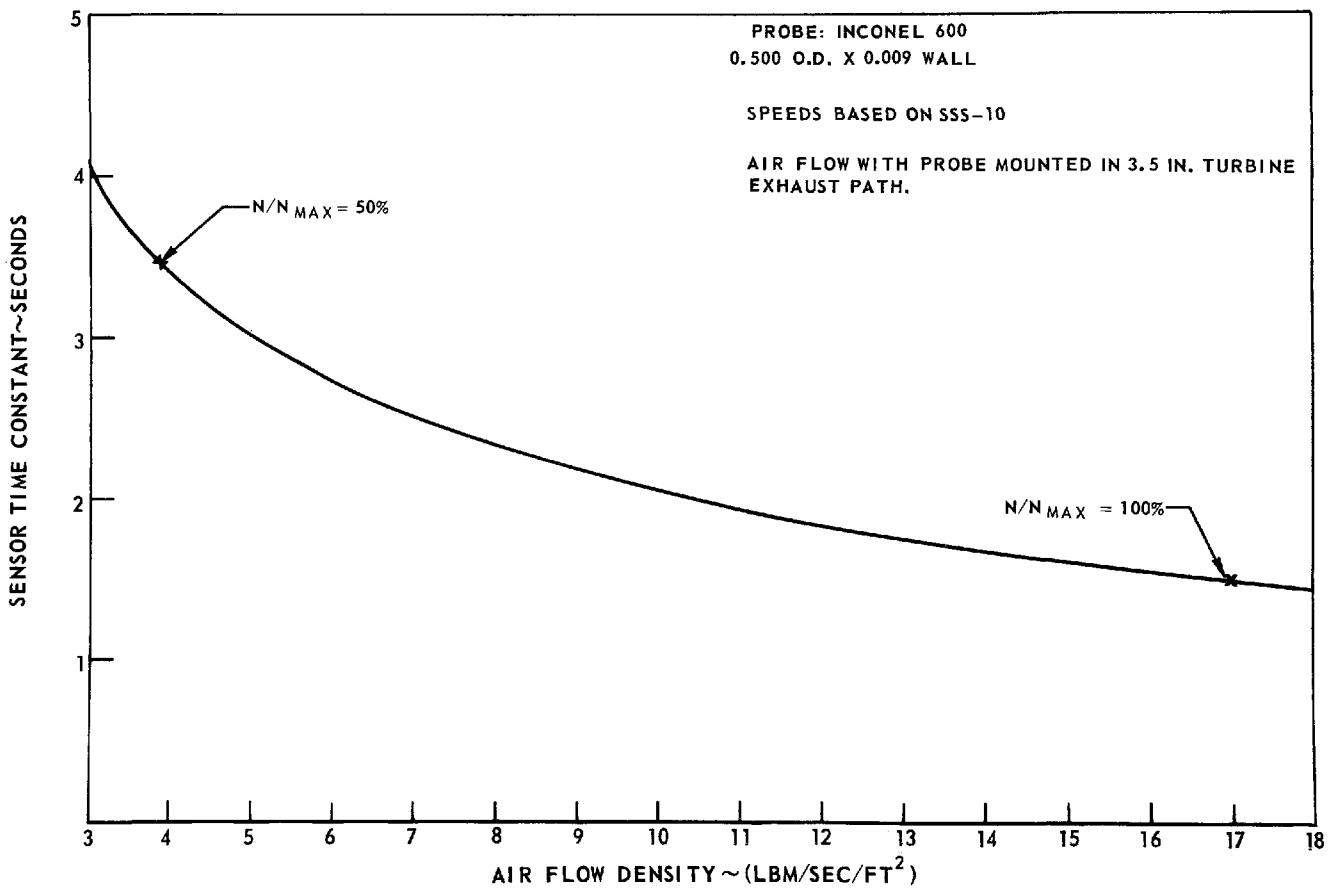

FIG. 61

ESTIMATED STARTING FUEL FLOW

SSS-10

ASSUMPTIONS: (1) START VALVE SET @ 90% N_{MAX}
(2) W_f/P_3 MAX = 0.65
(3) W_f/P_3 MIN = 0.20
(4) FUEL BURNER NOZZLE
$\Delta P_N = K W_f^2$

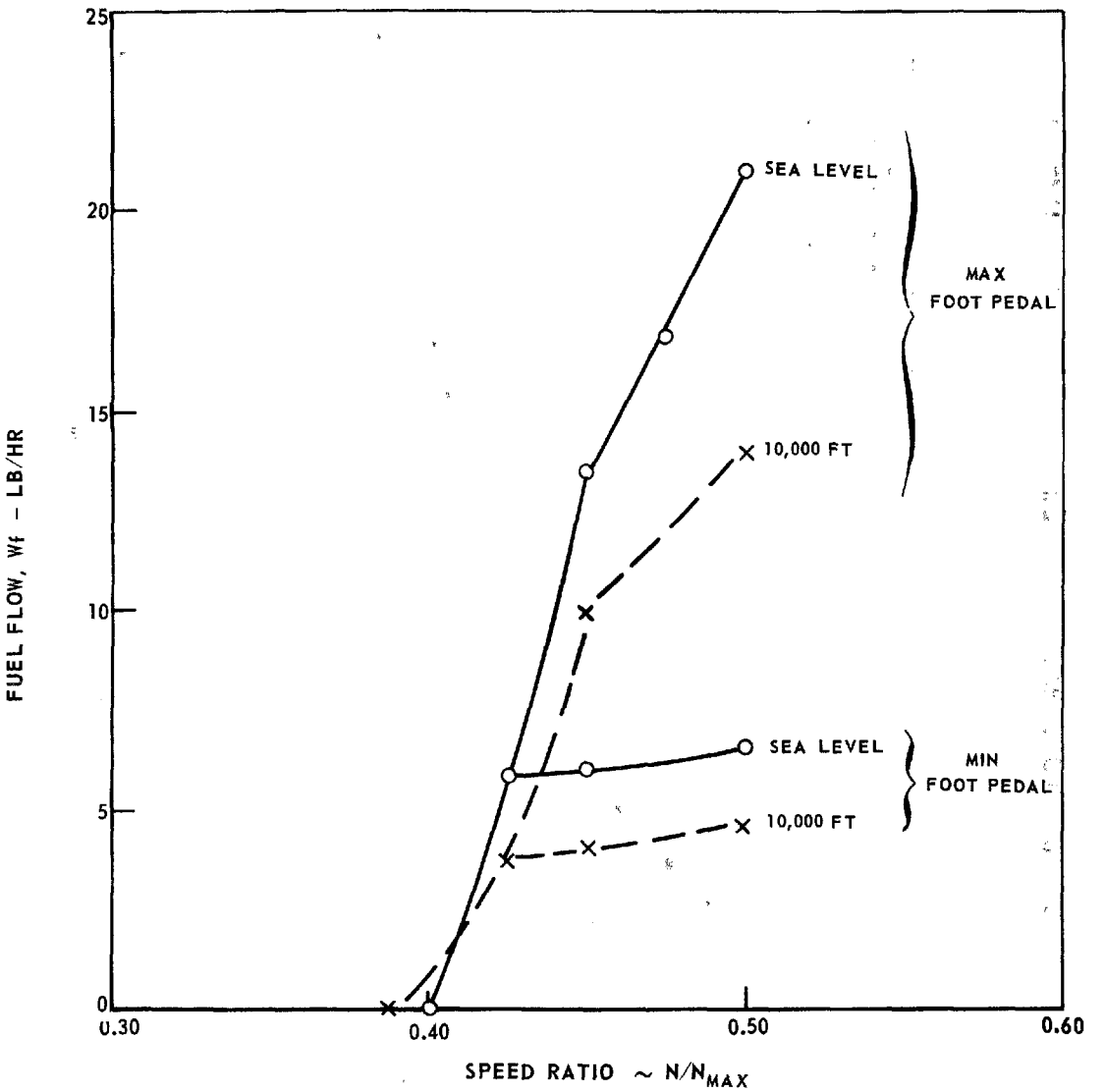

AUTOMOTIVE FUEL CONTROL DETAIL

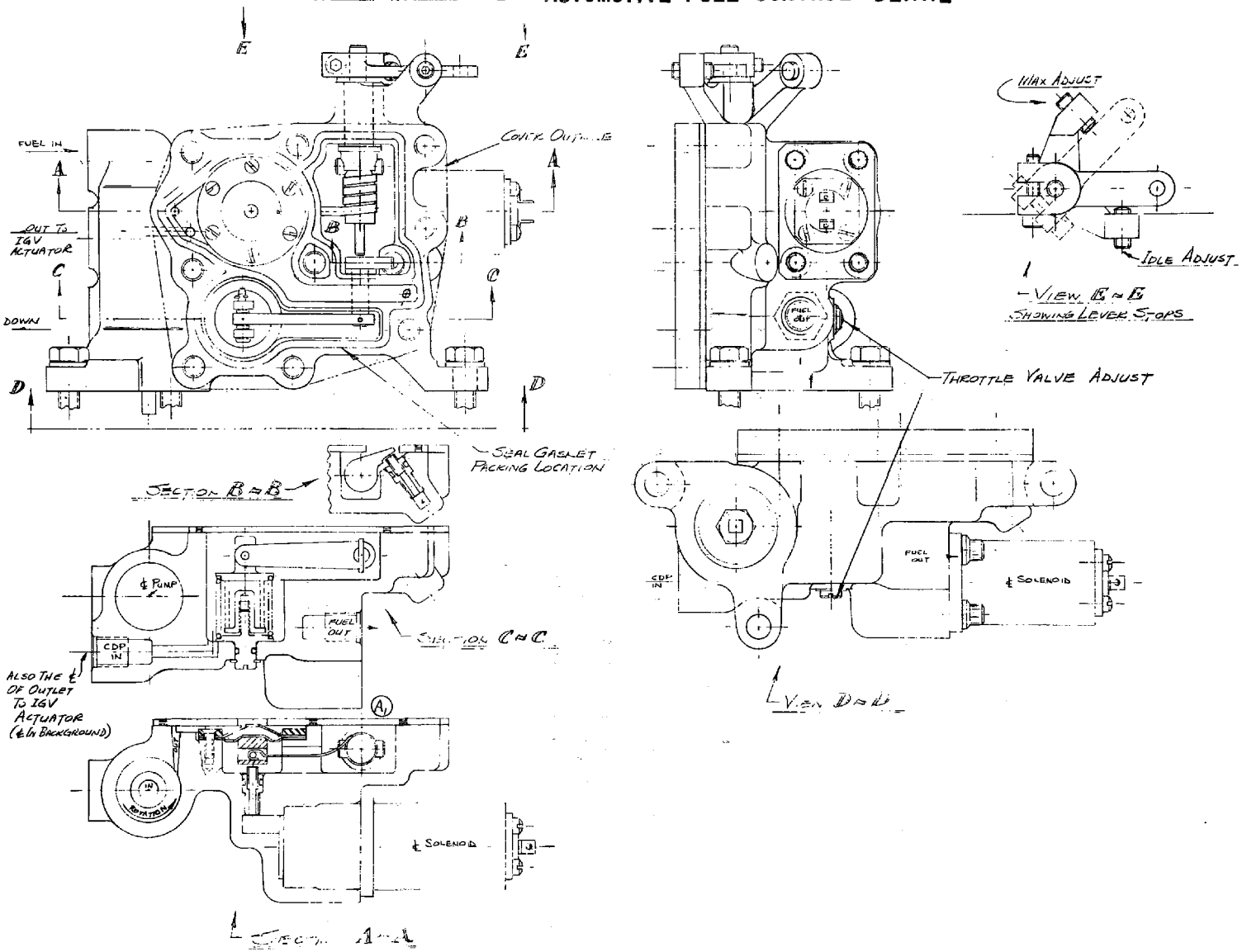

L-971249-7

FIG. 63

Physical Description

The selected fuel control has been studied carefully for determination of weight and cost while maintaining high standards of reliability, durability, flexibility, and maintainability. Several arrangements were examined prior to selection of the installation shown in Figs. 63 and 64. Realistic volumes and weights are obtained by preparing a detailed arrangement in this manner.

The fuel control package consists of three separate units connected by fuel and pneumatic lines. The fuel control unit is positioned on the engine gearbox to utilize the high-speed drive required for the fuel pump. The IGV actuator is mounted adjacent to the engine IGV linkage mechanism, thus insuring minimum linkage weight. The EGT sensor is mounted at a convenient location in the turbine exhaust gas stream. Standard bolt retentions are used for each unit, and special tools are not required for maintenance.

Main Housing and Control Cover Assembly

The housing is of die-cast aluminum for low cost and weight. It encloses the high-speed centrifugal pump, pressure regulating system and foot pedal linkage, shut-off solenoid and start valve, and the P3 sensor and throttle valve. The metering elements are closely grouped to minimize pressure drops within the control. Close spacing assures minimum volume and weight.

The unit is accessible for maintenance and adjustment after installation. Idle and maximum speed adjustments are externally accessible at the foot pedal input lever location. P3 bellows external adjustment is performed with a screwdriver. All internal subassemblies are accessible for scrutiny by removing the control cover bolts and control cover. Since no operating parts are attached to the cover, all internal parts remain undisturbed during inspection.

The fuel control features a metal gasket with integral, continuous packing for positive sealing. "Printed circuit" flow lines are incorporated in this gasket to simplify the housing casting. The cover is of die-cast aluminum for low cost and weight. Provisions in the cover are made for upstream and downstream throttle valve pressure taps which are also useful for purging air after fuel control installation. Hydraulic and pneumatic connections are made by use of standard open-end wrenches. Positive sealing is assured by utilizing "O"-seal packings in aircraft-type threaded fittings. All housing mounting bolts are standard, and likewise are readily installed by use of standard socket or open-end wrenches.

FUEL CONTROL-EXTERNAL VIEW

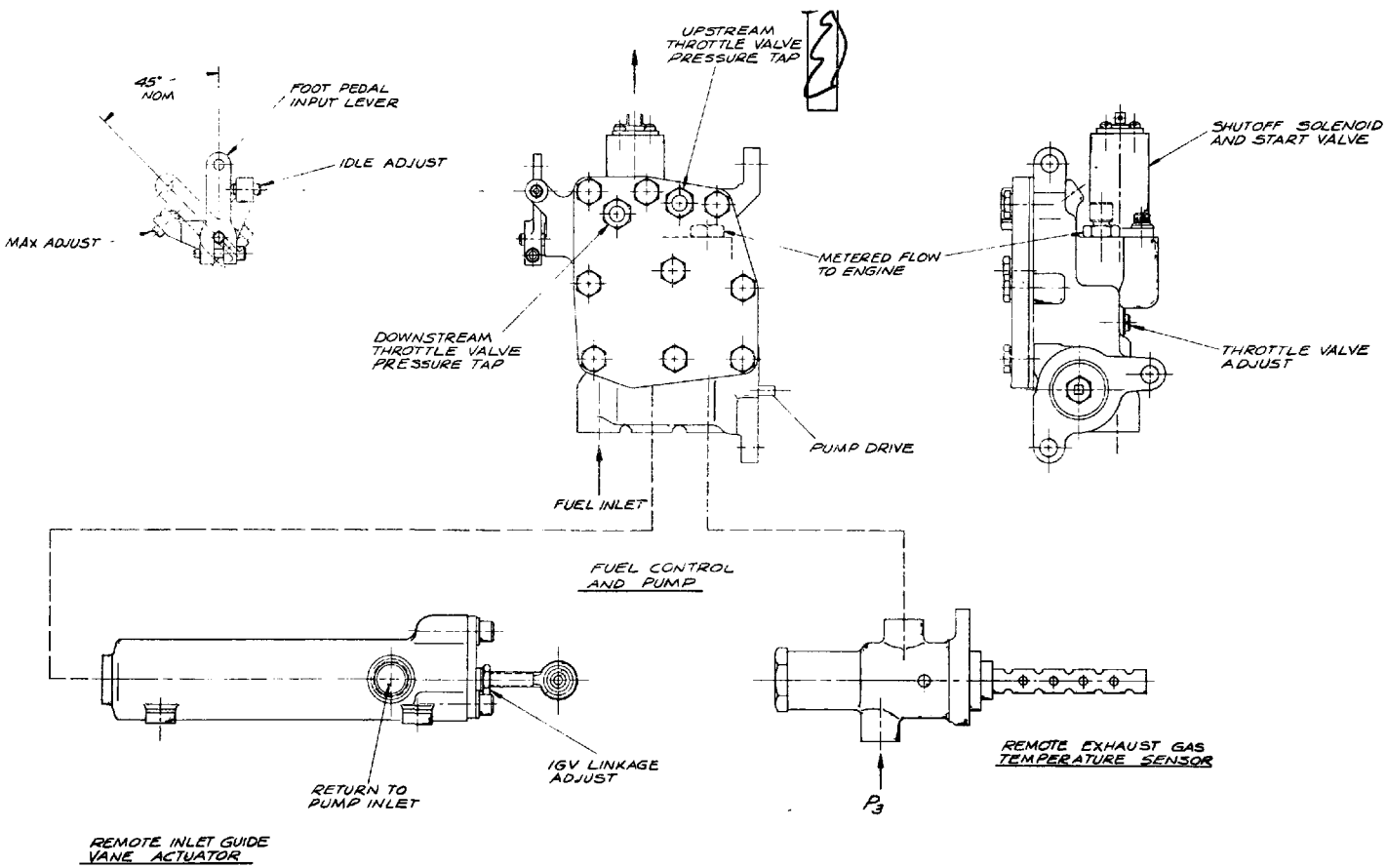

L-971249-7

FIG. 64

The high-speed centrifugal pump is a cartridge-type assembly, and is located low in the housing to minimize suction losses. The cartridge is restrained by a snap ring, and may be readily removed without disturbing the control calibration. Pump interface to the engine gearbox is a continuous surface to eliminate contamination to the drive shaft and bearing seal. A standard, face-type carbon seal mates with the anti-drive end of the pump shaft, thus allowing the high attendant surface speeds while effectively preventing fuel-to-air leakage.

The shut-off solenoid and integral start valve are located at the top of the control housing. Electrical terminals are oriented upward so that waterproof protectors can be effectively used. Metered fuel flow is upward from the control through the start valve, and then out to the engine. Any entrapped air is purged automatically by virtue of this arrangement.

The P3 sensor and throttle valve subassembly is located low within the main housing to allow the P3 connection to enter from the bottom; also, any condensate that forms in the bellows cavity drains out by gravity. An externally accessible throttle valve position adjustment screw is located at the side of the main housing for field adjustments, if required.

The pressure regulating system and foot pedal linkage shaft terminates at the side of the control opposite the engine, allowing flexibility of design of foot pedal linkage. Adjustment of idle and maximum-stop screws is possible with a standard Allen wrench. Self-locking inserts prevent screw rotation due to vibration.

Inlet Guide Vane (IGV) Actuator

The IGV actuator is a simple plunger-cylinder design mounted adjacent to the engine inlet guide vanes, and remote from the main control housing. The actuator housing is a permanent-mold aluminum casting for low cost and weight. An adjustable rod is provided at the end of the IGV piston shaft for exact actuator positioning with respect to the IGV linkage. Aircraft-type connections insure leak-proof sealing.

Exhaust Gas Temperature (EGT) Sensor

The exhaust gas temperature sensor is mounted in the turbine exhaust gas stream at the rear of the engine, remote from the main control housing. The sensor assembly consists of a cast iron housing and a slide valve actuated by a high-temperature bimetallic probe inserted in the gas stream. Orientation of the sensor is not critical, thus allowing flexibility in mounting location.

Component Weights

The estimated dry weights of the fuel control units, excluding electrical wiring and hydraulic and pneumatic tubing provisions and mounting bolts, are as follows:

Fuel control and pump	5.03 lb
IGV actuator	2.29 lb
EGT sensor	2.01 lb
Total estimated system dry weight	9.3 lb

The fuel control and pump weight is broken down as follows:

Housing	2.50 lb
Housing cover	0.57 lb
Housing cover bolts	0.24 lb
Gasket plate and packing	0.14 lb
Fuel pump and drive	0.37 lb
P3 sensor and throttle valve	0.16 lb
Shut-off solenoid and start valve	0.75 lb
Pressure regulating system and foot pedal linkage	0.30 lb
Total estimated dry weight	5.03 lb

External Connections Required

Fuel control

Hydraulic:
- fuel line to pump
- fuel line to engine
- fuel pressure line to IGV actuator

Pneumatic:
- signal line from EGT sensor to P3 sensing bellows cavity

Electrical:
- wiring to shut-off solenoid

Mechanical:
- foot pedal input lever linkage

Inlet guide vane actuator

Hydraulic:
- fuel pressure line to pump suction line
- fuel pressure line to pump discharge line

Mechanical:
- IGV linkage

Exhaust gas temperature sensor

Pneumatic:
- P3 line from engine compressor to EGT sensor
- Signal line from EGT sensor to fuel control

Summary of Fuel Control Analysis

This analysis indicates that an engine control mode based on scheduling Wf/P3 as a function of foot pedal position with a proportional turbine exhaust gas temperature bias results in a control of minimum complexity suitable for the RGSS-6, RCSS-8, or SSS-10 engines. However, additional study of the engine control system will be required to determine control design requirements.

It is recommended that engine, control, and transmission dynamics be studied in a comprehensive analysis of overall system performance in both acceleration and steady-state speed governing modes of operation. Results of this analysis will establish requirements such as: rate of change of "gear ratio" for the IVT as a function of engine speed error, exhaust gas temperature sensor time constant, and rate of change of P3 reduction with temperature. In addition, hot- and cold-day performance analysis of the acceleration mode can determine the feasibility of eliminating the need for an exhaust gas temperature sensor by establishing an appropriate maximum Wf/P3 limit for the SSS-10 engine.

Evaluation of engine performance at hot- and cold-day extremes without temperature bias of the IGV schedule is recommended to determine the feasibility of simplifying the control system by eliminating the requirement for temperature bias of the IGV. In addition, a determination of IGV system forces due to friction and aerodynamic loading will be required to establish actuator positioning accuracy.

Finally, it is recommended that further studies be conducted on the pumping and burner fuel nozzle system. These studies would be aimed at reducing fuel system pressure requirements, thereby enabling lower pump speeds to be utilized to assure long pump life. Perhaps a combination of pump and injector such as a "slinger nozzle" could be incorporated into the engine to further simplify the fuel control system.

ENGINE PERFORMANCE

Program Description

All engine cycle analyses were performed by Pratt & Whitney Aircraft (P&WA) using its proprietary State-of-the-Art Performance Program (SOAPP). The SOAP program is an engine cycle analysis system which easily organizes any type of engine configuration using any combination of components. It is particularly applicable for this optimization study because of the contract requirement to study a large number of alternative engine cycle parameters and configurations.

The engine, within SOAPP, is made up of components such as inlets, compressors, burners, turbines, heat exchangers, and reheat burners. The computations involving each of these components are made in subprograms called modules. These modules contain the latest calculation techniques and are continually updated for this purpose. The analyst may select any desired engine configuration which can have any of a number of compressor and turbine types and any pressure ratio, turbine inlet temperature, and value for other parameters of interest.

The SOAP program locates the modules in the machine library and links them together in a running engine calculation. The actual order of calculation is automatically determined by the program through a preprocessor program. The parameters, such as temperatures and pressures, are passed along downstream in the calculation and build up an array of values at each station for all of the parameters as the calculation flows toward the exit nozzle. There are four basic arrays that bind the engine deck into a running system. There is a continuity array which passes the values of parameters from module to module, the spool array which links the turbine with its compressor, the stream array which contains parameters that have only one value per stream, and the constants array which are the values associated with specific components.

The input conforms to preselected designations and runs directly from the input block to the modules. When a design point is run, the scaling constants for any compressor or turbine version are calculated so that the off-design points that follow are properly scaled.

Output

The output computed by the SOAPP for this study included the following items:

1. Percentage horsepower
2. Percentage speed
3. Horsepower

FIG. 65

DESIGN TORQUE AND SPEED CHARACTERISTICS

SINGLE – SHAFT GAS TURBINES

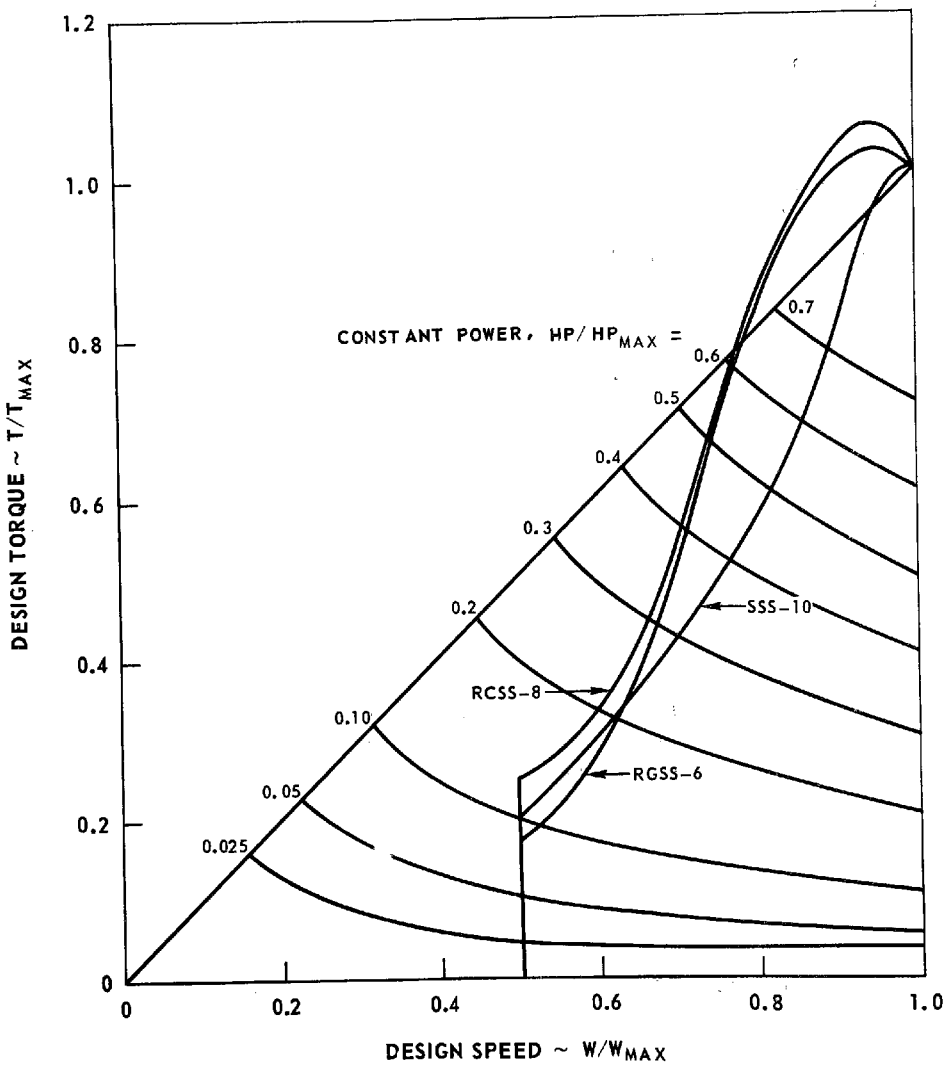

4. Speed
5. Fuel flow
6. Burner inlet temperature
7. Turbine inlet temperature
8. Turbine exhaust temperature
9. Engine exhaust temperature
10. Airflow
11. Compressor pressure ratio
12. Engine exhaust flow
13. Fuel-air ratio
14. Heat exchanger effectiveness
15. Engine torque
16. Percentage torque

Each computer output sheet contains printouts of these values for fixed horsepower and speed commands. Horsepower values were selected from 2% to 100% at the design speed, and appropriate values of horsepower were computed for design speeds ranging down to 50%. Eight different engine speeds were selected and approximately 40 points run for each engine condition.

Performance was generated for the following five ambient conditions:

1. Sea level, standard day
2. 5000-ft standard day
3. Sea level, 32 F
4. Sea level, 85 F
5. Sea level, 105 F

Therefore, the complete set of output data for Phase II consisted of five conditions for three engines, and approximately 40 points per engine, for a total of approximately 600 calculated engine operating points.

Although complete sets of data were generated for all three engines, the final changes which occurred during the optimization process were not necessarily included in the final output for each engine. Trends for various ambient conditions, however, were firmly established and it was judged not essential to rerun the entire 200 points for each final engine.

The final data consisted of the sea level, standard-day calculations for the simple-cycle engine, the regenerated engine, and the recuperated engine. The data were then plotted for each engine in order to determine the maximum torque characteristics, the fuel flow lines, temperature lines, etc. Lines for each operating point were determined by the maximum allowable turbine inlet temperature. For all three engines, this was 1900 degrees, corresponding to the use of uncooled turbines. Figure 65 shows the torque-speed characteristics for all three engines for standard-day conditions. Fuel flow is superimposed on the torque-speed curve for the RGSS-6

RGSS-6 TORQUE CHARACTERISTICS

DESIGN SPEED = 82,000 RPM

DESIGN POWER = 130 HP

T.I.T. = 1900 F

AMBIENT TEMP = 59 F

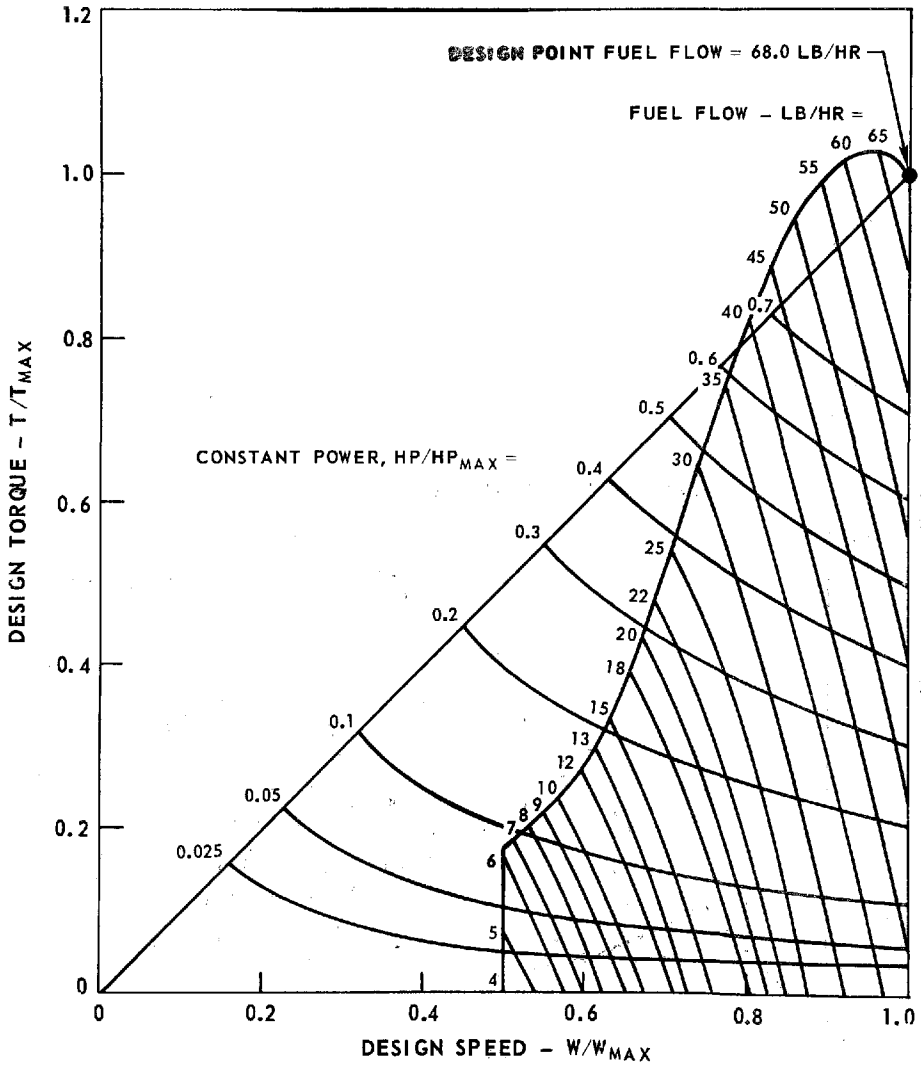

FIG. 67

RCSS-8 TORQUE CHARACTERISTICS

DESIGN SPEED = 95,000 RPM

DESIGN POWER = 130 HP

T.I.T. = 1900 F

AMBIENT TEMP = 59 F

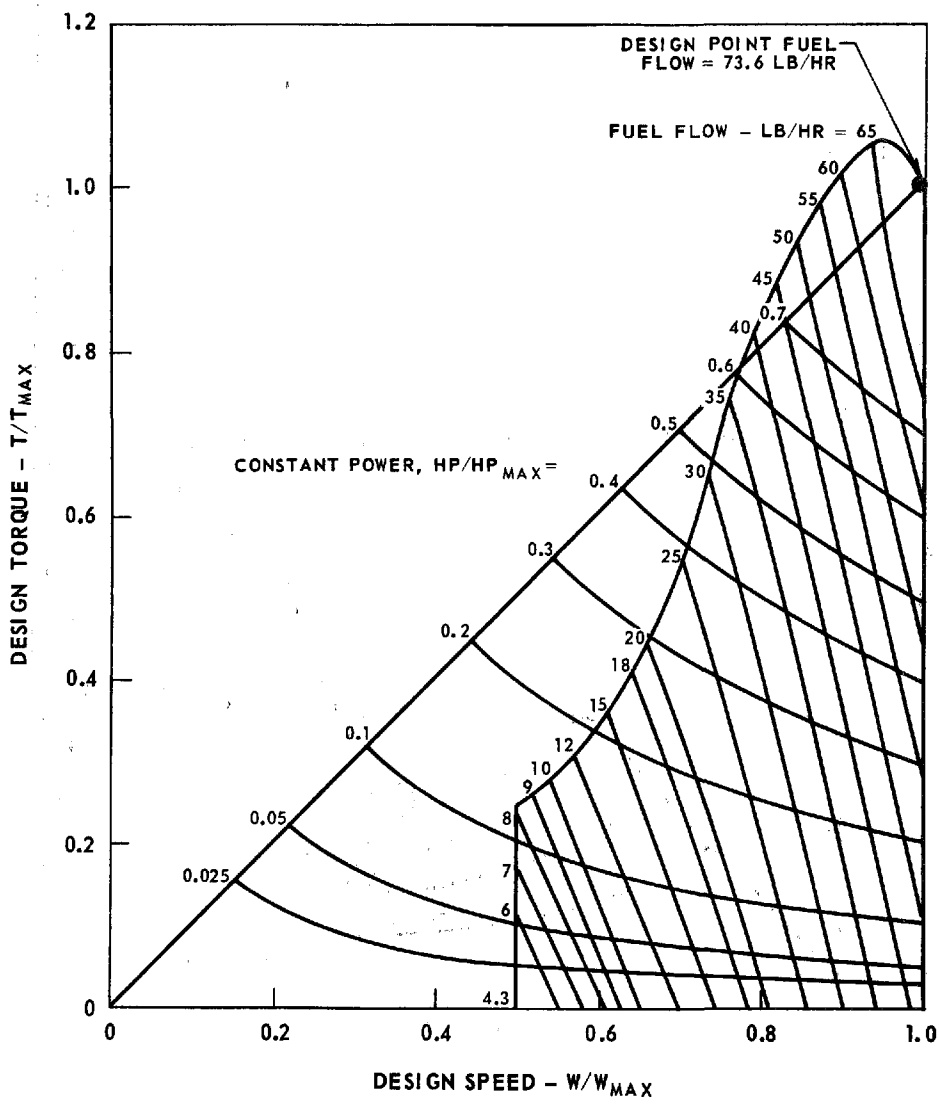

FIG. 68

SSS-10 TORQUE CHARACTERISTICS

DESIGN SPEED = 106,000 RPM

DESIGN POWER = 130 HP

T.I.T. = 1900 F

AMBIENT TEMP = 59 F

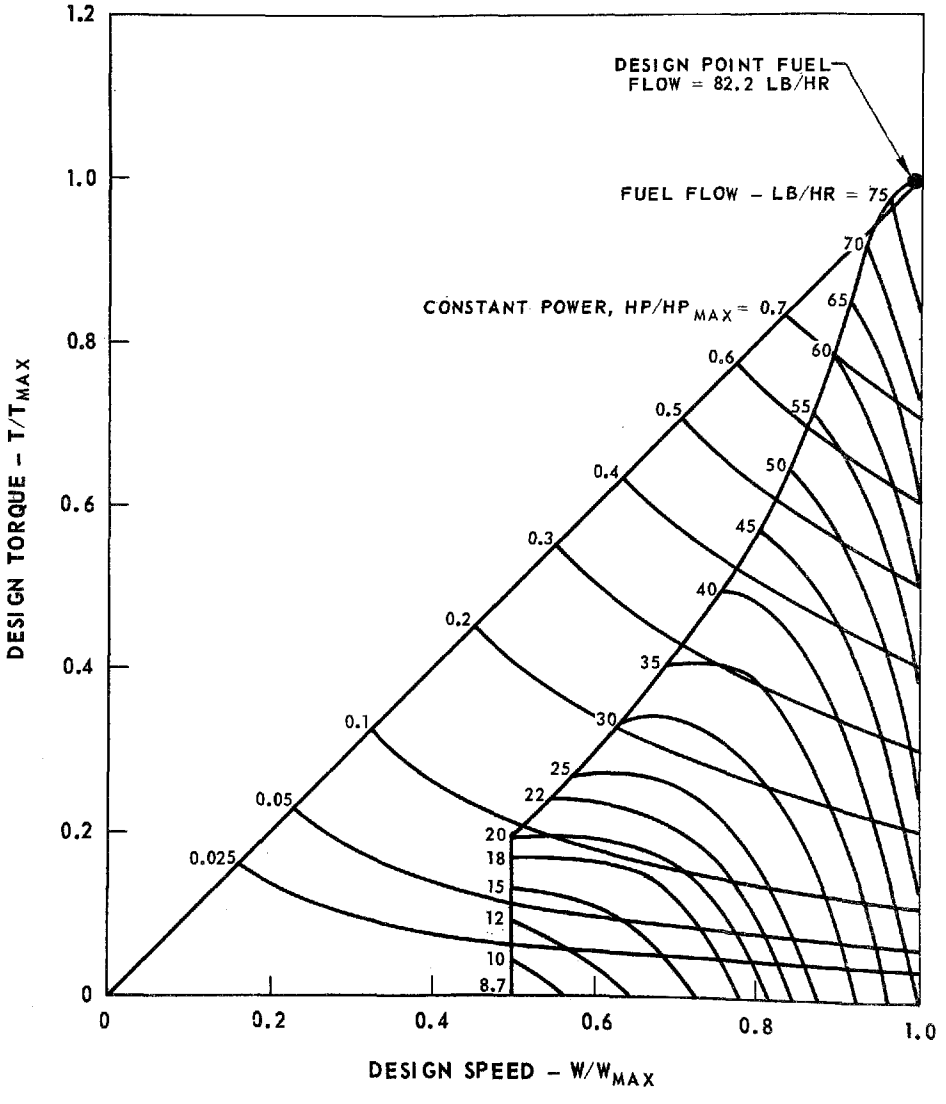

on Fig. 66, while fuel flows for the RCSS-8 and SSS-10, are plotted on Figs. 67 and 68, respectively.

Selection of Engine Operating Line

Engine operating lines were selected to provide common modes of operation for all three engines. Two considerations entered into the selection of these lines. These were: vehicle acceleration response and engine operating life.

With regard to engine acceleration response, there have been reservations relative to the capability of a gas turbine engine to provide response similar to that currently experienced by the owners of automobiles. The problem of response is many-fold. It includes a consideration not only of the engine itself and its steady-state torque capabilities, but of the engine inertia, the transmission characteristics, and the transient characteristics of the engine.

It is well known that the single-shaft engine suffers from much poorer torque-speed characteristics than its free-turbine counterpart. Thus, the single-shaft engine requires a fairly sophisticated transmission in order to provide suitable propulsion system characteristics for vehicles. On the other hand, the characteristics of the single-shaft engine are such that its maximum torque at any operating engine speed is instantly available. That is to say, an increment in fuel flow to the burner is immediately felt as a greater torque output through the turbine which is connected directly to the operating shaft. Free-turbine engines have a built-in transient lag since the additional energy added in the combustor is extracted first through the compressor turbine and is felt secondarily by the power turbine. Because of this response lag, many automotive gas turbine engines with a free-turbine configuration include variable geometry on the power turbine in order to extract more energy from the expanding gases for propulsion purposes.

Since a single-shaft engine requires a sophisticated transmission in order to serve as a practical propulsion system, the transmission itself can be used to solve response problems which remain. Specifically, the control system of the engine, transmission and accelerator pedal can be integrated so that the vehicle operator feels an instantaneous response to his pedal command, while the engine can simultaneously be allowed to accelerate to speeds where more torque is available, provided the engine's steady-state operating line is selected at some combination of speed and output which provides an acceleration margin at that speed. Figure 69 shows six potential operating lines. The first operating line (AA) is the maximum torque characteristic of the engine at any given speed. It is obvious that an engine operating on this line, to deliver steady-state power requirements, would be unable by itself to accelerate either the vehicle or itself without provisions in the transmission to drop the load. But this dropping of load would aggravate the response characteristics and be unacceptable to the motorist; thus line AA

ENGINE OPERATING LINES

RCSS-8

DESIGN SPEED = 95,000 RPM

DESIGN POWER = 130 HP

T.I.T. = 1900 F

AMBIENT TEMP = 59 F

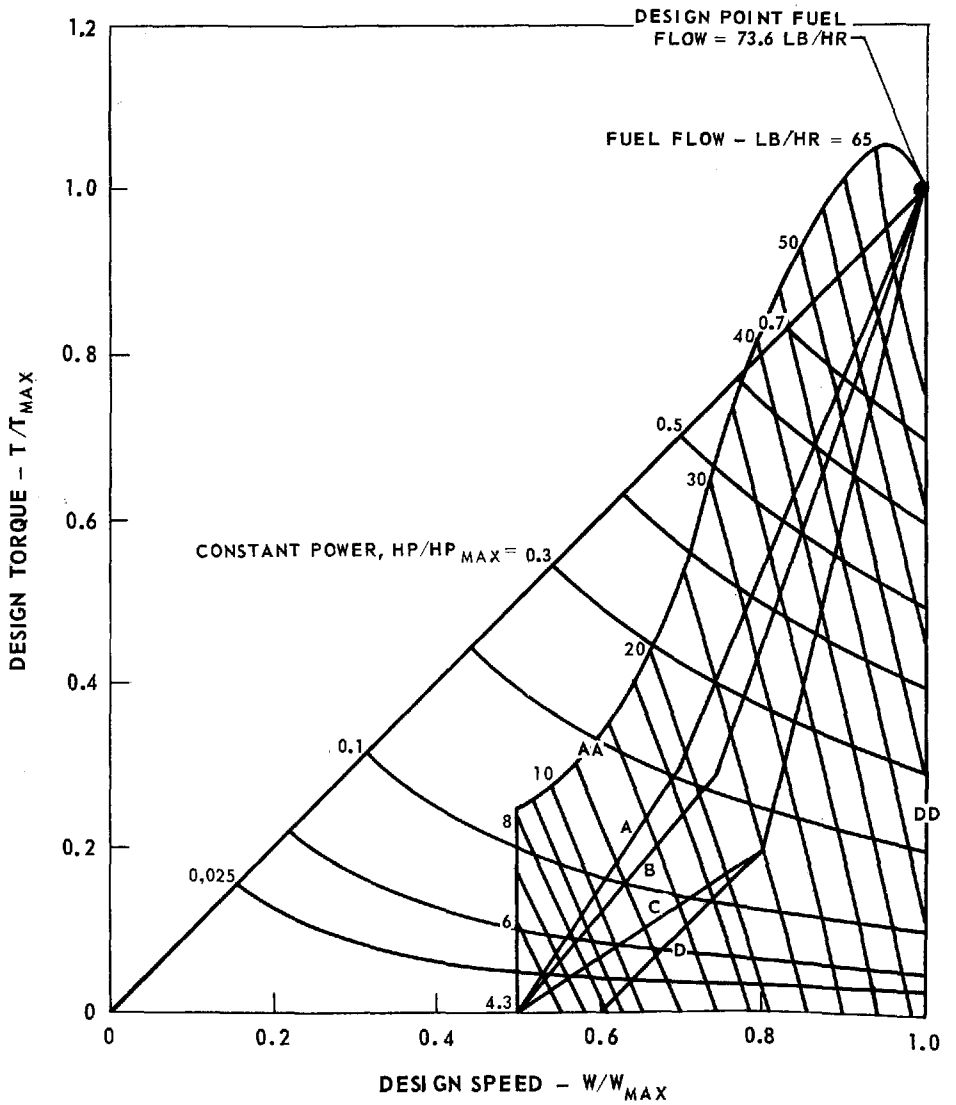

is not acceptable as an operating line. At the other extreme, operating line DD can provide an engine with 100% power response at any power requirement, but its fuel consumption would be unacceptable since it is always operating at maximum airflow.

The operating lines designated as A, B, C and D represent reasonable compromises between the extremes of fuel economy and response characteristics as represented by lines AA and DD. At this point in the development cycle, it cannot be stated with certainty which operating line is optimum or that any one would be optimum for all drivers. The infinitely variable transmission makes it feasible to offer several different operating lines to suit the driver's desires. For example, a driver-selected option can be visualized for performance with a fuel economy penalty, or vice versa. Considering the lines in sequence, line A provides the best fuel economy for the heat-exchanger engines but the least amount of response for all engines. Line B provides the best fuel economy for the simple-cycle engine, a somewhat poorer fuel economy for the heat-exchanger engines, but provides a more adequate response margin. Line C provides the greatest response margin of the three lines which start at the idle speed of 50%, but at the expense of fuel economy in all three engines. Line D represents an even greater margin of response, which is achieved by fixing idle speed at 60%. For the purposes of the present study, it is judged that line B represents the best overall combination of fuel economy and response for all three engines.

A second consideration in the establishment of the operating line is that of engine life. With reference to Figs. 66 and 67, it can be seen that the optimum fuel flow line for the heat-exchanger engines is coincident with the maximum torque line. This is because the greatest efficiency is achieved at the highest turbine inlet temperature for the engines of this configuration. But the stresses associated with high temperatures are such that the maximum turbine inlet temperature should not be used on a steady-state basis for more than 100 hours of engine operation in order to achieve the desired design life. Thus, the optimum fuel flow line for the heat-exchanger engines does not represent a practical operating line. On the other hand, transient excursions beyond the maximum turbine inlet temperature are allowable and acceptable. The simple rule of thumb of greatest validity is that, for steady-state operation, the turbine exhaust temperature at the design point should not be exceeded since the turbine exhaust temperature is closely related to the turbine metal temperature which is the determining factor in engine life calculations. The fuel control selected, which has been described previously, permits transient overtemperature subject to time-constant design parameters as a function of exhaust gas temperature. It assures that steady-state operation will not exceed allowable steady-state exhaust gas temperatures.

GAS TURBINE EXHAUST EMISSIONS

NITROGEN OXIDES

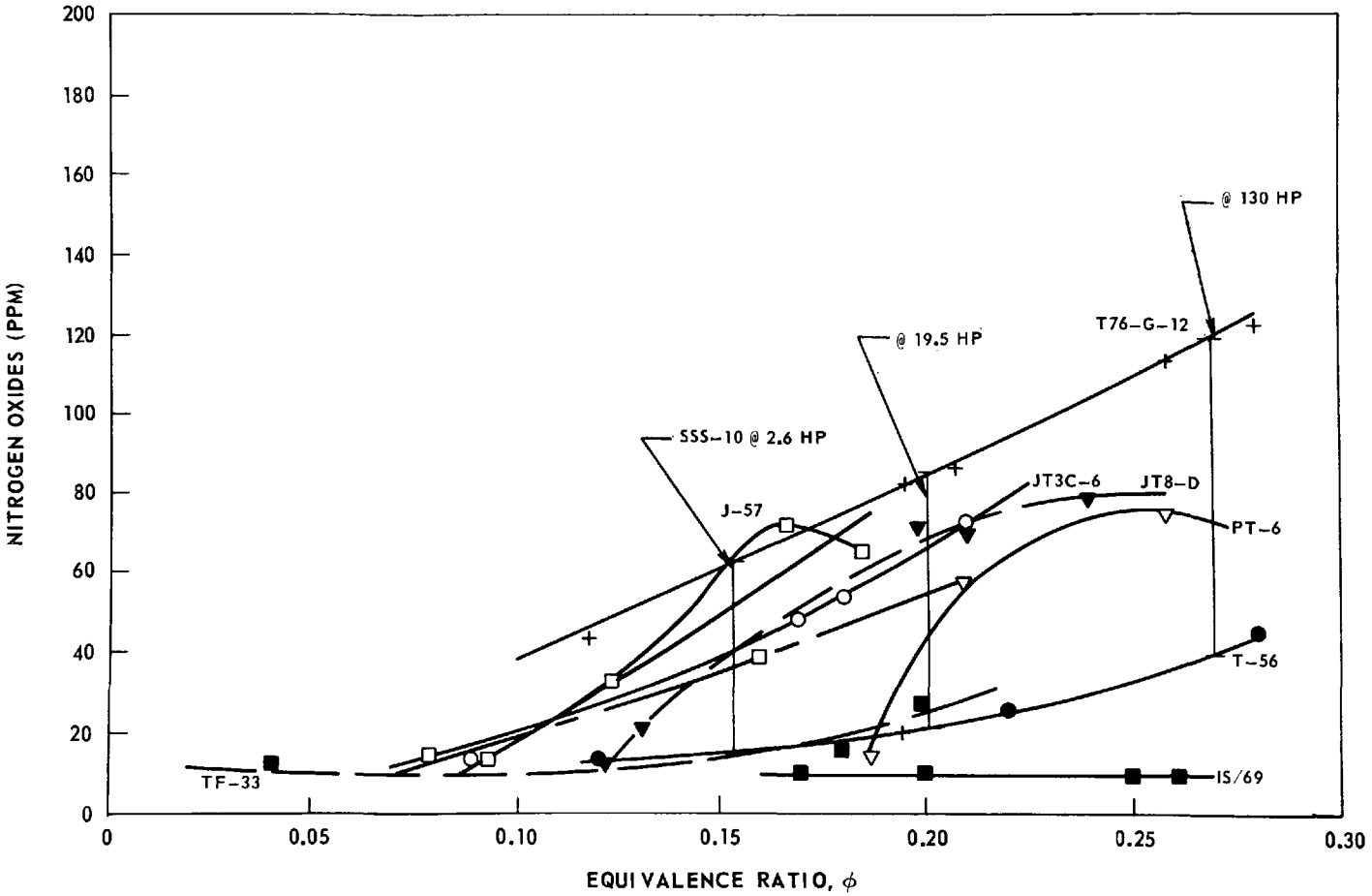

L-971249-7

FIG. 70

Emissions Characteristics

Emissions characteristics are based on state-of-the-art data as reported in various survey documents. In the case of the heat-exchanger engines, emissions measurements for state-of-the-art regenerated engines have been reported (Ref. 17). In the case of the simple-cycle engine, the data are developed from Ref. 18 which presents a survey of various simple-cycle aircraft engines. From these data, emissions index curves have been prepared suitable for input to the mission analysis program. These emissions index data are consistent with the operating lines discussed above, with emissions characteristics developed from fuel-air ratios (converted to equivalence ratios) which were reported as the output from the engine cycle analysis program.

Figure 70 presents NO_x exhaust emission data for a number of simple-cycle gas turbine engines from Ref. 18. The upper and lower values of NO_x are shown for three equivalence ratios corresponding to the operating line for the SSS-10 at powers of 2.6 hp, 19.5 hp and full horsepower. Figure 71 shows the same information for carbon monoxide. The bars shown are those believed to be typical of state-of-the-art, high-low values for simple-cycle gas turbine engines. It will be noted that the Contractor-produced PT6 engine is eliminated from this analysis since it is known that it is not typical, in carbon monoxide emissions, of low-emission combustors. Figure 72 presents these same data for unburned hydrocarbons. It will be noted that the extreme scatter of the UHC data renders it highly questionable and that there is practically no correlation between hydrocarbon output and carbon monoxide output. However, it is believed that hydrocarbon output is one of the most easily controlled emissions characteristics in the gas turbine engine.

Several emissions cases were run for both simple-cycle and heat-exchanger engines. In the case of the regenerated engine (RGSS-6), the emissions indices were derived from data reported on the General Motors GT-309 in Ref. 17, as was done in Ref. 1. The emissions indices for the RCSS-8 engine were slightly modified from those for the RGSS-6 to account for the lowered combustor inlet air temperature predictions as derived from the engine performance program. For the SSS-10, the emissions indices were derived from the T-56 engine (Allison Division of General Motors) as shown in Figs. 70, 71, and 72 for NO_x, CO, and UHC, respectively, correlated to the equivalence ratios calculated in the engine cycle analysis predictions. The corresponding equivalence ratios at 2.6, 19.5, and 130 hp are shown on these figures.

In addition, for all engines, emissions indices were approximated to indicate the levels required to meet Federal standards.

GAS TURBINE EXHAUST EMISSIONS

CARBON MONOXIDE

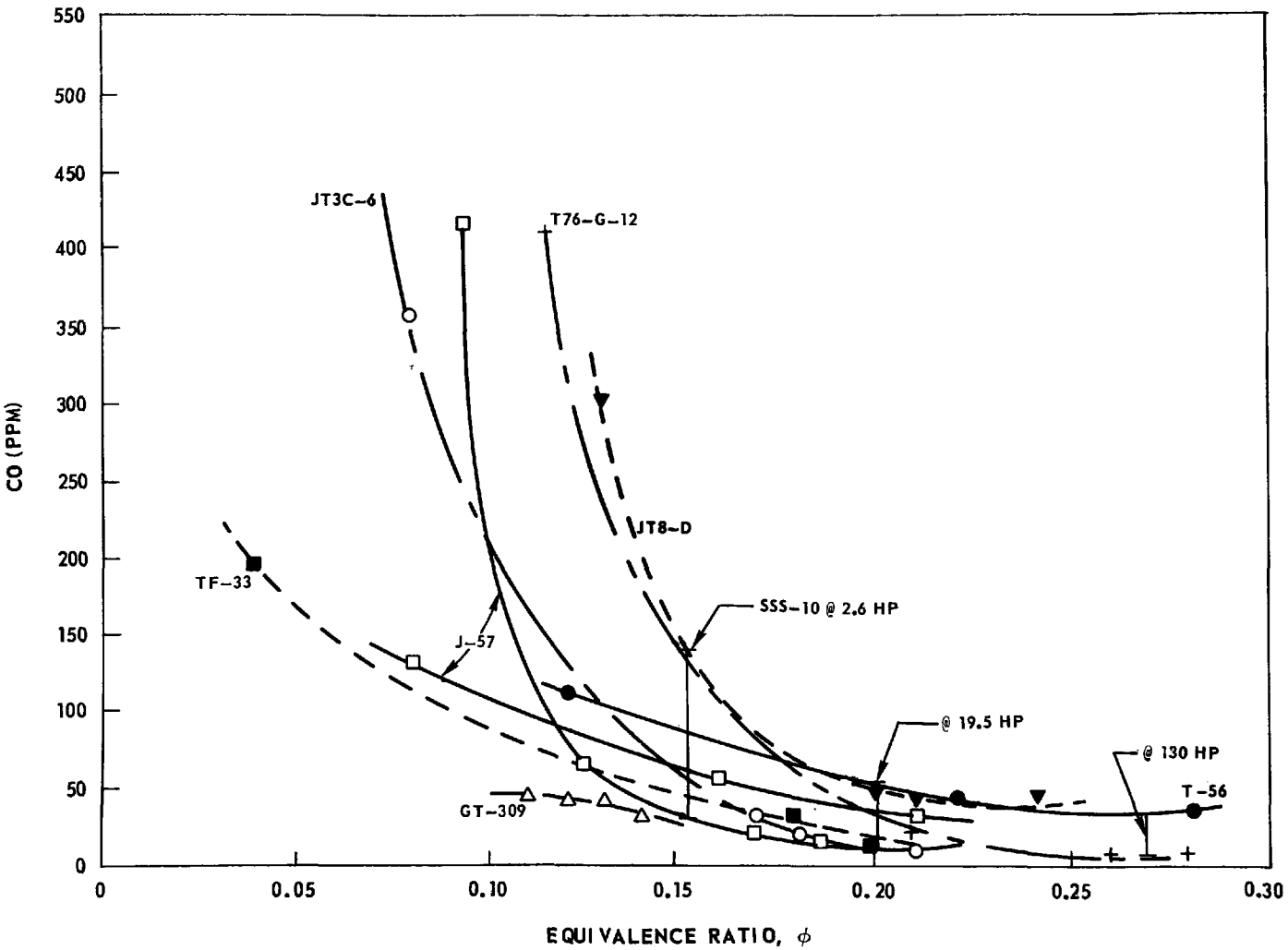

L-971249-7

FIG. 71

FIG. 22

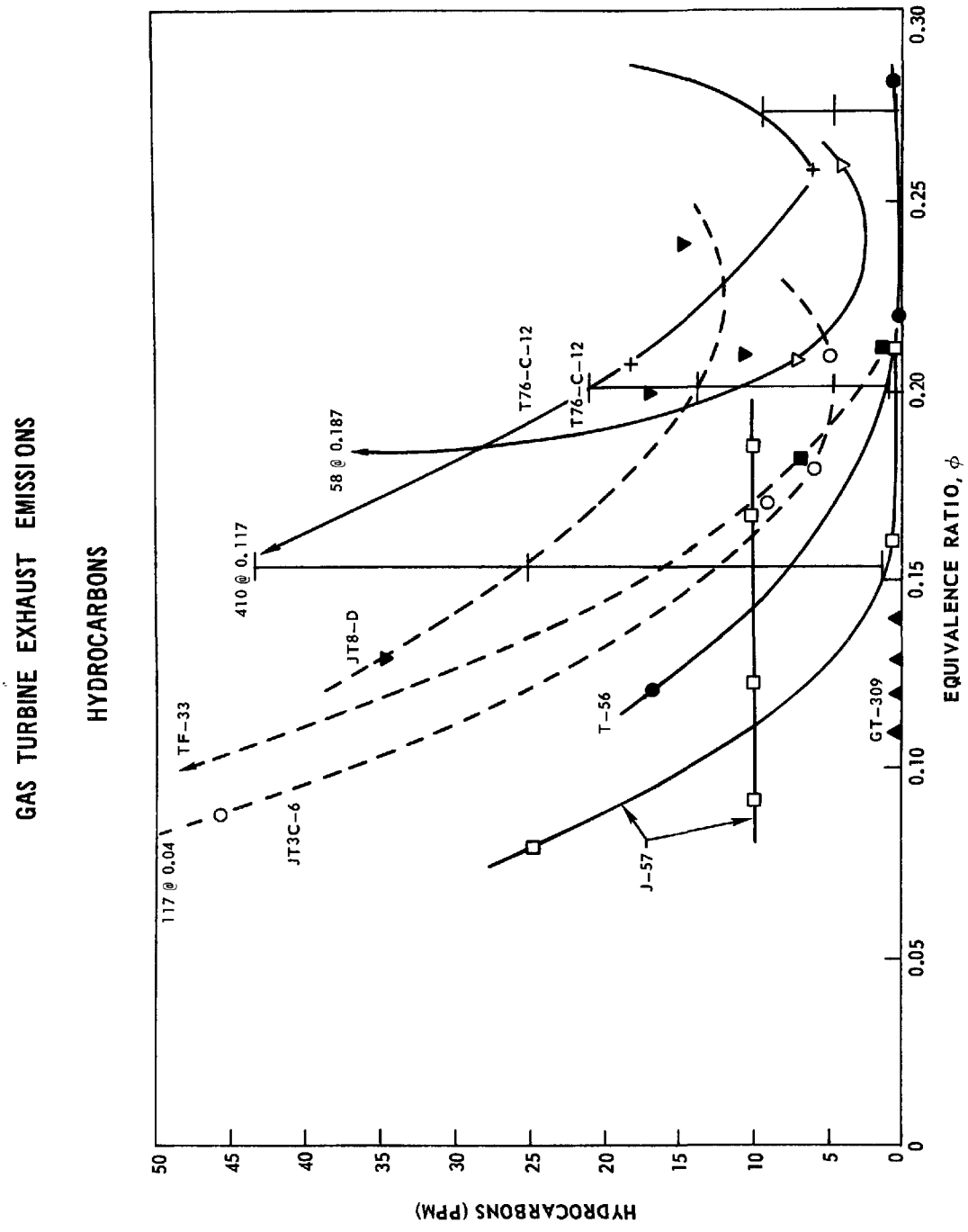
GAS TURBINE EXHAUST EMISSIONS
HYDROCARBONS
HYDROCARBONS (PPM)
EQUIVALENCE RATIO, ϕ
0
5
10
15
20
25
30
35
40
45
50
0.05
0.10
0.15
0.20
0.25
0.30
117 @ 0.04
TF-33
JT3C-6
JT8-D
410 @ 0.117
58 @ 0.187
T76-C-12
T76-C-12
T-56
J-57
GT-309

The emissions index data resulting from these selected curves for all three engines are shown in Figs. 97 through 103 and are discussed in the Emissions portion of the following section. These emissions index data serve as input in the vehicle mission analysis program for purposes of deriving emissions estimates.

VEHICLE EVALUATION

Transmission Modeling

The engines chosen for final optimization restricted the choice of available automatic transmissions to those compatible with the characteristically poor low-speed torque characteristics and narrow operating speed range of the single-shaft gas turbine. Further restrictions on the transmission are that it should be light-weight, durable, and have (assuming there are no off-the-shelf units available) the potential for mass producibility and low cost. Of the five basic types of transmission described in an earlier section (mechanical, hydromechanical, hydrokinetic, electrical and traction-drive), the GE HMT was chosen for evaluation. In addition, the Borg-Warner 8-speed mechanical transmission was chosen as an alternate for performance calculations.

Transmission Description - GE HMT

The GE HMT is an infinitely variable hydromechanical transmission designed to provide a stepless and continuously variable ratio change from full reverse to full forward and overdrive. The basic rotating elements are two hydraulic ball-pumps and a simple planetary gear set. The support items are a suitable control and two stroking actuators together with a small fixed-displacement charge pump. The input shaft from the engine is coupled directly to the sun gear of a planetary gear system and also drives the input hydraulic element. The output hydraulic element, which is hydraulically coupled to the input element, drives the ring gear. The planet gears, through their carrier, drive the output shaft. Ratio change is accomplished by varying ring gear speed and direction. This is done by changing the displacement of the input hydraulic element in response to signals from the ratio controller. The transmission incorporates a ratio control system which is programmed to reflect the desired torque for any particular engine speed. Approximately 60% of the torque is carried hydraulically, and 40% is carried mechanically through the sun gear.

The transmission weighs 165 lb dry and will use 20 lb of hydraulic fluid (SAE 10-30 motor oil is recommended). Rated and maximum input speeds are 3200 and 4200 rpm, respectively. However, these speeds will not be reached since 100% engine output speed is about 2700 rpm following the primary gear reduction. Nominal rated transmission output torque is 700 lb-ft (equivalent to wheel-spin torque for a 4000-lb vehicle with 50-50 weight distribution and a 2.86 rear-axle ratio).

The transmission efficiency data on which all HMT vehicle performance calculations were based are shown in Fig. 23. The analytical expression for transmission efficiency at the top of Fig. 23 fits the efficiency data over the range of input powers shown on the figure. This equation was used to extrapolate transmission efficiency when engine input power ratios (engine input power ÷ maximum power) were below 10%, since no data were available in that range. However, for the mission

FIG. 73

HYDROMECHANICAL TRANSMISSION INERTIA

GE HMT 870 (8.7 CU. IN./REV)

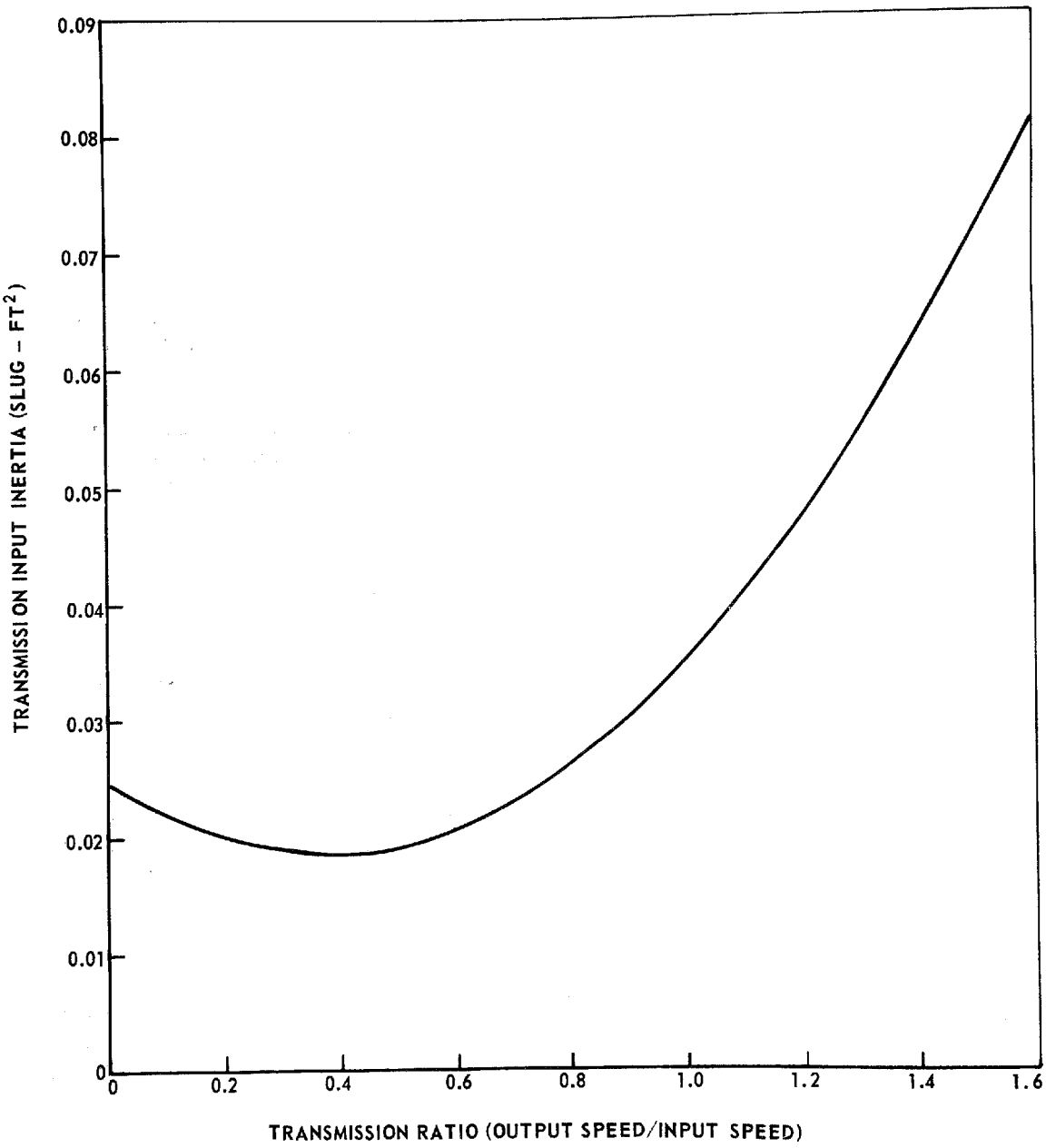

analysis work done in this study, the vehicles spend very little time at such low power levels. The rotational inertia of the 8.7 cu-in HMT, as a function of transmission ratio, is shown in Fig. 73.

Ratio Control

The transmission ratio is automatically controlled. For any road load condition, the control will select ratios to operate the engine according to a predetermined speed-load schedule. The speed-load schedule is established by the relationship of fuel control setting to controlled speed for each accelerator pedal position.

The optimum fuel flow line may be selected as the speed-load schedule, or some trade-offs may be desirable in the interest of overall vehicle performance to accommodate such factors as emissions, engine durability, high-speed power requirements and shape of the transmission efficiency curve.

The transmission control receives inputs of accelerator position and engine speed. If the accelerator is depressed, the transmission ratio controller calls for more engine speed. This signal is simultaneously fed by direct mechanical linkage to the engine fuel control. Since the engine speed cannot change as fast as the mechanical input from the accelerator, a speed difference signal is produced in the controller. This differential moves the controller output linkage to increase transmission ratio, unloading the engine and allowing it to accelerate. As engine speed increases, the speed error in the control approaches zero and transmission ratio stabilizes at a new value consistent with the engine torque for the particular engine speed selected by the operator and the horsepower load at the wheels. Viewed another way, if the accelerator and fuel control are maintained in a fixed position with the vehicle moving over varying terrain, the transmission will continually change ratio to maintain the desired engine torque value for the engine speed. Engine speed under this condition would be essentially constant.

Transmission Description - Borg-Warner 8-Speed Mechanical

The Borg-Warner 8-speed mechanical transmission consists of a four-speed planetary automatic gearbox preceded by a two-stage splitter which, in effect, doubles the number of ratios in the gearbox. The controlled slipping clutch can transmit constant torque to the wheels at any engine speed (below the clutch lock-up point) without multiplication. Its advantage is that the stall speed can be adjusted in the design process so that the engine can be completely idled or be completely engaged within a fairly narrow range. In addition, when the clutch is locked up, power is transmitted with a higher efficiency than associated with a hydraulic slipping device. The overall mechanical efficiency of the 8-speed gearbox is about 85% (not including clutch losses).

CONTROLLED SLIPPING-CLUTCH CHARACTERISTICS

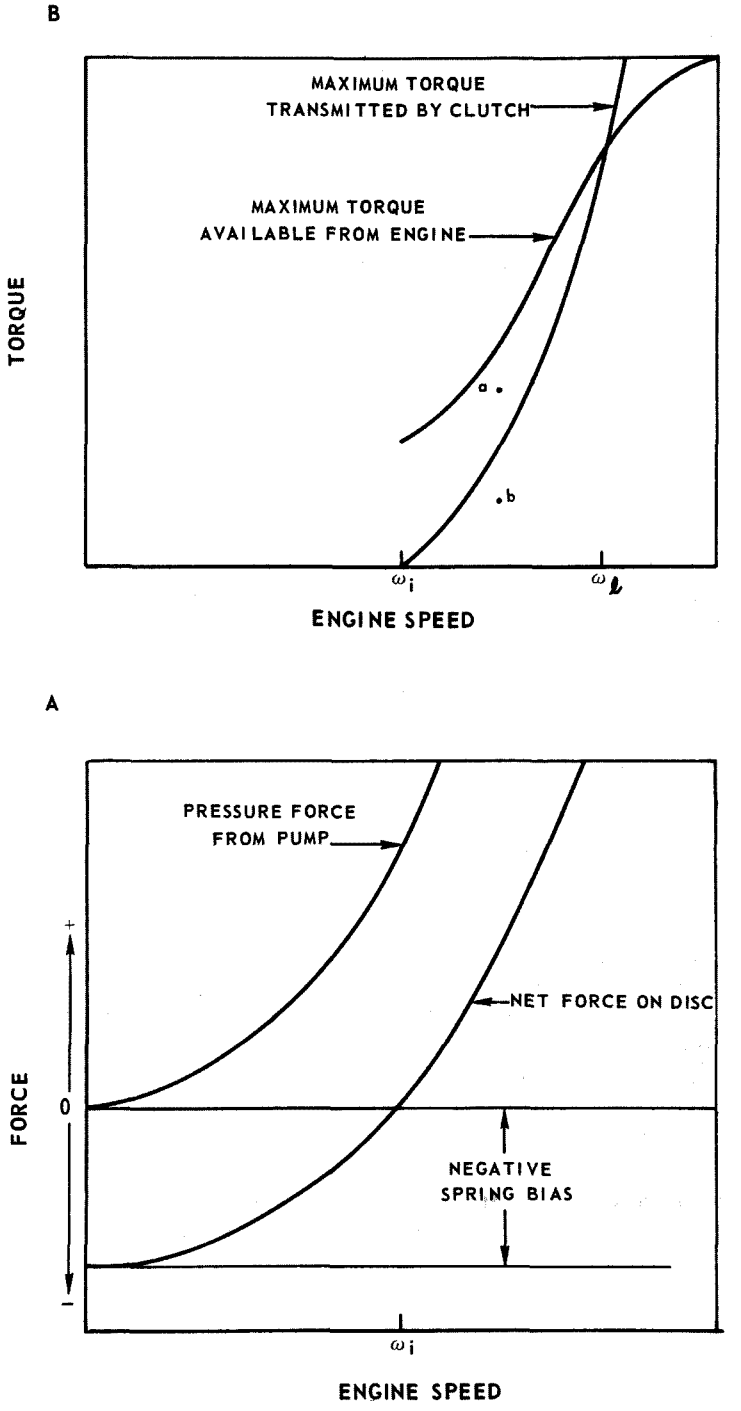

The clutch is a multiplate, oil-bath, disc-type design, about 9 in. in diameter. An oil cooler is required to dissipate excess heat. The torque transmitted by the clutch increases with increasing engine speed. This is done by applying increasing hydraulic pressure to the clutch pressure plate(s) against the action of a negative bias pressure from mechanical springs. The clutch system is designed so that engagement begins to occur at just above idle speed.

The action of the controlled slipping clutch can be more easily understood with the aid of Fig. 74. In Fig. 74A, the output pressure of the pump is shown increasing with the square of the engine speed. This pressure acts on the clutch pressure plate against the action of the negative spring bias (an opposing spring force). The sum of the pump and spring pressures is negative (that is, no pressure is applied to the clutch disc) until the engine speed increases to the value indicated by ω_i. At engine speeds above ω_i, the clutch begins to transmit torque because the pump pressure is greater than the negative spring bias, and a positive pressure, which increases with engine speed, is applied to the clutch disc.

Figure 74B shows the torque transmitted by the clutch, as a function of engine speed, superimposed on a typical single-shaft gas turbine torque curve. The value ω_i is the engine speed at which the clutch begins to transmit torque. The torque transmitted by the clutch increases as the square of the engine speed (because the torque transmitted is proportional to clutch pressure) until the speed ω_ℓ is reached. Beyond this speed, the maximum torque of the engine is less than the torque capacity of the clutch and the clutch will be locked. If an engine torque is commanded which is greater than the maximum torque that the clutch can transmit (say point a), the torque difference between the commanded and clutch torques will cause the engine to accelerate. If an engine torque is commanded which is less than the maximum clutch torque (point b, for example), the clutch will be locked. The speed ω_i would normally be selected as an idle speed and the speed ω_ℓ would be designated as the clutch lock-up speed. The values ω_i and ω_ℓ can be selected by the proper choice of clutch design parameters such as spring bias and pump characteristics.

Conversations with Borg-Warner personnel indicate that it will be possible to incorporate a device, known as an inertia valve, with the clutch system. The valve, which is sensitive to angular acceleration, would be used to limit the rate of change of engine speed during gear changes. The valve is held by a spring whose stiffness is such that the valve can bypass oil to the clutch (to allow slippage) for angular accelerations greater than the design value. The effect of the valve is to produce smoother, less jerky acceleration.

The inertia valve is not suitable for use with engines whose torque output is not a smooth function of time. For example, the discrete power strokes of the Otto-cycle engine produce transient accelerations of the crankshaft which would adversely affect the action of the valve. The continuous and smooth power production of the gas turbine, however, would render it suitable for use with the device.

TABLE IX

SELECTED PHYSICAL CONSTANTS AND BASE-LINE VEHICLE PARAMETERS

Acceleration of gravity	32.2 ft/sec^2
Air density (55 F)	0.0023769 $slug/ft^3$
Fuel density (gas turbine fuel)	7.0 lb/gal (0.143 gal/lb)
Heat content	18,400 Btu/lb
Rolling resistance coefficients	r_0 = 0.015
	r_1 = 2.15 x 10^{-5} lb/lb-fps
	r_2 = 1.85 x 10^{-7} lb/lb-fps^2
Wheel radius	1.1 ft
Product of frontal area and drag coefficient	12 ft^2
Weight distribution	50%-50%
Rear axle efficiency	0.95
Road-tire adhesion coefficient	1.0
Accessory power	
Fuel economy runs	1.3 hp
Acceleration performance runs	4.0 hp
Vehicle test weights (W_t) (Appendix V):	
RGSS-6	3970 lb
RCSS-8	4020 lb
SSS-10	3850 lb
Clutch inertia (8-speed transmission)	200 $lbm-in^2$
Transmission gear ratios (8-speed mechanical transmission):	

Gear	Ratio
1st	4.50
2nd	3.30
3rd	2.56
4th	2.06
5th	1.69
6th	1.40
7th	1.18
8th	1.00

Engine Sizing

The purpose of this task was to define the probable engine size (maximum power) and idle speed in order that the required off-design engine data could be generated for further engine optimization. To accomplish this, a computer program was written which predicts the maximum acceleration performance of a vehicle equipped with the GE-HMT transmission. Other results from this program, and two other programs written for this project, are discussed in later sections. The derivations for these programs are presented in Appendices I and II. The programs themselves, including sample printouts are described in Appendix III.

The criteria used to select the engine size and idle speed were the OAP vehicle acceleration performance goals of Ref. 19. These requirements are listed below. The parameter W_t is the vehicle test weight which is given in Table IX using standard OAP calculations. Table IX contains constants and base-line parameters used for all Vehicle Evaluations.

Acceleration from a standing start:

The minimum distance to be covered in 10.0 sec is 440 ft. The maximum time to reach a velocity of 60 mph is 13.5 sec. Ambient conditions are 14.7 psia, 85 F. Vehicle weight is W_t, and acceleration is on a level grade and is initiated with the engine at the normal idle condition.

Acceleration in merging traffic:

The maximum time to accelerate from a constant velocity of 25 mph to a velocity of 70 mph is 15.0 sec. Time starts when the throttle is depressed. Ambient conditions are 14.7 psia, 85 F. Vehicle weight is W_t, and acceleration is on level grade.

Acceleration, DOT High-Speed Pass Maneuver:

The maximum time and maximum distance to go from an initial velocity of 50 mph with the front of the automobile (18-foot length assumed) 100 feet behind the back of a 55-foot truck traveling at a constant 50 mph to a position where the back of the automobile is 100 feet ahead of the 55-foot truck is 15 sec and 1400 ft. The entire maneuver takes place in a traffic lane adjacent to the lane in which the truck is operated. The vehicle will be accelerated until the maneuver is completed or until a maximum speed of 80 mph is attained, whichever occurs first. Vehicle acceleration ceases when a speed of 80 mph is attained, the maneuver then being completed at a constant 80 mph. (This does not imply a design requirement limiting the maximum vehicle speed to 80 mph.) Time starts when the throttle is depressed. Ambient conditions are 14.7 psia, 85F. Vehicle weight is W_t, and acceleration is on level grade.

HOT-DAY ACCELERATION PERFORMANCE

GE HMT
SSS-10
W = 3050 LB
IDLE SPEED RATIO - W/W_{MAX}:
○—— 0.5
▽—— 0.6
□—— 0.7
ACCESSORY POWER = 1.3 HP

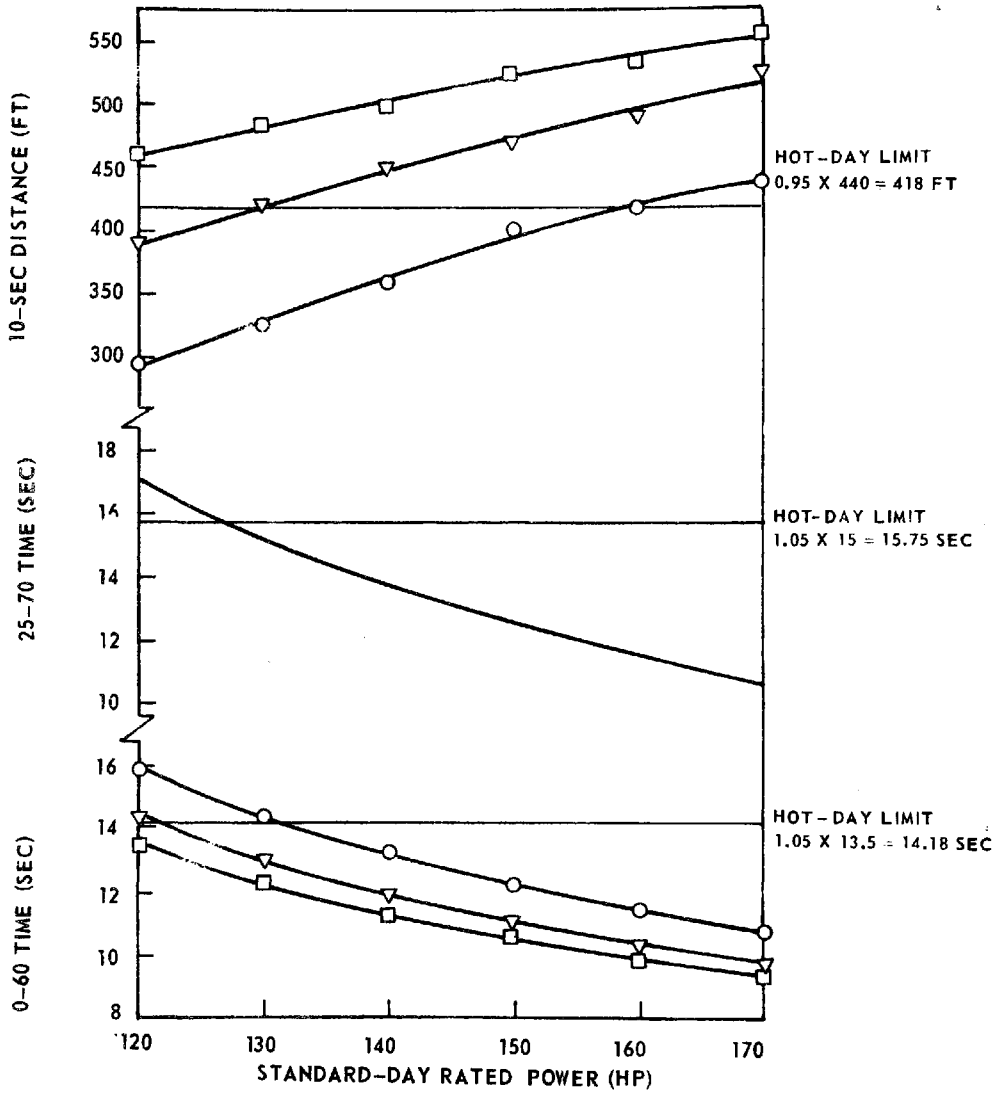

Reference 19 also states that the vehicle must be capable of providing the above acceleration performance within 5% of the stated values when operated at ambient temperatures from -20 to 105 F. For convenience, the OAP acceleration criteria are presented below in tabular form, for both the 85° and 105° days:

Performance Requirement	85° Day	105° Day (5% performance degradation)
0-60 mph acceleration time (sec)	13.5	14.2
Minimum distance covered in 10 sec (ft)	440	418
25-70 mph acceleration time (sec)	15.0	15.8
DOT High-Speed Pass Maneuver:		
Minimum time (sec)	15.0	15.8
Minimum distance (ft)	1400	1470

Because of the relatively severe degradation of performance with increasing temperature (about 15% loss of power between 59 to 105 F ambient temperature), the engines were sized on the basis of the hot-day (105°) requirements rather than the 85° ambient criterion.

Engine sizing was performed by inputting a matrix of (standard-day) engine powers and idle speeds into the HMT vehicle performance computer program to obtain a corresponding matrix of vehicle performance data. (The program corrects for the hot-day performance degradation.) The computed performance data consisted of the requirements for each of the OAP acceleration criteria (0-60 mph acceleration time, etc.). The performance data were then plotted to obtain the different combinations of engine size (maximum power) and idle speed which would just meet the OAP hot-day requirements. This process is illustrated in Fig. 75. The various combinations are formed by the intersections of the 105° day performance requirements (horizontal dashed lines) and the constant-horsepower lines on Fig. 75. The resulting engine power and idle speed pairs were then plotted as shown in Fig. 76. The locus of these points, for each acceleration criterion, divides the power and idle speed map of Fig. 76 into two regions. The region above and to the right of the locus contains power and idle speed combinations which will exceed the particular acceleration criterion. Conversely, all power and idle speed pairs below and to the left of the locus will not meet the acceleration requirements. Thus, the smallest engine size which will just meet all the OAP requirements will lie on the rightmost locus (of the three shown) for a given idle speed. Similarly, the lowest acceptable idle speed will lie on the uppermost locus for a given engine size. For the conditions shown in Fig. 76, the required size is 111 hp at an idle speed ratio of 0.60. The nominal unmodified standard-day engine rating to meet this requirement is 130 hp, assuming that 85% of standard-day torque is available at 105 F. Therefore, all three engines were specified to be rated at 130 hp at 59 F. A normal 50% idle speed was chosen because it is certain

OAP VEHICLE DESIGN GOAL PERFORMANCE ENVELOPE

- ENGINE SIZED FOR HOT-DAY (105 F) PERFORMANCE
- SSS-10 GAS TURBINE
- GE HMT
- VEHICLE WEIGHT = 3850 LB
- ACCESSORY POWER = 1.3 HP

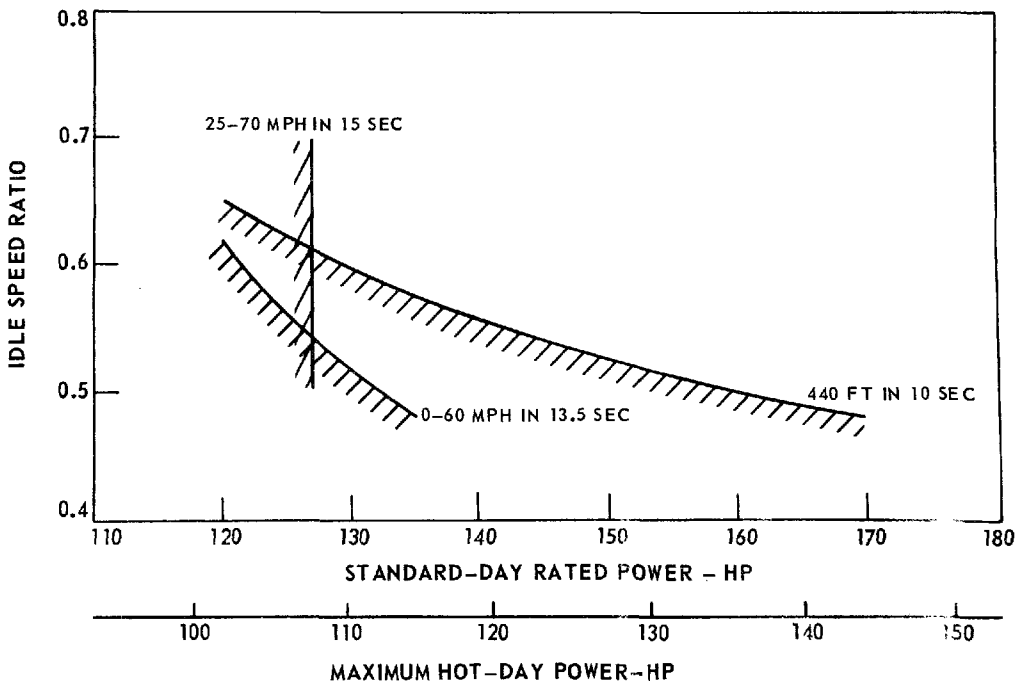

FIG. 76

For known values of r_1 and r_2, the radii of the remaining two gears are

$$r_3 = \frac{d - r_1 - r_2}{1 + \left(\frac{r_1}{r_2}\right) R_o}, \quad r_4 = \left(\frac{r_1 r_3}{r^2}\right) R_o \tag{6}$$

In Eq. (5), the gear face width (thickness), t, was assumed to be constant. However, the face width is a function of the power to be transferred and the rotational speed. This relationship is expressed as

$$D^2 t = \frac{31{,}500 \text{ hp } (R+1)^3}{k \omega R}, \tag{7}$$

where D = distance between gear center lines, in.
t = face width, in.
= input horsepower
R = reduction ratio
ω = pinion speed, rpm
= surface durability factor, lb/in.^{2}

Also:

$$D = r_1 + r_2 \tag{8}$$

where r_1 = pinion radius and r_2 = radius of mating gear. Equation (8) can also be written as

$$D = r_1(1 + R). \tag{9}$$

Substituting Eq. (9) into Eq. (7) yields

$$t = \frac{31{,}500 \text{ hp}}{k \omega_1 r_1^2} \left[\left(\frac{r_2}{r_1}\right) + 1\right] \tag{10}$$

INERTIAL ENERGY PARAMETER FOR DOUBLE-REDUCTION GEARING

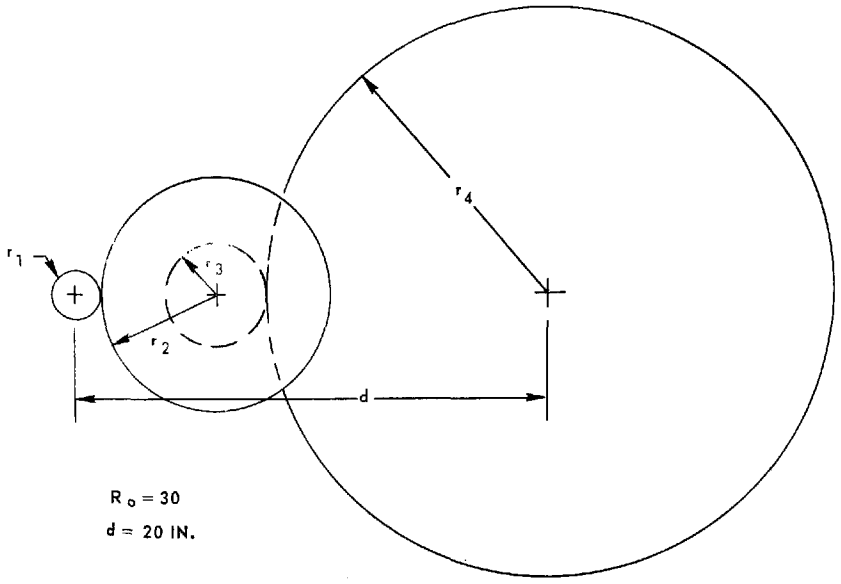

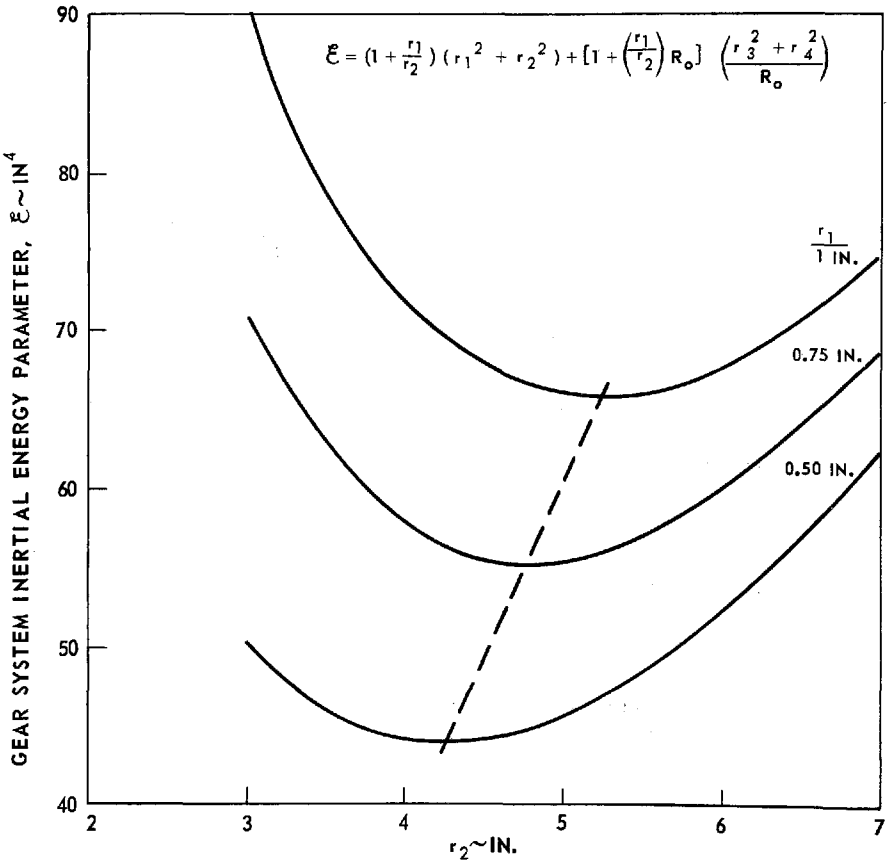

A face width parameter, τ, can be defined as

$$\tau_1 = \frac{\left[\left(\frac{r_2}{r_1}\right) + 1\right]}{r_1^2} \tag{11}$$

The second set of reduction gears can be analyzed in a similar manner, yielding

$$\tau_2 = \frac{r_2}{r_1 r_3^2}\left(\frac{\frac{r_2}{r_1} + R_o}{R_o}\right) \tag{12}$$

By applying Eq. (11) to the first two terms of Eq. (5), and Eq. (12) to the last two terms, Eq. (5), modified for gear thickness, becomes

$$\varepsilon = \left(1 + \frac{r_1}{r_2}\right)\left(r_1^2 + r_2^2\right) + \left[\frac{1 + \left(\frac{r_1}{r_2}\right) R_o}{R_o}\right]\left(r_3^2 + r_4^2\right) \tag{13}$$

Substituting Eq. (6) into Eq. (13) yields an expression for ε in terms of the characteristics of the pinion and mating gears.

$$\varepsilon = \left(1 + \frac{r_1}{r_2}\right)\left(r_1^2 + r_2^2\right) + \frac{(d - r_1 - r_2)^2}{1 + \left(\frac{r_1}{r_2}\right) R_o}\left[\frac{1}{R_o} + \left(\frac{r_1}{r_2}\right)^2 R_o\right] \tag{14}$$

Figure 37 presents the variation of the gear system inertial energy parameter, ε, with pinion gear and mating gear size. With a 0.5-in. radius pinion, the total inertial energy is about 30% less than that for the 1.0 in. radius pinion, for the minimum-ε cases. The 0.5-in. pinion requires a 4-in. mating gear. The corresponding third and fourth gears will have radii of 3.26 in. and 12.23 in., respectively.

Since the gearbox weight will be a small fraction of total vehicle weight, its weight effect on vehicle performance will be small. However, the gears' inertia directly affects the response of the engine to throttle changes and is therefore the dominant factor to be considered.

Figure 38 presents the radii of the third and fourth gears in the double reduction system. The radius of the final gear is rather large and contributes a significant amount to the total gear system inertial energy. The basic problem with using single-stage double reduction gearing is the relatively large span

FIG. 38

GEAR SIZE RELATIONSHIPS

d = 20 IN.

R_o = 30

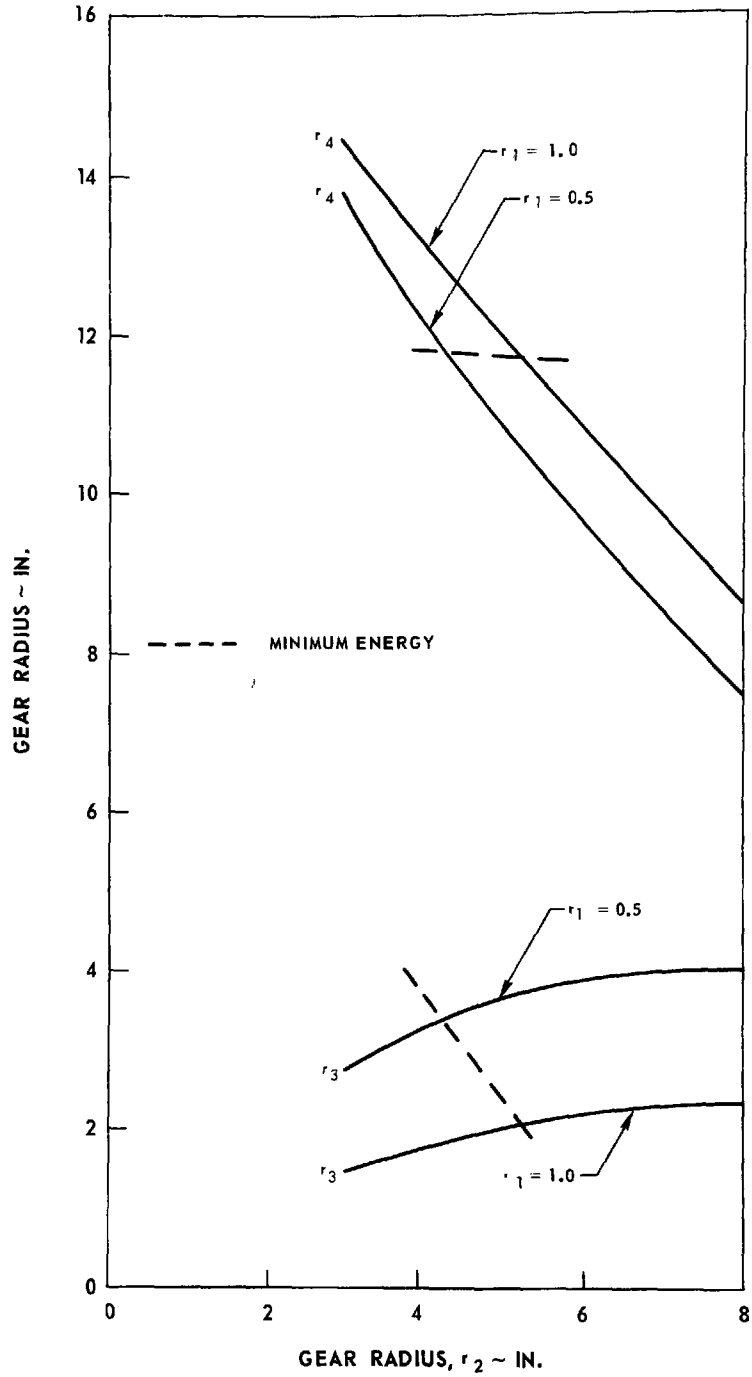

between the input and output shafts. If this distance were smaller, the final gear size could be reduced. The same effect can be achieved by adding a fifth gear the same size as the final gear, as an idler. A schematic is shown in Fig. 39.

With the idler in the system, the energy parameter, ε, is defined as

$$\varepsilon = r_1^4 + r_1^2 r_2^2 + \left(\frac{r_1}{r_2}\right)^2 r_3^4 + \frac{2\, r_4^4}{R_o} \,. \tag{15}$$

The gear radii r_3 and r_4 are:

$$r_3 = \frac{d - r_1 - r_2}{1 + 3\left(\frac{r_1}{r_2}\right) R_o} \,, \quad r_4 = \left(\frac{r_1 r_3}{r_2}\right) R_o \tag{16}$$

The inertia energy parameter, corrected for varying gear thickness becomes

$$\varepsilon = \left(1 + \frac{r_1}{r_2}\right)\left(r_1^2 + r_2^2\right) + \left[\frac{d - r_1 - r_2}{1 + 3\left(\frac{r_1}{r_2}\right) R_o}\right]^2 \left[1 + 2\left(\frac{r_1}{r_2}\right)^2 R_o^2\right] \left[\frac{1 + \left(\frac{r_1}{r_2}\right) R_o}{R_o}\right] \tag{17}$$

The inertial energy for this gear train system is about 50% lower than for the standard double reduction system, as seen by comparing Figs. 37 and 39. Also, the gear sizes are significantly reduced, as evidenced in Fig. 40. Now the largest gear is only 5 in. radius. Consequently, the double reduction system with an idler was chosen for the reduction gearbox in this study.

Installation Concepts

The installation of any power/transmission system in an automobile should provide for easy maintenance, minimal susceptibility to impact damage, and should not encumber the driver or passengers. The selection of a single-shaft gas turbine offers great flexibility as to installation in a full-size six-passenger sedan, because of its small size and light weight. The HMT was chosen as a candidate transmission for purposes of examining the installation problem. The engine and transmission can be mounted transversely and neatly connected with a double

INERTIAL ENERGY PARAMETER DOUBLE-REDUCTION GEARING WITH IDLER

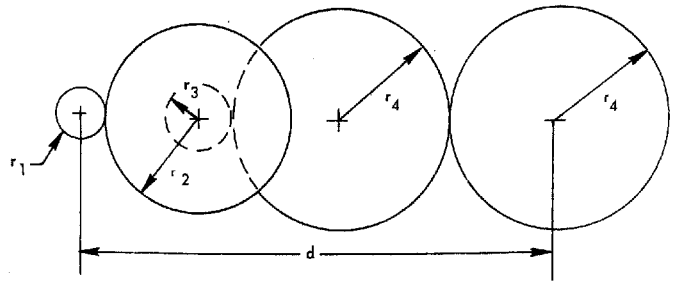

d = 20 IN.

$R_o = 30$

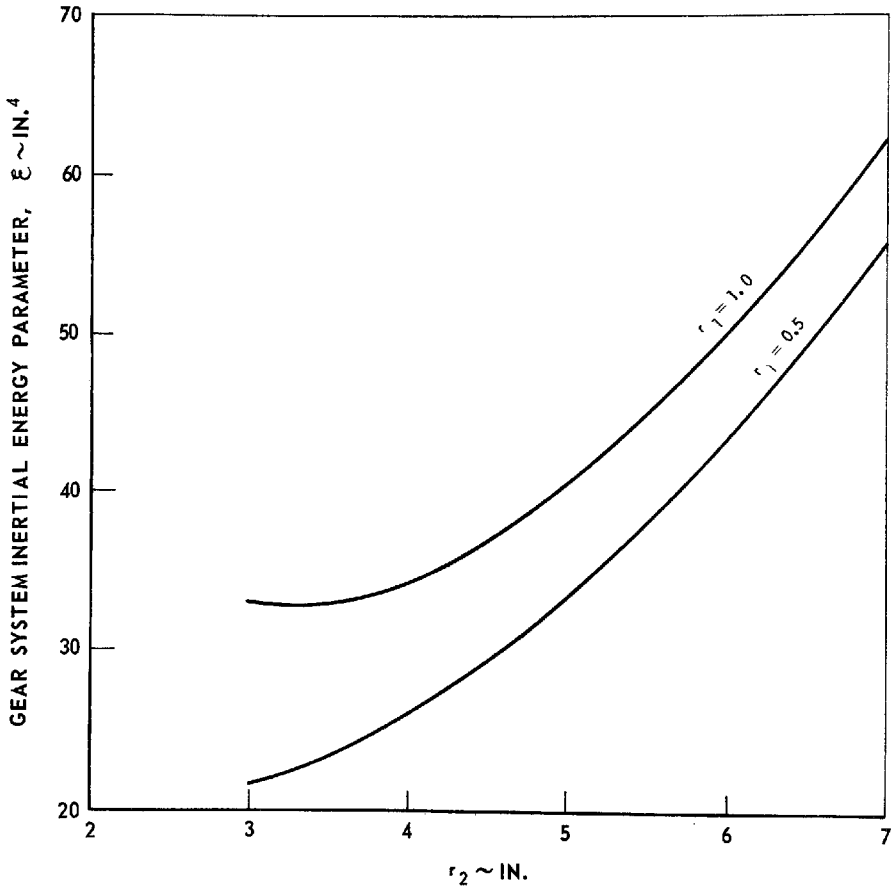

DOUBLE REDUCTION GEARING

GEAR SIZE RELATIONSHIPS

d = 20 IN.
R_o = 30

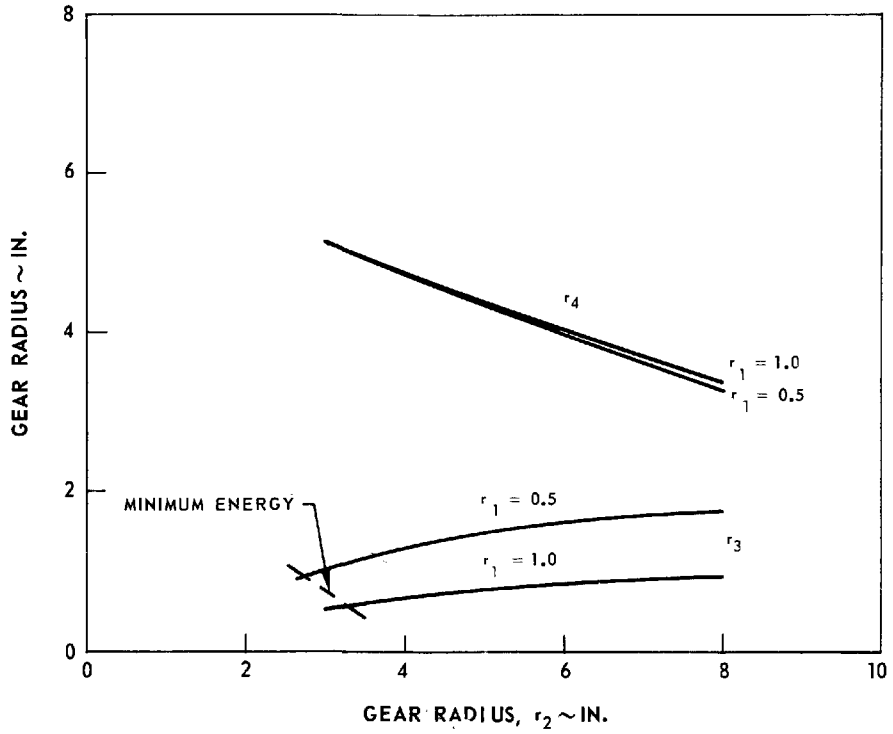

FIG. 41

INSTALLATION SKETCH, SINGLE-SHAFT GAS TURBINE WITH HMT, FRONT WHEEL DRIVE

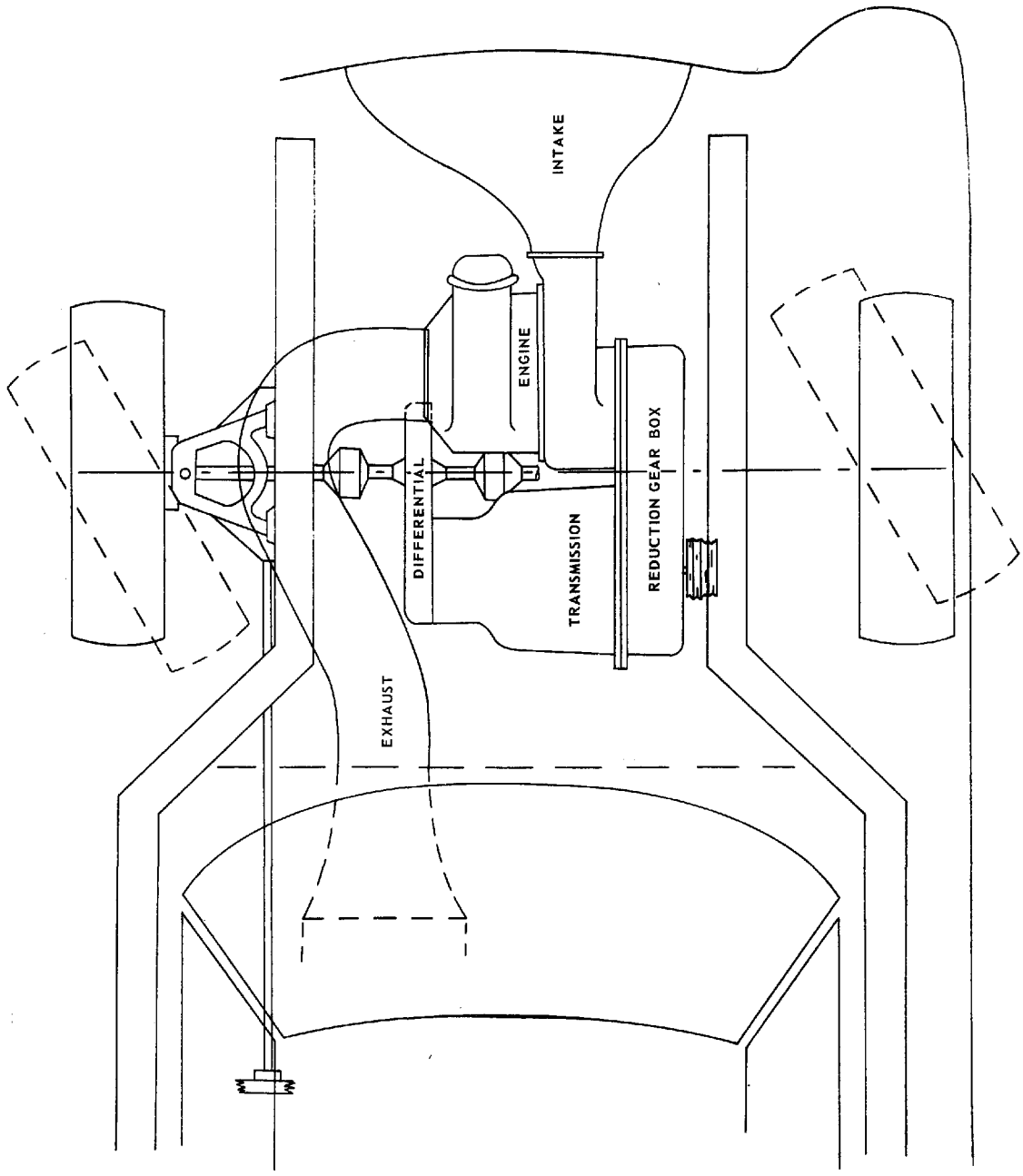

reduction gearbox incorporating an idler. The final drive would be through the epicyclic differential. This arrangement is so compact that a front-wheel drive (FWD) configuration could easily be developed. Such a system is shown in Figs. 41, 42, and 43 for a simple-cycle engine. Drive-line flexibility can be provided with Rzeppa joints. Figure 41 shows the entire unit neatly mounted between the frame members.

The air intake is shown only schematically; an actual system would incorporate a filter system and moisture trap. The exhaust system is conceived to be a straight-through system which is muffled by long-strand fiber glass, contained by inner walls perforated according to the noise profile over the length of the system. The 6-in. exhaust pipe will flatten beneath the vehicle to provide road clearance. The accessory drive is taken from the idler gear of the reduction gearbox in the form of a series of pulley belts. Because of the low engine torque, a belt-drive starter can be incorporated.

The installation shown would allow a large, flat floor space for the front-seat occupants, and more importantly provides a large amount of empty space between the engine and grill of the vehicle, which is vital in avoiding serious and expensive damage in light, to moderate, collisions. It is felt that the insurance companies will watch closely the development of the low-emission systems and would most certainly impose high rates on any system which is excessively vulnerable to light collisions. An example would be a collision in which a standard vehicle sustains a broken grill, a smashed radiator, and fan. A new radiator core costs about $60 and the fan about $25. This same collision would only bend the intake ducting for the single-shaft gas turbine-powered vehicle. Conversely, a Rankine-cycle system would probably sustain damage to the condensor, vapor generator, regenerator, condensor fans, and considerable plumbing. If such components were repairable at all, the total labor costs would be very high, and replacement costs would be similarly severe.

The same basic unit would also make an attractive rear-engine installation, as shown in Figs. 44 and 45. The air intake would be through openings near the rear of the car, using either protruding scoops or flush grilles, depending on the pressure distribution and airflow in that particular area, as well as styling features.

The exhaust would be serpentined to provide sufficient length for muffling and exhaust-gas cooling. Note that the rear-engine system also provides substantial crush-structure between the rear bumper and the engine.

The regenerated and recuperated single-shaft configurations are somewhat larger than the simple-cycle unit, but can still be installed quite nicely in the same basic configurations. Figures 46 and 47 illustrate the front-drive system using the recuperated engine. Note that the engine and transmission are reversed to allow hood clearance over the engine. The rear-drive installation for the recuperated engine is shown in Figs. 48 and 49.

L-971249-7

FIG. 42

INSTALLATION SKETCH, SSS-10 WITH HMT, FRONT-WHEEL DRIVE

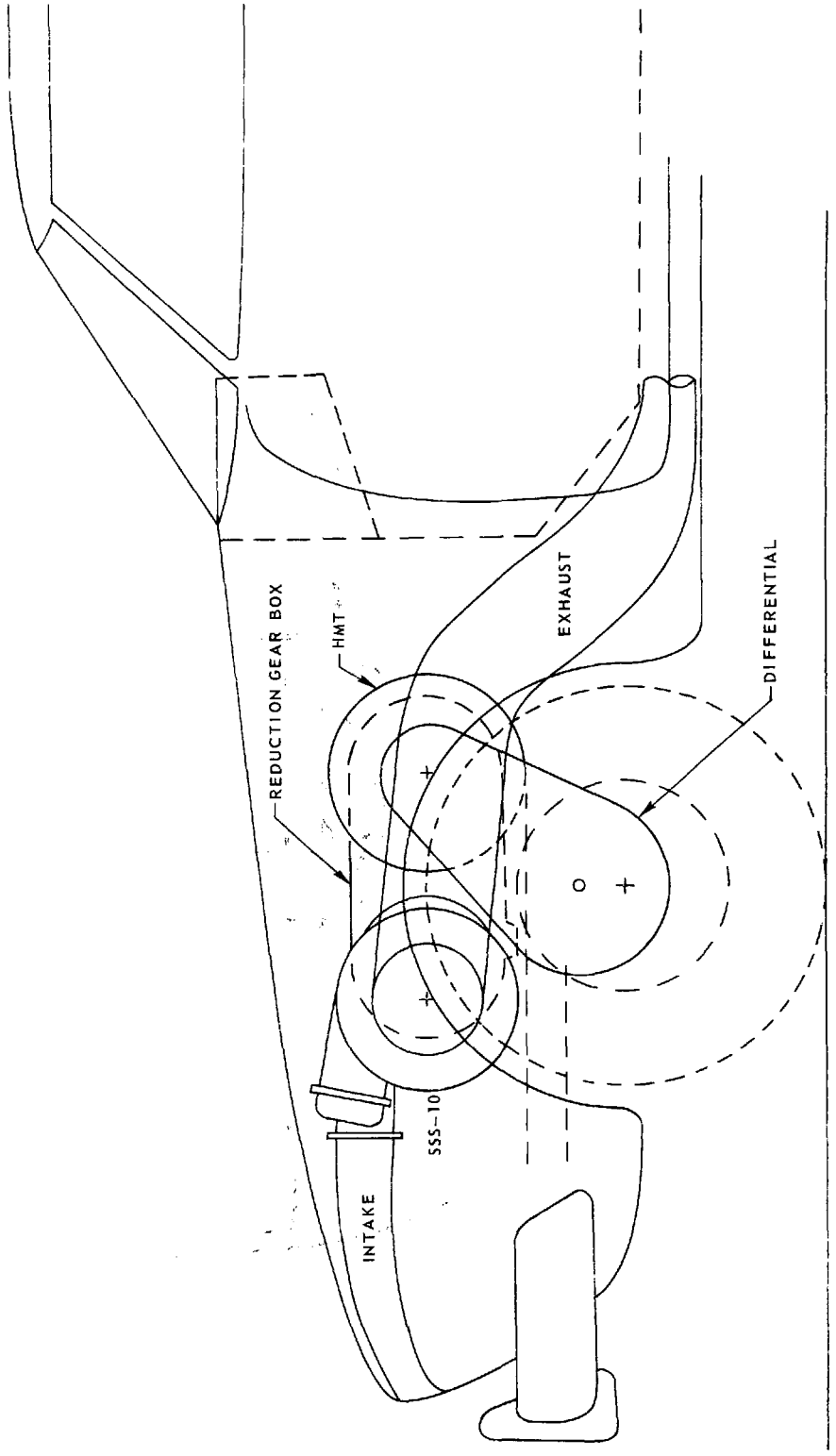

FIG. 43

INSTALLATION SKETCH, SSS-10 WITH HMT, FRONT-WHEEL DRIVE

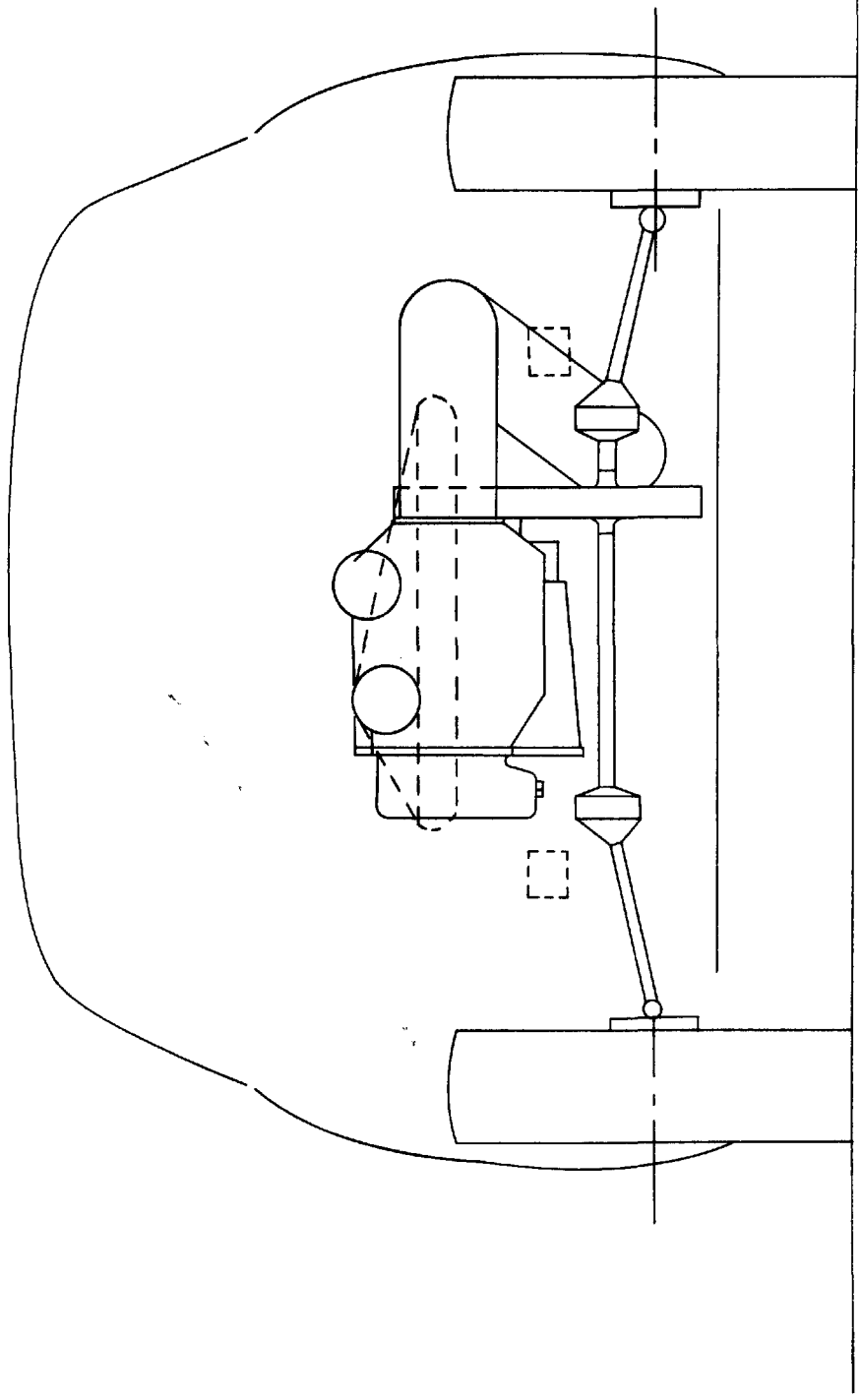

FIG. 44

INSTALLATION SKETCH, SINGLE-SHAFT GAS TURBINE WITH HMT, REAR-WHEEL DRIVE

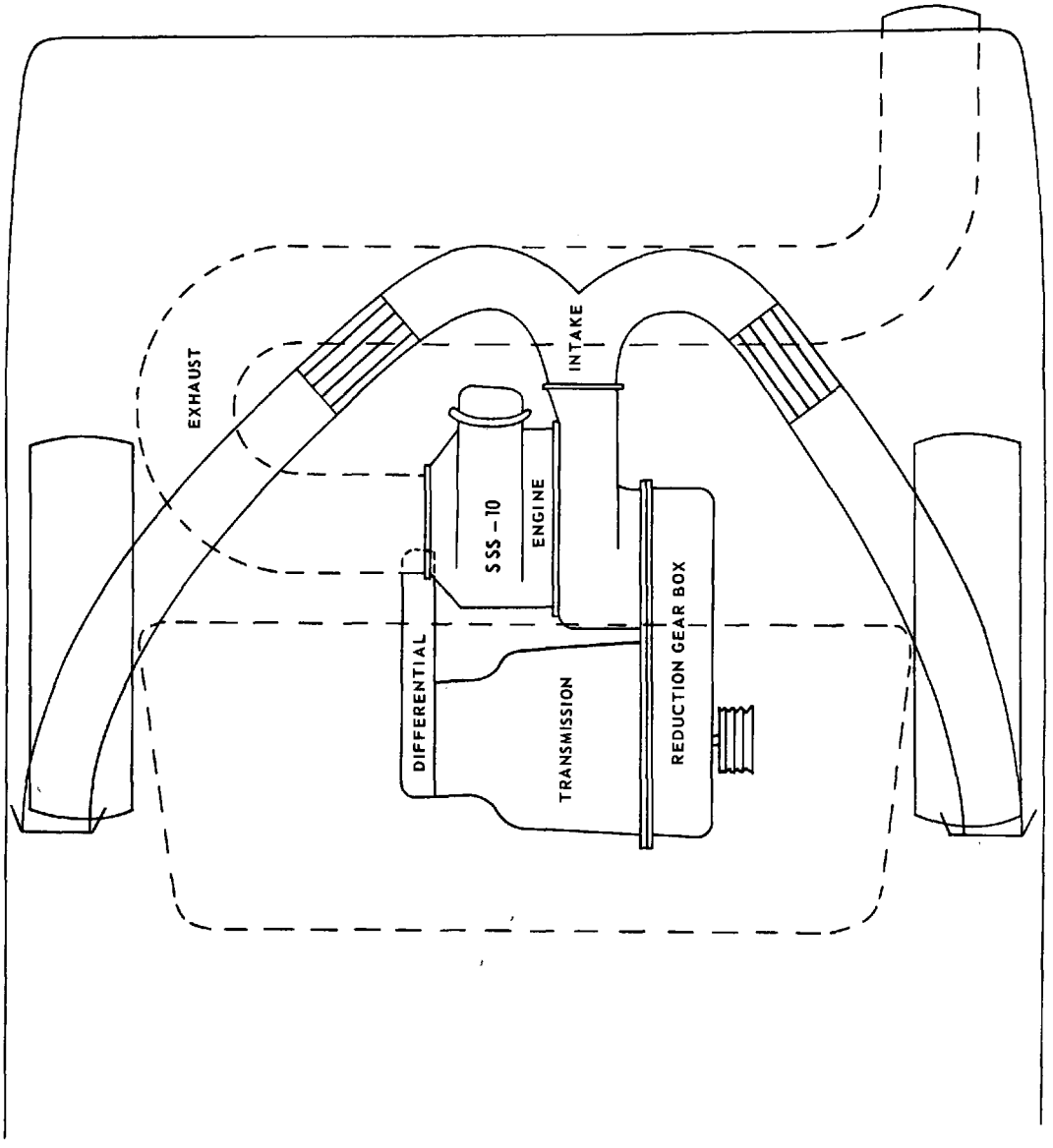

FIG. 45

INSTALLATION SKETCH, SSS-10 WITH HMT, REAR-ENGINE DRIVE

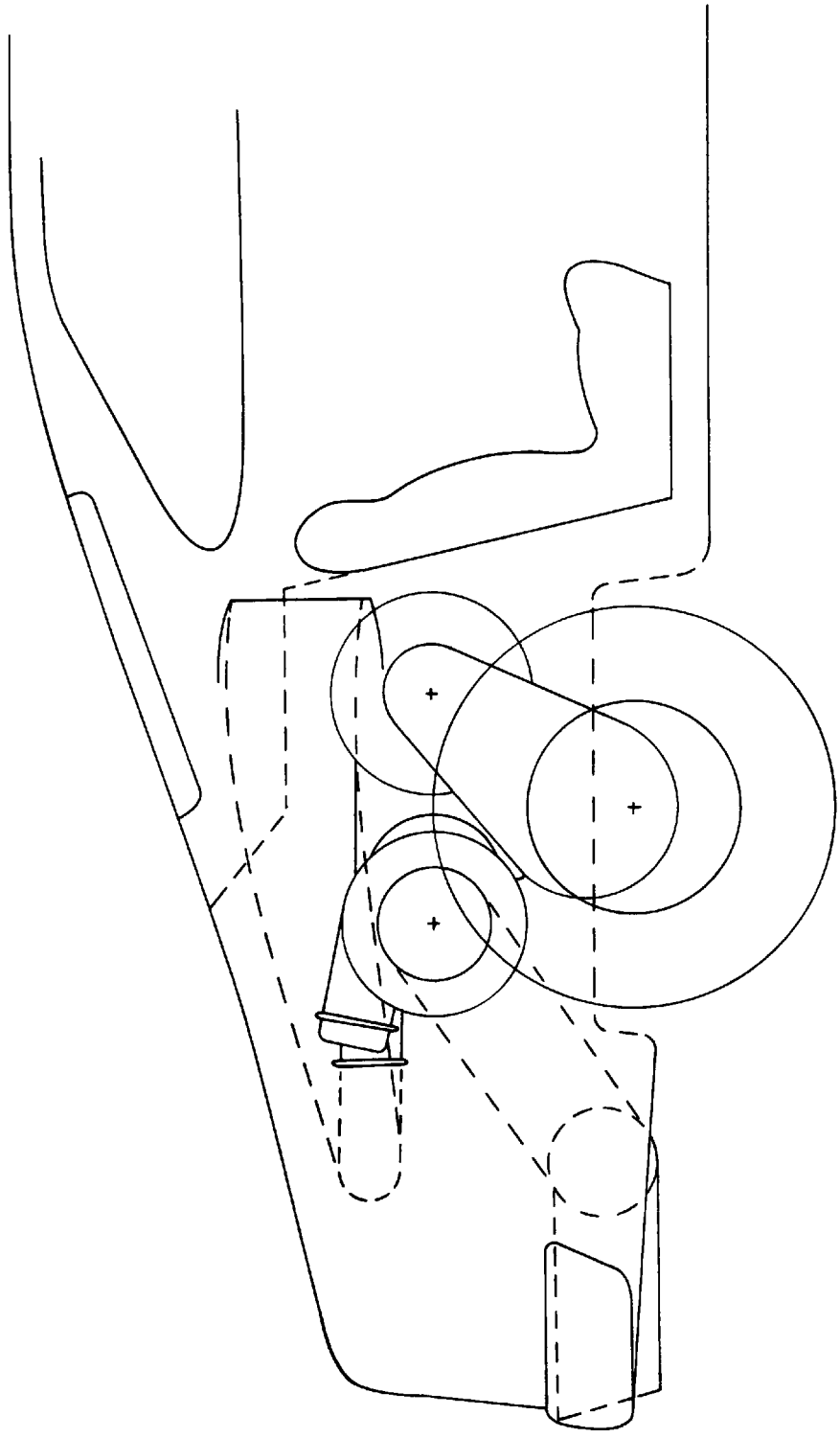

L-971249-7

FIG. 46

INSTALLATION SKETCH, RCSS-8 WITH HMT, FRONT-WHEEL DRIVE

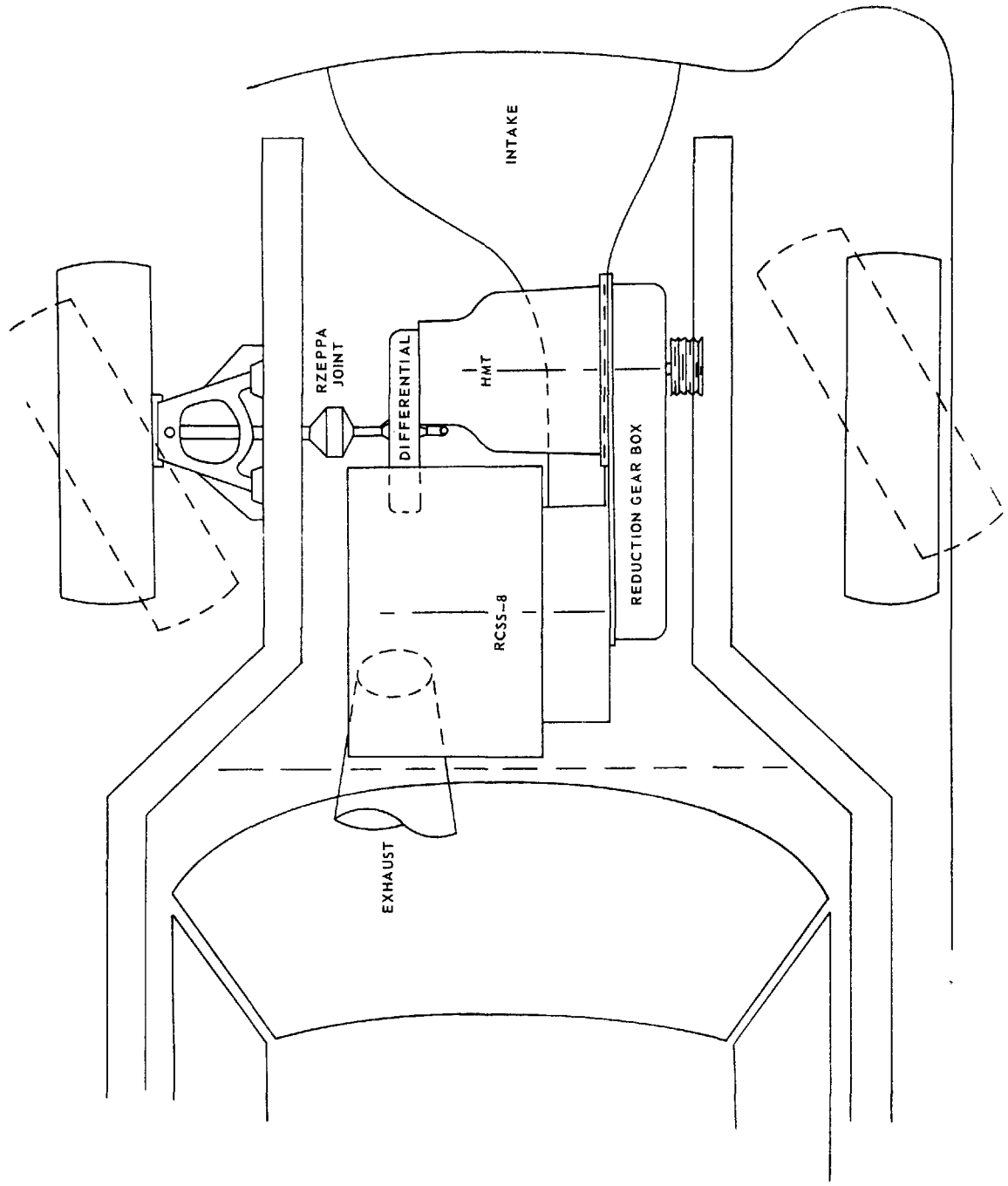

L-971249-7

FIG. 47

INSTALLATION SKETCH, RCSS-8 WITH HMT, FRONT-WHEEL DRIVE

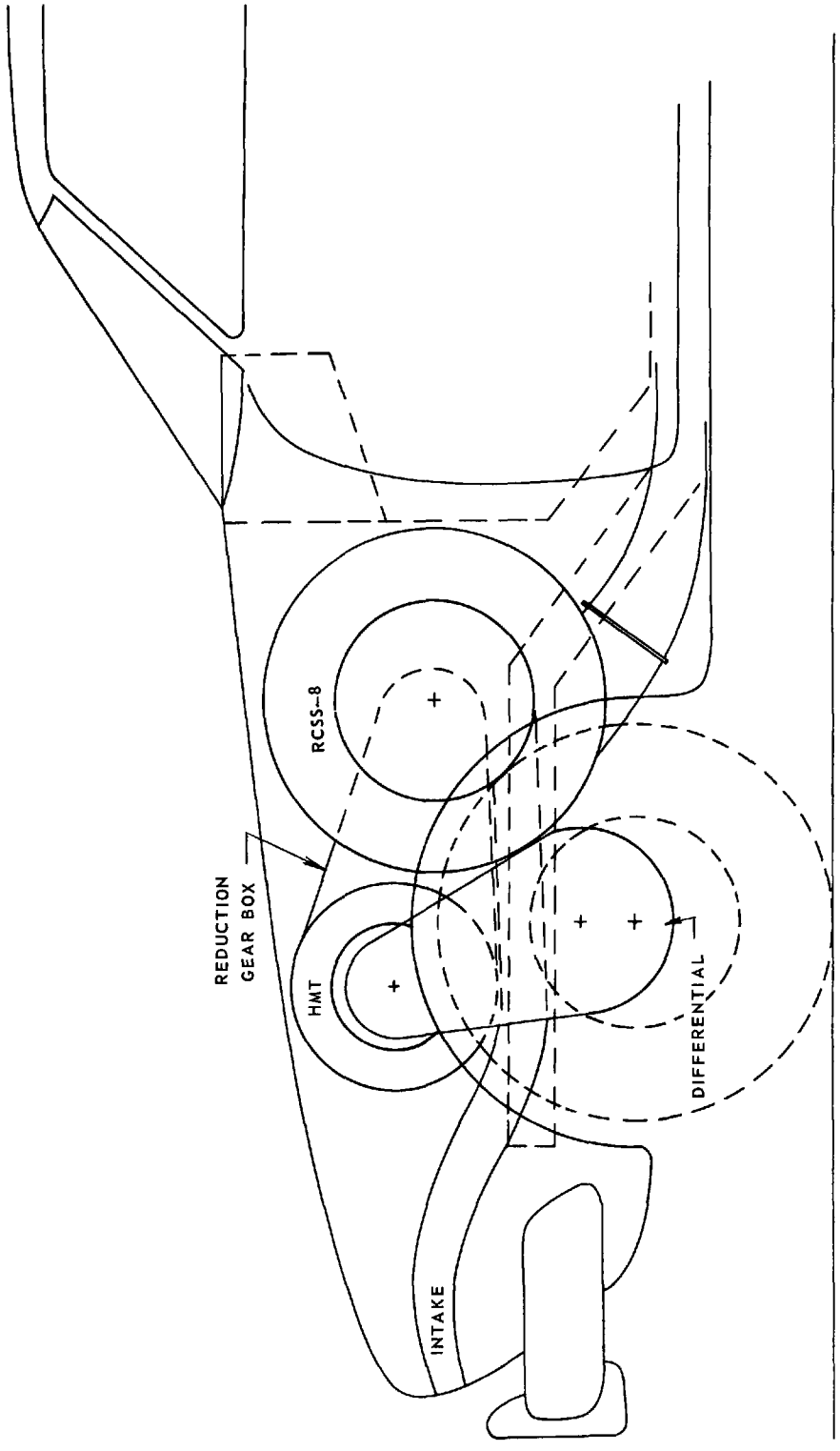

L-971249-7

FIG. 48

INSTALLATION SKETCH, RCSS-8 WITH HMT, REAR-ENGINE DRIVE

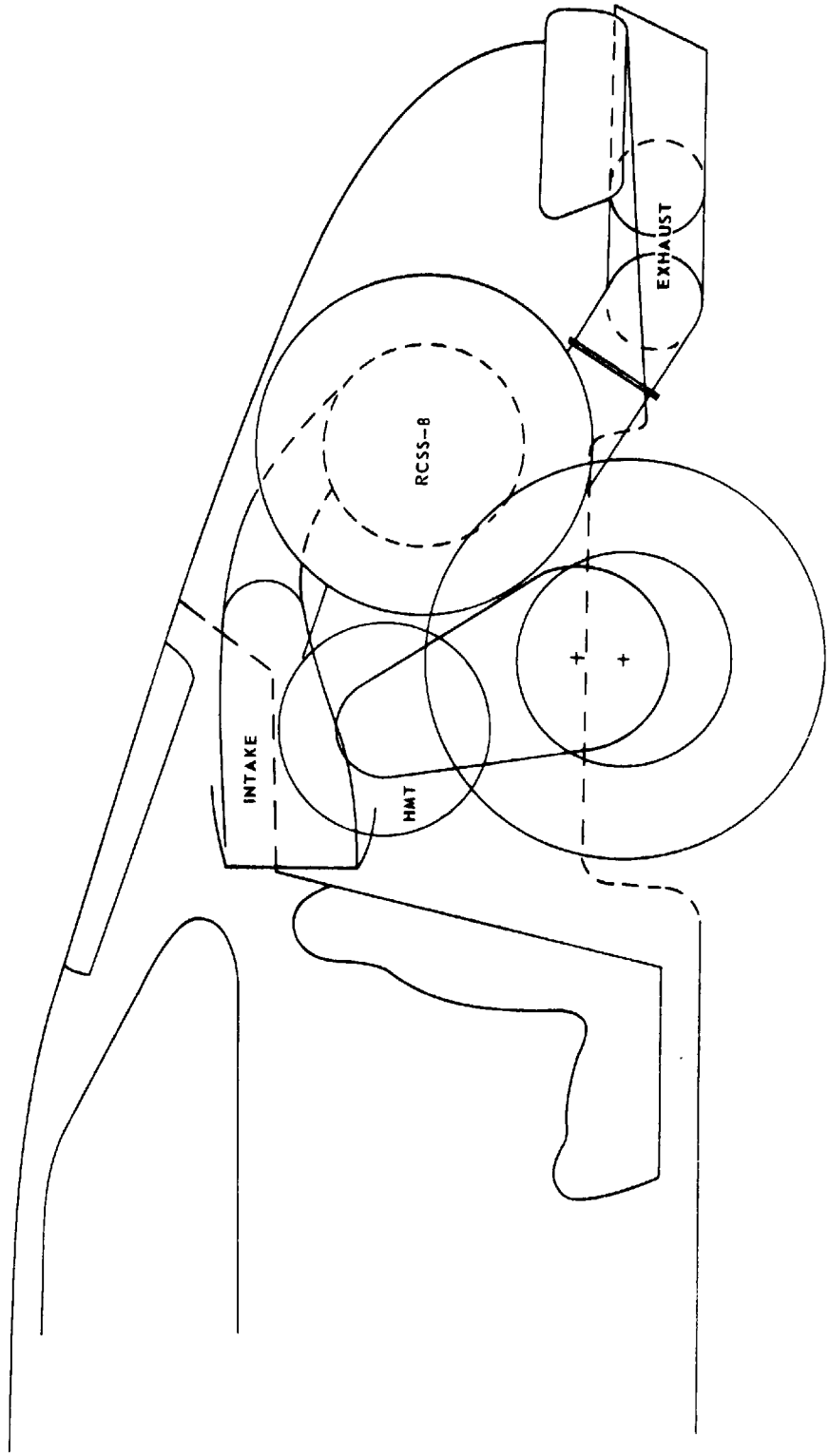

INSTALLATION SKETCH, RCSS-8 WITH HMT, REAR-ENGINE DRIVE

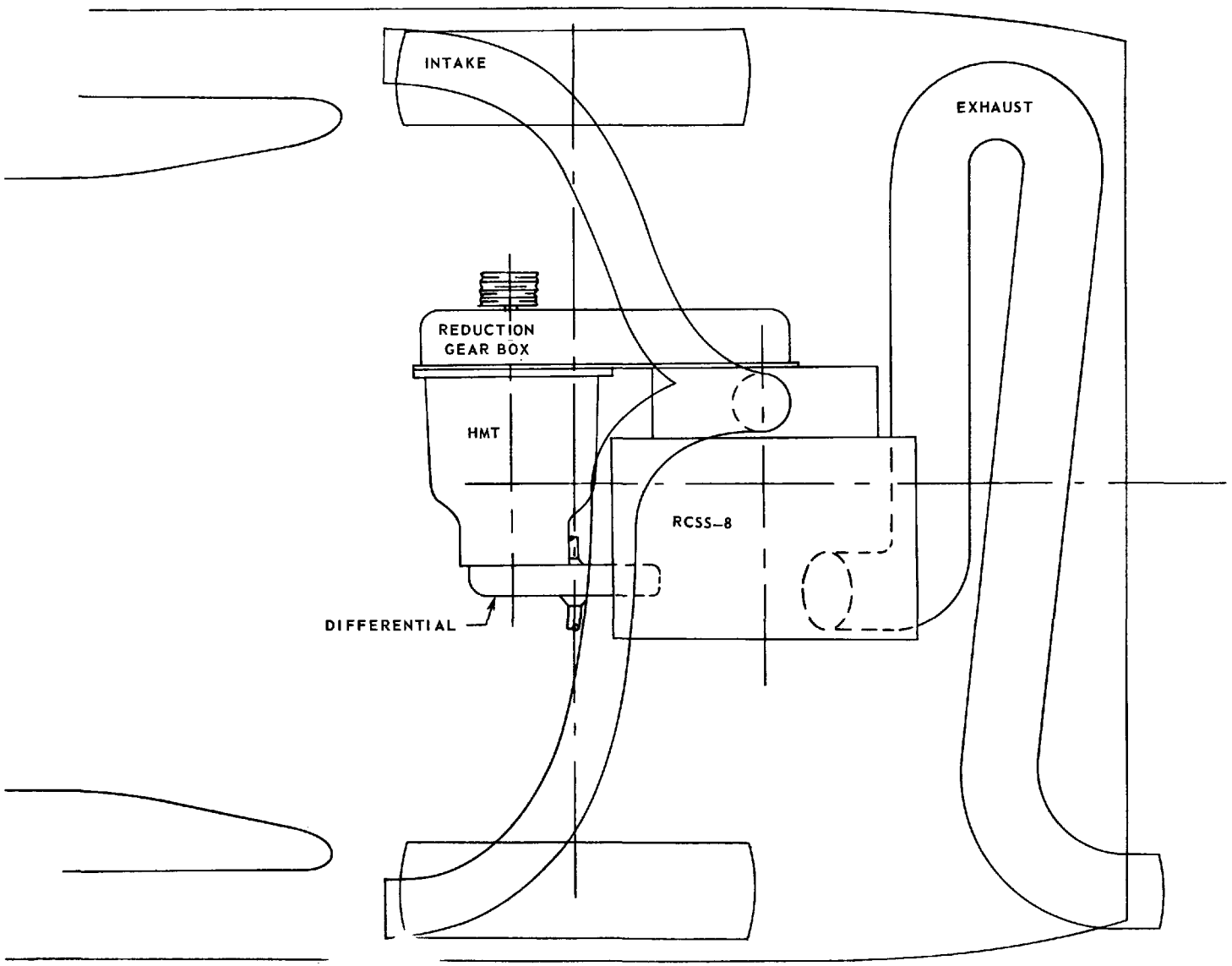

L-971249-7

FIG. 49

INSTALLATION SKETCH, RGSS-6 WITH HMT, FRONT-WHEEL DRIVE

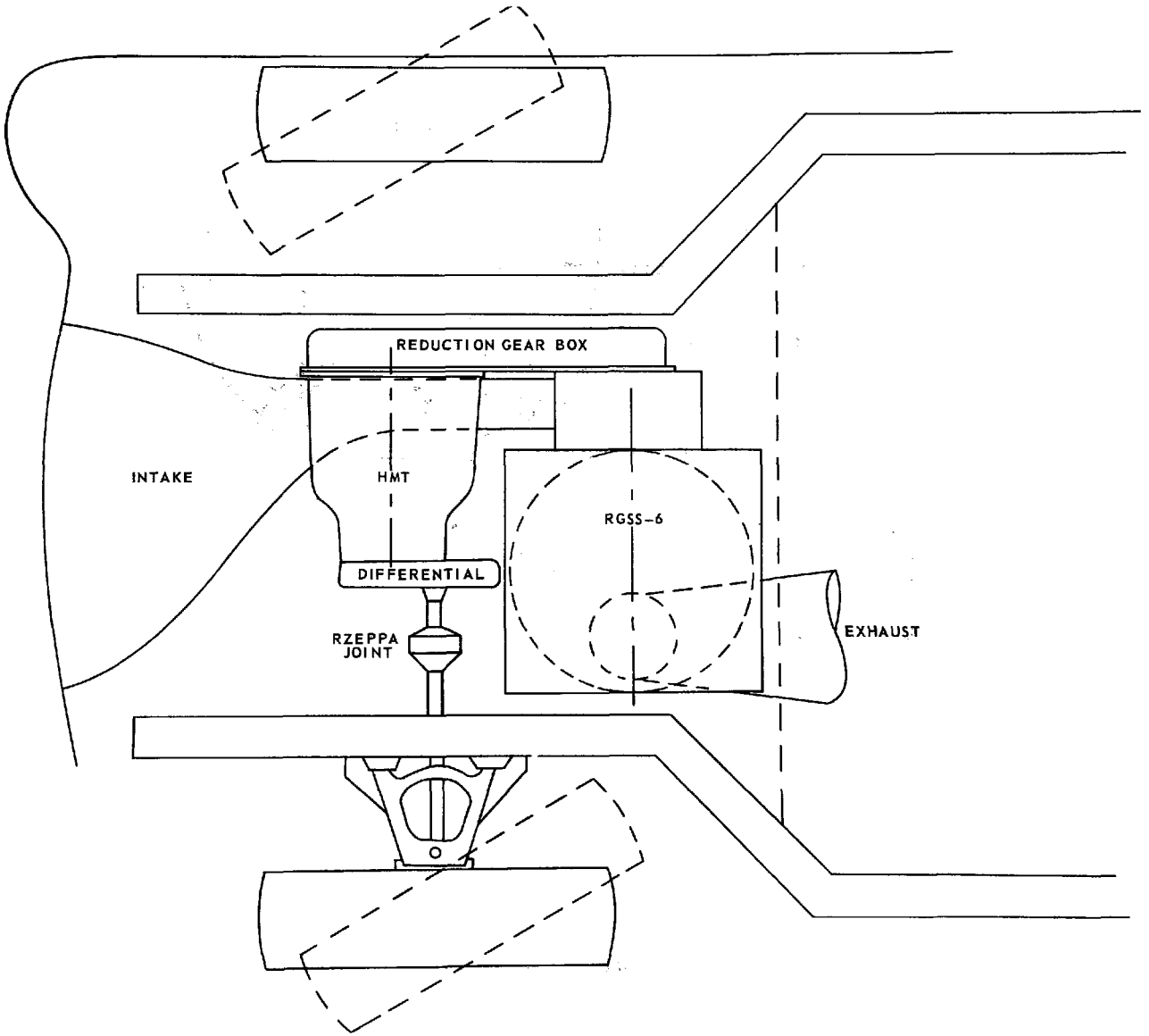

FIG. 50

L-971249-7

FIG. 51

INSTALLATION SKETCH, RGSS-6 WITH HMT, FRONT-WHEEL DRIVE

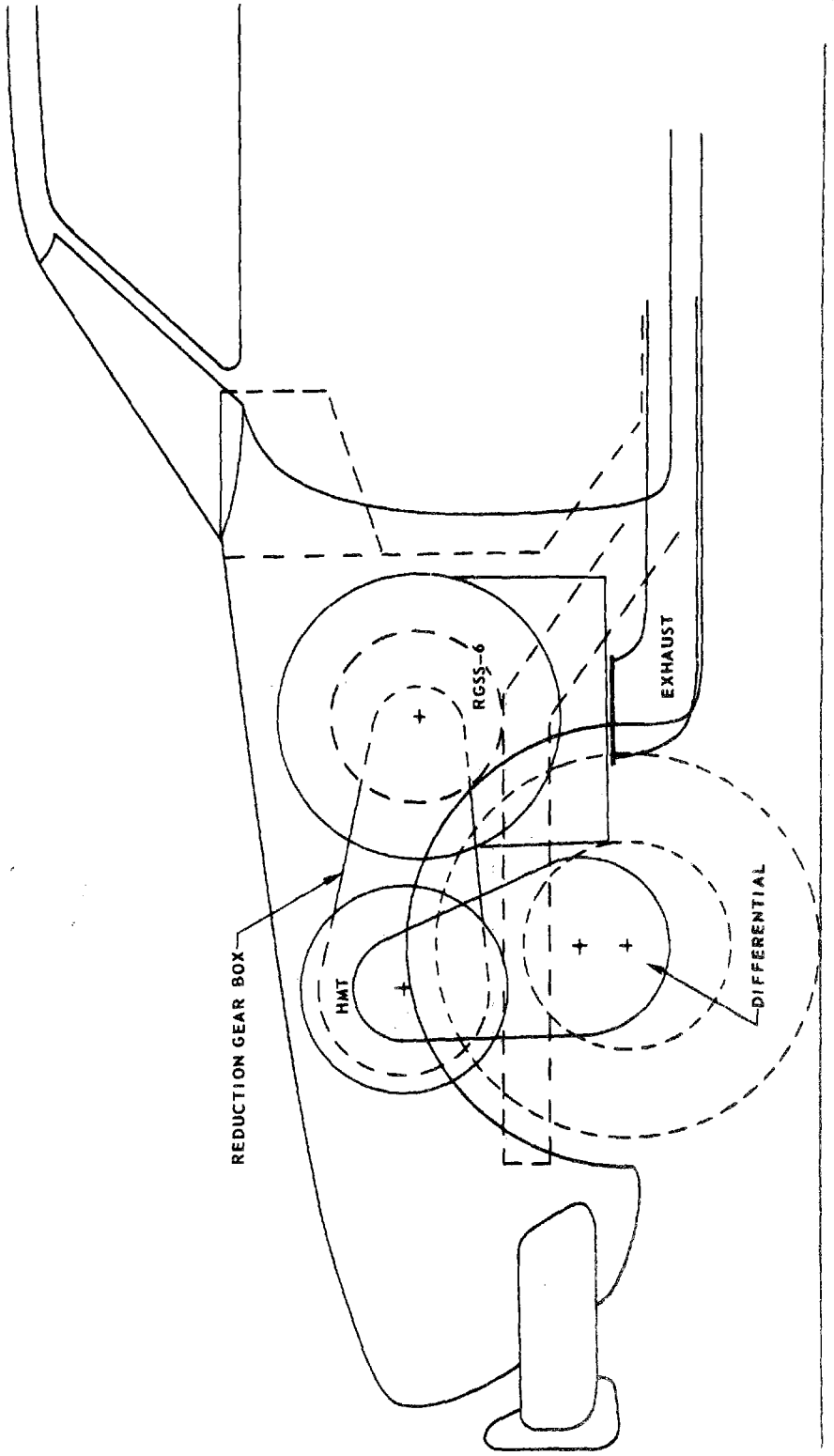

The large regenerated engine is shown in Figs. 50 and 51 for the front-wheel drive vehicle. The rear-engine system is very similar to the recuperated engine installation.

Fuel Control

Introduction

This section summarizes the study program conducted by the United Aircraft Hamilton Standard Division for a fuel control for an automotive gas turbine. The program was undertaken to conceptually design fuel control systems for three different engines; namely, single-shaft simple-cycle, single-shaft recuperative, and single-shaft regenerative engines. The fuel control system discussed in this report satisfies the requirements for all three engines when used in conjunction with the General Electric infinitely variable HMT transmission.

The selected mode of control for this application consists of a fuel flow/compressor discharge pressure (Wf/P3) schedule with exhaust gas temperature (EGT) limiting. A detailed discussion of the reasons for this mode selection is presented later. In addition, a schematic diagram and a control packaging concept have been generated and are discussed at length.

The control evolved during this study program is basically a hydromechanical unit with an integral fuel pump, a remote inlet guide vane (IGV) actuator and a remote EGT sensor. Specific design features of the control include the following:

1. Control of starting, acceleration, and deceleration fuel flow
2. Automatic start sequencing as a function of pump (and engine) speed
3. Exhaust gas temperature limiting
4. Automatic IGV actuation as a function of pump (and engine) speed
5. Foot pedal bias of fuel flow
6. Electrical shut-off
7. Automatic altitude compensation from sea level to 10,000 feet

Although the control which was conceptually designed for this application is hydromechanical, electronic implementation was also considered. Similar control logic was used for an electronic control, and a logic diagram and wiring schematic were prepared. Both methods of control implementation were then costed, and costs

to manufacture either the hydromechanical or electronic version compared favorably. However, it was decided that the electronic implementation presented a somewhat larger uncertainty than the hydromechanical version in both cost and performance. Therefore, a program decision was reached to implement the control hydromechanically. However, for future programs of this nature, it is recommended that an electronic control be given consideration. Electronic implementation may prove beneficial if the automotive engine requirements become somewhat more sophisticated.

Control Mode Determination

General

The mode of control presented is the result of discussions with UARL and UACL relating to implementation of a low-cost fuel control for the single-shaft regenerative and recuperative engines (RGSS-6 and RCSS-8) and the single-shaft simple-cycle engine (SSS-10). Fuel control requirements for these engines were considered in conjunction with the General Electric IVT-870 infinitely variable hydromechanical transmission, and although engine temperature, pressure, and fuel flows differ for the three engines, the operating characteristics allow a common mode of control for all three engines. Thus, only the detailed requirements of the SSS-10 have been considered in sizing control components, with the assumption that differences in the temperature, pressure, and flow requirements of the other two engines would have a negligible effect on cost, weight, and complexity.

Review of Engine and Control Requirements

A typical engine performance map, shown in Fig. 52, indicates engine fuel requirements for steady-state and acceleration operation of the engine. The maximum acceleration fuel flow is limited by turbine inlet temperature considerations.

The steady-state operating line is a result of the infinitely variable transmission controlling engine speed (as a function of foot pedal position) by varying transmission drive ratio to hold engine speed constant when the foot pedal is in a fixed position. Thus, the fuel control is not required to provide engine speed governing (as is required on aircraft engines) because of the combination of a fixed-shaft engine and an infinitely variable transmission. Therefore, fuel control requirements are reduced to providing acceleration and deceleration fuel limits and auxiliary functions such as IGV, starting, and shut-off functions.

Traditional aircraft engine control methods of controlling turbine inlet temperature during acceleration are by open-loop scheduling of fuel flow as a function of speed, inlet temperature, and compressor discharge pressure (P3) level. These techniques would result in excessive control cost and complexity for

FIG. 52

SSS-10 TORQUE CHARACTERISTICS

DESIGN SPEED = 106,000 RPM

DESIGN POWER = 130 HP

T.I.T. = 1900 F

AMBIENT TEMP = 59 F

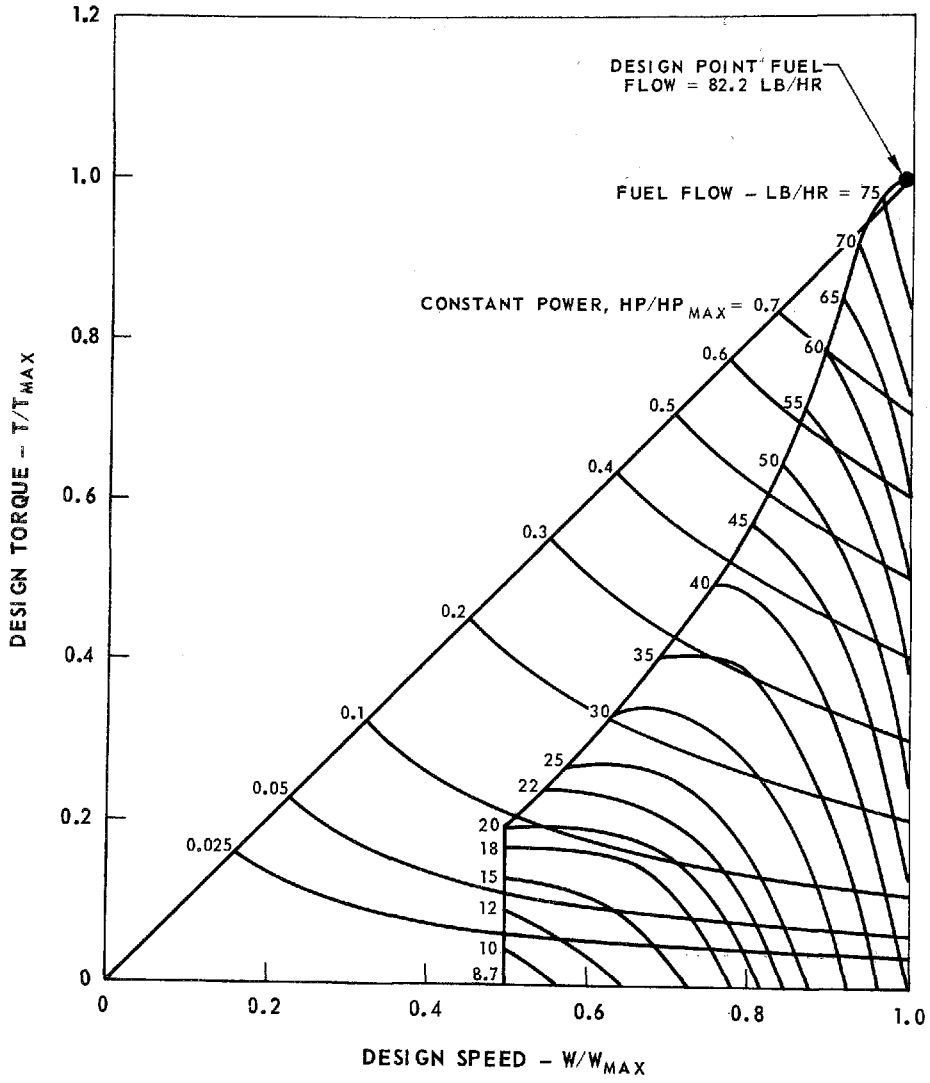

TURBINE EXHAUST GAS TEMPERATURE (EGT) VS TURBINE INLET TEMPERATURE (TIT)

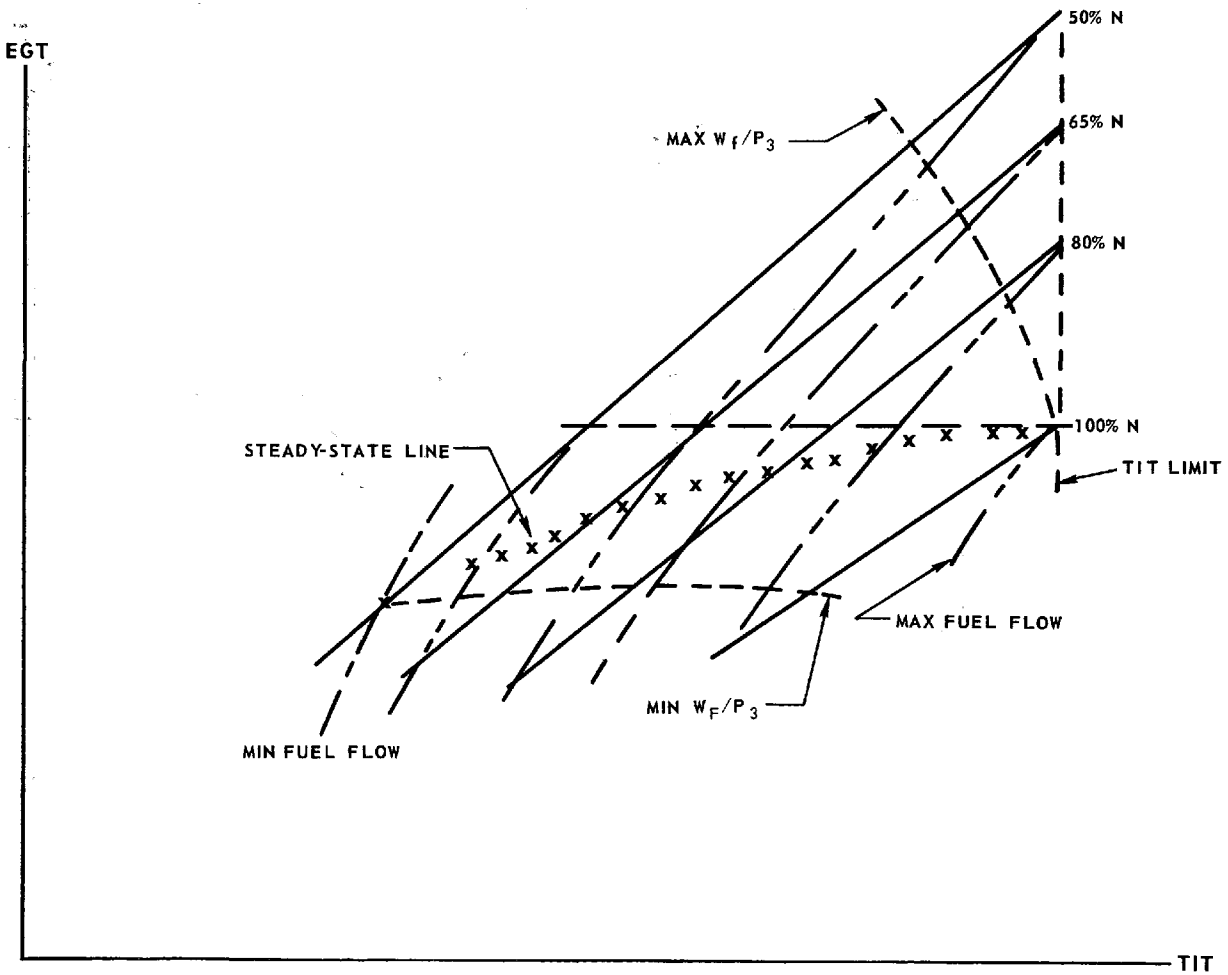

FIG. 53

FUEL FLOW PARAMETER

SSS-10

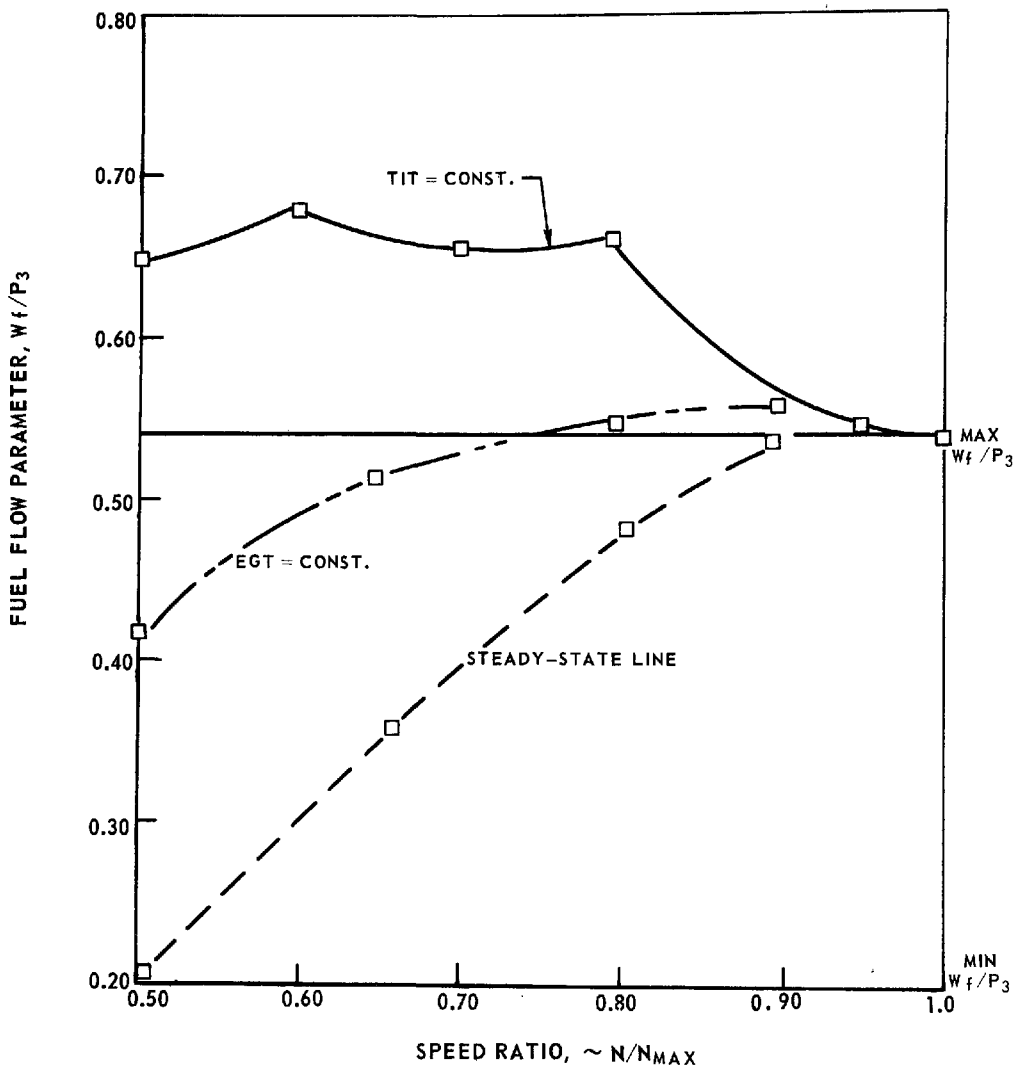

EFFECT OF OUTPUT SHAFT SPEED ON SSS-10 FUEL ECONOMY

AMBIENT TEMPERATURE = 59 F

VEHICLE WEIGHT = 3850 LB

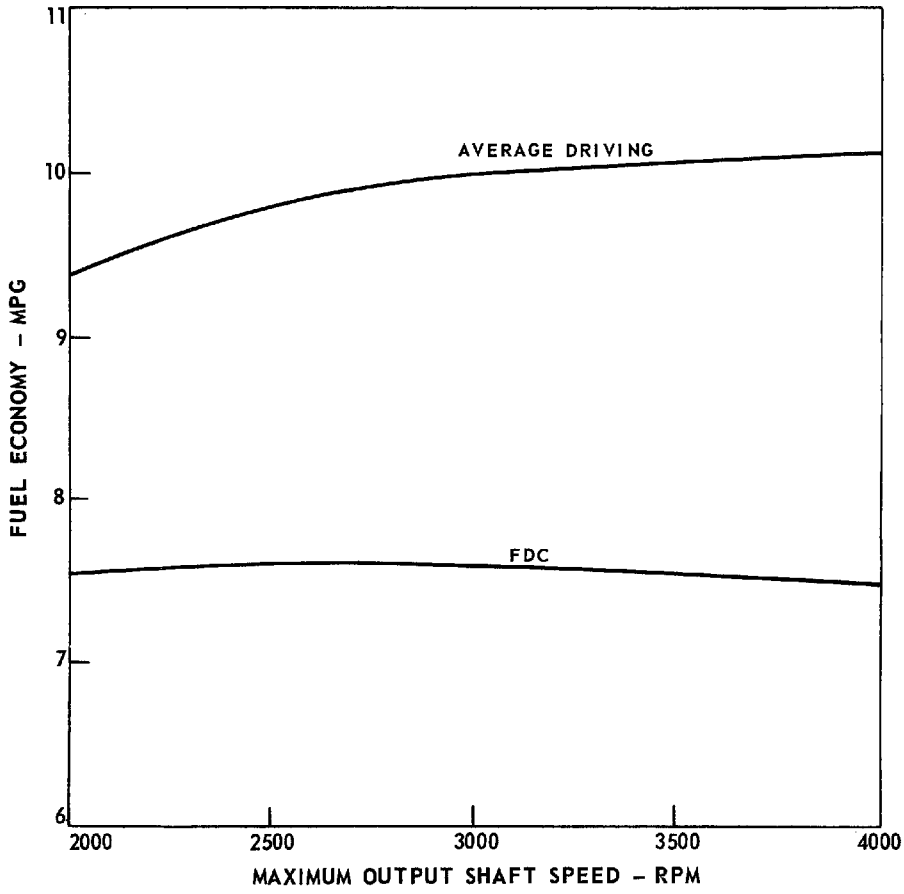

FIG. 95

EFFECT OF GAS GENERATOR INERTIA ON SSS-10 FUEL ECONOMY

AMBIENT TEMPERATURE = 59 F

VEHICLE WEIGHT = 3850 LB

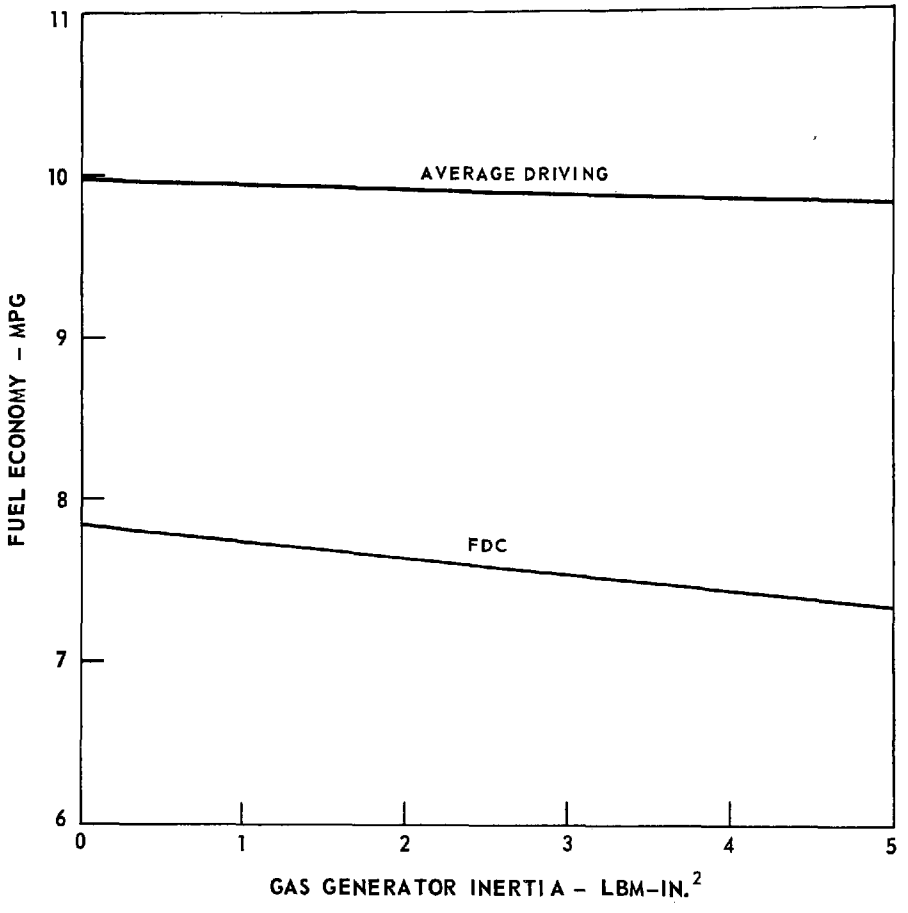

EFFECT OF ACCESSORY POWER ON SSS-10 FUEL ECONOMY

AMBIENT TEMPERATURE = 59 F

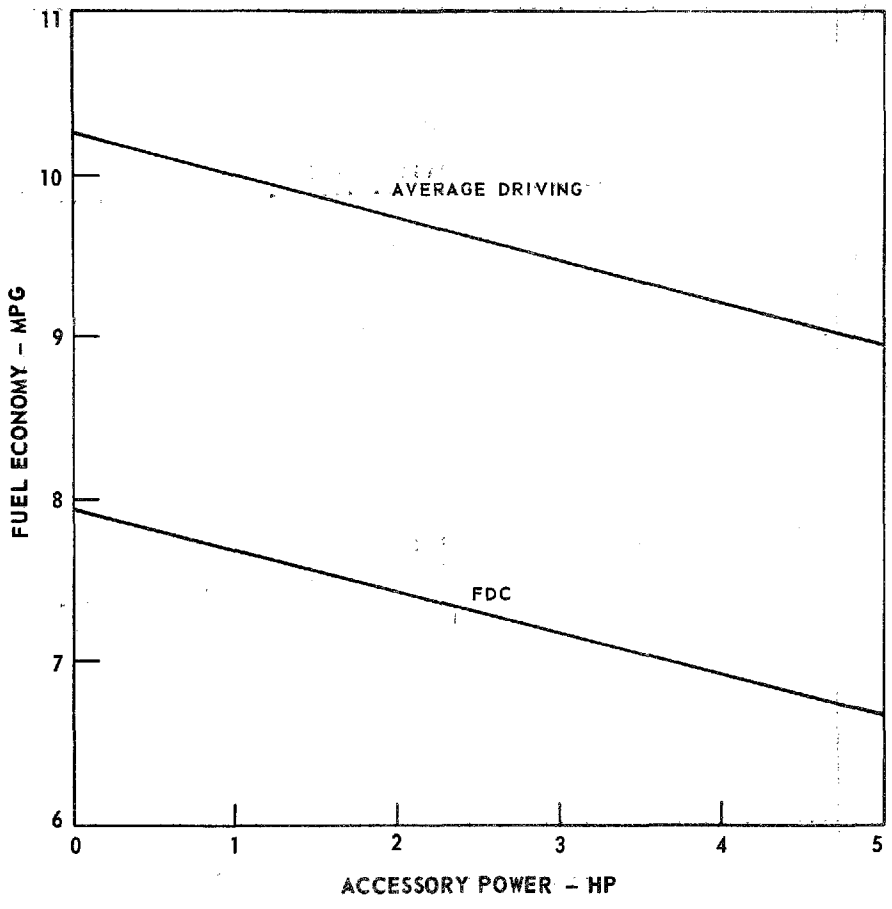

TABLE XI

EFFECT OF CHOICE OF OPERATING LINE

ON FUEL ECONOMY

		Fuel Economy (mpg)			
Engine	Fuel Flow Line	FDC	Suburban Route	Country Route	Composite
RGSS-6	A	13.04	19.26	17.29	16.08
	B (base-line)	12.16	17.52	16.13	14.90
	C	9.85	13.14	13.41	11.88
	D	8.77	12.19	13.41	11.10
RCSS-8	A	12.07	17.80	16.29	14.97
	B (base-line)	11.20	16.15	15.06	13.79
	C	9.00	12.00	12.54	10.95
	D	8.00	11.15	12.54	10.20
SSS-10	A	7.48	10.98	12.00	9.75
	B (base-line)	7.51	11.01	12.02	9.77
	C	7.11	10.24	11.49	9.21
	D	6.82	9.90	11.49	8.97

effect on average mpg is slight, the change being due to the change in FDC economy. The latter is adversely affected by increases in engine inertia because of the continuous variations in vehicle (and therefore engine) speed.

The effect on fuel economy of accessory power is shown in Fig. 96 for the SSS-10. Both average and FDC economy figures are adversely affected by increases in the accessory load. Decreases of 13% and 16% for the average and FDC fuel economies, respectively, are incurred for a change in accessory load from 0 to 5 hp.

The fuel economy results for the various engine operating lines described in the Engine Performance Section (Fig. 69) are shown in Table XI. Operating line A shows somewhat better fuel economy than line B (the base-line operating schedule) for the two regenerated engines, and approximately the same fuel economy for the SSS-10 engine. This result is due to the character of the respective fuel flow maps. For the heat-exchanger engines, the lines of constant fuel flow are fairly straight and parallel, with negative slopes. Thus, line A, being above and to the left of line B, produces better fuel economy for the RGSS-6 and RCSS-8 (see the fuel flow maps of Figs. 66 and 67). The constant fuel flow lines for the SSS-10, however, are flatter in the region of lines A and B, and the fuel economy of this engine is therefore less sensitive to the selection of the operating line than either the RGSS-6 or the RCSS-8. The fuel flow line of the simple-cycle engine (Fig. 68), in fact, became tangent to the lines of constant power (for low-to-medium power settings) and there exists an optimum fuel flow line which comprises the locus of the points of tangency.

Line C reduces the fuel economy for all three engines, but the reduction is less severe for the SSS-10 by the above reasoning. Line D, which utilizes a 60% idle speed ratio, produces further penalties in fuel economy, with decreases of 28%, 29% and 10% on the FDC for the RGSS-6, RCSS-8 and SSS-10 engines, respectively.

Emissions Results

For the purposes of calculating vehicle emissions over the Federal Driving Cycle, basic data were expressed in terms of an emissions index (lb of pollutant produced per 1000 lb fuel consumed) as a function of engine power setting for each of the important constituents. Figure 97 shows the emissions index (EI) for oxides of nitrogen (NO_x) for the RGSS-6 engine. Line A, representing existing data for automotive engines, was taken directly from Ref. 1. Line B is the estimated variation of EI required to just meet the Federal standards for NO_x. Figure 98 shows similar data for the RCSS-8. The NO_x EI data for the SSS-10 engine are shown in Fig. 99. Line A is representative of data for the T-56 engine as described earlier, and line B is an estimate of the EI variation which would just meet the Federal standards for NO_x emissions.

FIG. 97

EMISSIONS INDEX FOR NITROGEN OXIDES (NO_X)

(EXPRESSED AS NO_2)

RGSS-6

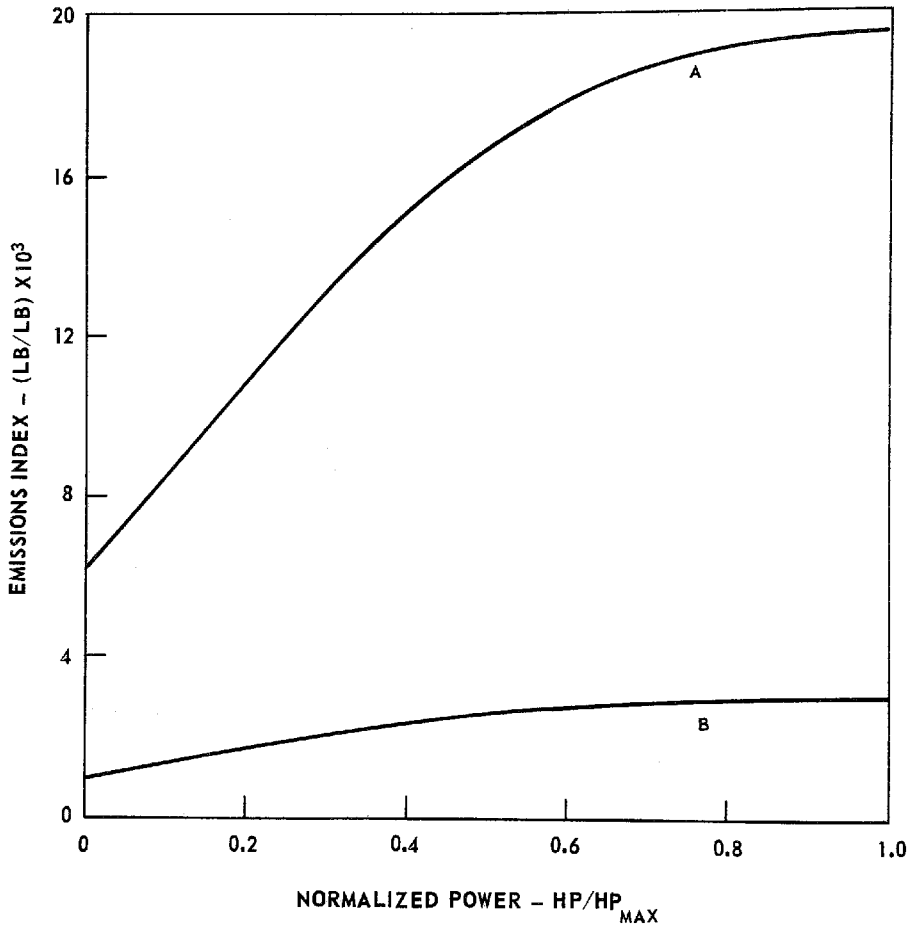

FIG. 98

EMISSIONS INDEX FOR NITROGEN OXIDES (NO_X)

(EXPRESSED AS NO_2)

RCSS-8

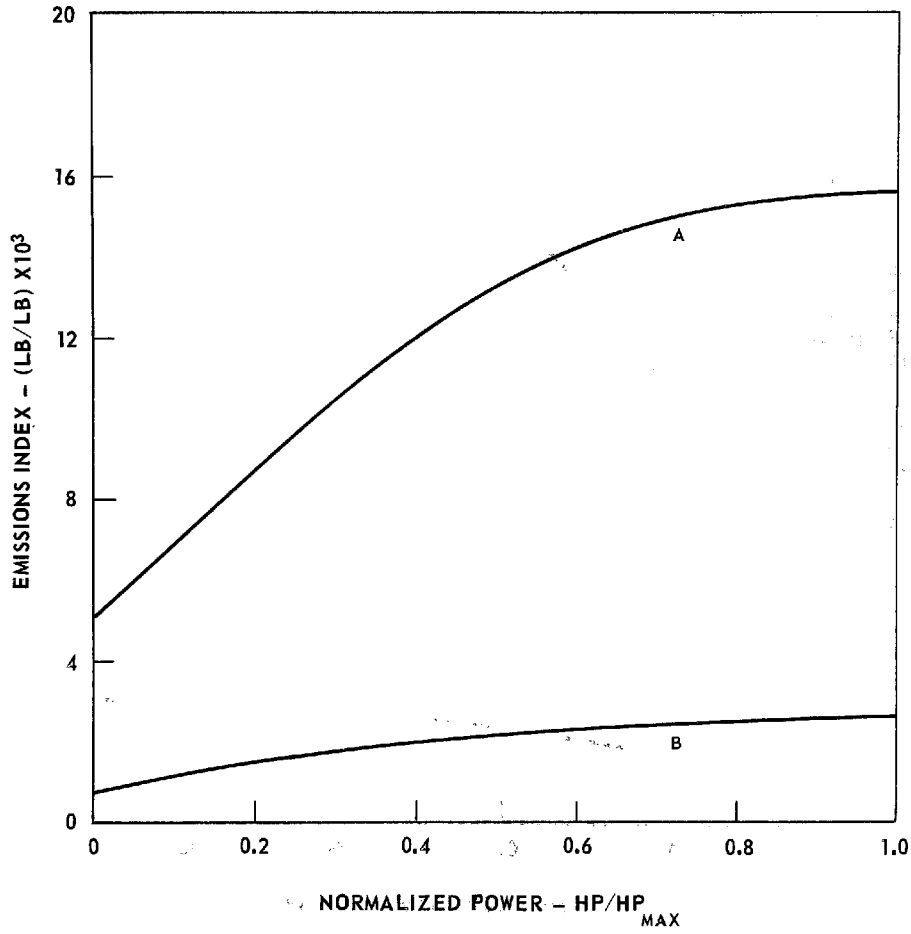

FIG. 99

EMISSIONS INDEX FOR NITROGEN OXIDES (NO_X)

(EXPRESSED AS NO_2)

SSS-10

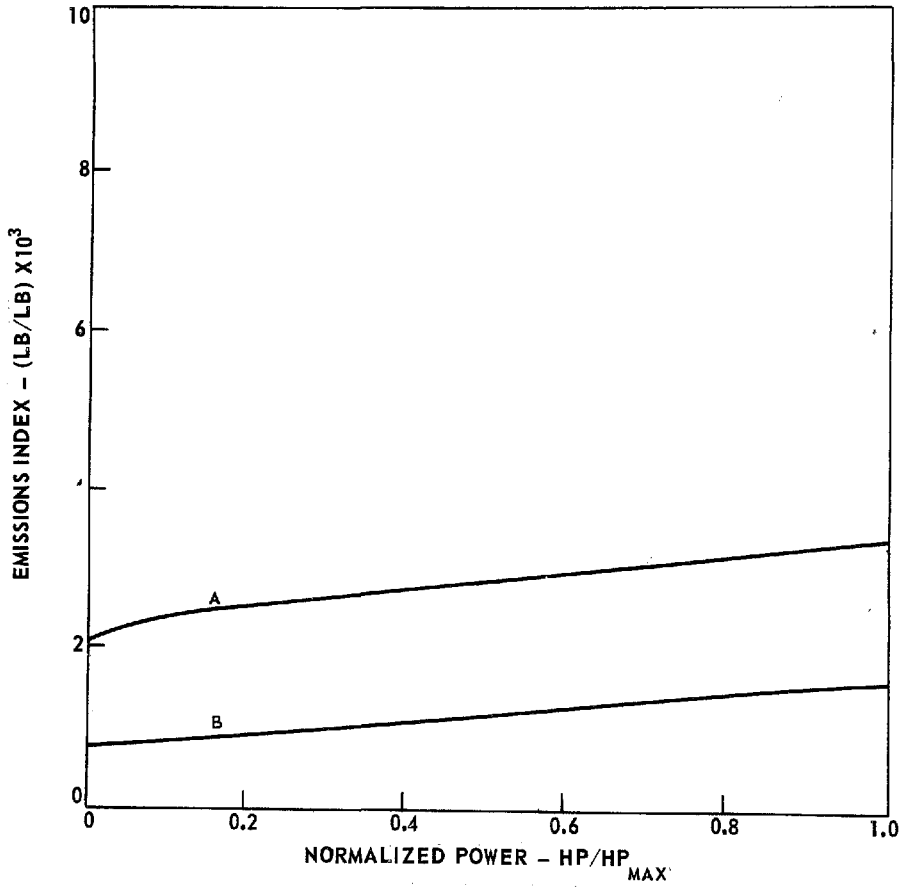

EMISSIONS INDEX FOR CARBON MONOXIDE (CO)

RGSS-6
RCSS-8

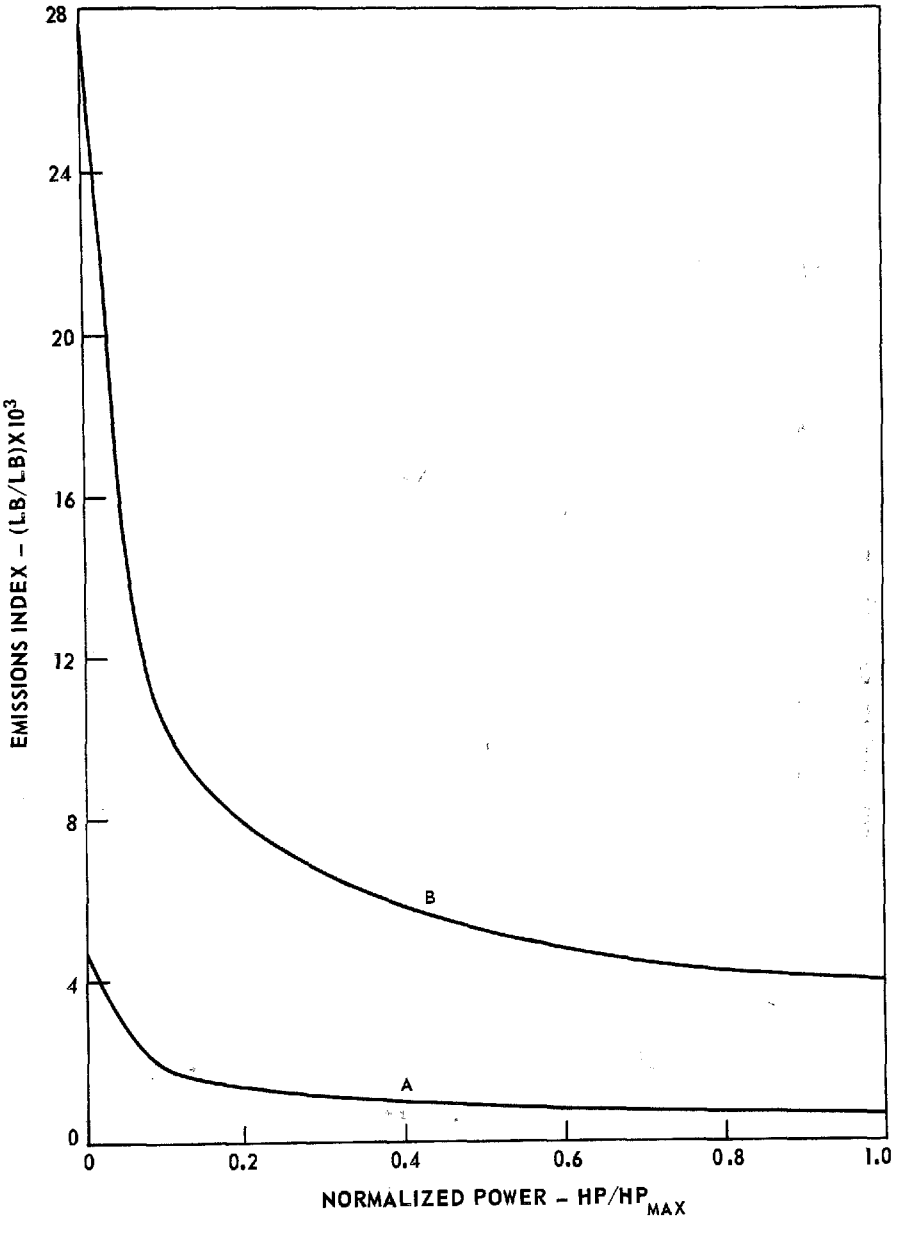

TABLE XII

FEDERAL DRIVING CYCLE EMISSIONS DATA

Baseline Vehicles
Ambient Temperature = 59 F
Engine Operating Line B (Fig. 69)

		Emissions (gm/mi)		
Engine	Emissions Index Line & Source Figs. 97 Through 103	CO	UHC (as C_6H_{14})	NO_x (as NO_2)
RGSS-6	A - GT 309	0.53	0.15	2.72
	B - Typical Required	2.90	0.38	0.41
RCSS-8	A - Modified GT309	0.57	0.16	2.38
	B - Typical Required	3.13	0.41	0.41
SSS-10	A - T-56	1.86	0.31	1.03
	B - Typical Required	2.58	0.40	0.41
	Federal Standards	3.40	0.41	0.40

The carbon monoxide (CO) EI variations for the RGSS-6 and RCSS-8 engines are shown in Fig. 100. Line A was taken from Ref. 1, and line B is the estimated CO allowable to approximately meet the requirements. Figure 101 shows CO EI variations for the SSS-10 engine, where line A represents data for the T-56 engine, and line B is an estimate of the CO EI variation allowable to still approximately meet the requirements.

The unburned hydrocarbons (UHC) EI data for the RGSS-6 and RCSS-8 engines are shown in Fig. 102. Lines A and B were derived as described above for the heat-exchanger engines. Figure 103 shows the UHC estimates for the SSS-10 engine. Line A is based on the T-56 data, and line B is the estimate for allowable emissions.

The emissions results as calculated for the base-line vehicles operating over the Federal Driving Cycle (FDC) are shown in Table XII along with the current Federal Standards. All results were derived for the base-line vehicles using engine operating line B of Fig. 69. The existing EI data for the heat-exhanger engines (line A) yield NO_x emissions greater than the Federal Standards by a factor of 6. The corresponding CO and UHC levels are well below the standards. A reduction in the NO_x EI levels for the RGSS-6 and RCSS-8 (line B, Figs. 97 and 98, respectively) is required to meet NO_x standards, but a substantial increase in CO and UHC is also allowable.

The T-56 data used to derive curve A for the SSS-10 engine yield NO_x emissions of 1.03 gm/mi. This value is greater than the allowable standard by a factor of 2.5, but still well below the NO_x levels of the RGSS-6 and RCSS-8. The EI data of curve B, for the SSS-10, yield 0.41 gm/mi of NO_x, with CO and UHC emissions of 2.58 and 0.40 gm/mi, respectively.

The effect of vehicle weight on emissions is shown in Fig. 104 for the SSS-10 engine. Increasing vehicle weight causes the CO and NO_x production to rise, although the variation of CO with weight is slight. The UHC emissions decrease with increasing vehicle weight because the negative slope of the UHC EI curve of Fig. 103 more than offsets the increases in average power and fuel consumed which occur with increasing weight. Figure 105 shows the effect on emissions (for the SSS-10) of varying the rear-axle ratio. The CO emissions are relatively unaffected, but the NO_x emissions attain a minimum at an axle ratio of about 2.75. The UHC emissions experience a "weak" maximum at the same axle ratio. The effect of accessory power on emissions for the SSS-10 engine is shown in Fig. 106. The trends are similar to those indicated in Fig. 104, and the UHC emissions decrease with increasing accessory power. The NO_x emissions are strongly influenced by the accessory power loading, with an increase of 22% occurring as the accessory load increases from 0 to 5 hp.

FIG. 101

EMISSIONS INDEX FOR CARBON MONOXIDE (CO)

SSS-10

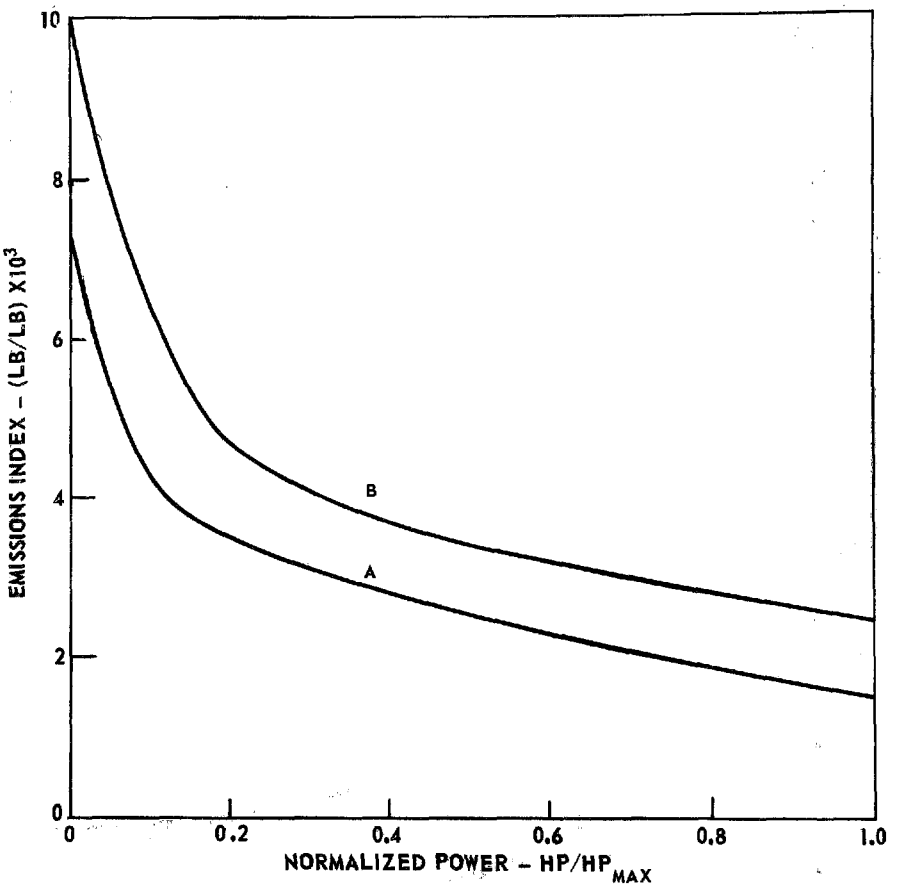

EMISSIONS INDEX FOR UNBURNED HYDROCARBONS (UHC) (EXPRESSED AS C_6H_{14})

RGSS-6

RCSS-8

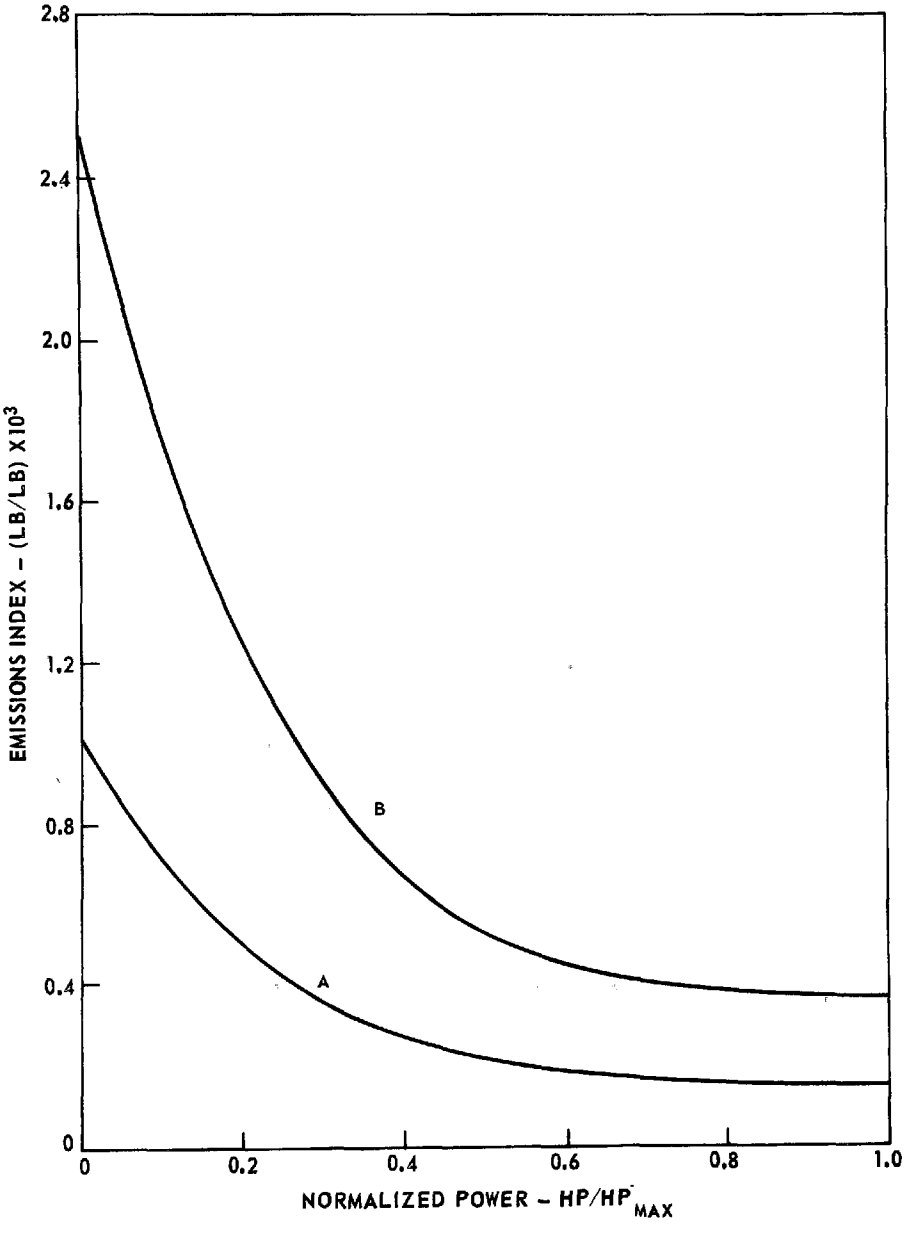

FIG. 103

EMISSIONS INDEX FOR UNBURNED HYDROCARBONS (UHC) (EXPRESSED AS C_6H_{14})

SSS-10

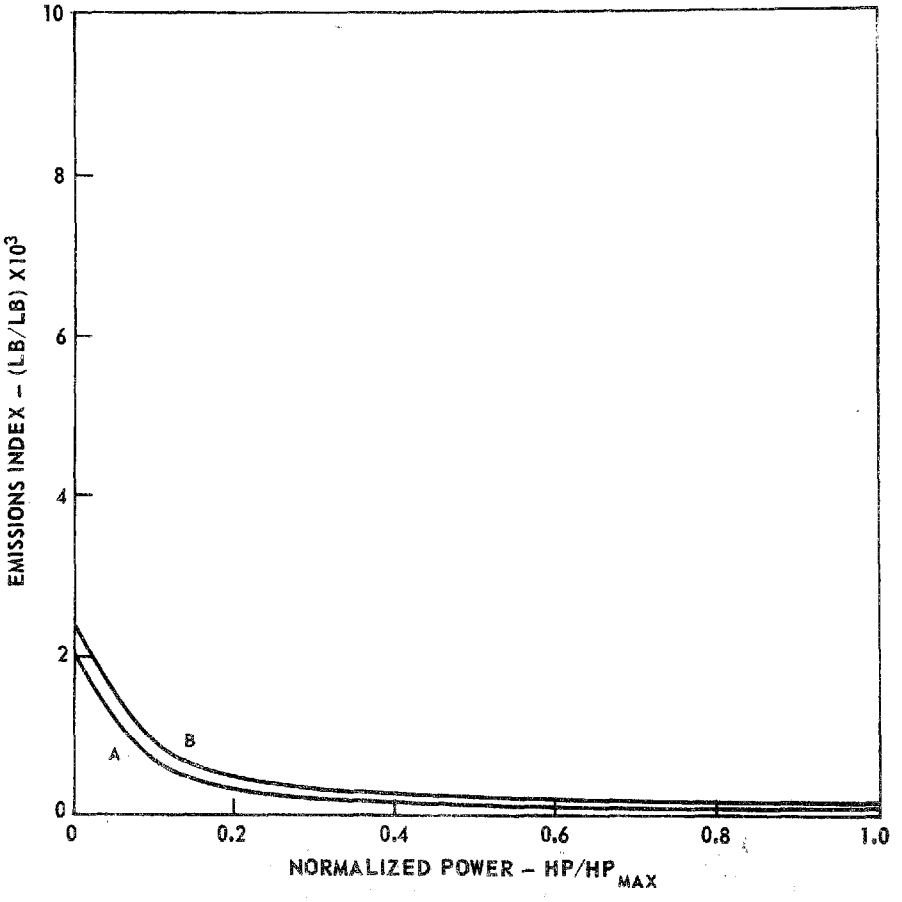

EFFECT OF VEHICLE WEIGHT ON EMISSIONS

SSS-10 ENGINE
FEDERAL DRIVING CYCLE
AMBIENT TEMPERATURE = 59 F
HYDROMECHANICAL TRANSMISSION
MAXIMUM POWER = 130 HP (59 F)
EMISSIONS INDEX C~LINES

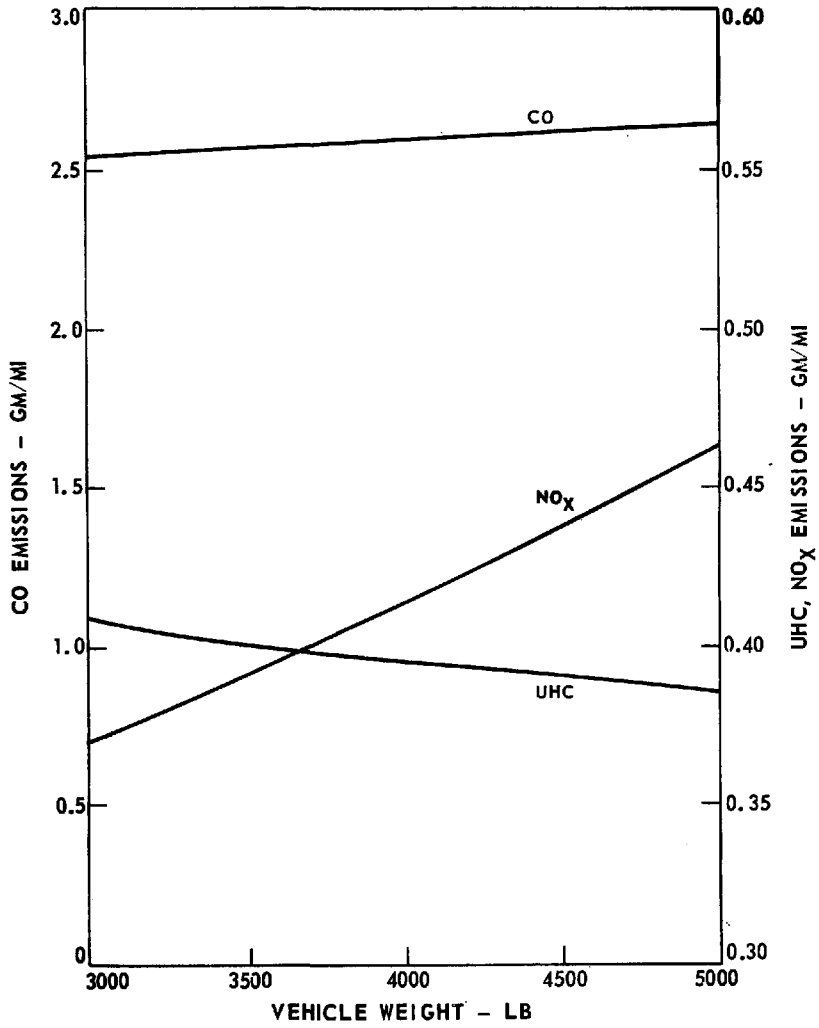

FIG. 105

EFFECT OF REAR-AXLE RATIO ON EMISSIONS

SSS-10 ENGINE
FEDERAL DRIVING CYCLE
AMBIENT TEMPERATURE - 59 F
HYDROMECHANICAL TRANSMISSION
MAXIMUM POWER - 130 HP
EMISSIONS INDEX C-LINES

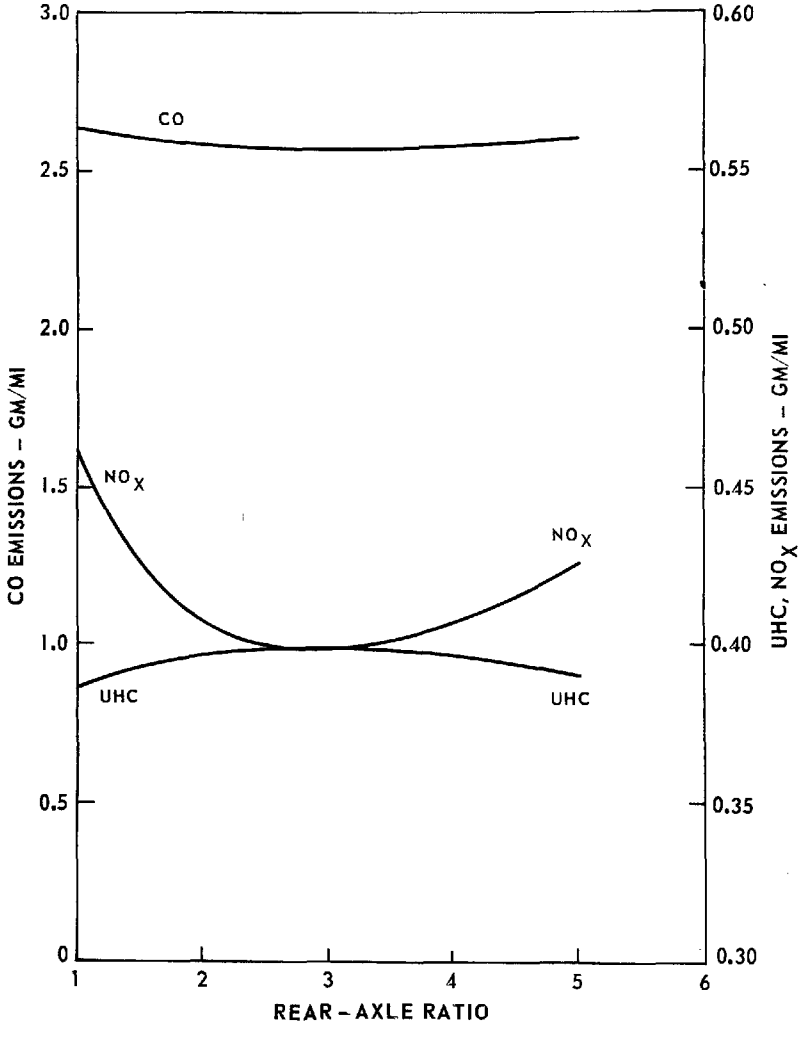

EFFECT OF ACCESSORY POWER ON EMISSIONS

SSS-10 ENGINE
FEDERAL DRIVING CYCLE
AMBIENT TEMPERATURE = 59 F
HYDROMECHANICAL TRANSMISSION
MAXIMUM POWER = 130 HP
EMISSIONS INDEX C-LINES

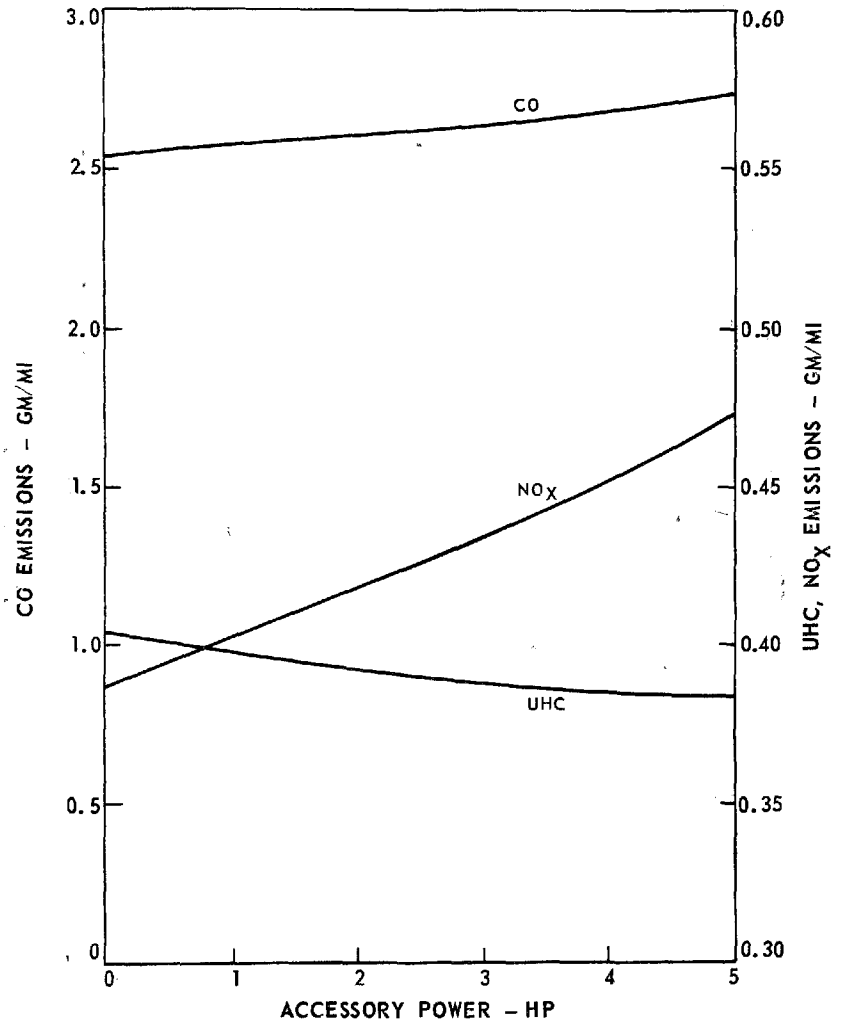

ECONOMIC ANALYSIS

The economic analysis is concerned with the estimated owning and operating costs to the vehicle owner over the life of the vehicle. The vehicle life has been specified by OAP to be 15,000 miles annually for seven years, or a total of 105,000 miles.

The figure of merit used in this economic analysis is the total lifetime cost (TLC) of the engine since the costs associated with the remainder of the vehicle are assumed to be constant regardless of the engine type. In a later section, some of the effects of the propulsion system upon the vehicle itself are also considered. The total lifetime costs include the initial engine cost as derived from the direct manufacturing cost, the cost of capital, fuel, repairs, and maintenance. The method of calculation employed is discussed below.

Direct Manufacturing Cost Estimates

Manufacturing cost estimates were prepared for each engine design. Figures 107, 108 and 109 show the parts content for the RGSS-6, RCSS-8 and SSS-10, respectively. The part numbers are keyed to Tables XIII, XIV and XV, respectively, for the RGSS-6, RCSS-8 and SSS-10, which present the manufacturing cost estimates.

These estimates of direct manufacturing costs are defined as the sum of the direct materials costs and the direct labor costs. It should be noted that the most important value for each of these engines is the combined total of direct materials plus direct labor (the latter value of which is converted from minutes to dollars at an appropriate wage). This distribution is emphasized because in those circumstances where a component part most likely would not be made in an engine-maker's facility, estimates of both labor and materials could not be made. As a result, the noted direct labor times correspond only to the estimated time allocated to the engine in the engine-maker's facilities.

The specific component parts defined in each of the three tables constitute over 91% of the total parts costs for each engine, and 100% of the parts whose direct cost is $1.00 or more. Each of the noted parts, as well as some included under the miscellaneous category, was examined individually to determine its weight, material, and machining requirements. The background in production methods used for the study reported in Ref. 1 was relied upon extensively to support the analyses of the present study. However, whereas manufacturing cost estimates of Ref. 1 included purchased part costs with an allowance for machinery amortization in addition to the cost of the basic materials, the results presented in Tables XIII through XV are for basic materials only.

FIG. 107

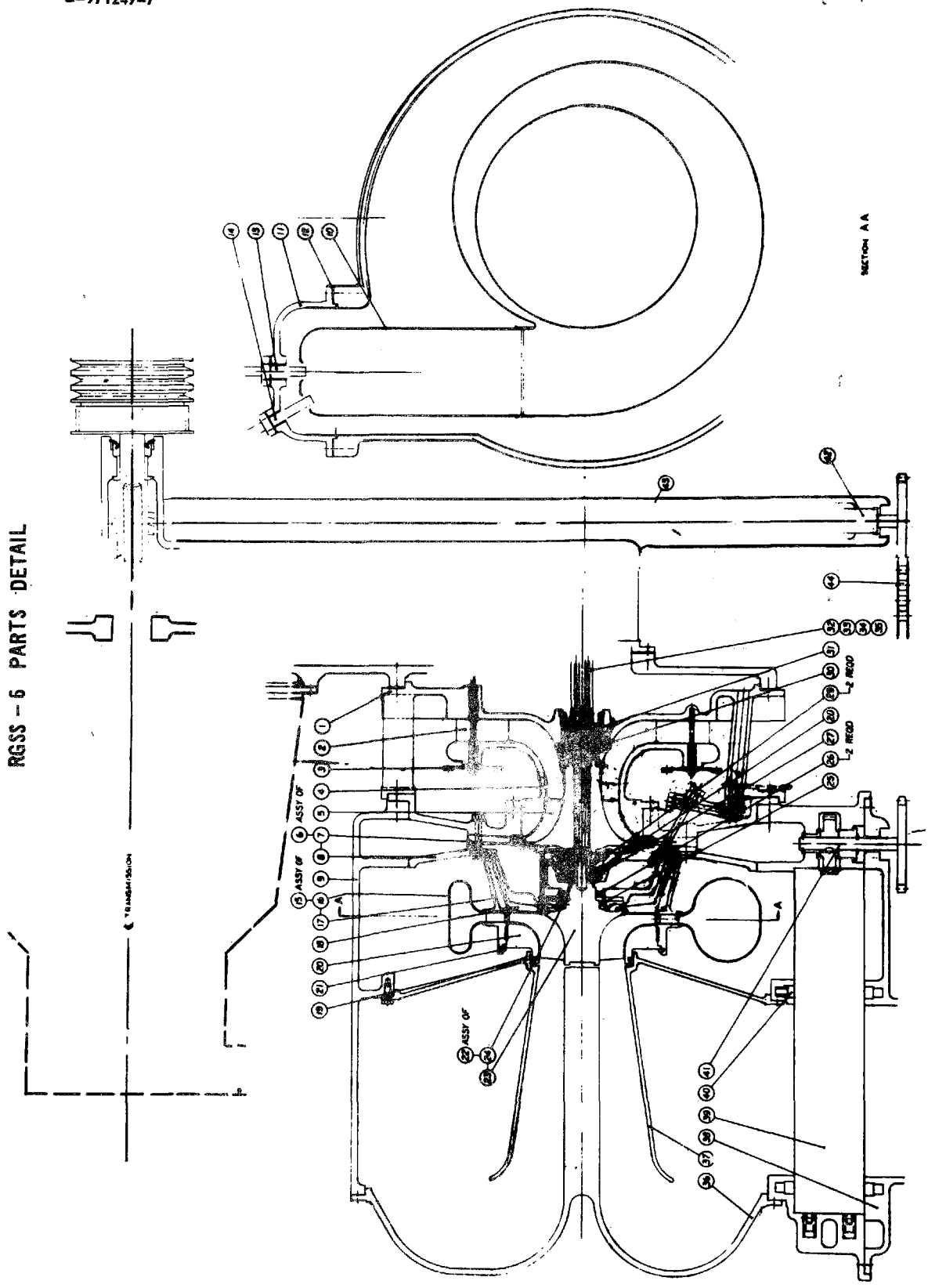
RGSS - 6 PARTS DETAIL
SECTION A-A
TRANSMISSION
ASSY OF
ASSY OF
ASSY OF
2 REQD
2 REQD

TABLE XIII

RGSS-6 DIRECT MANUFACTURING COST ESTIMATES

Part No.*	Item	Material**	Direct Material Cost - $	Direct Labor - Min.
4	Compressor Shroud	Ductile Cast Iron	3.85	2.8
5	Impeller	AMS 4928	18.55	9.8
8	Diffuser Case	Ductile Cast Iron	7.85	18.4
9	Pressure Vessel	Ductile Cast Iron	26.60	6.0
10	Combustor Can	Hastelloy -X (IN 625)	3.20	2.0
16	Combustor Scroll	Hastelloy -X IN 625)	18.10	4.0
17	Turbine Nozzle	WI-52 (IN 738)	24.00	9.8
18	Turbine Shroud-Front	WI-52 (IN 738)	15.95	2.5
20	Turbine Shroud-Rear	WI-52 (IN 738)	4.35	2.1
23	Turbine Rotor	U700 (IN 100)	20.30	9.5
24	Turbine Shaft	SAE 4340	1.50	5.8
26,30	Shaft Seals (3)	Carbon & Cast Iron	2.50	incl.
27,31	Bearings, Antifriction (3)	52 CB	10.50	incl.
36	Cover, Press. Vessel-Rear	Heat Resist. Cast Iron	3.05	2.0
37	Exhaust Diffuser	Heat Resist. Cast Iron	3.35	3.0
38	Cover, Regen. Disk Housing	Ductile Cast Iron	6.70	6.0
39	Regenerator Disk	CERCOR (Ceramic)	16.30	incl.
40	Regen. Support, Seals, Gears, etc.	Ductile Cast Iron	80.50	19.0
42,44	Regen. Drive Pulley, etc.	- - -	1.50	3.0
45	Case, Reduction Gearbox	Cast Iron	5.70	3.5
45	Reduction Gears	Gear Steel	13.40	43.1
45	Cover, reduction gearbox	Cast Iron	7.35	4.5
	Miscellaneous	- - -	20.55	11.2
	Fuel Control	- - -	39.50	incl.
	Oil Pump	- - -	4.50	incl.
	Alternator, Starter, Voltage Regulator	- - -	14.55	incl.
	Final Assembly & Test	- - -	- - -	35.0
	Subtotal		$374.20	202.7
	Direct Labor @ $5/hr		16.95	
	Total Direct Mfg. Cost		$391.15	

*See Fig. 107

**Alternate materials for certain high-cost parts shown in parenthesis. Final specification to depend on cost.

L-971249-7

FIG. 108

RCSS-8 PARTS DETAIL

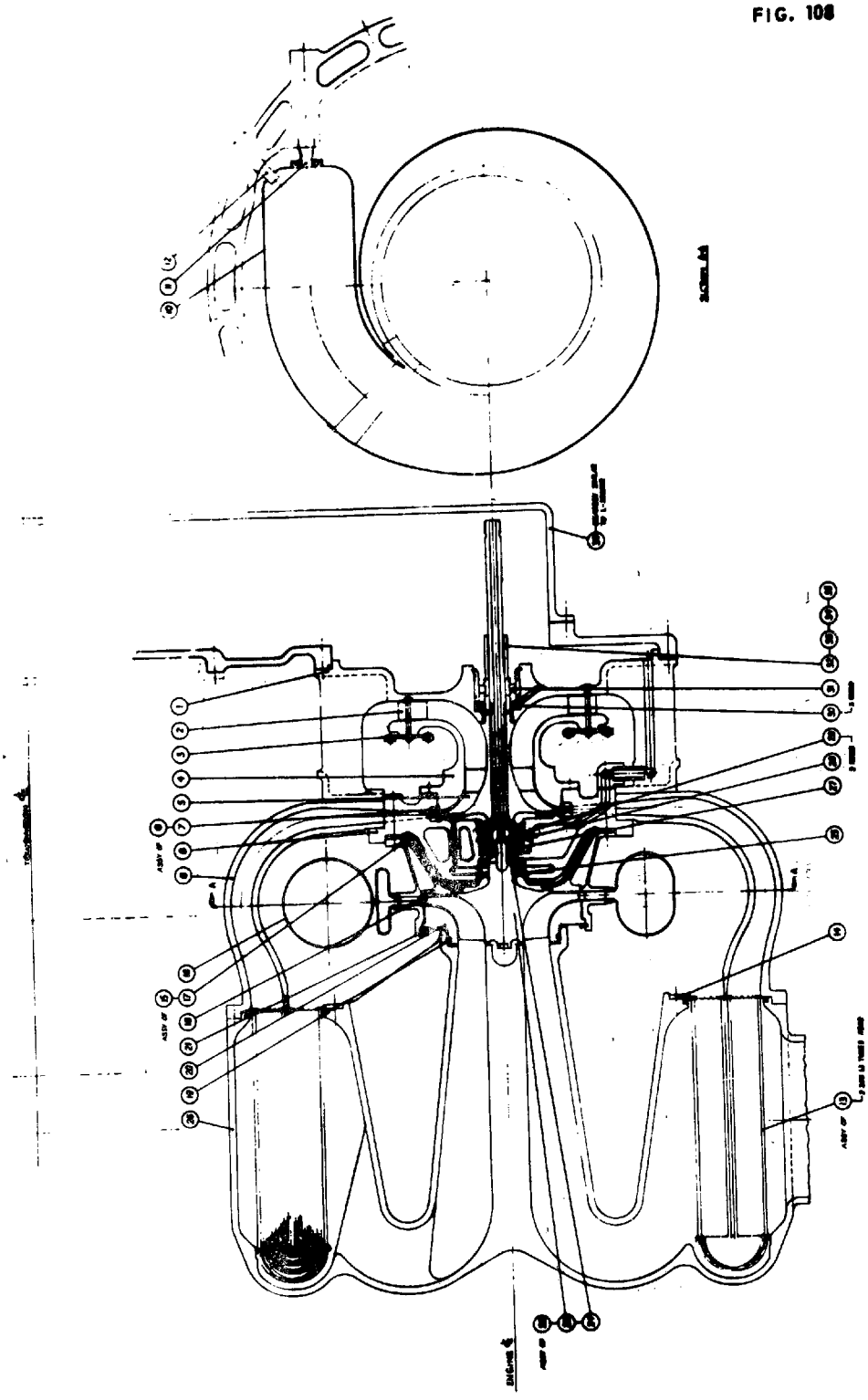

TABLE XIV

RCSS-8 ESTIMATED DIRECT MANUFACTURING COST

Part No.*	Item	Material**	Direct Material Cost - $	Direct Labor - Min.
4	Compressor Shroud	Ductile Cast Iron	1.90	2.7
5	Impeller	AMS 4928	13.70	6.0
8	Diffuser Case	Ductile Cast Iron	3.50	14.0
9	Diffuser-to-Recup. Casing	Ductile Cast Iron	12.50	3.0
10	Combustor Can	Hastelloy-X (IN 625)	3.50	2.5
13	Recuperator	Type 304 Stainless	77.45	43.0
16	Combustor Scroll	Hastelloy-X (IN 625)	15.80	4.0
17	Turbine Nozzle	WI-52 (IN 738)	20.30	10.1
18	Turbine Shroud-Front	WI-52 (IN 738)	13.10	3.6
20	Turbine Shroud-Rear	WI-52 (IN 738)	4.65	2.2
23	Turbine Rotor	U700 (IN 100)	19.80	9.1
24	Turbine Shaft	SAE 4340	1.05	5.0
26	Recuperator Casing	Ductile Cast Iron	10.95	8.5
27,31	Bearings, Antifriction (3)	52 CB	10.50	incl.
30	Shaft Seals (3)	Carbon & Cast Iron	2.50	incl.
36	Case, Reduction Gearbox	Cast Iron	5.70	3.5
36	Reduction Gears	Gear Steel	13.40	43.1
36	Cover, reduction gearbox	Cast Iron	7.35	4.5
37	Exhaust Diffuser	Heat Resist. Cast Iron	5.65	3.0
	Miscellaneous		16.85	9.1
	Fuel Control		39.50	incl.
	Oil Pump		4.50	incl.
	Alt., Start., Volt. Reg.		14.55	incl.
	Final Assembly & Test		----	30.8
	Subtotal		$333.45	207.7
	Direct Labor @ $5/hr		17.35	
	Total Direct Mfg. Cost		$350.80	

*See Fig. 108

**Alternate materials for certain high-cost parts shown in parenthesis. Final specification to depend on cost.

L-971249-7

FIG. 109

SSS-10 PARTS DETAIL

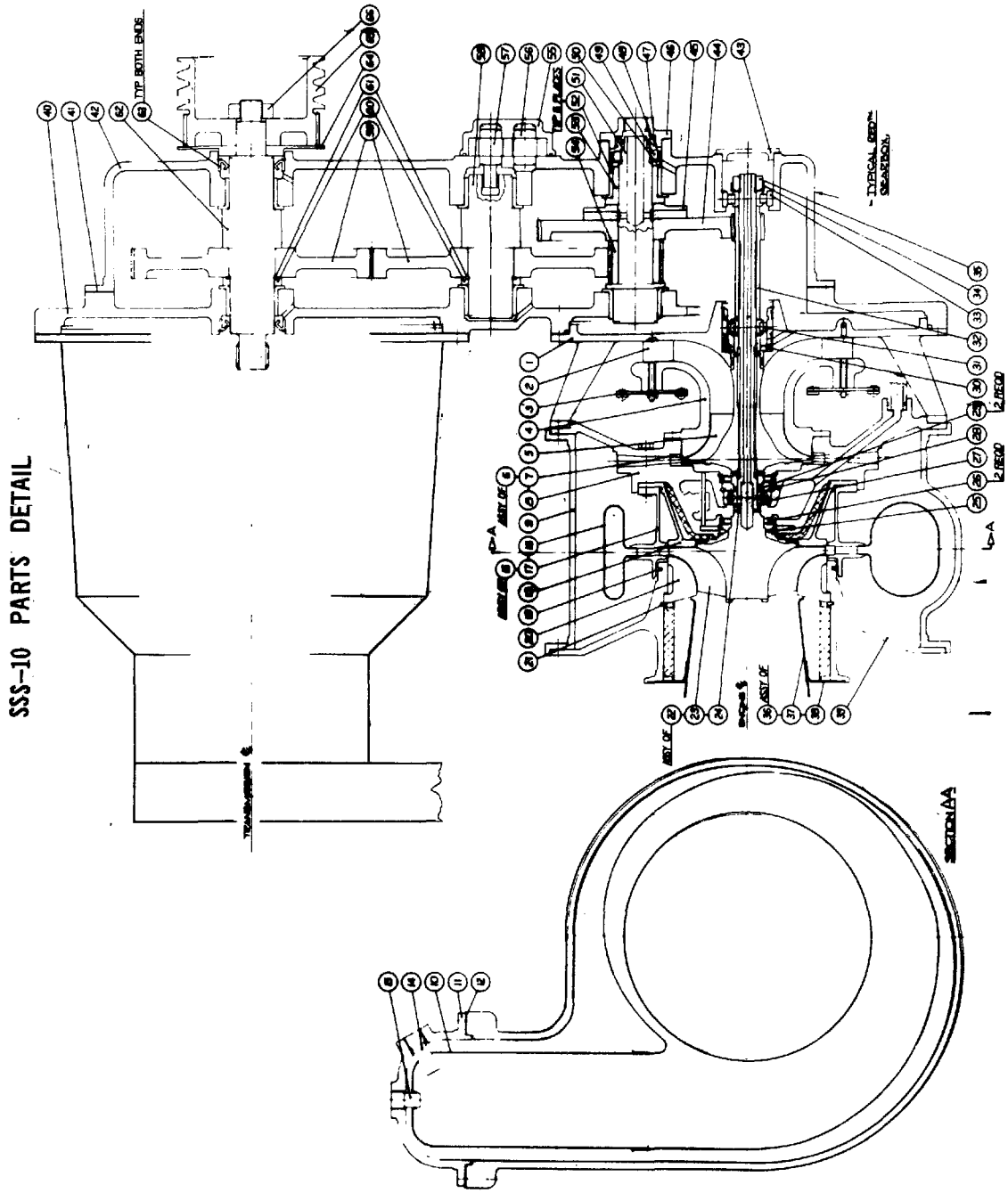

TABLE XV

SSS-10 DIRECT MANUFACTURING COST ESTIMATES

Part No.*	Item	Material**	Direct Material Cost - $	Direct Labor - Min.
4	Compressor Shroud	Ductile Cast Iron	1.30	2.6
5	Impeller	6-2-4-6 Titanium	13.35	5.7
8	Diffuser Case	Ductile Cast Iron	4.95	16.0
9	Pressure Vessel	Ductile Cast Iron	3.00	6.0
10	Combustor Can	Hastelloy-X (IN 625)	2.25	2.0
16	Combustor Scroll	Hastelloy-X (IN 625)	16.05	4.0
17	Turbine Nozzle	WI-52 (IN 738)	16.40	10.7
18	Turbine Shroud - Front	WI-52 (IN 738)	8.10	2.2
20	Turbine Shroud - Rear	WI-52 (IN 738)	5.15	2.3
23	Turbine Rotor	U700 (IN 100)	19.60	8.6
24	Turbine Shaft	SAE 4340	1.30	5.5
26,30	Shaft Seals (3)	Carbon & Cast Iron	2.50	incl.
27,31,33	Bearings - Antifriction (3)	52 CB	10.50	incl.
39	Cover, Pressure Vessel - Rear	Cast Iron	2.80	1.9
40	Case, Reduction Gearbox	Cast Iron	5.70	3.5
42	Cover, Reduction Gearbox	Cast Iron	7.35	4.5
44,59	Gears, Reduction	Gear Steel	13.40	43.1
	Miscellaneous		15.40	9.5
	Fuel Control		39.50	incl.
	Oil Pump		4.50	incl.
	Alt., Start., Volt. Reg.		14.55	incl.
	Final Assembly and Test		----	21.0
	Subtotal		$207.65	149.1
	Direct Labor @ $5/hr		12.45	
	Total Direct Mfg. Cost		$220.10	

*See Fig. 109

**Alternate materials for certain high cost parts shown in parenthesis. Final specification to depend on lowest cost.

The following assumptions were common to all three engine designs in this analysis. All cast iron parts were estimated for a material cost of between 15¢ and 20¢ per pound, depending on whether or not a high-temperature version of this material was required. For all components, material cost estimates were based on the weights before machining and, as such, include a scrap allowance. However, in most circumstances, this scrap allowance never exceeds 20%, a practice which is quite typical of the high-volume, price-conscious automotive industry. Materials such as coated WI-52 or its alternate IN 718, both of which could be specified for investment-cast parts, were assumed to cost slightly less than $3 per lb. Hastelloy-X, which was used in burner cans and high-temperature sheet metal parts, was estimated at $4.50 per lb in sheet form. In all engines, both the inducer/impellers and the turbine rotors were assumed to be produced by advanced forging techniques. One approach to advanced forging is the superplastic method (Gatorizing) which recently has been perfected at the Pratt & Whitney Aircraft Division of UAC. Previous analyses and consultations with Corporate personnel familiar with this process made it possible to say that in high-volume production the raw material costs for superplactically forged parts will cost approximately $7 per lb, a value which is practically independent of the type of material specified. Furthermore, it is believed that because of the nature of this production process, labor times of approximately 3 min per lb (for small parts) would be required in the forging, trimming and finishing operations of each part.

As noted above, the direct costs of purchased parts include profit, overhead and machinery depreciation allowances in addition to the costs of labor and materials. Previous consultation with suppliers of these high-volume-production items has led to the discovery that in most cases, the O.E.M. prices quoted by a manufacturer of a part are approximately 1.8 to 2.0 times the direct production cost of that component. As a result, all purchased component price data were divided by this price/manufacturing cost ratio to reflect the present best estimate of direct production cost for each of these items. In general, items which were included in the vendor-purchased category were seals, bearings, starters, alternators, voltage regulators, oil pumps, fuel controls and heat exchangers (where necessary). Prices for these items were obtained from specialist vendors who either supply these items directly to the automotive industry or who had an intimate working knowledge of the prices of the various parts.

In the case of the regenerator or recuperator of the RGSS-6 and RCSS-8 engines, detailed analyses of the various heat exchanger components were made. The ceramic-type regenerator actually represents a complicated mechanism incorporating a chain-driven gear drive, a disk holder and the disk sealing mechanism. A previous study (Ref. 1) indicated that the heat recovery approach to automotive gas turbine design is expensive, and, from the results generated in this study, this conclusion is substantiated. Of the nearly $100 indirect material costs associated with the regenerator, the ceramic disk and its support and drive mechanism constitute

approximately $40, whereas the direct cost of the sealing mechanism is estimated to cost over $50. Discussions with the major manufacturer of this type of dynamic seal have revealed that unless severe compromises are made on the part of the engine maker, there is little chance that direct production costs of the seals can be reduced, even in high-volume production.

The recuperative type of heat exchanger represents a different problem because a large tube area must be provided to attain a reasonable effectiveness for the thermodynamic engine cycle. As a result, 2140 tubes, each with a diameter of 0.125 in. and an average length of slightly more than 23 in., are required. With Type-304 stainless steel formed from strip stock 0.010 in. thick, the base price of the tubes alone becomes $64.50. The addition of end headers increases this cost to slightly more than $77 per unit. Total labor time is estimated at a conservative 43 minutes per unit even with the use of highly automated equipment. As a result, the estimated cost of the heat exchanger on the recuperative-design automotive gas turbine engine is only slightly less than the heat exchanger in the regenerated RGSS-6 engine. It must be emphasized, however, that there is currently no assurance that satisfactory recuperators can be manufactured by these techniques with these materials, and that a large-scale development program would be necessary to develop not only more accurate cost estimates, but a realistic assessment of the practical problems involved.

Although no specific analysis was made, it is believed that the accuracy of the material cost estimates are within ±10 to 15% based on a root-mean-square component-by-component analysis. This estimate of accuracy is approximately the same as that noted in Ref. 1 since all engine components were analyzed in a similar manner. Estimates of the direct labor probably have a higher statistical error, although even a larger error would not significantly affect the results noted because labor constitutes such a small portion of the total direct cost. Within a given organization, a rather large multiplier normally is applied to labor to account for overhead items (such as equipment amortization) which are intrinsic to an individual firm's operations. Such overheads have not been included in this analysis because this multiplier is an accounting convenience, is not a consistent value, and is not necessarily a strong function of direct labor hours. Consequently, it is believed that the results presented in Tables XIII, XIV and XV represent an estimate of the direct charges associated with the production of each engine which reasonably could be attained in the 1976-77 period.

Cost of Capital

The cost of capital includes those costs related to investments either by the owner or his creditors and/or to the value of the vehicle. In order to apportion these costs it is necessary to make several assumptions. First, as mentioned above, it is assumed that the nonpropulsion system portions of the vehicle behave in an identical fashion for all engines and, consequently, will not enter into the

evaluation of the candidate engines and their propulsion systems. Secondly, it is assumed that depreciation rates, interest rates, tax rates, etc., are unaffected by the type of engine and that the only differences among the systems will be those determined by the relative initial prices. It is further assumed that there is a direct relation between manufacturing cost and retail price and that this relation is represented by a factor of 2.7 in order to mark up the direct manufacturing cost to the original discounted retail price as per Ref. 1. Finally it is assumed that these costs will continue to be incurred in accordance with historical trends.

The capital costs involved are those resulting from depreciation, interest lost, finance charges, taxes, and collision and comprehensive insurance. All of these may be reflected back to the original purchase price of the engine in terms of probable lifetime percentage values.

Depreciation over the lifetime of the vehicle can be defined as the total of the retail sales price minus the total of the trade-in (wholesale) price or allowance. On a percentage basis, this sum is divided by the original sales price. Statistics of Ref. 20 indicate that the average car bought new is traded at 3.9 years, and that the average car bought used is traded at an average age of 7 years. If it is assumed that all the study vehicles depreciate and resell on the same historical basis, which includes the dealer's profit and cost on each of the two resales, a depreciation value of approximately 120% relative to the original value of the vehicle can be derived using Ref. 21 data for standard-sized Ford and Chevrolet six-passenger V-8 sedans.

Appendix IV describes the historical data used to establish the cost of ownership of conventional automobiles. On this basis, it can be determined that the overall cost of capital historically amounts to approximately 166% of the original price of the vehicle. Thus, the cost of capital for the engines considered in this study may be derived by multiplying their direct manufacturing cost by 2.7 (to account for average retail price) and further multiplying this figure by 1.66 (to account for depreciation, interest, taxes, finance charges and insurance costs).

Cost of Fuel

The cost of fuel to the owner can be established by multiplying the 105,000 miles driven by the assumed fuel cost in dollars per gallon and dividing the product by the miles per gallon for the prescribed OAP driving cycle for each candidate engine. The difficulty in applying this figure lies in estimating the price of the fuel. Retail pricing in the petroleum industry is a complex subject and results in highly varying practices. The competitiveness of this business results in large swings which bear little or no immediate relation to the actual cost of refining.

In the long run, however, it does appear that fuel costs must be related to refining costs and to supplies. The prime feature of the fuel for the gas turbine engines considered in this report is the lower pump delivered price. There are no octane requirements nor cetane requirements, and straight-run distillery fuels (either gasoline or light oils) would provide satisfactory fuel for the engines. Since refining costs for gasoline (and particularly high-octane gasolines and most particularly gasolines without lead) suitable for operation in motor vehicles are necessarily higher than for turbine fuels, it appears safe to assume that, at least for the foreseeable future, average pump prices for turbine fuels should be lower than those for gasoline. This situation would be true even if the entire vehicle production were converted, immediately, from Otto-cycle to gas turbine engines, since in any given year only 10% of the vehicle population is replaced, and presumably the majority of refinery output for motor vehicles would continue to be gasoline.

The assumed gas turbine fuel cost in this study has been assumed to be 31¢/gal.* The cost could easily range from 25¢ to 40¢, particularly for varying localities and times, and quite obviously the engine with the higher rate of fuel consumption is more sensitive to increased fuel prices.

Cost of Repairs and Maintenance

The basic data for estimating the repair and maintenance costs are the historical data described in Appendix IV. Maintenance and repair estimates for the three candidate gas turbine engines are also compared on this use basis and involve estimation of frequency of repair as well as estimates of mechanic labor and direct manufacturing costs of the parts involved. In this case, the retail spare parts cost is arrived at by multiplying the direct manufacturing cost estimate by 3.5.

The maintenance estimate for the three candidate engines is shown in Table XVI and the lifetime repair estimate is shown in Table XVII. It will be noted in Table XVI that periodic maintenance is reduced considerably over that required historically, and tune-up requirements become a minor item in the cost of maintaining a vehicle. Primarily as a result of this situation, the repair and maintenance costs of the gas turbine engines are predicted to be quite attractive in comparison with conventional engines.

Quite naturally, it is most difficult to predict the cost of repairs and maintenance for new systems. Such predictions must always be only approximate prior to the accumulation of sufficient amounts of historical data. While it cannot be stated that the repair and maintenance costs for any of the gas turbine engines would fall within the range assumed, it is felt that the estimates made here are logical extrapolations based on present knowledge.

*A fuel cost of 33¢/gas was assumed for the preliminary candidate selection process described earlier; however, at the request of OAP, the value was changed to 31¢/gal for the final engine selection.

TABLE XVI

ESTIMATED GAS TURBINE MAINTENANCE COSTS

Annual:	(15,000 mi)	
	Check and adjust belts	$ 5
	Replace ignitor	2
	Replace fuel filter	3
	Check and calibrate control	8
	Replace air filter	6
		$24
Biennial:	(30,000 mi)	
	Replace belts	10
	Replace ignitor	2
	Replace fuel filter	3
	Check and calibrate control	8
	Replace air filter	6
	Check balance	5
	Change oil (SSS-10 only)	7
		$41
	Check heat exchanger (RGSS-6;RCSS-8 only)	20
		$61

Total Maintenance Costs (4 Annual, 3 Biennial):

RGSS-6 = $279
RCSS-8 = $279
SSS-10 = $219

TABLE XVII

GAS TURBINE REPAIR ESTIMATES

Repair Item	Engine	Frequency[1]	Material Cost ($)	Labor Hours	Total per Repair ($)	Lifetime Cost ($)
Repair Casings	All	0.1	0	4	40	4
Replace and Repair:						
Combustor	RGSS-6	0.6	12.80	2	33	20
	RCSS-8	0.6	14.00	4	54	32
	SSS-10	0.6	9.00	2	29	17
Fuel Nozzle	All	1.2	2.00	1	12	14
Ignitor	All		Included in Maintenance			
Scroll	RGSS-6	0.2	72	4	112	22
	RCSS-8	0.2	48	4	88	18
	SSS-10	0.2	48	4	88	18
Turbine Nozzle	RGSS-6	0.6	98	7	168	100
	RCSS-8	0.6	81	7	151	91
	SSS-10	0.6	65	6	125	75
Shrouds	RGSS-6	0.3	80	8	160	54
	RCSS-8	0.3	72	8	152	46
	SSS-10	0.3	52	7	122	37
Wheel	RGSS-6	0.2	81	8	161	32
	RCSS-8	0.2	80	8	160	32
	SSS-10	0.2	80	7	150	30
Seals	All	0.6	20	7	90	54
Bearings	All	0.6	41	7	111	66
Reduction Gearing	All	0.3	52	4	92	19
Regen. Core	RGSS-6	0.8	64	2	84	67
Regen. Seals	RGSS-6	1.2	320	2	340	410
Recup. Seals	RCSS-8	0.8	310	2	330	264
Total Lifetime Repair Costs -	RGSS-6					$862
	RCSS-8					$640
	SSS-10					$334

[1] Frequency of repair over total lifetime; where less than 1.0, only fraction of vehicles would require repair; e.g., one in ten vehicles would require casing repair.

TABLE XVIII

TOTAL LIFETIME COSTS FOR PROPULSION SYSTEM - (TLC_{ps})

Engine	Fuel Economy mpg*	Fuel Economy Cost** $	Cost of Maintenance $	Cost of Repairs $	DMC $	Cost of Capital*** $	TLC_{ps} $
RGSS-6	14.9	2180	279	862	391	1760	5081
RCSS-8	13.8	2360	279	640	351	1520	4859
SSS-10	9.8	3330	219	334	220	990	4873

* OAP driving cycle
** Fuel @ 31¢/gal
*** 4.5 X DMC

Results

The results of the economic analysis are shown in Table XVIII. As can be seen, the total lifetime costs are extremely close for the three candidate engines. Certainly, they are too close to clearly favor one engine over the other in view of the accuracy of the assumptions entered.

Originally it had been thought that the economic analysis would provide a basis for recommending the selection of one engine over the others. However, it is obvious that the figures shown in Table XVIII are not sufficiently different to allow the selection of any one engine. Therefore, a different selection procedure had to be especially devised to meet the primary objective of the study. This procedure is described in the next section.

RECOMMENDED ENGINE SELECTION

The available information and best estimates concerning the performance, cost, and other relevant characteristics of the various types of engines considered (including, for comparison, present and future Otto-cycle engines) are summarized and discussed briefly in this section, and recommendations are made as to which of these engines is most likely to satisfy the requirements for clean, economical prime movers for automobiles.

Emissions

Nitrogen Oxides

Nitrogen oxides (NO_x) are the most dangerous of the pollutants attributable to the motor vehicle and have been consistently judged as representing the most serious pollution problem. Independent sources have estimated its harmfulness as much as 50 times higher than that for carbon monoxide. The problem of controlling NO_x is not only the most important of those facing the automobile industry; it is also generally considered to be the most difficult.

The results of this study show the SSS-10 to have a major advantage with regard to NO_x production. It is believed to be virtually certain that combustors can be developed at reasonable cost for engines of the SSS-10 type which will permit them to meet the 1976 Federal Emissions Standards of 0.4 g/mi for NO_x. As noted in the previous section, this requirement represents approximately a 60% reduction in what is considered the state of the art for NO_x emissions of untreated simple-cycle engines. There is some indication that, because of low values for UHC and CO emissions, slight increases in typical UHC production and a doubling of typical CO production may be allowable in striving for the NO_x standard. Preliminary results of UACL combustor testing programs* have been inconclusive in this regard, and definitive results are not in hand at the time of publication of this report.

In the case of the heat-exchanger engines, it is far less certain that the NO_x standards can be met. Unconventional combustor design is almost certain to be called for and, even if the required NO_x reduction is demonstrated in test stands, considerable question exists as to the likelihood of accommodating the combustor design in a feasible automotive engine design, and whether such a design can be manufactured at competitive costs.

---

* A combustor development program is under way at UACL, with UARL participation, to demonstrate that the desired emissions levels can be achieved, under EPA Contract 68-04-0015. Both regenerated and simple-cycle combustors are being developed, and other contractors are also working with EPA support.

The Otto-cycle engine is very unlikely to achieve the required level of NO_x production by 1976. Reference 22, for example, describes a maximum-effort automobile which will produce NO_x emissions still too high by a factor of two. It is expected that Wankel engines will have similar problems in meeting the standards.

Therefore, not only does the SSS-10 have a significant advantage in meeting NO_x standards, it appears that it is the only practical engine with a high probability of achieving this requirement.

Unburned Hydrocarbons (UHC) and Carbon Monoxide (CO)

The production of both UHC and CO is related primarily to the efficiency of combustion. They are, therefore, more easily controllable than the production of NO_x, which is fundamentally related to the combustion process itself. In addition, their importance from a health standpoint is considerably less than that associated with NO_x. All of the candidate gas turbine engines have inherently very low production levels of CO and UHC, unlike the Otto-cycle engine. However, even the Otto-cycle engine may meet the UHC and CO standards by using post-combustion treatment, at least for the majority of vehicles when they are produced.

Both the regenerative and recuperative gas turbine engines are certain to achieve these standards, since compliance has already been demonstrated by similar engines. Even in the case of the simple-cycle engine, whose basic rate of production of CO and UHC is somewhat higher than the regenerative engines, there is little doubt that the standards will be met.

Production Variability

Production variability has been noted as of extreme importance in the case of production-line Otto-cycle engines, which will rely heavily on post-combustor treatment devices (such as catalytic converters) to convert a highly noxious exhaust stream into a relatively pure one. The natural state of emissions for Otto-cycle engines is some ten to one hundred times worse than that required to meet the standards, and in many cases the natural state is made even worse in an attempt to lower NO_x. Consequently, if a converter with a design efficiency of 98%, for example, delivers only 96% efficiency as a result of normal production-line tolerance stackups, the emissions will obviously double. On the other hand, the gas turbines are inherently clean-burning engines, so that production-line tolerance stackups will not result in significantly altered emissions levels. The only area of possible concern would be a complex combustor design, such as may be required for the heat-exchanger engines. The possibility of emission-performance degradation due to tolerance stackups will have to be addressed for these burners, and appropriate quality-control measures will have to be used.

Deterioration in Service

A major element in the emissions evaluation is the likelihood of satisfactory emissions performance over the lifetime of the vehicle. In the case of the SSS-10, its emissions performance is likely to be constant, varying by no more than 20 to 25% in the extreme, with such variations as do occur being caused primarily by lifetime degradations of power and component efficiency. In the case of the heat-exchanger gas turbine engines, a slightly lower degree of lifetime performance is expected because of heat exchanger leakage. Also, unconventional combustors will undoubtedly be required to meet the NO_x requirements in the heat-exchanger engines, which may break down with consequent increase in emissions. In the case of the Otto-cycle engine, there is presently no assurance that the required add-on equipment can be made to last even 50,000 mi, i.e., half of the lifetime of the car. As a result, in-service inspections would be required to check deterioration at considerable inconvenience and cost to the owner.

Emissions Summary

In summary, it is believed that the SSS-10 engine possesses distinct advantages with regard to the all-important emissions area. It is the only practical engine with a high assurance of meeting the NO_x goals. It, together with the heat-exchanger gas turbines, offers the only reasonable approach among the engines considered here for low lifetime-average CO and UHC formation.

Initial Price and Production Cost Uncertainties

It is believed that the strongest measurable factor governing buyer appeal for a given set of vehicle options is the initial price. Historically, most prospective car buyers are far more concerned with the initial price of the vehicle than with its operating or lifetime costs.

Table XIX presents an analysis of price estimates which are based on (a) vehicle weight estimates and (b) engine manufacturing cost estimates. For purposes of standardization, OAP evaluation procedures require that the non-propulsion system portion of the standard six-passenger vehicle weight be fixed at 2700 lb. In actuality, the weight of such components as springs, brakes, tires, wheels, etc., are affected strongly by propulsion system weights. Automobile manufacturers tend to expect to save about one additional pound in vehicle weight for every pound saved in the engine weight. A somewhat more conservative value for this ratio can be derived as follows, based on a component breakdown of vehicle weights originally established by Hoffman (Ref. 23). Of the total vehicle weight, the trim and glass (total of 690 lb) are assumed to be unaffected by propulsion system weight, but the rest of the vehicle is assumed to vary with the ratio of the propulsion system weight saved to the gross weight. Thus,

TABLE XIX

VEHICLE WEIGHT AND PRICE ESTIMATES

Line	Item	Computation	SSS-10	RCSS-8	RGSS-6	Base-Line OC	OC-76
1	Engine		lb 235	lb 475	lb 515	600	800
2	Radiator		0	0	0	60	70
3	Starter		25	25	25	20	20
4	Generator		20	20	20	20	20
5	Engine with Accessories	Σ lines (1)-(4)	280	520	560	700	910
6	Transmission		180	180	180	160	160
7	Rear Axle and Drive Line		100	100	100	170	170
8	Battery		50	50	50	45	45
9	Fuel and Tank $\left(1.37\left(\frac{p \times 200}{FDC}\right)\right)$ (200-mi range fuel)		250	170	160	175	215
10	Exhaust		75	65	65	50	50
11	Propulsion Accessories	Σ lines (6)-(10)	655	565	555	600	640
12	(W_p) Propulsion System	(5)+(11)	935	1085	1115	1300	1550
13	Adjusted Gross Weight	$\frac{(12) + 1690}{0.548}$	4400	4650	4700	5000	5420
14	Nonpropulsive Variable Items	(13) - (12) - 1690	1775	1875	1895	2010	2180
15	Nonpropulsive Fixed Items		690	690	690	690	690
16	Vehicle without Propulsion System	(14) + (15)	2465	2565	2585	2700	2870
17	Curb Weight	(13) - 0.75 (9) - 1000	3210	3525	3580	3870	4260
18	Curb Weight without Engine	(17) - (5)	2930	3005	3020	3170	3450
19	Price Less Engine	\$0.90 x (18)	\$2640	\$2700	\$2715	\$2850	\$3010
20	DMC Engine		220	350	390	200	444
21	Price of Engine	2.7 x (20)	595	945	1055	540	1200
22	Automobile Retail Price	(19) + (21)	\$3235	\$3645	\$3770	\$3390	\$4210
23	Change Relative to Base Line OC		\$-155	\$+245	\$+380	\$ 0	\$+820

L-9712497

$$W_g = W_p + 1690 + \frac{2010}{5000}\left(W_g\right)$$

where W_g is the gross weight, 690 lb is the invariant portion of the body (trim and glass), and 1000 lb is the weight of passengers and luggage to be added to the fully fueled curb weight in order to reach the gross weight, and where 2010 lb is the variable portion of the 5000-lb gross weight of a conventional automobile.

This yields the following relationship for adjusted gross weight:

$$W_g = 1.672\ W_p + 2826$$

which indicates that about an additional 2/3 lb is saved for each pound saved in the propulsion system.

Table XIX shows the vehicle weight and price estimates using this system for five selected vehicles. The first vehicle is based on the SSS-10 engine; the second the RCSS-8; and the third the RGSS-6. The fourth column represents a vehicle employing a base-line Otto-cycle engine and is designated "base-line OC." This vehicle represents a conventional 4000-lb six-passenger automobile with standard V-8 engine, as described in Ref. 1, and is, nominally, a 1970 vehicle. The final column represents the estimate for a vehicle employing a pollution-treated 1976 Otto-cycle engine*.

Line 1 contains the engine weight. The first three columns are those derived from the design portion of this study. The OC-76 weight is derived by increasing the size of the base-line OC engine in order to partially compensate for performance reductions caused by emissions treatment devices and by adding 100 lb of various pollution control devices. The radiator for the OC-76 is increased slightly to account for the greater inefficiency and larger size of the propulsion system. The transmission weights for the gas turbine engines are listed as 25 lb higher than the conventional three-speed automatic with torque converter. This is a conservative estimate, since the weight could well be less depending upon the transmission selected. The rear axle and drive-line weight for the gas turbine engines is considerably less by virtue of the lighter front-wheel drive selected . Fuel and tank weights are calculated on the basis of a 200-mi range for the Federal Driving Cycle.

---

* The data for weights in this study have been generated by UARL for a contract for the Department of Transportation.

From the calculated propulsion system weights shown on line 12, the adjusted gross weight is then derived using the formula shown above. From this weight, the key figure which is obtained (i.e., the curb weight of the vehicle without its engine) is shown on line 18. The price of the vehicle less its engine is shown in line 19, using the relationship that the price equals the weight multiplied by 90¢/lb. The direct manufacturing cost of the engine is shown in line 20 and is converted into a price of the engine by multiplying it by 2.7, as per Ref. 1. Finally, the automobile retail price is calculated by adding the price of the engine to the price of the vehicle-less-engine. As can be seen, the SSS-10 has the lowest price of any of the vehicles, and the difference between it and that for the future predicted Otto-cycle engine is almost $1000. Also, the SSS-10 vehicle costs $400 less than the RCSS-8 vehicle and more than $500 less than the RGSS-6 vehicle.

While a preliminary analysis of this sort cannot be considered to be conclusive, it strongly suggests that on the grounds of low weight and low manufacturing cost the SSS-10 engine has a clear advantage not only over the other two candidate gas turbine engines but with regard to future predicted Otto-cycle engines.

Production Cost Uncertainty

No gas turbine has as yet been successfully placed in large-scale mass production. Therefore, the manufacturing cost estimates presented in this report, although the best that can be made at this time, are subject to several uncertainties.

Manufacturing cost estimates for the SSS-10 engine will probably be quite close to those predicted here, since parts for which a large degree of uncertainty exists are not of particularly high value. The greatest production uncertainty is associated with the RCSS-8 engine because enough is not known to determine, with confidence, the specification of the material used, or manufacturing techniques involved, in the recuperator.

In the case of the regenerated engine, the major uncertainties stem from the fact that production costs of ceramic cores are apparently not achieving target values, so that it may actually be cheaper to purchase stainless steel regenerator cores than ceramic cores (Ref. 24). Considerable uncertainty also exists regarding the eventual cost of satisfactory seals for this duty, so that the manufacturing cost estimates for the RGSS-6 may be considerably higher than those estimated here.

Considerable uncertainty also exists regarding the production costs of treated Otto-cycle engines, primarily because of the difficulty in defining the required system.

Fuel Economy

The national average fuel consumption for all passenger cars is less than 14 miles per gallon (Ref. 16); this figure includes all of the compacts and intermediates as well as the heavier standard-sized cars studied herein. UARL calculation of 11.4 mpg for present standard cars operating on the OAP composite cycle appears to be consistent with this figure. The base-line SSS-10-powered vehicle, which is predicted to deliver 9.8 mpg for the OAP cycle, burns 15% more fuel than this standard car (OC-70), while the RGSS-6 at 14.9 mpg burns 24% less fuel. With a 15% fuel cost differential (31¢/gallon vs 35¢/gallon), the present auto and the future SSS-10-powered vehicle have almost equal fuel costs for the OAP cycle, whereas the costs for the RGSS-6 would be about one-third lower. Thus, the fuel economy of the SSS-10 is believed to be adequate.

This situation suggests that the regenerated-cycle gas turbine might be offered as an extra-cost fuel-economy option, which might be attractive for light commercial vehicles, economy-conscious consumers, etc. For passenger cars, however, most of the buying public would probably not avail itself of this option*.

The OAP specification for fuel economy calls for 10 mpg over the Federal Driving Cycle**. The heat-exchanger gas turbines considered herein are expected to exceed this specification by delivering between 11 and 12 mpg. However, the base-line SSS-10, as configured herein, is predicted to deliver only 7.5 mpg over the Federal Driving Cycle using the GE hydromechanical transmission (HMT).

---

* Several relevant precedents are the following: (1) The overdrive, which at about $100 extra over the standard transmission, delivered a 10 to 20% improvement in fuel economy, saved on wear and tear on the engine, and furnished an automatic passing gear, has disappeared from the market because of disinterest by the public. (2) Economy engines, such as six cylinder vs eight, four vs six, etc., low compression (regular fuel) vs high compression (premium fuel), generally have had only a very limited appeal. (3) Extra-performance options (four carburetor barrels vs two) enjoy significant sales, despite their poorer economy and higher first cost. (4) A 1971 study by General Motors based on a nationwide sample of 15,630 new car buyers of ten different makes of B-body sized cars (see Table XX) indicated that the largest single group of car buyers surveyed (Chevrolet owners) ranked gas economy 21st out of the 26 reasons most often mentioned as factors important in determining final selection; in fact, only 7.8% of the Chevrolet buyers mentioned gas economy, while the average for buyers of all the ten makes surveyed was 10.4% (ranging from a low of 4.6% for the Pontiac to 23.6% for the Ambassador).

** It is questionable whether future Otto-cycle engines can achieve this figure; a more likely achievement for these engines is only 8 to 9 mpg.

TABLE XX

REASONS FOR CHOOSING CHEVROLET

	% Responding		% Responding
Previous Experience with Make	64.7%	Interior Roominess	25.2
Exterior Styling	49.3	Dealer Service	24.9
Future Resale Value	46.9	Dealer Location	24.4
Dependability	37.9	Perf. Engine Response	22.3
Reputation of Car	36.1	Delivery Made When Wanted	20.3
Riding Comfort	35.8	Durability	18.7
Handling Ease	35.4	Overall Operating Economy	18.5
Final Cost - Deal Offered	33.0	Quality of Workmanship	12.8
Interior Styling	28.0	Safety Features	11.7
Wanted Larger Car	25.9	Sales Effort by Salesman	9.7
		GAS ECONOMY	7.8
		All Others	40.2
		Total	629.4

NOTE: Figures total more than 100% because of multiple answers

SOURCE: Automotive Industries, April 1, 1972

It should be pointed out that the SSS-10, as configured herein, is a first-generation engine with considerable potential, not only for growth, but for modifications which could improve the performance of even the initial version. Accordingly, further optimization studies were conducted to investigate the possibility of meeting the 10-mpg goal with both demonstration and production SSS-10 powered automobiles. Several vehicle and engine design options are available to achieve this goal, and these options, together with reasonable assumptions of their magnitude and effect, are detailed in Appendix V and discussed below.

Of the likely vehicle design options, the use of the Tracor transmission (rather than the GE HMT, together with a reduced vehicle test weight achievable with the lightweight SSS-10) and slightly lower aerodynamic and tire resistance values, results in a predicted FDC fuel economy of 8.4 mpg and an overall fuel economy of 11.6 mpg. When these vehicle design options are combined with potential improvements resulting from engine reoptimizations aimed at improving low-speed fuel economy, a value of 10.0 mpg for the FDC may be achievable for a 1974 demonstrator vehicle. Associated with these design options is an improvement in fuel economy on the OAP composite driving cycle to 12.8 mpg, as compared with the predicted value of 9.8 mpg for the base-line vehicle.

For production automobiles in the 1977 to post-1980 time periods, further engine refinements can be foreseen which might raise fuel economy on the FDC to 10.5 to 11 mpg and, on the OAP composite driving cycle, to values exceeding 14 mpg. These values are in the range predicted for the 1974 base-line RGSS-6 and RCSS-8 powered autos* and are considerably better than predictions for future Otto-cycle engines.

In summary, the heat exchanger gas turbines offer superior fuel economy, but it is believed that the SSS-10 demonstration engine offers adequate fuel economy for most owners, especially when measured against the current performance of comparable engines (and potentially superior fuel economy when compared with likely future Otto-cycle engines). Sufficient opportunity exists to substantially improve SSS-10 fuel economy for the demonstration if this is required, while in the future, with anticipated improvements in gas turbine (and transmission) technology, even the simple-cycle gas turbine is likely to exceed current fuel economies, and advanced heat-exchanger gas turbines may even exceed the fuel economy of current automotive diesel engines.

Fuel Availability

Related to fuel economy (which is an owner problem) is the problem of conservation of petroleum resources (which is a national and, ultimately, global problem).

---

* Many of the same improvements could be considered for the heat-exchanger engines also, thereby offering still better fuel economy for these types.

In this connection, not only the mpg on an absolute basis but also the refinery yields must be considered. Future gasolines which have been proposed for Otto-cycle engines (Ref. 25) will not only be more costly to refine, but the process will yield less gasoline per gallon of refinery stock than current gasolines. The heat-exchanger engines are given the highest rating in this respect, the Otto-cycle engine the lowest, while the SSS-10 would rate somewhere in between*.

Size and Weight

The size and weight of the engine is considered to be of prime importance to the vehicle producer. It is obvious that a small, lightweight engine can be utilized in a much larger variety of vehicles than one which must be tailored to each installation. The increased size and weight of the treated Otto-cycle engine is surely a great deterrent to the future flexibility of automobile design. The same is true for the heat-exchanger gas turbines. Conversely, the small size and light weight of the SSS-10 engine makes it adaptable to a wide variety of vehicles from compacts, through intermediates, to standard automobiles. In addition, the smaller size and weight of the gas turbines, and particularly the simple-cycle SSS-10, allows a greater compatability with the devices which are required by new Department of Transportation regulations concerning safety, all of which will certainly add weight to the car.

Further advantages of reduced size and weight relate to the ability of packaging the complete reduced-size propulsion unit in either the front or the rear of the vehicle, as shown in Figs. 41 through 45. Both a front installation with front drive and a rear installation with rear drive permit improved traction, eliminate a long driveline (thus improving interior space flexibility), and permit additional overall savings in the weight and cost of the vehicle.

Reliability and Maintainability

All of the gas turbines studied should be more reliable and more maintainable than the future piston engine, based on the greater simplicity as well as on past experience in numerous gas turbine installations in ground vehicles. This

---

* In the future, as petroleum resources may become scarcer and higher-priced, it is quite likely that vehicle designs may turn to highly efficient forms of motive power, such as fuel cells. This event, however, is considered to be at least several vehicle generations in the future, and is not of particular concern at this time.

predicted reliability extends not only to a no-breakdown situation, but to a good cold-start capability. Furthermore, the simplest form of gas turbine engine is expected to have the highest reliability and maintainability of those studied. Estimates for the repair and maintenance costs of future Otto-cycle engines indicate increases of from 30 to 50% in order to keep the more complicated and less reliable pollution control equipment operating. (As indicated previously, the failure of these devices can result in pollution worse than that emitted by the untreated Otto-cycle engine.)

On the basis of these considerations, the SSS-10 engine is judged to have the best reliability and maintainability potential of all engines considered.

Technological Risk

For the gas turbine engines considered herein, the greatest technological risk lies in the development of the RCSS-8 because of the largely unproven design of its recuperator. The second largest technological risk is assigned to the RGSS-6 because considerable question still exists regarding the lifetime of acceptably priced seals and ceramic disks. On the other hand, the SSS-10 incorporates proven technology in a conservative design in which the major unknowns relate primarily to eventual production cost rather than technological uncertainty. Hence, the SSS-10 is considered to involve the least technological risk of all engines considered.

To place these technological risks in perspective, it should be observed that, although an Otto-cycle engine does not in itself represent any technological risk, building one which can drastically reduce its naturally dirty emissions to acceptable limits involves a considerable technological risk, because there is at present no known acceptable technological procedure to achieve the Federal Standards by 1976 (Ref. 26). In this sense, a large technological risk must be assigned to the Otto-cycle engine.

Development Time and Costs

The development time and costs are governed by the technological risk. Therefore, because of its simplicity and its extrapolation from direct state-of-the-art technology, the SSS-10 is expected to require the shortest development time and probably the lowest development costs. The successful demonstration of the heat-exchanger gas turbines could probably be accomplished at a cost not greater than about 1-1/2 times that of the simple-cycle engine. However, although the estimates on development time and costs for developing pollution-treated Otto-cycle engines are uncertain at this time, they are likely to be considerably higher than those which would be required to successfully demonstrate the SSS-10 engine.

Noise

All engines should be equally capable of low-noise operation. The heat exchanger acts as a noise suppressor and results in a quieter engine for the RCSS-8 and RGSS-6. The SSS-10 is likely to require an exhaust noise silencer. Possible solutions include fixed ceramic cores and fiberglass mufflers, and a cheap and simple installation appears probable.

Exhaust Heat

The SSS-10 will run with hotter exhaust gases, and the localized heat flux at the tailpipe is a problem. Possible solutions include finning of ducts, and dilution with outside air. The exhaust from the regenerated engines, on the other hand, is cooled, and is less likely to be a problem. There is also a similar heat problem associated with the future Otto-cycle engine, since the OC exhaust will be heated and kept warm by the combination of converters and reactors acting in its exhaust system.

Critical Materials

With respect to the requirement for critical materials, the SSS-10 is slightly ahead of the other gas turbine engines under consideration because the critical materials used in the heat exchangers associated with regenerated or recuperated engines are not required in the simple-cycle engine.

Drivability

With an appropriate transmission, the SSS-10 should be as responsive and as capable of engine braking as the best of present engine-transmission combinations. The responsiveness of future Otto-cycle engines may not be up to this standard especially if they are not maintained perfectly, based on observations of current "semi-cleaned-up" engines.

The heat retention characteristics of the heat exchangers used in the RGSS-6 and RCSS-8 will affect the performance felt by the driver somewhat (i.e., degrade the responsiveness); should this prove to be a severe problem, it will require control system sophstications which will add to the cost of these already expensive engines.

Results of Engine Selection Processes

In view of all of these considerations, it is believed that the SSS-10 engine is the most likely to meet the EPA goals because:

1. It has the potential for the lowest emissions of any of the engines considered herein and has a high probability of achieving the Federal Standards.

2. It leads to the lowest predicted automobile price of any of the low-emission engines, particularly including the future Otto-cycle engined vehicle.

3. Its predicted fuel economy is adequate based on conservative estimates, and considerable potential exists for significant improvement over present Otto-cycle engined vehicles.

4. Its simplicity, small size, proven technology, and potential low manufacturing cost lead to high reliability, low technological risk, low development costs, installation flexibility, good drivability, and fewer demands on critical resources.

The heat-exchanger engines are also believed to be far better alternatives for vehicular power plants than the expected future pollution-treated Otto-cycle engine. They have the advantage over the SSS-10 of lower fuel consumption (with the implied lesser demand on petroleum resources), at the expense of greater cost, complexity, and somewhat lesser responsiveness (or greater control complexity) in the single-shaft, fixed-turbine nozzle configuration considered here, and hence may be desirable for commercial applications (taxis, buses, trucks) for which fuel economy is crucial. Therefore, it is believed that development and demonstration of all three of the gas turbine engines considered herein could certainly be justified on the basis of the nation's future needs, since the development costs are likely to be modest in terms of national needs and in terms of expenditures being made currently to modify Otto-cycle engines.

Since it is believed that engines generally similar to the RGSS-6 are being currently developed by at least one automobile company it would seem prudent to additionally develop only the RCSS-8 as an alternative to the SSS-10 engine. Although its development involves a greater technological risk than the SSS-10, a developed RCSS-8 would provide a backup engine which might prove more cost effective if future fuel prices increased more rapidly than the future costs of labor and materials.

DEVELOPMENT PROGRAM

Demonstration Program

A development program has been laid out aimed at a demonstration of the performance and emissions characteristics of an SSS-10 powered automobile. The goal of the program would be to achieve the performance levels of the base-line vehicle as reported herein, including emissions levels below those specified by law for 1976 vehicles. A total of five pre-production prototype engines would be built and installed in three demonstration vehicles, with the demonstration to consist of approximately 100 hours of essentially trouble-free operation with each automobile. It is estimated that thirty months would be required for this program (see Fig. 110).

Functionally, the development program consists of three closely related areas: the engine, the transmission, and the vehicle. From the standpoint of time, the development program is divided into three phases. Phase 1 is 8 months in length and consists primarily of the engine design effort and supporting component tests; Phase 2, 16 months in length, consists primarily of test and development of the engines, up to and including proof test; and Phase 3, 6 months in length, comprises the installation of the engines and transmissions into suitably designed demonstration vehicles, and culminates in the actual vehicle demonstration for a three-month period.

In order to complete the demonstration by the end of 1974, the program must be started by July 1, 1972. Since the program is highly compressed, lower program costs would probably result from a 3 to 6 month stretchout (from the nominal 30-month program, to 33 to 36 months). However, this stretchout may not be permissible because of the urgency of the automotive pollution problem and the possibility that interim emissions treatment to Otto-cycle engines may be either ineffective or involve unacceptable performance or cost penalties.

Engine Development

The engine development encompasses a design and assembly program, an extensive engine test program, a support test program, and a component test program. A detailed design of 8 months comprises the major effort in Phase 1. Coincident with the last five months of the detailed design phase, long-lead-time hardware items which can be clearly defined are procured. This procurement phase extends for four months into Phase 2 for those items which have short lead times and those items which are not completely defined until the end of the detailed design exercise.

The engine test program involves tests in eleven areas; i.e., performance, controls, stress and vibration, lubrication and gearing, bearings, emissions,

L-971249-7

FIG. 110

RECOMMENDED DEVELOPMENT AND DEMONSTRATION PROGRAM

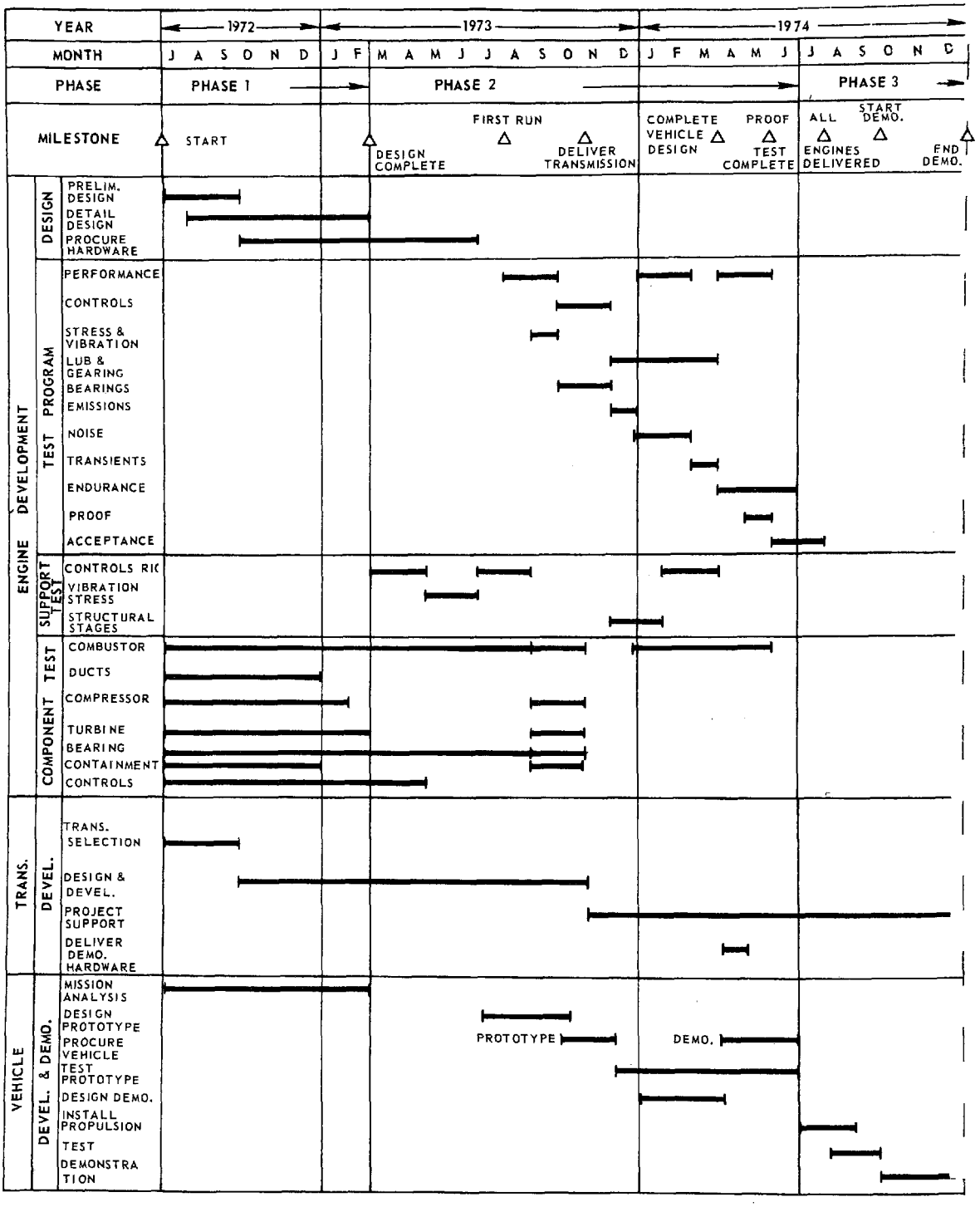

noise, transients, endurance testing, proof testing, and acceptance testing. The first engine run is predicted to occur on the first of August, 1973, thirteen months following start. Two dynamometers and an outdoor test stand are required.

The first engine assembly is tested on the performance test stand using the first dynamometer rig for two months, incurring some 40 hours of engine running. The performance testing continues at two other separated intervals, all on the same dynamometer, for a total of 160 hours of testing. Controls testing takes place on the second dynamometer and occupies 40 test hours. Stress and vibration testing is also accomplished on the second dynamometer and totals 20 hours. The lubrication system and gearing tests are also run on the second dynamometer and total 150 hours. Bearings and air system tests are run on the first dynamometer and total 50 hours. Emissions tests are run on the first dynamometer and total 20 hours. Noise tests are accomplished on an outside noise rig constructed for the purpose of the program and total some 30 hours. Transient performance is run on a test vehicle and requires 20 hours. Endurance testing is also accomplished with a test vehicle and totals 100 hours. Proof testing is accomplished on either available dynamometer and totals 70 hours. Finally, acceptance tests for the engines for the demonstrator vehicle are run on any available dynamometer and total 40 hours. The total number of engine hours projected during the development phase of the program is 700.

Transmission Development

The transmission development program should be conducted in parallel with Phases 1 and 2 of the engine development program. The transmission development program must be preceded by a transmission selection program. Its outcome will be to select optimum transmissions for use with the SSS-10 engine. The design and development of at least two transmissions should be pursued. This duplication is required since the engine and vehicle performance depends significantly on the type of transmission used, and it is advisable not to make the success of the demonstration dependent upon only one transmission. At least two transmissions should be delivered for testing in the prototype vehicle. This delivery would occur on the first of November, 1973. (If during the prototype testing part of the engine test program one transmission proves to have outstanding characteristics, it will be selected for delivery during the actual demonstration, and a second transmission will not be required.)

Vehicle Development and Demonstration

The vehicle development program is involved in the first two phases of the development and demonstration program, and the vehicle demonstration culminates Phase 3 of the effort.

The first requirement is a mission analysis program in support of the engine design effort; it will investigate various duty cycles for the vehicle, and will

serve to specify the engine and transmission characteristics in such a fashion as to insure the optimum combination of design parameters.

The prototype vehicle will be designed and procured in the vehicle development and demonstration program, and will be tested in the engine test program. The vehicles will be "off-the-shelf" vehicles, so that the design and modification discussed herein pertains only to the modification required to make it suitable for accepting and demonstrating the SSS-10.

The delivered propulsion systems will be installed in these vehicles and two months are provided for internal testing prior to delivery to the designated EPA facility for actual demonstration purposes. The demonstration is shown in the program as consisting of three months, during which time 100 hours of demonstration will be accomplished on each of the three vehicles provided. It is anticipated that the demonstration will include emissions testing, performance testing, fuel mileage testing, maintenance testing, and various other demonstrations as prescribed by EPA.

Future Production

The normal procedure for the introduction of new concepts for automobiles is that, following successful completion of a demonstration of the type described above, field experience is gained. On the basis of this experience, a production prototype is designed and tested prior to the initiation of limited production (< 100,000 units annually). Thus, from hardware program start to full mass production of over 80% of a given vehicle population, the introduction of a new product might cover a minimum of 10 years. Within this period, 3 to 4 years would be devoted to the design and demonstration of the concept (similar to the program described above), 2 to 3 years for design and development of the production prototype, an additional 3 to 4 years for fleet testing, and production planning, and 2 to 4 years (and sometimes up to 10 years depending on demand) for production build-up. On the basis of this approach, the SSS-10 could not be expected to reach large-scale production until after 1980. However, the normal product phase-in considerations, which are largely governed by economics, are superseded in this case by the urgent requirement for engines with low emissions.

A comprehensive study is required to establish what is possible in terms of placing a simple engine such as the SSS-10 into production on a crash basis. It is believed that an integrated program closely developed in concert with a vehicle manufacturer could result in limited production (100,000 vehicles or less per year) at a relatively early date, i.e., within 2 or 3 years of a successful demonstration (1977-78), and possibly sooner (at still greater cost and risk). The major requirements which are not met by the above recommended demonstration program which would be required for this limited production include extensive fleet

testing of vehicles, subsequent redesign of the engine for production, and the design, manufacture, and assembly of the required production line.

Since the general configuration and the general manufacturing requirements of the designated engine are expected to be known fairly early in the program, considerable progress can be made toward integrating the manufacturing facility with the development program. Production machinery can be generally specified and, in many cases, procured long before the exact final form of the required production tooling is known (i.e., the size and location of drills, the exact program for numerically controlled machine, the exact dies, molds, etc., for castings and forgings).

It is obvious that this concurrent development procedure would involve some waste; nevertheless, the proposed limited production in 1977 is consistent with the reported progress which has been made toward the production of Wankel engines. The additional effort required would be well within the capabilities of the present automobile companies, and a ready market could be expected to exist for the SSS-10 vehicle even if its initial production costs were higher than those estimated in this report.

On the other hand, it does not appear practical to envision the entire changeover of an industry to this type of engine in any calendar year close to 1975. Extensive owner and consumer testing such as might be derived from limited production runs should certainly be required before a massive changeover of the present industry takes place. If it is assumed that the engine does go into limited production in 1977, several years of extensive consumer operation of these production cars is desirable, and it is difficult to imagine that a complete industry changeover could occur prior to 1980 without unprecedented effort. Nevertheless, an extraordinary effort might be justified on the basis of national impact, and the general requirements for implementation, i.e., placing the engine into high-volume production, should be the subject of additional study.

Costs

A costing effort was not conducted for the development program outlined here. The costs would depend on the basic objectives of the program and other factors, and would require far more extensive analysis than that permitted by the scope of this contract. Nevertheless, it is possible to make a rough estimate for comparison with costs which are currently being incurred in the search for a low-emission vehicle.

It is quite probable that the entire recommended development and demonstration program discussed above and shown in Fig. 110 (excluding that required to prepare for limited production) could be accomplished for less than $10 million. This cost would include the procurement and development of five engine sets and three complete demonstrator vehicles, including the running of the demonstration

for 300 vehicle-hours. It would also include transmission and control costs, although any estimates for transmission development are necessarily speculative at this time because of lack of definition of the optimum transmission(s).

REFERENCES

1. Wright, E. S., L. E. Greenwald, and W. R. Davison: Manufacturing Cost Study of Selected Gas Turbine Automobile Engine Concepts. UARL Report K-911017-4. August 1971.

2. Kenny, D. P.: A Novel Low-Cost Diffuser for High-Performance Centrifugal Compressors. Journal of Engineering for Power. January 1969.

3. Groh, F. G., G. M. Wood, R. S. Kulp, and D. P. Kenny: Evaluation of a High Hub/Tip Ratio Centrifugal Compressor. ASME Paper No. 69-WA/FE-28.

4. Kenny, D. P.: Supersonic Radial Diffusers. Lecture Series No. 39 on Advanced Compressors. AGARD-LS-39-70.

5. Morris, R. E., and D. P. Kenny: High Pressure Ratio Centrifugal Compressors for Small Gas Turbines. Prepared for the 31st Meeting of the Propulsion and Energetics Panel of AGARD, "Helicopter Propulsion Systems," June 10-14, 1968, Ottawa.

6. Morris, R. W.: High Pressure Ratio Radial Compressors and Turbines. Diesel and Gas Turbine Progress, December 1970.

7. Okapuu, U., and G. S. Calvert: An Experimental Cooled Radial Turbine. High Temperature Turbines, AGARD Conference Proceedings No. 73 (preprint), September 21-25, 1970.

8. Okapuu, U., and G. S. Calvert: Cooled Radial Turbine for High Power-to-Weight Applications. AIAA Paper No. 69-524.

9. Langton, R. L., and R. E. V. Westerhout: Aerodynamic Testing and Instrumentation of Components for Small Gas Turbines. SAE 670941.

10. Slabiak, Walter: An A-C Individual Wheel Drive System for Land Vehicles. SAE Transactions, Paper No. 660134. 1967.

11. Sedlock, Edward: Advanced Electrical Machinery and Component Development. P&WA Report 66-972.

REFERENCES (cont'd)

12. Kress, James, H.: Hydrostatic Power-Splitting Transmissions for Wheeled Vehicles. SAE Transactions, 1968, Paper No. 680549.

13. McLean, A. F.: Case for the Single-Shaft Vehicular Gas Turbine Engine. IME Symposium, Warwick, England April 9, 1969.

14. Yeaple, F.: Metal-to-Metal Traction Drives. Product Engineering, Oct. 1971.

15. Cope, E. M., and C. L. Gauthier: Cost of Operating an Automobile. U.S. Department of Transportation Report, February 1970.

16. Anon.: 1969 Automobile Facts and Figures. Automobile Manufacturers Association, 1969.

17. Anon.: Vehicle Design Goals - Six Passenger Automobile. Office of Air Programs Division of Advanced Automotive Power Systems Development, Revision C, May 28, 1971.

18. Corenlius, W. and W. R. Wade: The Formation and Control of Nitric Oxide in a Regenerative Gas Turbine Burner, SAE.

19. Bujac, J. N. Jr., and R. Mantler: Impact of National Environmental Policy Act of 1969 on the Advanced Technology Turbine Engine. Proceedings of the National Conference on Environmental Effects on Aircraft and Propulsion Systems, May 10, 1971.

20. Katona, G.: 1969 Survey of Consumer Finances, U Michigan.

21. Anon.: NADA Official Used Car Guide. National Automobile Dealers Used Car Guide Company, Eastern Edition, November 1971.

22. Brehab, W. M.: Mechanisms of Pollutant Formation and Control from Automotive Sources. Presented at Nineteenth Annual Lecture Series, Milwaukee Section, Society of Automotive Engineers, March 5, 1971.

23. Hoffman, G. A.: Hybrid Power Systems for Vehicles. Symposium on Power Systems for Electric Vehicles, U.S. Department of Health, Education, and Welfare. National Center for Air Pollution Control, 1967.

REFERENCES (cont'd)

24. Best, G. C., and E. E. Flanigan: Allison GT-404-The VIP Engine-Versatile Industrial Power. ASME 72-6T-93, San Fransisco, March 26-30, 1972.

25. Oil & Gas Journal, Editorial Vol. 70, No. 3, January 17, 1972, p. 45.

26. Anon.: Semi-Annual Report by the Committee on Motor Vehicle Emissions of the National Academy of Sciences to the Environmental Protection Agency Washington, D. C., January 1, 1972.

27. Winfrey, R.: Economic Analysis for Highways. International Textbook Company, 1969.

28. Anon.: Automobile Insurance and Tax Data Extracted from a 14-State Study by National Automobile Association. United Services Automobile Association, December 1971.

29. Anon.: 1968 Owner's Manual, Ford Motor Company, 1967.

30. Anon.: Flat Rate Manual 1971. The Irving-Cloud Publishing Company, 1971.

31. Anon.: Automotive Parts and Accessories Catalogue No. 295. J. C. Whitney and Company, 1971.

32. Claffey, Paul J.: Running Costs of Motor Vehicles as Affected by Road Design and Traffic. Paul J. Claffey and Associates, National Cooperative Highway Research Program. Report No. 111, Highway Research Board, 1971.

33. Guedet, R. H. and J. E. Louis: Dual Mode Hydromechanical Transmission as Applied to Gas Turbines. ASME 69-6T-13 Cleveland, March 9-13, 1969.

APPENDIX I

VEHICLE DYNAMICS WITH THE GE HYDROMECHANICAL TRANSMISSION

Two computer programs were written to estimate vehicle performance using the GE hydromechanical transmission (HMT). One program performs full-power acceleration calculations based on the OAP vehicle performance specifications given in Ref. 17, and the other program computes fuel economy and emissions for the Federal Driving Cycle (FDC) as well as for simplified country and suburban driving.

The basic assumptions used in the development of these programs are as follows:

- Level road
- No wind
- Air density is related to ambient temperature by the perfect gas law
- Steady-state engine torque curves apply during engine and vehicle acceleration
- OAP resistance equations apply

The physical constants used in this study are given in Table IX.

The apparent increase in rotational inertia of a rotating mass due to speed reduction is fundamental to the engine dynamics given in Appendices I and II, and a brief digression to discuss its derivation is appropriate here. Consider the rotating mass, connected to a torque source by means of an ideal reduction gear system (no mass, no losses), shown in the sketch below.

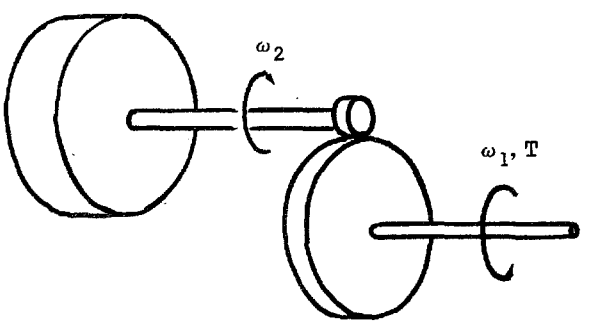

Let I = rotational inertia

T = applied torque

R = ω_2/ω_2

ω_1 = speed of shaft through which torque is applied

ω_2 = speed of rotating mass

in some consistent set of units.

From dynamics, the applied power is equal to the time rate of change of kinetic energy, or

$$T\omega_1 = \frac{d}{dt}\left(\tfrac{1}{2} I \omega_1^2\right)$$

$$= I \omega_1 \dot{\omega}_1 \quad . \tag{I-1}$$

Now

$$\omega_2 = R\omega_1 \quad , \tag{I-2}$$

and putting Eq. (I-2) into Eq. (I-1) and rearranging, one has,

$$\dot{\omega}_1 = T/R^2 I \quad , \tag{I-3}$$

which is the rotational form of Newton's Second Law, referred to the torqued shaft. The inertia of the rotating mass as seen from the torqued shaft appears to be increased by the factor R^2.

Viewed another way, a change in speed of the torqued shaft from ω_{1_i} to ω_{1_f}, where the subscripts i and f denote initial and final stages, respectively,

corresponds to a change in kinetic energy of the rotating mass of $\frac{1}{2} I(\omega_{2_f}^2 - \omega_{2_i}^2)$ or $\frac{1}{2} R^2 I(\omega_{1_f}^2 - \omega_{2_f}^2)$. The factor R^2 appears again when the energy change is expressed in terms of a speed different from the speed of the rotating mass.

As described in the main text, the GE-HMT responds to an increase in throttle setting by "unloading" the engine to allow its speed to come up to the controlled speed as determined by the throttle setting and the engine operating line. The rate of engine acceleration following an increase in throttle setting is determined by the transmission response time. Because the response time of the HMT is relatively short (fractions of a second), it would be possible, say, to be driving at some steady speed, depress the accelerator pedal, and have the vehicle slow down as the transmission "downshifts" to allow the kinetic energy of the vehicle to help bring the engine to its controlled speed. After the engine attained controlled speed, the vehicle would then accelerate at constant engine speed. The deceleration, of course, is undesirable, and in practice the transmission would be controlled in such a way as to permit a smooth flow of power to the wheels while at the same time bringing the engine to its controlled speed. The effect of this HMT response to a change in throttle setting has been included in the acceleration dynamics by means of a hypothetical "torque-split" which is described further on.

For this analysis, the engine is assumed to be a torque source, with no rotational inertia, connected in series with a rotational inertia equal in resistance to the sum of the engine and the transmission inertias. The GE-supplied curve of transmission inertia versus ratio (output speed ÷ input speed), shown in Fig. 73, was used for this analysis. It should be noted that, in order for the engine and transmission inertias to be added, the inertia values must be referenced to the same rotational speed. Thus, if transmission input speed is used as a reference, the engine inertia referred to the gas generator shaft must be multiplied by the square of the total engine reduction gear ratio (gas generator speed ÷ output shaft speed) before being added to the transmission inertia.

The sketch below will be used to derive the equations of motion for an HMT vehicle.

Equations of Motion - Full-Power Acceleration

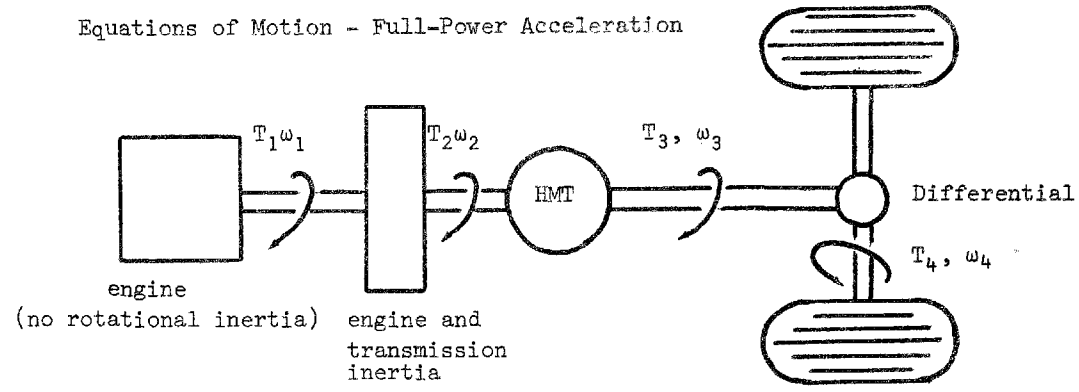

A free-body diagram of the lumped engine and transmission inertias yields the equation of motion for the engine:

$$\omega_2 = \frac{30}{\pi} \frac{T_1 - T_2}{I} \quad , \tag{I-4}$$

where I = combined engine and transmission inertia (slug-ft^2), referred to the engine output speed

T_1 = engine output torque, minus accessory load (generator, etc.) (lb-ft)

T_2 = resisting torque of transmission as seen by the engine (lb-ft)

$\dot{\omega}_2$ = engine acceleration (rpm/sec)

The engine output shaft speed (ω_1) is equal to the transmission input shaft speed, by definition. The transmission input torque (T_2) is related to ω_1 and T_1 by means of the hypothetical torque-split described by the equation below.

$$T_2 = T_1 \left(\frac{\omega_1 - \omega_{idle}}{\omega_{max} - \omega_{idle}} \right)^n \quad , \tag{I-5}$$

where ω_{idle} = engine idle speed (rpm)

ω_{max} = maximum engine speed (rpm)

η = dimensionless torque-split exponent

The purpose of the function described by Eq. (I-5) is to simulate the effect of the transmission response to full-throttle acceleration. For a fixed value of η, the resisting torque of the transmission (T_2) will be an increasing function of engine speed such that, initially, when the engine is at idle, all of the engine torque (T_1) is available to accelerate the engine. As engine speed increases, the fraction of the total engine torque available to accelerate the engine decreases (although the difference T_1-T_2, which causes the acceleration of the engine, may increase) until the engine reaches maximum speed and all of its torque goes into accelerating the vehicle. Increasing the value of η will increase the initial engine acceleration at the expense of vehicle acceleration. Thus, a high value of η will allow the engine to reach its maximum speed sooner than a relatively lower value. Viewed another way, the engine will be at its maximum speed at a lower vehicle speed for the greater value of η.

It is emphasized that the torque split of Eq. (I-5) is merely a device to simulate the effect of transmission response. However, the technique was believed to be satisfactory, by GE personnel, for estimating vehicle performance (Ref. 3).

At any instant the transmission output shaft speed may be computed from Eq. (I-6) assuming no wheel slippage:

$$\omega_3 = \frac{30}{\pi} \frac{R_a}{r_\omega} \, v \quad , \tag{I-6}$$

where r_ω = driving wheel radius (ft)

R_a = rear-axle ratio

v = vehicle speed (fps)

ω_3 = transmission output shaft speed (rpm)

Application of the definition of transmission efficiency, Eq. (I-7), yields an expression for the transmission output torque, (Eq. (I-8).

$$\eta_t = \frac{\text{power out}}{\text{power in}} = \frac{T_3\omega_3}{T_2\omega_2} \tag{I-7}$$

Thus

$$T_3 = \eta_t T_2 \left(\frac{\omega_2}{\omega_3}\right) \quad , \tag{I-8}$$

where T_3 = transmission output torque (lb-ft)

η_t = transmission efficiency.

The transmission efficiency is found as a function of input power and output speed from Fig. 23. The torque applied to the wheels can be found by an application of the definition of rear axle efficiency:

$$T_4 = \eta_a T_3 \left(\frac{\omega_3}{\omega_4}\right) \tag{I-9}$$

where T_4 = rear-axle torque (lb-ft)

η_a = rear-axle efficiency

ω_4 = rear-axle speed (rpm)

The aerodynamic and rolling resistance forces are given by Eqs. (I-10) and (I-11), respectively, and the vehicle acceleration is given by Eq. (I-12).

$$F_{aero} = \tfrac{1}{2}\rho C_D A v^2 \tag{I-10}$$

$$F_{roll} = W\left(r_o + r_1 v + r_2 v^2\right) \tag{I-11}$$

$$a = \frac{g}{W'}\left(\frac{T_4}{r_w} - F_{aero} - F_{roll}\right) \tag{I-12}$$

where a = vehicle acceleration (ft/sec^2)

A = vehicle frontal area (ft^2)

C_D = aerodynamic drag coefficient

F_{aero} = aerodynamic resistance force (lb)

F_{roll} = rolling resistance force (lb)

g = acceleration of gravity (ft/sec^2)

r_0, r_1, r_2 = rolling resistance coefficients (units of lb and fps)

r_w = radius of driving wheel (ft)

W = vehicle weight (lb)

W' = apparent vehicle inertial weight (lb)

ρ = ambient air density ($slug/ft^3$)

The apparent inertial weight W' is equal to the gravitational weight plus the equivalent weight of rotating masses such as the wheels, axles, etc.

Equations (I-4) and (I-12) may be integrated to derive the full-power acceleration history of the vehicle.

Equations of Motion - Driving Cycle Computations

The problem of computing vehicle performance for a driving cycle is somewhat different than for a full-power acceleration. For a given driving cycle, the transmission output, rather than input, conditions are known at discrete and specified intervals of time, and there are in general no differential equations of motion to integrate. Rather, quantities such as fuel consumed and emissions produced are calculated for each point, summed over all points of the driving cycle, and then averaged as needed, in the computation of fuel economy in miles per gallon.

Let a and v be the acceleration and speed, respectively, of a vehicle at some point in a driving cycle. Then a rearrangement of Eq. (I-12) allows solution for the required torque (T_4) at the driving wheels.

$$T_4 = r_w \left(\frac{W'a}{g} + F_{aero} + F_{roll} \right) \qquad \text{(I-13)}$$

The transmission output speed (ω_3) can be obtained from Eq. (I-6) and the transmission output torque (T_3) can be solved for from Eq. (I-9):

$$T_3 = \frac{T_4}{\eta_a} \frac{\omega_4}{\omega_3} \qquad \text{(I-14)}$$

Now, knowing the transmission output torque and speed, it is necessary to find the input torque and speed in order to determine the engine operating point (torque and speed).

Since the transmission efficiency map (Fig. 23) is expressed in terms of input power and output speed, it is necessary to implement a trial-and-error procedure to find the transmission input conditions. A separate subroutine was devised to perform this function for the HMT. In essence, the computational procedure of the subroutine finds, by a trial-and-error algorithm, a transmission input power which satisfies both the efficiency map of Fig. 23 and the definition of overall transmission efficiency, Eq. (I-7). Now the engine operating speed must be found, since at this point only the transmission input power, but not the particular combination of torque and speed (T_2 and ω_2, respectively), is known. This is accomplished by referring to the operating line of the engine, expressed as a function of power and speed. Then, with the transmission input power and speed known, the input torque is obtained from the definition of power.

Finally, the engine output torque is calculated as the sum of the transmission input torque, the accessory-load torque, and the torque required to accelerate the engine to its next operating point in the driving cycle. The engine acceleration torque can be estimated by performing the above computations for the next interval or point on the driving cycle to determine the engine operating speed. Then the average engine acceleration torque during the present interval is assumed to be the torque required to accelerate the engine from its present speed to the speed at the next point at a uniform rate. This is expressed

mathematically by Eq. (I-15).

$$T_{accel} = \frac{\pi}{30} I\left(\frac{\omega_{next}-\omega_{now}}{\Delta t}\right) , \qquad \text{(I-15)}$$

where T_{accel} = average engine acceleration torque (lb-ft)

Δt = time interval between the present and next driving cycle intervals (sec)

ω_{next} = engine speed for the next point on the driving cycle (rpm)

ω_{now} = present engine speed (rpm)

The term of Eq. (I-15) in parentheses is the assumed average engine acceleration (rpm/sec) during the present interval.

APPENDIX II

VEHICLE DYNAMICS WITH THE BORG-WARNER AUTOMATIC TRANSMISSION

The basic assumptions and physical constants used in the Borg-Warner transmission vehicle derivations are given in Appendix I and Table IX. Additional assumptions applying to the multispeed transmission analysis are as follows:

- Maximum acceleration only
- Engine and clutch inertias are lumped together
- Gearbox efficiency is constant
- Inertias and losses in the gearbox (including internal clutches and bands) are neglected as such, but are assumed to be included with the lumped, constant gearbox efficiency.
- Upshifts occur only at maximum engine speed
- Clutch has inertia valve mechanism to limit engine deceleration on upshifts
- Coefficient of friction between clutch surfaces is uniform and constant
- Clutch output shaft speed drops instantaneously at each upshift.

For the purposes of this analysis, the vehicle acceleration dynamics have been divided into three sections which correspond to three different regimes of clutch operation (for maximum acceleration). The clutch pressure plate (or engine) speed is referred to as the clutch input speed and the clutch disc (or gearbox input) speed is referred to as the clutch output speed. The clutch performance map of Fig. 111 will be useful for understanding the ensuing discussion. The three modes of clutch operation are as follows:

Regime 1 - Engine acceleration. Clutch input speed is greater than clutch output speed and the engine is accelerating under the torque difference between the maximum available engine torque and the torque transmitted by the clutch for a given engine speed (see Fig. 74). The clutch input and output speeds

CLUTCH PERFORMANCE MAP

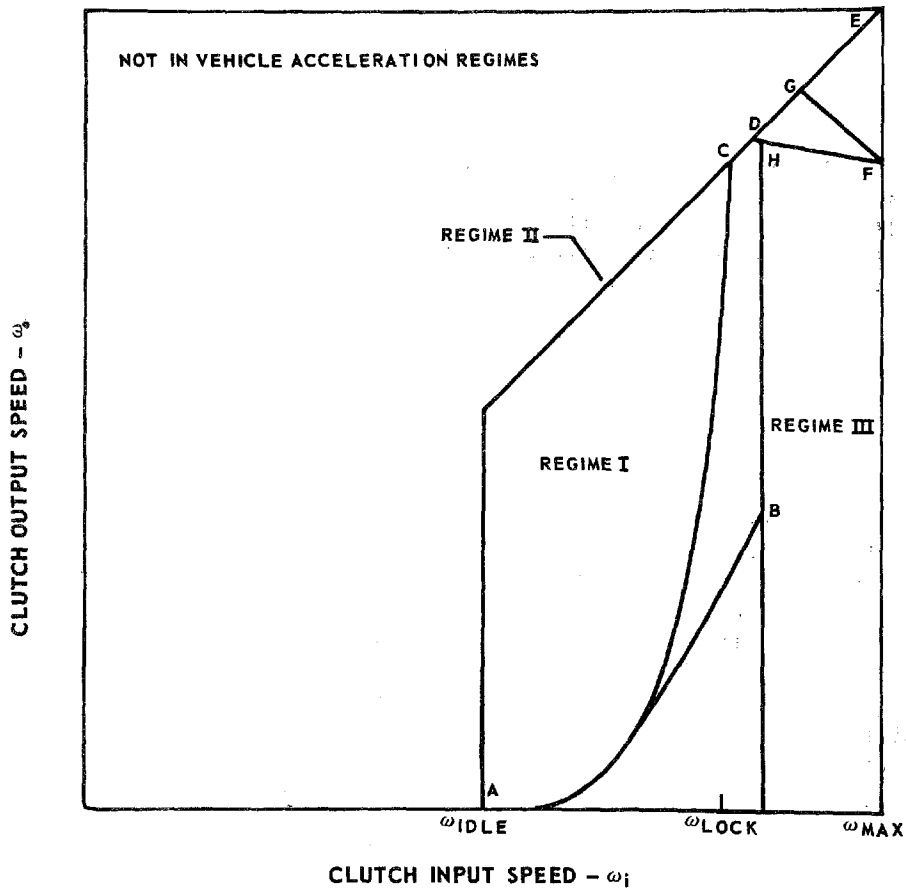

(ω_i and ω_0, respectively) are defined for Regime 1 by the relations below. The subscripts "idle" and "lock" refer to the engine idle and clutch lockup speeds, respectively.

$$\omega_{idle} \leq \omega_i \leq \omega_{lock} \tag{II-1}$$

$$0 \leq \omega_0 < \omega_i \tag{II-2}$$

Regime 2 - Engine acceleration. The clutch is locked and clutch input and output speeds are the same. The clutch speeds for this regime are defined by Eq. (II-3). The subscript "max" refers to maximum engine speed.

$$\omega_i = \omega_0 \leq \omega_{max} \tag{II-3}$$

Regime 3 - Engine deceleration. This regime occurs immediately after an upshift when the clutch output shaft speed drops following the gear change. Clutch input speed is greater than clutch output speed and the engine is decelerating at a constant rate under the bypass action of the inertia valve. The clutch speeds for Regime 3 are defined by the equations below.

$$\omega_{lock} < \omega_i \leq \omega_{max} \tag{II-4}$$

$$\omega_0 < \omega_i \tag{II-5}$$

The equations of motion are different for each clutch performance regime, and are derived separately. Before proceeding with the derivations it should be noted that because of the action-reaction principle, the clutch output torque is equal to the input torque, regardless of the input and output speeds. Because of this, and the definition of clutch efficiency, the clutch efficiency is numerically equal to the clutch slip ratio (output speed ÷ input speed). The engine is assumed to be a torque source with no rotational inertia, connected in series with a rotational inertia equal in resistance to the sum of the engine and clutch inertias. As in the case of the GE-HMT, the engine inertia is referenced to the engine output (clutch input) speed.

The sketch below will be used to derive the equations of motion. For generality, the number of speeds in the transmission was considered variable rather than fixed (8-speed).

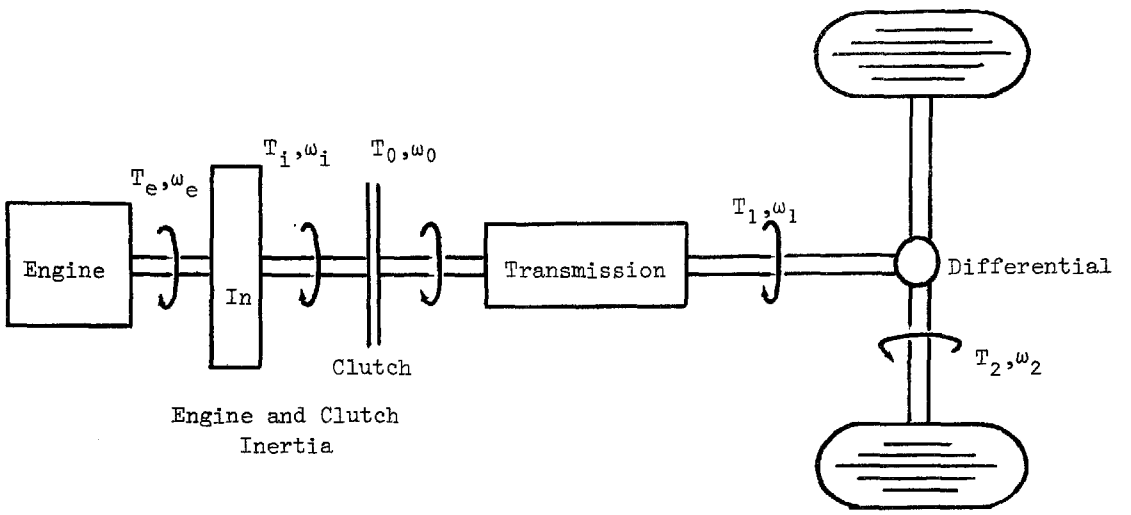

Regime 1

A free-body diagram of the combined engine and clutch inertias yields the following equation for the engine acceleration

$$\dot{\omega}_e = \left(\frac{30}{\pi}\right) \frac{T_e - T_i}{I} \quad , \qquad \text{(II-6)}$$

where I = combined engine and clutch inertias (slug-ft^2)

T_e = engine output torque (lb-ft)

T_i = torque transmitted by clutch (lb-ft) - see Fig. 74

$\dot{\omega}_e$ = engine acceleration (rpm/sec)

Because of the action-reaction principle, T_o (clutch output torque) is equal to T_i

(clutch input torque), and ω_i (clutch input speed) is equal to ω_e (engine speed) by definition.

The transmission output speed and torque are given by Eqs. (II-7) and (II-8), respectively. Equation (II-8) was obtained from the definition of transmission efficiency.

$$\omega_1 = \omega_0/R_n \tag{II-7}$$

$$T_1 = \eta_t T_o R_n \quad , \tag{II-8}$$

where $R_n = \omega_0/\omega_i$ = transmission gear reduction ratio for the n^{th} gear

T_1 = transmission output torque (lb-ft)

η_t = transmission gearbox efficiency

ω_1 = transmission output speed (rpm)

In a similar fashion, the rear-axle speed and torque are given by Eqs. (II-9) and (II-10), respectively.

$$\omega_2 = \omega_1/R_a \tag{II-9}$$

$$T_2 = \eta_a T_1 R_a \quad , \tag{II-10}$$

where $R_a = \omega_1/\omega_2$ = rear-axle gear reduction ratio

T_2 = rear-axle torque (lb-ft)

η_a = rear-axle effiency

ω_2 = rear-axle speed (rpm)

For compactness, let F_{res} (lb) be the sum of the aerodynamic and rolling resistance which are given in Eqs. (I-10) and (I-11) in Appendix I. Then the vehicle acceleration is given by Eq. (II-11).

$$a = \frac{g}{W'}\left(\frac{T_2}{r_w} - F_{res}\right) \quad , \tag{II-11}$$

where a = vehicle acceleration (ft/sec^2)

g = acceleration of gravity (ft/sec^2)

W' = equivalent inertial weight of vehicle (lb)

Equations (II-6) and (II-11) may be integrated to yield the full-power acceleration history of the vehicle during Regime 1 clutch operation. This mode of acceleration ends when the clutch output speed becomes equal to the clutch input (engine) speed. The clutch output speed (ω_o) can be determined as a function of the vehicle speed by applying the kinematical expression for the rotational speed of a wheel which is rolling without slipping, and then combining with Eqs. (II-7) and (II-9). The result of these manipulations is given by Eq. (II-12).

$$\omega_o = R_a R_n \frac{30}{\pi} \frac{V}{r_w} \tag{II-12}$$

Regime 2

The equations of motion derived for Regime 1 also apply to Regime 2, but since the clutch is locked ($\omega_o = \omega_i$), the engine and vehicle equations of motion can be combined. One may begin by taking Eq. (II-11) for the vehicle acceleration and using Eqs. (II-8) and (II-10) to express T_2 in terms of the clutch torque, T_i (which is equal to T_o). The result is Eq. (II-13).

$$a = \frac{g}{W'} \left(\frac{\eta_a \eta_t R_a R_n T_i}{r_w} - F_{res} \right) \tag{II-13}$$

In Eq. (II-6) the engine acceleration may be expressed in terms of the vehicle acceleration by noting that ω_e equals ω_o (because the clutch is locked), differentiating Eq. (II-12), and substituting the result into Eq. (II-6). The result is Eq. (II-14).

$$a = \frac{r_w}{R_a R_n} \left(\frac{T_e - T_i}{I} \right) \tag{II-14}$$

Finally, eliminating T_i between Eqs. (II-13) and (II-14), and rearranging, yields Eq. (II-15) which expresses vehicle acceleration directly in terms of engine torque.

$$a = \frac{\frac{\eta_a \eta_t R_a R_n T_e}{r_w} - F_{res}}{\frac{W'}{g} + \eta_a \eta_t \left(\frac{R_a R_t}{r_w}\right)^2 I} \qquad \text{(II-15)}$$

Equation (II-15) is identical to Eq. (II-11) except for extra terms in the denominator which may be considered as augmenting the inertial mass of the vehicle. The additional term is due to the effect of the kinetic energy that must be supplied to the engine inertia as the vehicle accelerates. This term can add 50% or more to the effective mass of a gas turbine vehicle in first gear because of the gear reductions involved.

Equation (II-15) may be integrated to yield the acceleration history of the vehicle while the clutch is locked. The engine speed is related to the vehicle speed in this regime by Eq. (II-12). Equation (II-15) is valid until the engine attains maximum speed at which point an upshift is assumed to occur.

Regime 3

The equations of motion for the vehicle during Regime 3 acceleration are the same as those for Regime 1 except that the engine is now decelerating (after the upshift) at a constant rate due to the effect of the inertia valve. Assuming a constant rate of engine deceleration, Eq. (II-6) may be rewritten to solve for the clutch input torque.

$$T_i = T_e + \frac{\pi}{30} I \alpha \quad , \qquad \text{(II-16)}$$

where α = engine deceleration (rpm/sec).

The effect of the engine deceleration is to cause an apparent increase in the amount of torque available from the engine. The additional torque, of course, arises from the kinetic energy surrendered by the rotating engine as it decelerates. Equations (II-7) through (II-11) apply to Regime 3, and Eq. (II-11) may be integrated to yield the acceleration history during Regime 3 clutch operation.

Sequence of Clutch Operation

For the dynamic model of the controlled slipping clutch used in this report, the following describes the sequences of clutch operation which occur during a full-power acceleration. It is assumed the vehicle is initially at rest with the transmission in first gear, and the engine at idle. Time begins when the acceleration pedal is (instantaneously) floored. The clutch performance map of Fig. 111 will be used to illustrate the discussion.

When the acceleration is begun, the state of the clutch is represented by point A on Fig. 111. Here, the engine is at idle and the output shaft of the clutch is stalled because the vehicle has not yet begun to move. The subsequent motion of the vehicle can now describe various types of trajectories on the clutch performance map depending on the choice of vehicle parameters, particularly the effective engine inertia. For a vehicle with a relatively small engine inertia, the engine will quickly accelerate to clutch lockup speed (ω_{lock}) and then remain constant while the vehicle speed increases to bring the clutch output speed to ω_{lock}. This mode of acceleration is described by trajectory ABHD on Fig. 111. During the portion of the curve BHD, the engine speed is constant and the vehicle accelerates under constant torque. When the clutch output shaft reaches ω_{lock} (point D), the clutch locks up (because clutch torque becomes equal to engine torque at this point) and the remainder of the first gear acceleration is in Regime 2 along line DGE.

For large engine inertias, the vehicle (and hence clutch output shaft) may accelerate more rapidly in comparison with the engine, and the output shaft speed of the clutch may increase to match the input speed before ω_{lock} (curve AC), and the clutch will be locked for the duration of first gear (line CDGE).

At point E an upshift occurs and the output shaft speed drops to point F. This commences Regime 3 operation and the engine begins to decelerate at a constant rate while the vehicle continues to accelerate. If the engine deceleration is rapid enough, the engine will reach ω_{lock} before the clutch output and input speeds have matched, and the clutch will then hold the engine speed at ω_{lock} until the output shaft catches up with it (Regime 1). The remainder of the acceleration in this gear will then be in Regime 2 until the engine reaches maximum speed (path FHDGE).

If the engine deceleration rate is low, the output shaft speed of the engine will increase to meet the engine speed, and lockup will occur (path FGE). At point E, the next upshift occurs and the process repeats. Successive upshifts do not in general follow the same trajectories because vehicle acceleration varies with speed.

It should be noted that the preceding description of the clutch and gearbox operation was derived from the dynamics of the idealized mathematical models used in this study. The dynamics of an actual vehicle may be somewhat different due to the various internal transmission losses and inertias which were neglected in this analysis. These factors would tend to soften the sharply defined rates of change indicated by the model; for example, instantaneous clutch lockup. Despite these qualifications, the net acceleration predictions are believed to be accurate.

APPENDIX III

COMPUTER PROGRAM DESCRIPTION

This appendix describes the three vehicle performance computer programs which were written for this study. Program users' instructions, including listings of all programs and subroutines, are included in a separate volume (L-971249-8). The vehicle dynamics on which the three programs are based are described in Appendices I and II.

Vehicle Acceleration Program - Hydromechanical Transmission

This program was written to predict the acceleration performance and top speed of a vehicle equipped with the GE-HMT transmission. The program output consists of a time history of the vehicle's acceleration, including parameters such as speed, elapsed distance, engine speed and power, and transmission efficiency. For each case (a particular vehicle), the program calculates the acceleration history of the vehicle from a standstill to top speed. While this is occurring, the program monitors the vehicle's performance and performs interpolations to derive the acceleration data for the OAP performance goals, such as 0-60 mph acceleration time, etc. At the end of each case, the program prints a summary of the OAP acceleration performance. A print option permits suppression of the acceleration history printout so that only the heading, which consists of a summary of the engine and vehicle data, and the OAP acceleration results are printed. A sample printout, with the acceleration history suppressed, is shown in Table XXIa.

The program utilizes a variable step size (in time) for integrating the vehicle's motion. The calculations are set up so that below 15 mph the step size is 0.1 sec, because of high engine acceleration rates. Above 15 mph, the step size is calculated such that the vehicle speed change between intervals is 1.0 mph. In addition, the intervals are calculated so that the vehicle speeds appear as integer values on the printout. Above 80 mph, a step size of 2.0 sec is used. The program is fairly rapid, with an average execution time (on a UNIVAC 1108) of about 4 sec for each case.

The OAP performance goals state that acceleration times are measured from the instant when the accelerator is depressed. Thus the acceleration history, with the vehicle initially at a standstill, is initiated with the engine at idle, and the program computes the subsequent build-up of engine and vehicle speeds.

TABLE XXIa

SAMPLE COMPUTER PRINTOUT

* * * UARL VEHICLE PERFORMANCE PROGRAM - MAXIMUM ACCELERATION CAPABILITY * * *

(SINGLE-SHAFT GAS TURBINE ENGINE, GE HYDROMECHANICAL TRANSMISSION)

ENGINE DATA

MAXIMUM POWER (HP) =	130.0
MAXIMUM G.G. SPEED (RPM) =	106000.
MAXIMUM OUTPUT SHAFT SPEED (RPM) =	2700.
ENGINE GEAR REDUCTION =	39.3/1
IDLE SPEED FRACTION =	.500
IDLE SPEED (RPM) =	1350.
GAS GENERATOR INERTIA (LBM-IN**2) =	2.30
OUTPUT SHAFT INERTIA (SLUG-FT**2) =	.76
ENGINE NUMBER =	3
PERFORMANCE DEGRADATION FACTOR =	.85

INITIAL ENGINE SPEED FRACTION (AT 25 MPH) = .624
ENGINE RUNUP TIME, SEC (AT 25 MPH) = 1.115

INITIAL ENGINE SPEED FRACTION (AT 50 MPH) = .736
ENGINE RUNUP TIME, SEC (AT 50 MPH) = .840

VEHICLE AND PERFORMANCE DATA

VEHICLE WEIGHT (LB) =	3850.
ACCESSORY POWER (HP) =	4.0
CDA PRODUCT (FT**2) =	12.
ROLLING RESISTANCE COEFFICIENTS	
F0 (LB/LB) =	.015
F1 (LB/LB-MPH)*E-05 =	2.15
F2 (LB/LB-MPH**2)*E-07 =	1.85
REAR AXLE RATIO =	2.00/1
WEIGHT FRACTION ON DRIVING WHEELS =	.50
TRANSMISSION TORQUE SPLIT EXPONENT =	1.00
AMBIENT TEMPERATURE (F) =	105.
ROAD-TIRE ADHESION COEFFICIENT =	1.0

* * SUMMARY OF ACCELERATION PERFORMANCE * *

(EPA VEHICLE DESIGN GOALS - SIX PASSENGER AUTOMOBILE)

* 0-60 MPH ACCELERATION TIME (SEC) =	16.40
* DISTANCE COVERED IN 10 SEC FROM STANDSTILL (SEC) =	332.4
* 25-70 MPH ACCELERATION TIME (SEC) =	18.48
* DOT HIGH-SPEED PASS MANEUVER TIME (SEC) =	14.45
* DOT HIGH-SPEED PASS MANEUVER DISTANCE (FT) =	1332.4
* TOP SPEED (MPH) =	93.8

However, mathematical difficulties with the transmission torque-split model preclude starting acceleration runs from nonzero vehicle speeds. For these cases, which begin at 25 and 50 mph for the OAP maneuvers, the engine is assumed to be initially at rated (maximum) speed. The resultant performance is then corrected by adding on a calculated engine run-up time from the 25- and 50-mph steady-state engine speeds.

Vehicle Acceleration Program - Borg-Warner Mechanical Transmission

This program predicts the acceleration performance of a vehicle equipped with the Borg-Warner mechanical transmission and a controlled slipping clutch. The program output, like the HMT acceleration program, consists of a time history of the vehicle's acceleration, including vehicle speed, elapsed distance, engine speed and power, power lost in the clutch, and the transmission gear number. The acceleration is initiated from a standstill with the engine at idle, and interpolations are performed during the acceleration to compute the OAP performance data. The program terminates when the vehicle has reached top speed or when the DOT high-speed pass maneuver has been completed, whichever comes first. At the end of each case, the program prints a summary of the OAP acceleration performance data. A print option permits suppression of the acceleration history printout so that only the heading and summary are printed, as in the HMT program.

A variable computation step size is used which depends on the vehicle acceleration and the clutch performance regime. The step sizes are based on a vehicle speed change of 0.5 mph or a change of engine speed of 5% of the difference between the idle and lock, or lock and maximum speeds (depending on the clutch regime), whichever is smaller. The total computation time for each case is short, averaging about 3 sec on a UNIVAC 1108. A sample printout is shown in Table XXIb.

Because of the close ratio spacing of the transmission (small rpm changes at each shift), Borg-Warner feels that the transmission shifts should be controlled only by engine speed, and not influenced by throttle position as in conventional automatic transmissions. This means that, for a given vehicle speed, the engine speed is the same regardless of throttle position. Thus, the 25-70 mph acceleration time and DOT high-speed pass maneuver interpolations are not corrected for engine run-up time as in the case of the HMT.

TABLE XXIb
SAMPLE COMPUTER PRINTOUT

L-971249-7

* * * DARL VEHICLE PERFORMANCE PROGRAM - MAXIMUM ACCELERATION CAPABILITY * * *

(SINGLE-SHAFT GAS TURBINE ENGINE, N-SPEED SLIPPING CLUTCH TRANSMISSION)

ENGINE DATA

MAXIMUM POWER (HP) =	130.0
MAXIMUM G.G. SPEED (RPM) =	62000.
MAXIMUM OUTPUT SHAFT SPEED (RPM) =	7000.
ENGINE GEAR REDUCTION =	11.7/1
IDLE SPEED FRACTION =	.500
IDLE SPEED (RPM) =	3500.
GAS GENERATOR INERTIA (LB-IN**2) =	2.50
OUTPUT SHAFT INERTIA (SLUG-FT**2) =	.11
ENGINE NUMBER =	1
PERFORMANCE DEGRADATION FACTOR =	.85
CLUTCH LOCKUP SPEED FRACTION =	.850
RATIO(1)=	4.50
RATIO(2)=	3.30
RATIO(3)=	2.56
RATIO(4)=	2.06
RATIO(5)=	1.69
RATIO(6)=	1.40
RATIO(7)=	1.18
RATIO(8)=	1.00

VEHICLE AND PERFORMANCE DATA

VEHICLE WEIGHT (LB) =	3970.
ACCESSORY POWER (HP) =	4.0
CDA PRODUCT (FT**2) =	12.
ROLLING RESISTANCE COEFFICIENTS	
F0 (LB/LB) =	.015
F1 (LB/LB-MPH)*E-05 =	2.15
F2 (LB/LB-MPH**2)*E-07 =	1.85
REAR AXLE RATIO =	6.11/1
AMBIENT TEMPERATURE (F) =	105.

* * SUMMARY OF ACCELERATION PERFORMANCE * *

(EPA VEHICLE DESIGN GOALS - SIX PASSENGER AUTOMOBILE)

* 0-60 MPH ACCELERATION TIME (SEC) =	22.76
* DISTANCE COVERED IN 10 SEC FROM STANDSTILL (SEC) =	106.8
* 25-70 MPH ACCELERATION TIME (SEC) =	19.22
* 50 HIGH-SPEED PASS MANEUVER TIME (SEC) =	14.36
* 50 HIGH-SPEED PASS MANEUVER DISTANCE (FT) =	1327.3

Fuel Economy and Emissions Program - Hydromechanical Transmission

The purpose of this program is to estimate the fuel economy and emissions of a vehicle which uses the GE HMT. The program output consists of a summary of the fuel economy (mpg) and emissions produced over the Federal Driving Cycle (FDC), and for steady-state speeds of 20, 30, 40, 50, 60, and 70 mph. The fuel economy in Btu/mi and the average power for each of the above cases are also given. Finally, the average mpg for the simplified suburban and country routes, and for the composite of the latter two routes and the FDC, are given. A sample printout is shown in Table XXII. A print option permits a listing of various vehicle parameters such as engine power, engine speed, and transmission efficiency for each of the 1370 intervals of the FDC. The program requires about 25 sec of Univac 1108 computing time for each case.

At each point (or interval) in the cycle, the fuel consumed and the emissions produced are calculated in the following manner. Knowing the vehicle speed and acceleration, the road-load torque is computed. Then, as described in the section on vehicle dynamics, the transmission input torque and speed are computed and added to the engine accessory load torque plus an additional torque which is calculated to account for engine acceleration effects. Then, knowing the engine output speed and torque (engine operating point), the fuel flow is computed by numerical interpolation from the engine fuel flow map which is stored in tabular form.

The pollutant emissions produced during the interval are obtained by numerical interpolation for the emissions indices (lb of pollutant produced per 1000 lb of fuel consumed) for each species and then multiplying the index by the fuel consumed. Finally, the fuel consumed and pollutants produced are summed over all the intervals of the cycle and then averaged as required.

TABLE XXII
SAMPLE COMPUTER PRINTOUT

L-971249

* * * UARL VEHICLE PERFORMANCE PROGRAM - FUEL ECONOMY * * *

(SINGLE-SHAFT GAS TURBINE ENGINE, GE HYDROMECHANICAL TRANSMISSION)

ENGINE DATA

MAXIMUM POWER (HP) =	130.0
MAXIMUM G.G. SPEED (RPM) =	106000.
MAXIMUM OUTPUT SHAFT SPEED (RPM) =	2700.
ENGINE GEAR REDUCTION =	39.3/1
IDLE SPEED FRACTION =	.500
IDLE SPEED (RPM) =	1350.
GAS GENERATOR INERTIA (LBM-IN**2) =	2.30
OUTPUT SHAFT INERTIA (SLUG-FT**2) =	.76
TRANSMISSION NO-LOAD POWER (HP)	.00
ENGINE NUMBER =	3
OPTIMUM FUEL FLOW LINE NUMBER =	2
EMISSIONS INDEX FLOW NUMBER =	3

VEHICLE AND PERFORMANCE DATA

VEHICLE WEIGHT (LB) =	3850.
ACCESSORY POWER (HP) =	1.3
CDA PRODUCT (FT**2) =	12.
ROLLING RESISTANCE COEFFICIENTS	
F0 (LB/LB) =	.015
F1 (LB/LB-MPH)*E-05 =	2.15
F2 (LB/LB-MPH**2)*E-07 =	1.85
REAR AXLE RATIO =	2.00/1
AMBIENT TEMPERATURE (F) =	60.

* * SUMMARY OF VEHICLE PERFORMANCE * *

	FDC	20 MPH	30 MPH	40 MPH	50 MPH	60 MPH	70 MPH
FUEL ECONOMY (MPG)	7.51	8.68	11.21	12.51	12.63	12.22	11.47
FUEL ECONOMY (BTU/MI)	17156.	14842.	11485.	10292.	10196.	10540.	11230.
CO EMISSIONS (GM/MI)	2.582	2.614	1.768	1.398	1.163	1.064	1.004
UHC EMISSIONS (GM/MI)	.397	.443	.243	.169	.109	.078	.066
NOX EMISSIONS (GM/MI)	.407	.322	.257	.242	.254	.286	.339
AVERAGE POWER (HP)	14.3	10.3	14.2	19.8	27.6	39.1	55.3

AVERAGE SUBURBAN FUEL ECONOMY (MPG) = 11.01

AVERAGE COUNTRY FUEL ECONOMY (MPG) = 12.02

AVERAGE FUEL ECONOMY FOR EQUAL PARTS OF
RURAL DRIVING, SUBURBAN DRIVING, AND FDC (MPG) = 9.77

APPENDIX IV

HISTORICAL ENGINE-RELATED OWNERSHIP COSTS

For analysis purposes, present engine-related auto ownership costs have been separated into four major categories: fixed costs, out-of-pocket running costs, maintenance costs, and repair costs. Each of these categories is divided into its components which will be discussed in detail later.

At the outset it is assumed that the car will be driven by three owners over a seven-year lifetime for a total distance of 105,000 miles at a constant rate of 15,000 miles per year. The initial purchaser of the car is assumed to own and operate it for the first four years, the second owner for two years, and the third for one year. Data from Ref. 16 indicate that this would be a typical ownership history. An ownership cost history for the engine-transmission complex is shown in Table XXIII, details of which are discussed below.

Fixed Costs

Fixed costs are taken as those costs which are mainly independent of odometer mileage. These include the capital costs (depreciation, interest, and/or finance charges) plus insurance and taxes.

The engine-transmission share of the original selling price of a 1971 medium-priced 4-door sedan has been separately established as $518 for the engine and $160 for the transmission for a total of $678. Data from Ref. 21 indicate that the wholesale value of a car (and, presumably, all its components) can be closely approximated by a declining-balance depreciation rate of 27.7% per year. That is, at the end of any year the car's wholesale value is 72.3% of what is was one year previously. Extrapolation of the ratio of wholesale-to-retail prices to the time of initial sale indicates an initial wholesale value of 84.5% of the original retail sales price. Hence, an initial wholesale value of $573 is found for the engine-transmission complex.

Statistical data on automobile financing (Ref. 16) indicate that about one-third of all new car buyers pay cash and that the remaining two-thirds finance. It is assumed that those who finance pay one-third cash and borrow the balance for three years at 12% with uniform annual payments. From this it follows

TABLE XXIII

Engine/Transmission-Related Ownership Costs
1971 Automobile
(Costs in Dollars)

	Year								
	0	1	2	3	4	5	6	7	ΣYears
Miles	-	15000	15000	15000	15000	15000	15000	15000	
ΣMiles	-	15000	30000	45000	60000	75000	90000	105000	
Fixed Costs:									
Cash Cost	678	- - -	- - -	- - -	218	- - -	- - -	50	
Loan	298	210	111	- - -	70	37	- - -	- - -	
Equity	275	204	188	217	87	76	82	59	
Value	573	414	299	217	157	113	82	59	
Depreciation	-	264	115	82	60	105	31	23	
Interest	-	36	25	13	- - -	8	4	- - -	
Vestcharge	-	16	12	11	13	5	5	5	
Insurance	-	25	25	25	6	6	6	6	
Taxes	-	77	10	10	10	17	10	10	
Total Fixed Costs		418	187	141	89	141	56	94	1126
Fuel & Oil Costs		387	387	387	387	387	387	387	2709
Maintenance:									
Interval - 6 mos		28	42	28	42	28	42	28	
Interval - 12 mos		43	43	43	86	43	43	43	
Interval - 24 mos		-	40	-	40	-	40	-	
Total Maintenance		71	125	71	168	71	125	71	702
Repairs:									
Distributor (14)*		12	12	12	12	12	12	12	
Exhaust (39)		-	-	26	-	-	26	-	
Water Pump (52)		-	-	24	-	-	24	-	
Carburetor (45)		-	-	29	-	-	29	-	
Fan Belt (51)		-	-	-	4	-	-	4	
Fuel Pump (52)		-	-	-	15	-	-	15	
Generator (52)		-	-	-	32	-	-	32	
Transmission (66)		-	-	-	-	178	-	-	
Engine Block (70)		-	-	-	-	93	-	-	
Radiator (76)		-	-	-	-	-	16	-	
Oil Pump (109)		-	-	-	-	-	-	18	
Total Repairs		12	12	91	63	283	107	81	649
Grand Total		888	711	690	707	882	675	633	5186

*Interval, months

that, in aggregate, new car purchases are financed 56% cash and 44% by loan. Thus a hypothetical purchaser pays $380 cash for the engine-transmission and borrows $298. His initial equity, however, is the difference between the initial wholesale value and the loan, $275, and not the $380 which he actually paid.

In addition to the 12% typical loan interest, a vestcharge of 6% on the owner's equity is also levied. This is in accordance with principles discussed in Ref. 24 and represents the income which might be expected from an appropriate alternative investment.

Depreciation is charged at the aforementioned rate of 27.7% of the previous year-end value except that the first year's depreciation figure includes the difference between initial cost and initial wholesale value. This same exception applies to the fifth year, which is the first year of ownership by the car's second owner.

Financing the second ownership follows the same principles as the first but with somewhat different proportions. Automobile financing statistics (Ref. 16) indicate that 52% of second-hand car buyers pay all cash and that 48% finance. Here again, those who finance are assumed to pay one-third down and two-thirds on account at 12%, but this second loan is assumed to mature in two years instead of three. This process results in a hypothetical second owner paying 68% cash and borrowing 32%. Meanwhile, the ratio of wholesale value to retail price has declined from an original 84.5% to 72.0%. Thus, the second buyer's cost is 1.39 times wholesale value, whereas the comparable first buyer's cost factor was 1.183.

Reference 28 was used as the source for insurance and tax costs. These data (averages of 5 U. S. cities) can be regarded as at least typical though not necessarily equal to national averages. The data of Ref. 28 were first expressed as percentages of initial cost and applied in that manner to the present application.

The philosophy regarding insurance is that liability, property damage, and medical payments are properly chargeable to the driver, not the vehicle, and should not be shared as an engine-transmission cost. Comprehensive (fire and theft) and collision ($50 deductible) were found to be 0.9% and 2.8%, respectively, of initial cost. It was assumed that comprehensive would be carried for the life of the car but that collision would be carried only for the first three years.

Sales tax averaged 3% for the 5 cities examined and is applied in this instance to both retail sales of the vehicle. A federal excise tax of 7% is applied to the initial sale of the vehicle. The annually recurring taxes, registrations, licenses, inspections, etc., averaged 1.41% and are applied here throughout the car's life.

TABLE XXIV

ENGINE MAINTENANCE COSTS

Interval (mos. or kmi.)	Item	Cost. $	
6	Change oil	5	
	Change oil filter	5	= 14
	Clean breather cap	4	
	Check and adjust belts	4	
12	Replace plugs	12	
	Replace points	5	
	Replace PCV	3	= 43
	Replace fuel filter	3	
	Clean cooling system	5	
	Tune-up	15	
24	Replace belts	10	
	Replace hoses	15	= 40
	Replace air filter	5	
	Change coolant	10	

It will be noted that the total capital (fixed) costs of $1126 amount to 166% of the original price.

Out-of-Pocket Running Costs

Engine-related out-of-pocket costs are simply fuel and oil consumption. Here, the fuel consumption rate of Ref. 15 was used, 13.8 miles per gallon*, and an oil consumption rate of 3/4 qt/1000 mi, not including oil changes, was assumed. Fuel (gasoline for conventional cars) was assumed to cost 34.9¢/gal, including state and federal tax, and oil, 70¢/qt.

Maintenance Costs

Routine maintenance operations and mileage intervals are shown in Table XXXIV. These are typical of owner's manual recommendations (Ref. 29). Also shown are estimated costs by item. A summary of these costs appears in the maintenance cost section of Table XXIII. The service station flat-rate manual (Ref. 30) and parts catalogues (Ref. 31) were used as guides in estimating maintenance costs.

Repair Costs

In spite of maintenance, component failures do occur, necessitating occasional repairs. The engine-transmission components, the average mileages at which they require repairs, and the average costs of repairs are listed in the Repairs Section of Table XXIII. These data were taken from Ref. 32 and represent repair experience on fleets of cars owned and operated by the Bureau of Public Roads and by the highway departments of each of the 50 states. Although the data of Ref. 32 do not so specifically state, it has been established that these fleets were subjected to a schedule of maintenance comparable to Table XXIV in addition to the repair work presented.

Total costs for each year of a car's life are shown at the bottom of Table XXIII and, in addition, are graphically illustrated in Fig. 112. The "present worth" of each of these total annual costs is established in Table XXV. The sum of the "present worths" provides a final single figure for purposes of ownership cost comparison, the "present worth" of total ownership costs of an engine-transmission combination over a seven-year useful life.

---

*This estimate is inconsistent with Ref. 15, which indicates a 13.96 mpg national average for cars of all weights, including subcompacts and compacts. UARL simulations consistently indicate that the mileage for the 4000-lb car is 11 to 11.5 mpg, depending on driving cycle, which is more consistent with the Ref. 15 data.

ENGINE-TRANSMISSION RELATED OWNERSHIP COSTS, 1971 AUTOMOBILE

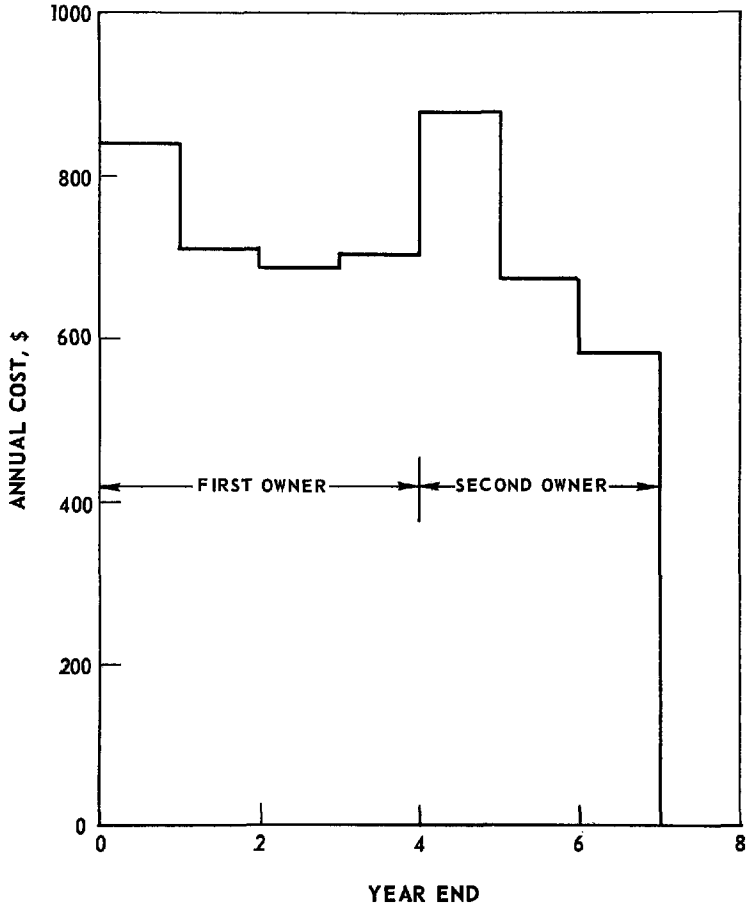

TABLE XXV

PRESENT WORTH OF OWNERSHIP COSTS
1971 Automobile

Year	Cost	PWF (0.06)	PW	ΣPW
1	841	0.9434	793	793
2	711	0.8900	633	1426
3	690	0.8396	579	2005
4	707	0.7921	560	2565
5	882	0.7473	659	3224
6	675	0.7050	476	3224
7	583	0.6651	388	4088

APPENDIX V

DESIGN OPTIONS FOR IMPROVED FUEL ECONOMY

The study ground rules and the conservative design assumptions result in base-line engines which result in vehicle fuel economies far short of the ultimate potential of these engines. In this appendix a number of design options are considered which serve to increase the fuel economy. With these options, the SSS-10 could achieve the OAP design goal of 10 mpg in a 1974 demonstration engine, and exceed it in subsequent production engines.

Transmission Design Options

An extended optimization study of engine and transmission combinations is required and has been recommended to OAP. Aside from the obvious result that transmission efficiency improvements lead to corresponding fuel economy improvements, additional benefits of transmission optimization can be attained by:

1. permitting the engine to be sized smaller in order to achieve identical performance, thus providing better part-load fuel economy, and

2. providing better response and thus permitting lower idle speeds and better idle fuel consumption.

Reasonable expectations of the result of such a study are that fuel economy could be increased by from 10 to 20% over the FDC as a result of using currently proposed, but more efficient, transmission concepts, and optimizing the engine and transmission together. Furthermore, potential improvements exceeding 50% can be postulated. Several transmission concepts appear worthy of more detailed investigation, and are discussed in the following:

General Electric Hydromechanical Transmission (GE HMT)

The GE HMT was specified for the base-line vehicle in this study since it has been demonstrated in actual hardware, provides excellent drivability, and has prospects for reasonable manufacturing cost with a relatively low technological risk. A major drawback, however, is that its average efficiency over the FDC is only 50%. This efficiency could undoubtedly be improved by readily conceived modifications which might include an overdrive, for example, to provide maximum efficiency for both the FDC and for freeway operation. This effect can be seen by referring to Figs. 91 and 92. For example, specification of an overdrive which allows a 2:1 drive axle ratio at speeds greater than 35 mph, and 3:1 at speeds less

TABLE XXVI

SSS-10 Fuel Economy Optimization

Line	Modification	Driving Cycle FDC	OAP Suburban	OAP Country	OAP Composite
1	Base-line	7.51	11.01	12.02	9.77
2	GE HMT With Overdrive	7.90	11.34	12.02	10.07
3	Sundstrand DMT	8.05	11.56	12.65	10.47
4	Borg Warner n-speed	8.26	12.12	13.21	10.74
5	Tracor	7.76	12.55	12.82	10.47
6	Transmission η = 100%	9.04	13.64	13.82	11.71
7	3700# Vehicle Test Weight	7.61	11.11	12.12	9.88
8	3480# Vehicle Test Weight	7.77	11.26	12.26	10.04
9	Aero Drag of 80%	7.61	11.24	12.93	10.07
10	Radial Belted Tires	7.92	12.05	13.10	10.50
11	Combined Vehicle Modifications 5,8,9 & 10	8.38	13.95	14.94	11.63
12	Engine Reoptimization	9.00	12.12	11.50	10.84
13	Combined System Modifications: (1974)	10.05	15.35	14.23	12.77
14	(1977-78 Performance)	10.55	16.12	14.95	13.41
15	(Post-80 Performance)	11.08	16.89	15.66	14.05

than 35 mph, would improve fuel economy by permitting maximum efficiency for both operating modes. This modification plus a 3% efficiency gain at low-power operation (below 10% power) would yield the results shown on line 2 in Table XXVI (7.90 mpg on the FDC, with corresponding improvements on the other driving cycles examined).

Sundstrand Dual-Mode Transmission (DMT)

The Sundstrand DMT has been described in Ref. 33 as it pertains to commercial applications. Like the GE HMT, it is a split-path combination hydrostatic and mechanical device which provides infinitely variable output characteristics. It is more efficient, particularly in the lower speed ranges, at the expense of greater complexity and a probable higher manufacturing cost. Although exact performance data of a suitably sized DMT were not evaluated, an average increase of efficiency of 15% in the low-speed range and 5% in the high-speed range might be expected. Efficiency improvements of this magnitude would lead to the results shown in line 3 of Table XXVI.

Borg-Warner n-Speed Transmission

The Borg-Warner-suggested concept (Ref. 1) of a 6, 8 or 10-speed geared transmission coupled to the SSS-10 through a controlled-speed slipping clutch would provide relatively high transmission efficiency at the expense of some off-optimum engine operation and the possible requirement for a somewhat larger engine to provide equivalent performance. The overall effect expected might be to provide a fuel economy gain of approximately 10%, as shown on line 4 of Table XXVI (8.26 mpg on the FDC).

Tracor Transmission

Data on the performance of the Tracor traction (friction) drive transmission was furnished by EPA for consideration. These data are shown in Fig. 113, and were adapted for use in the simulation program as shown in Fig. 114. The results of the fuel economy evaluation using this data is shown on line 5 of Table XXVI (7.76 mpg on the FDC).

Other Transmission Possiblities

Other likely transmission possibilities include modified torque converter automatics, geared multispeed manuals, variable-sheave pulley and chain traction devices, other toroidal devices, etc. The last three in particular show high promise for higher overall transmission efficiency. While detailed study is required to establish the feasibility of any of these devices, line 6 shows the fuel economy which would be obtained if transmission efficiency (η) was 100%. In other words, this line represents the theoretical limit for a base line vehicle with no transmission losses other than reduction gearing and rear axle losses.

TRACOR TRANSMISSION EFFICIENCY FOR VARIOUS OUTPUT/INPUT SPEED RATIO

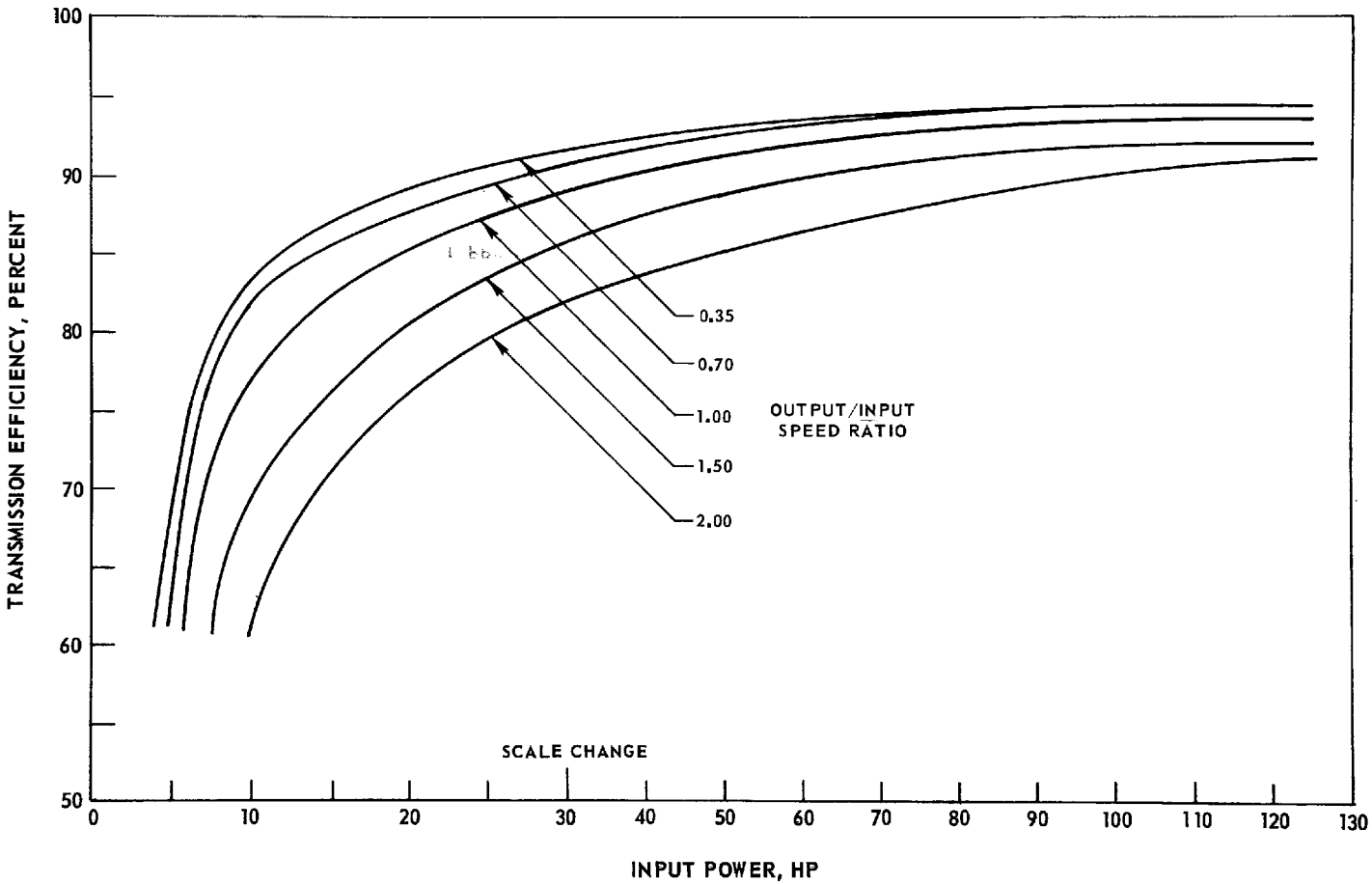

FIG. 113

L971249-7

ASSUMED TRACOR TOROIDAL TRANSMISSION EFFICIENCY FOR VARIOUS VEHICLE SPEEDS

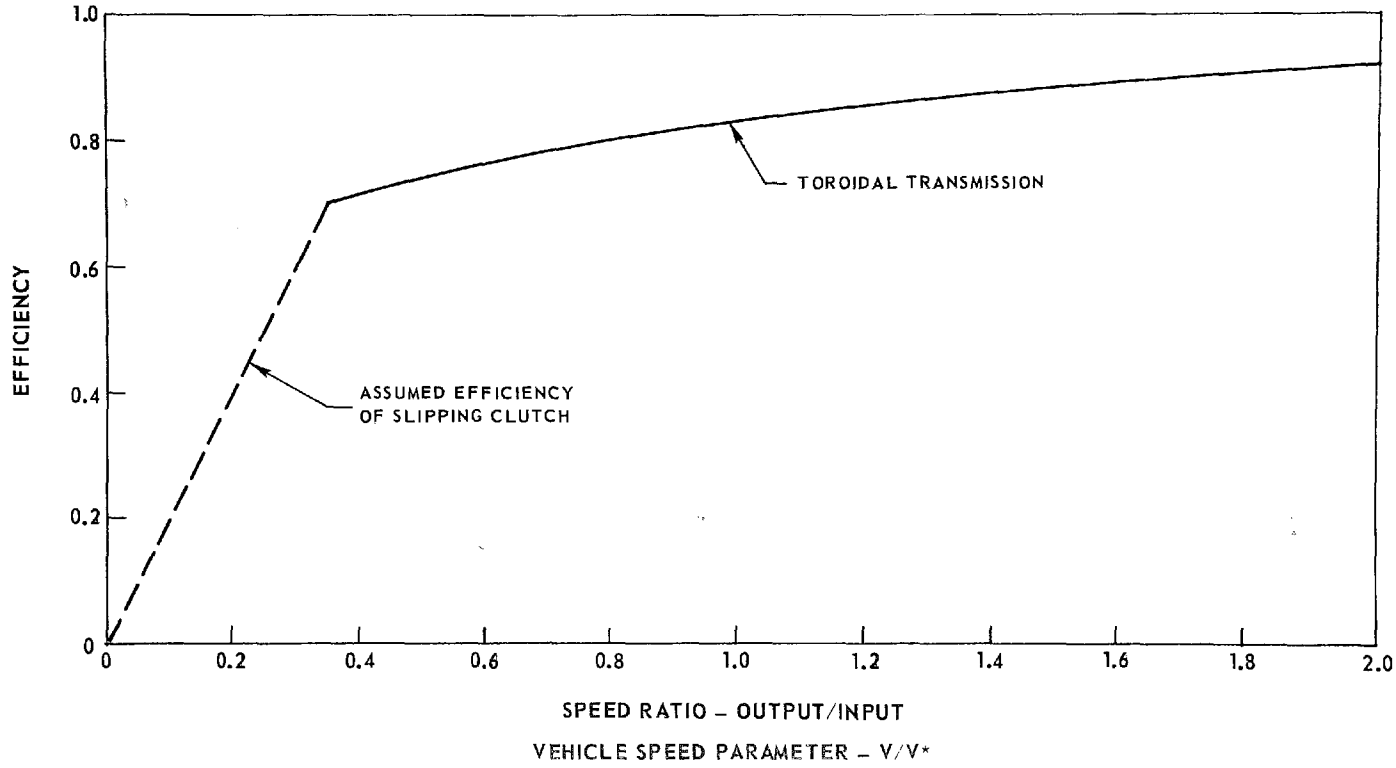

FIG. 114

Probable Vehicle Test Weight

The section of this report concerning RECOMMENDED ENGINE SELECTION (page 221) presented estimates of likely vehicle weight, which were shown in Table XIX. It is strongly believed that the SSS-10 has a significant advantage in that its low weight can further reduce the overall weight of the vehicle designed for its use, with a corresponding beneficial effect on fuel economy. From line 13 of Table XIX, an estimated adjusted gross weight of 4400 lb is shown. Deduction of 700 lb as per OAP specifications would then lead to a vehicle test weight of 3700 lb. The effect on fuel economy of a reduction from 3850 lb for the baseline vehicle to 3700 lb can be derived from Fig. 93 and is shown on line 7 of Table XXVI (7.61 mpg on the FDC).

Additional weight savings may be possible. For example, the Tracor transmission is estimated to weigh 130 lb versus the 185 lb assumed in Table XIX. In addition, its higher input speed permits weight reduction in the engine gearbox of approximately 30 lb. If this transmission proves to be satisfactory, vehicle weight would decrease by an additional 142 lb [1.67 x (55 + 30)]. Fuel weight will also decrease for a vehicle delivering 10 mpg over the FDC, from the 187 lb assumed in Table XII, to 140 lb. An additional decrease of 220 lb (142 + 1.67 x 47) would account for both of these effects, and the results on fuel mileage are shown on line 8 of Table XXVI for the resulting 3480-lb test weight vehicle. (Note, this result accounts for the weight reduction, but not the efficiency improvement of the Tracor transmission. Multiple effects are discussed later.)

Vehicle Resistance

It is obvious that vehicle resistance determines a large part of the power required to propel the vehicle, and thus has a first-order effect on fuel consumption. As discussed in the Vehicle Evaluation Section, OAP-specified resistance equations call for a standard vehicular frontal area, air drag coefficient, and rolling drag coefficient in order to provide a common basis for analytical evaluation of competing propulsion systems. In the design of the demonstration vehicle, there is opportunity to reduce the resistance expected for the actual vehicle. For example, the small size of the SSS-10 would probably permit a somewhat smaller aerodynamic cross section (A) than the 25 ft^2 specified by the OAP, while the reduction of radiator cross section and some underpanning (which may be required in any event for the exhaust system) could also reduce the air drag coefficient (C_{AD}). The present $C_{AD}A$ value of 12 ft^2 (0.48 x 25) could be reduced 20%, to 9.6 ft^2, with a C_{AD} of 0.40 and an A of 24 ft^2 (or, alternatively, a C_{AD} of 0.44 and a frontal area of 21.8 ft^2).

*U.S.Government Printing Office: 1974--747-787/318 Region No. 4

The changes in fuel economy for the base-line vehicle solely due to a reduction in aerodynamic resistance of this magnitude are shown in line 9 of Table XXVI.

With regard to reducing rolling resistance, it is well known that the use of radial belted tires reduces tire resistance considerably. Line 10 of Table shows the effect on fuel consumption of the base-line vehicle when radial belted tires are substituted with a 20% reduction in rolling resistance.

Combined Vehicle Modifications

All of the above fuel economy optimization procedures have been considered independently of each other. A detailed study of the system interactions has not been made, but a cursory analysis clearly indicates that significant fuel economy improvements are possible when the above elements are combined in a reasonable fashion. Line 11 presents the expected results from such a cursory analysis pertaining to combining certain of the above vehicle modifications. The calculations were made from the combination of the Tracor transmission (line 5), an expected vehicle test weight of 3480 lb (line 8), aerodynamic design improvements (line 9), and radial belted tires (line 10). Fuel mileage on the FDC is now shown to be 8.38 mpg, while overall mileage is 11.63 mpg. These figures represent improvements of 11% and 14%, respectively, in mpg, over those for the base-line vehicle. Note that potential improvements in the engine itself have not been considered, as yet.

Engine Reoptimization

In the course of an actual engine development program, considerable opportunity exists for further reoptimization of the engine to improve its fuel consumption. Improvement goals for three candidate areas for reoptimization might be as follows: (1) reduce idle speed an additional 5% of design speed in order to reduce idle fuel consumption by an additional 8 to 10%; (2) improve the intake and exhaust ducting arrangements to reduce the predicted installation losses at low airflow in order to improve low part-power fuel economy by an additional 5%; (3) reoptimize all engine components and rematch as necessary to further reduce idle and low-power fuel consumption by 5 to 10%, accepting, if necessary, a concurrent 10% reduction in full-power fuel consumption.

The net result of successful pursuit of these three goals would be to improve FDC fuel economy of the SSS-10 by 20%, with a concomittant reduction on the OAP Country cycle of 5%. This result is shown on line 12 of Table XXVI, showing 9.00 mpg on the FDC.

Combined System Modifications

The combination of the suggested vehicle modifications (line 11) and engine efficiency improvement goals (line 12) results in the system estimates shown on line 13, in which the OAP specification of 10 mpg over the FDC is indicated. Considerable further study is needed to establish the probability of achieving the performance shown on line 13. However, it is clear that a reasonable possibility of making significant improvements in the fuel economy of the SSS-10 demonstrator automobile exists.

With regard to eventual production automobiles, further development of the engine and refinement of the optimization processes described above lead to expectations of future performance 5 to 10% better than shown, for 1977-78 and post-1980 periods, respectively. The resulting values are shown in lines 14 and 15. (It should be noted that the estimated post-1980 performance of the SSS-10 exceeds that predicted for the RCSS-8 base-line vehicle.)

A large difference exists between the transmission possibilities of line 6 and the line 5 data used for the values shown in lines 11, 13, 14 and 15. The assumption of satisfactory development of high-efficiency transmissions combined with the other modifications described above would yield fuel mileage estimates of up to 17 mpg for the post-1980 period.

The proper optimization of any system with complicated interactions, such as a new type of low-polluting automobile, involves not only a large analytical effort, but extensive field and customer testing. Therefore, the above comments on fuel economy optimization should not be regarded as definitive, but rather indicative that if fuel economy is important enough, the SSS-10 automobile has the potential to deliver over 10 mpg on both the FDC and the OAP composite cycles.

Driving Cycle Effects

The relative fuel economy of the several engines considered herein depends on the driving cycle. The OAP driving cycle contains a very small proportion of freeway driving; only 1/9 (by time) of the driving is at 70 mph and an additional 1/9 at 60 mph. This preponderance of slow-speed operation penalizes the SSS-10 engine with its somewhat worse part-load fuel consumption. The following table illustrates this effect for both the base-line vehicle and the post-1980 fuel-economy-optimized vehicle (line 15) of Table XXVI.

	Base-line SSS-10 Mileage (line 1)	¢/mi* Relative Cost	OC-70 Mileage	¢/mi* Relative Cost	Post-1980 Fuel Economy Optimized SSS-10 Mileage (line 15)	Cost
FDC	7.5	4.1	9.5	3.7	11.1	2.8
OAP Suburban	11.0	2.8	12.6	2.8	16.9	2.0
OAP Country	12.0	2.6	12.5	2.8	15.7	2.0
OAP Overall**	9.8	3.2	11.3	3.1	14.1	2.2
60 mph	12.2	2.5	12.9	2.7	15.7	2.0
50 mph	11.5	2.7	11.5	3.0	15.0	2.1

Thus, the urban driver (FDC) of the base-line SSS-10 auto will find his fuel cost higher (0.4¢/mi) by about the same amount that the freeway driver (70 mph) finds his cost lower (0.3¢/mi), while the typical driver of the base-line SSS-10 auto (OAP Overall) will notice no significant difference (0.1¢/mi). The driver of the post-1980 SSS-10 vehicle will have a consistent 0.7¢/mi to 0.9¢/mi cost saving compared with present experience.

* SSS-10 fuel at 31¢/gal; OC-70 fuel at 35¢/gal.

** Combination of equal portions of FDC, OAP Suburban, and OAP Country, by time.